Investigations into the removal and destruction of bacterial biofilms by sodium hypochlorite irrigant delivered into an *in vitro* model

A thesis submitted to the University College of London in fulfilment of the requirements for the degree Doctor of Philosophy

By

Saifalarab Mohmmed BDS (Iraq), MSc (Iraq)

University College London

2017

UCL Eastman Dental Institute

Biomaterials and Tissue Engineering Research Division

University College London

DECLARATION

I, Saifalarab Mohmmed confirm that the work presented in this thesis is my own. Where information has been derived from other sources, I confirm that this has been indicated in the thesis.

Saifalarab Mohmmed

ABSTRACT

Aims: To investigate the influence of canal design (closed, open), irrigant concentration, agitation, canal complexity, and biofilm type on the efficacy of sodium hypochlorite to remove biofilm. To examine the extent of biofilm destruction following irrigation protocols.

Methodology: Standardized *in vitro* models were developed (Endo-Vu block, flow cell, and 3D printing root canal models). The canal consisted of two halves of an 18 mm length, size 30 and taper 0.06, with or without a lateral canal of 3 mm length, and 0.3 mm diameter. Biofilms were grown for 10 days, and stained using crystal violet. The model was attached to an apparatus and observed under a fluorescent microscope. Following 60 s of 9 mL NaOCl irrigation using syringe and needle, the irrigant was either left stagnant or agitated using gutta-percha, sonic and ultrasonic methods for 30 s. Images were captured every second using an external camera. The residual biofilm percentages were measured using image analysis software. The SPSS software was used for statistical analysis. The residual biofilms were observed using confocal laser scanning, scanning electron, and transmission electron microscope.

Results: The removal of biofilm by NaOCl was more extensive in the open than in the closed canal. The concentration and extent of the needle had an influence on the amount of the residual biofilm. Ultrasonic agitation increased the biofilm removal from the main canal (90.13%) and lateral canal (66.76%). Extensive destruction of residual biofilm was observed in the ultrasonic groups. More residual multi-species biofilm than single species biofilm was identified ($p = 0.001$).

Conclusion: The 3D-printing model provides a reliable method to investigate irrigation procedure. The closed canal adversely affect the efficacy of NaOCl. Concentration and position of the needle affect the efficacy of NaOCl. The results recommend the ultrasonic method for NaOCl agitation. The multi-species biofilm was more resistant than the single species biofilm.

ACKNOWLEDGEMENTS

I would like to express my sincere gratitude and thanks to:

My primary supervisor Professor Jonathan c. Knowles for his encouragement, and professional contribution to improve my academic education.

My secondary supervisor Dr Morgana E. Vianna, for her endless support, teaching, advice, and help throughout the study.

The Ministry of Higher Education and Scientific Research of Iraq for funding my PhD study as a part of educational scholarship programme.

Dr Nicky Mordan for her invaluable assistance, and help with the image analyses.

Dr Stephen Hilton and Dr Matthew Penny for their assistance in printing of the root canal model.

Dr Adam Roberts for his supervision and assistance during PCR amplification procedure to identify the bacterial strains.

Professor Kishor Gulabivala as this study is based on his ideas and concepts originated, developed and under his investigation.

Dr. Paula Ng for her advice in the experiments related to chapter 3 of this study.

Dr Graham Palmer and Dr George Georgiou for their help with the iodometric titration of NaOCl and ordering materials.

Dr Haitham Hussain for providing assistance in the microbiology laboratories.

Dr Aviva Petrie and Mr David Boniface for their assistance in reviewing the statistical analyses.

Mrs Angela Cooper for her advice and support to improve my skills in academic writing.

Mr Jonathan Brittain; Acteon UK Southern Territory Manager for loaning the Satelec® P5 ultra-sonic device.

Finally, I would like to thank my mother, brother, and wife for their support and encouragement throughout my study.

CONTENTS

DECLARATION 2
ABSTRACT 3
ACKNOWLEDGEMENTS 4
CONTENTS 5
List of figures 11
List of tables 20
PUBLICATIONS 23
PRESENTATIONS 23
Chapter 1 24
Introduction 24
1.1. Introduction 24
1.2. Literature review 26
1.2.1. Composition of the root canal microbiota and pathogenesis of apical periodontitis 26
1.2.2. The biofilm concept 30
1.2.3. Formation of biofilm 31
1.2.4. Resistance of biofilm to antimicrobial agent 34
1.2.5. Role of root canal treatment in management of an intracanal biofilms 37
1.2.6. Root canal irrigation solutions 38
1.2.7. Physical and chemical efficacy of NaOCl in root canal treatment 39
1.2.8. Fluid dynamics concept of irrigation 42
1.2.9. Factors influencing the penetration of an irrigant within the root canal system 45
1.2.10. Overcoming the problems of irrigant penetration 46
1.2.11. Agitation of irrigant solution 48
1.2.12. Investigations of efficacy of irrigants against root canal microbiota 50
1.3. Statement of the problem 54
1.4. Null hypothesis 56
1.5. Aim of the study 56
Chapter 2 57
Development and optimization of the materials used in the study 57
2.1. Introduction 57
2.2. Investigation to test potential substratum materials for development of an *in vitro* biofilm model. 58
2.2.1. Justification of the investigation 58

2.2.2. Materials and Methods 59
2.2.3. Results 67
2.2.4. Discussion 75
2.2.5. Conclusion 79
2.3. The effect of needle position on the velocity distribution of irrigant in the root canal system 80
2.3.1. Justification of the investigation 80
2.3.2. Materials and methods 81
2.3.3. Results 83
2.3.4. Discussion 85
2.3.5. Conclusion 87
Chapter 3 88
Investigations into the effect of root canal design (closed, open) on the efficacy of 2.5% NaOCl to remove bacterial biofilms or organic films 88
3.1. Introduction 88
3.2. Material and methods 89
3.2.1. Preparation of simple anatomy canal models 89
3.2.2. Longitudinal sectioning of the canal models 90
3.2.3. Allocation of models to experimental groups 90
3.2.4. Preparation and application of stained organic films (hydrogel, collagen) on the canal wall (subgroups 1, 2) 91
3.2.5. Generation of single species biofilm (*Enterococcus faecalis*) on the surface of the root canal models (subgroup 3) 92
3.2.5.3. Generation of single species biofilm on the canal surface of the model 93
3.2.6. Re-apposition of the model halves 94
3.2.7. Irrigation experiments 95
3.2.8. Image analysis 97
3.2.9. Measurement of available chlorine and pH of outflow NaOCl 97
3.2.10. Data analysis 98
3.3. Results 99
3.3.1. Observations of irrigation experiments 99
3.3.2. Results of statistical analyses 101
3.4. Discussion 108
3.5. Conclusion 112
Chapter 4 113
Investigations into the efficacy of sodium hypochlorite to remove bacterial biofilm or organic film simulating biofilm from a slide surface of a flow cell 113
4.1. Introduction 113
4.2. Materials and Methods 114

4.2.1. Allocation of the flow cell slides to experimental groups 114
4.2.2. Preparation and application of stained organic films (hydrogel, collagen) on the slide (groups 1, 2) 114
4.2.3. Preparation of microbial strain and determination of the standard inoculum 115
4.2.4. Generation and staining of single species *E. faecalis* biofilm on slide surface 115
4.2.5. Irrigation experiments 116
4.2.6. Recording of organic film or biofilm removal by the irrigant 117
4.2.7. Image analysis 117
4.2.8. Assessment of composition of bubbles between NaOCl and bacterial biofilm film (collagen, hydrogel) 117
4.2.9. Data analyses 117
4.3. Results 118
4.3.1. Results of statistical analysis 118
4.3.2. Results of GC-MS analysis of the outflow NaOCl 120
4.4. Discussion 121
4.5. Conclusion 124
Chapter 5 125
The effect of sodium hypochlorite concentration and irrigation needle extension on *Enterococcus faecalis* biofilm removal from a simulated root canal model 125
5.1. Introduction 125
5.2. Materials and Methods 125
5.2.1. Construction of transparent root canal models and distribution to experimental groups 125
5.2.2. Preparation of microbial strain and determination of the standard inoculum 127
5.2.3. Generation of single species biofilm (*E. faecalis*) on the surface of the apical 3 mm of the canal model 128
5.2.4. Staining of biofilms grown on the surface of the models 128
5.2.5. Re-apposition of the model halves 128
5.2.6. Irrigation experiments 128
5.2.7. Recording of biofilm removal by the irrigant 129
5.2.8. Image analysis 129
5.2.9. Measurement of available chlorine and pH of outflow NaOCl 129
5.2.10. Data analyses 130
5.3. Results 130
5.4. Discussion 134
5.5. Conclusion 137

Chapter 6 138

Investigations into the effect of different agitation methods using sodium hypochlorite as an irrigant on the rate of bacterial biofilm removal from the wall of a simulated root canal model 138

6.1. Introduction 138

6.2. Materials and Methods 139

6.2.1. Construction of transparent root canal models and distribution to experimental groups 139

6.2.2. Preparation of microbial strain and determination of the standard inoculum 139

6.2.3. Generation of single species biofilm (*E. faecalis*) on the surface of the apical 3 mm of the canal model 139

6.2.4. Staining of biofilms grown on the surface of the models 139

6.2.5. Re-apposition of the model halves 139

6.2.6. Irrigation experiments 140

6.2.7. Recording of biofilm removal by the irrigant 142

6.2.8. Image analysis 142

6.2.9. Measurement of available chlorine and pH of outflow NaOCl 142

6.2.10. Preparation of the samples for confocal laser scanning microscope (CLSM) 142

6.2.11. Preparation of the samples for scanning electron microscope (SEM) 144

6.2.12. Preparation of the samples for transmission electron microscope (TEM) 144

6.2.13. Data analyses 145

6.3. Results 146

6.3.1 Statistical analysis 146

6.3.2. Microscopic images analysis 149

6.4. Discussion 161

6.5. Conclusion 164

Chapter 7 165

Investigations into the *in situ Enterococcus faecalis* biofilm removal and destruction efficacies of passive and active sodium hypochlorite irrigant delivered into lateral canal of a simulated root canal model 165

7.1. Introduction 165

7.2. Materials and Methods 166

7.2.1. Construction of transparent root canal models with lateral canal and distribution to experimental groups 166

7.2.2. Preparation of microbial strain and determination of the standard inoculum 167

7.2.3. Generation of single species biofilm (*E. faecalis*) on the surface of the apical 3 mm of the canal model 167

7.2.4. Staining of biofilms grown on the surface of the models 167
7.2.5. Re-apposition of the model halves 167
7.2.6. Irrigation experiments 167
7.2.7. Recording of biofilm removal by the irrigant 168
7.2.8. Image analysis 168
7.2.9. Preparation of the samples for confocal laser scanning microscope (CLSM) 168
7.2.10. Preparation of the samples for scanning electron microscope (SEM) 169
7.2.11. Preparation of the samples for transmission electron microscope (TEM) 169
7.2.12. Data analyses 169
7.3. Results 170
7.3.1 Statistical analysis 170
7.3.2. Microscopic images analysis 173
7.4. Discussion 187
7.5. Conclusion 190
Chapter 8 191
Investigations into the removal of multi-species biofilm and biofilm destructive efficacy of passive and active NaOCl irrigant delivered into a simulated root canal model 191
8.1. Introduction 191
8.2. Materials and Methods 192
8.2.1. Construction of transparent root canal models and distribution to experimental groups 192
8.2.2. Preparation of microbial strains and determination of the standard inoculum 192
8.2.3. Generation of multi-species biofilm on the surface of the apical 3 mm of the canal model 194
8.2.4. Staining of biofilms grown on the surface of the models 194
8.2.5. Re-apposition of the model halves 195
8.2.6. Irrigation experiments 195
8.2.7. Recording of biofilm removal by the irrigant 196
8.2.8. Image analysis 196
8.2.9. Preparation of the samples for confocal laser scanning microscope (CLSM) 196
8.2.10. Preparation of the samples for scanning electron microscope (SEM) 196
8.2.11. Preparation of the samples for transmission electron microscope (TEM) 196
8.2.12. Data analyses 197
8.3. Results 197
8.3.1 Statistical analysis 197
8.3.2. Microscopic images analysis 200

8.4. Discussion 213
8.5. Conclusion 216
Chapter 9 217
General discussion and conclusions 217
9.1. General discussion 217
9.2. Suggestions for future work 227
9.3. General conclusion 227
References 229
11.1. Appendix 1 259
..... 259
11.2. Appendix 2 260
11.2.1. Identity of the strains used in the study 260
11.2.2. DNA extraction 260
11.2.3. Protocol of polymerase chain reaction (PCR) technique 261
11.2.4. Protocol of gel electrophoresis of nucleic acids 262
11.2.5. Protocol of DNA Sequencing 263
11.3. Appendix 3 267
11.3.1. The distributions of zeta potential of the test materials 267
11.4. Appendix 4 268
11.4.1. Evaluation of the effect of sterilisation method on the surface structure of the biofilm model substrata 268
11.4.1.3 Results 269
11.5. Appendix 5 275
11.5.1. Iodometric Titration of NaOCl 275

List of figures

Figure 1.1: Schematic diagram illustrating the stages of biofilm formation....……..…33

Figure 2.1: Mean values and standard deviation of the contact angle (θ) at the interface between the substratum and polar (water, glycerol), and non-polar (diiodomethane) liquids..……..……..68

Figure 2.2: Mean and standard deviation values of the surface free energy of the biofilm model stratified by the type of the substratum……..69

Figure 2.3: Images depict the lack of antibacterial activity of the substrata materials against *E. faecalis* bacteria after 24 (a) and 48 (b) hours incubation in Mueller-Hinton agar……69

Figure 2.4: SEM images illustrate that the *E. faecalis* biofilm grown onto the surface of the dentine (a1, aii), Endo-Vu (b1, bii), Polystyrene (ci, cii), Accura (di, dii), and Photopolymer (ei, eii) after ten-day incubation……71

Figure 2.5: Microscopy images of crystal violet stained *E. faecalis* biofilm on one of the (a) dentine, (b) Endo-Vu, (c) Polystyrene, (d) Accura, and (e) Photopolymer sample surfaces ……..……...73

Figure 2.6: Mean and standard deviation values of percentage area of surface coverage with biofilm, stratified by substratum material (dentine, Endo-Vu, Polystyrene, Accura, and Photopolymer). ……..74

Figure 2.7: Sketch of the design of the computational fluid dynamics model.……....82

Figure 2.8: CFD images illustrate the velocity magnitude of irrigation during 10-step times (0.001 – 0.01 seconds) in the root canal geometry just apical to the tip of the irrigation needle place at 3 mm from the apical terminus.……84

Figure 2.9: CFD images illustrate the velocity magnitude of irrigation during 10-step times (0.001 – 0.01 seconds) in the root canal geometry just apical to the tip of the irrigation needle place at 2 mm from the apical terminus.……..……85

Figure 3.1: Photographic images illustrate the sectioning procedure of an Endo-Vu block into two sagittal halves: (a) sample and wheel position; (b) transverse sectioning of the model; (c) sagittal sectioning of the model.……...90

Figure 3.2: Schematic diagram illustrating the set-up of the apparatus.……..93

Figure 3.3: Photographic image illustrates the set-up of the apparatus used to generate single species biofilm (*E. faecalis*) on the canal model……..…….93

Figure 3.4: Photographic images illustrating the re-assembling of the two halves of the canal model: (a) sagittal halves of the canal model; (b) silicone gasket and organic film positions; (c) front view of the model; (d) side view of the model…….95

Figure 3.5: Sketch illustrating the set-up of equipment for recording of the organic film or biofilm removal by NaOCl irrigation protocol using a camera connected to a 2.5× lens of an inverted fluorescent microscope. The irrigant was delivered using a syringe with a 27-gauge side-cut open-ended needle, which was attached to a programmable precision syringe pump. The residual biofilm was quantified using computer software (Image-pro Plus 4.5). Outflow irrigant was collected in a plastic tube using a vacuum pump. The amount of available chlorine (%) and pH were measured using iodometric titration and a pH calibration meter respectively…..……..97

Figure 3.6: Images illustrate the stained hydrogel film on the canal surface of the open canal model: (a) before and (c) after 60 seconds of irrigation using NaOCl in an open canal model. Image-pro plus 4.5 software depicts the respective stained organic film in red (b, d)…….....99

Figure 3.7: Images illustrate stained collagen film on the canal surface of the open canal model (a) before and (c) after 60 seconds of irrigation using NaOCl in an open canal model. Image-pro plus 4.5 software depicts the respective stained organic film in red (b, d)…….....99

Figure 3.8: Images illustrate stained *E. faecalis* biofilm on the canal surface of the open canal model (a) before and (c) after 60 seconds of irrigation using NaOCl in an open canal model. Image-pro plus 4.5 software depicts the respective stained biofilm in red (b, d)……..……100

Figure 3.9: Images depict residual stained (a) hydrogel, (b) collagen film, and (c) biofilm on the canal surface of an open canal model after 60 seconds of irrigation with water…….....100

Figure 3.10: Image showing the presence of air bubbles after 25 seconds of irrigation for the biofilm removal using NaOCl in a closed canal model……..……..101

Figure 3.11: Mean percentages (95% confidence intervals) of residual biofilm or residual stained film (hydrogel, collagen) covering the root canal surface over duration (s) of irrigation. (a) NaOCl irrigation delivered into closed canal, (b) NaOCl irrigation delivered into open canal, (c) Water irrigation delivered into closed canal, (d) Water irrigation delivered into open canal……..…….102

Figure 4.1: (a) Image of flow cell with test material (hydrogel) applied on slide surface, and (b) schematic diagram of the direction of irrigant (2.5% NaOCl) delivery into the flow cell……..…116

Figure 4.2: Spectra of Gas Chromatography mass spectrometry of the experimental groups. (a) Biofilm group; (b) collagen group; (c) hydrogel group; and (d) control group……..…121

Figure 5.1: Image illustrates the design of the root canal model. Each half of a simulated canal is of 18 mm length with 1.38 mm diameter at the coronal portion and 0.3 mm diameter at the apical portion. The lower view shows the printed two halves and when they are reassembled, a straight simple canal of 18 mm length, apical size 30, and a 0.06 taper is created……..……..127

Figure 5.2: Schematic diagram illustrating the set-up of the equipment for recording residual biofilm by irrigant delivered at flow rate of 0.15 mL s^{-1} using an inverted fluorescent microscope……..……129

Figure 5.3: Mean percentages (95% CI) for root canal surface-area coverage with biofilm over duration (s) of canal irrigation using needle place at (a) 3 mm or (b) 2 mm from the canal terminus and delivered at flow rate of 0.15 mL s-1 for each group, stratified by type of irrigant (Total n = 60, n = 10 per group)……..……..131

Figure 6.1: Sketch illustrating the set-up of equipment for recording of the biofilm (biofilm was generated on the apical portion (3 mm) of the canal model) removal by active or passive NaOCl irrigation protocol using a camera connected to a 2.5× lens of an inverted fluorescent microscope. The irrigant was delivered using a syringe with a 27-gauge side-cut open-ended needle, which was attached to a programmable precision syringe pump for 60 s. Following that, the irrigant was kept either stagnant or agitated using manual, sonic, or ultrasonic agitation methods for 30 s. The residual biofilm was quantified using computer software (Image-pro Plus 4.5). Outflow irrigant was collected in a plastic tube using a vacuum pump. The amount of available chlorine (%) and pH were measured using iodometric titration and a pH calibration meter respectively……...141

Figure 6.2: Image illustrates the set-up of the equipment to examine the residual biofilm. Confocal laser scanning microscope was used to observe and record images of the live/dead cells within the residual biofilm. A template was used to control the viewing fields (0.3 mm^2) which were located in the top, middle, and bottom of the tested area. The areas were imaged manipulated using ImageJ® software……...143

Figure 6.3: Median values of the residual biofilm (%) covering the root canal surface-area over duration (s) of passive irrigation followed by passive or active irrigation protocols, stratified by type of irrigation (n = 10 per group)……..……....146

Figure 6.4: CLSM images (0.3 mm^2) from within the root canal to illustrate (a) *E. faecalis* biofilm grown for 10 days and stained using Live/Dead® viability stain with the green colour indicating live cells and the red colour showing the dead bacteria (control). (ai) residual biofilm at 3 mm from the canal terminus after passive irrigation protocol. (b) Passive irrigation group; (i) residual biofilm at 2 mm from the canal terminus; (ii) residual biofilm at 1 mm from the canal terminus. (c) manual-agitation group; (i) residual biofilm at 2 mm from the canal terminus; (ii) residual biofilm at 1 mm from the canal terminus. (d) Sonic agitation group; (i) residual biofilm at 2 mm from the canal terminus; (ii) residual biofilm at 1 mm from the canal terminus. (e) Ultrasonic agitation group; (i) residual biofilm at 2 mm from the canal terminus; (ii) residual biofilm at 1 mm from the canal terminus……..…….152

Figure 6.5: SEM images illustrate (a) *E. faecalis* biofilm grown for 10 days onto the surface of the root canal model (control). (ai) residual biofilm at 3 mm from the canal terminus after passive irrigation protocol. (b) Passive irrigation group; (i) residual biofilm

at 2 mm from the canal terminus; (ii) residual biofilm at 1 mm from the canal terminus. (c) manual-agitation group; (i) residual biofilm at 2 mm from the canal terminus; (ii) residual biofilm at 1 mm from the canal terminus. (d) Sonic agitation group; (i) residual biofilm at 2 mm from the canal terminus; (ii) residual biofilm at 1 mm from the canal terminus. (e) Ultrasonic agitation group; (i) residual biofilm at 2 mm from the canal terminus; (ii) residual biofilm at 1 mm from the canal terminus……..156

Figure 6.6: TEM images illustrate (ai) *E. faecalis* biofilm grown for 10 days onto the surface of the root canal model (control). (aii) residual biofilm at 3 mm from the canal terminus after passive irrigation protocol. (b) Passive irrigation group; (i) residual biofilm at 2 mm from the canal terminus; (ii) residual biofilm at 1 mm from the canal terminus. (c) manual-agitation group; (i) residual biofilm at 2 mm from the canal terminus; (ii) residual biofilm at 1 mm from the canal terminus. (d) Sonic agitation group; (i) residual biofilm at 2 mm from the canal terminus; (ii) residual biofilm at 1 mm from the canal terminus. (e) Ultrasonic agitation group; (i) residual biofilm at 2 mm from the canal terminus; (ii) residual biofilm at 1 mm from the canal terminus……..161

Figure 7.1: Image illustrates the design of the complex root canal mode (main and lateral canals. Each half of a simulated canal is of 18 mm length with 1.38 mm diameter at the coronal portion and 0.3 mm diameter at the apical portion. The lower view shows the printed two halves and when they are reassembled, a straight simple canal of 18 mm length, apical size 30, and a 0.06 taper is created with lateral canal of 3 mm length, 0.3 mm diameter……166

Figure 7.2: Sketch illustrating the set-up of equipment for recording of the biofilm (biofilm was generated on the apical portion (3 mm) of the main and lateral (3 mm) canals model) removal by active or passive NaOCl irrigation protocol using a camera connected to a 2.5× lens of an inverted fluorescent microscope. The irrigant was delivered using a syringe with a 27-gauge side-cut open-ended needle, which was attached to a programmable precision syringe pump. The residual biofilm was quantified using computer software (Image-pro Plus 4.5). ……..167

Figure 7.3: Image illustrates the set-up of the equipment to examine the residual biofilm in the lateral canal. Confocal laser scanning microscope was used to observe and record images of the live/dead cells within the residual biofilm. A template was used to control the viewing fields (0.3 mm^2) which were located in the top, middle, and bottom of the tested area. The areas were imaged manipulated using ImageJ® software……169

Figure 7.4: Mean (95% CI) percentages values of the residual biofilm (%) covering the root lateral canal surface-area over duration (s) of syringe irrigation followed by passive or active irrigation protocols, stratified by type of irrigation (n = 10 per group)……..171

Figure 7.5: CLSM images (0.3 mm^2) from within the lateral canal to illustrate (ai) *E. faecalis* biofilm grown for 10 days and stained using Live/Dead® viability stain with the green colour indicating live cells and the red colour showing the dead bacteria (control). (aii, aiii, and aiv) residual biofilm at 3 mm from the lateral canal after passive irrigation, manual, sonic protocols respectively. (b) Passive irrigation group; (i) residual biofilm at 2 mm from the lateral canal terminus; (ii) residual biofilm at 1 mm from the lateral canal terminus. (c) manual-agitation group; (i) residual biofilm at 2 mm from the lateral canal terminus; (ii) residual biofilm at 1 mm from the lateral canal terminus. (d) Sonic agitation group; (i) residual biofilm at 2 mm from the lateral canal terminus; (ii) residual biofilm at 1 mm from the lateral canal terminus. (e) Ultrasonic agitation group; (i) residual biofilm at 2 mm from the lateral canal terminus; (ii) residual biofilm at 1 mm from the lateral canal terminus.……..……176

Figure 7.6: SEM images illustrate (ai) *E. faecalis* biofilm grown for 10 days. (aii, aiii, and aiv) residual biofilm at 3 mm from the lateral canal after passive irrigation, manual, sonic protocols respectively. (b) Passive irrigation group; (i) residual biofilm at 2 mm from the lateral canal terminus; (ii) residual biofilm at 1 mm from the lateral canal terminus. (c) manual-agitation group; (i) residual biofilm at 2 mm from the lateral canal terminus; (ii) residual biofilm at 1 mm from the lateral canal terminus. (d) Sonic agitation group; (i) residual biofilm at 2 mm from the lateral canal terminus; (ii) residual biofilm at 1 mm from the lateral canal terminus. (e) Ultrasonic agitation group; (i) residual biofilm at 2 mm from the lateral canal terminus; (ii) residual biofilm at 1 mm from the lateral canal terminus.……..…….181

Figure 7.7: TEM images illustrate (ai) *E. faecalis* biofilm grown for 10 days. (aii, aiii, and aiv) residual biofilm at 3 mm from the lateral canal after passive irrigation, manual, sonic protocols respectively. (b) Passive irrigation group; (i) residual biofilm at 2 mm from the lateral canal terminus; (ii) residual biofilm at 1 mm from the lateral canal terminus. (c) manual-agitation group; (i) residual biofilm at 2 mm from the lateral canal terminus; (ii) residual biofilm at 1 mm from the lateral canal terminus. (d) Sonic agitation group; (i) residual biofilm at 2 mm from the lateral canal terminus; (ii) residual biofilm at 1 mm from the lateral canal terminus. (e) Ultrasonic agitation group; (i) residual biofilm at 2 mm from the lateral canal terminus; (ii) residual biofilm at 1 mm from the lateral canal terminus.……...187

Figure 8.1: Sketch illustrating the set-up of equipment for recording of the multi-species biofilm (biofilm was generated on the apical portion (3 mm) of the canals model) removal by active or passive NaOCl irrigation protocol using a camera connected to a 2.5× lens of an inverted fluorescent microscope. The irrigant was delivered using a syringe with a 27-gauge side-cut open-ended needle, which was attached to a programmable precision syringe pump. The residual biofilm was quantified using computer software (Image-pro Plus 4.5).……..…….....195

Figure 8.2: Image illustrates the set-up of the equipment to examine the residual multi-species biofilm. Confocal laser scanning microscope was used to observe and record images of the live/dead cells within the residual biofilm. A template was used to control the viewing fields (0.3 mm^2) which were located in the top, middle, and bottom of the tested area. The areas were imaged manipulated using ImageJ® software……...196

Figure 8.3: Mean (95% CI) percentages values of the residual biofilm (%) covering the root lateral canal surface-area over duration (s) of irrigation for each group stratified by the type of irrigant agitation (n = 10 per group).…….……198

Figure 8.4: CLSM images (0.3 mm^2) from within the canal to illustrate (ai) *E. faecalis* biofilm grown for 10 days and stained using Live/Dead® viability stain with the green colour indicating live cells and the red colour showing the dead bacteria (control). (aii) residual biofilm at 3 mm from the canal terminus after passive irrigation. (b) Passive irrigation group; (i) residual biofilm at 2 mm from the canal terminus; (ii) residual biofilm at 1 mm from the canal terminus. (c) manual-agitation group; (i) residual biofilm at 2 mm from the canal terminus; (ii) residual biofilm at 1 mm from the canal terminus. (d) Sonic agitation group; (i) residual biofilm at 2 mm from the canal terminus; (ii) residual biofilm at 1 mm from the canal terminus. (e) Ultrasonic agitation group; (i) residual biofilm at 2 mm from the canal terminus; (ii)residual biofilm at 1 mm from the canal terminus…...203

Figure 8.5: SEM images illustrate (ai) *E. faecalis* biofilm grown for 10 days. (aii) residual biofilm at 3 mm from the canal terminus after passive irrigation. (b) Passive irrigation group; (i) residual biofilm at 2 mm from the canal terminus; (ii) residual biofilm at 1 mm from the canal terminus. (c) manual-agitation group; (i) residual biofilm at 2 mm from the canal terminus; (ii) residual biofilm at 1 mm from the canal terminus. (d) Sonic agitation group; (i) residual biofilm at 2 mm from the canal terminus; (ii) residual biofilm at 1 mm from the canal terminus. (e) Ultrasonic agitation group; (i) residual biofilm at 2 mm from the canal terminus; (ii) residual biofilm at 1 mm from the canal terminus……208

Figure 8.6: TEM images illustrate (ai) *E. faecalis* biofilm grown for 10 days. (aii) residual biofilm at 3 mm from the canal terminus after passive irrigation. (b) Passive irrigation group; (i) residual biofilm at 2 mm from the canal terminus; (ii) residual biofilm at 1 mm from the canal terminus. (c) manual-agitation group; (i) residual biofilm at 2 mm from the canal terminus; (ii) residual biofilm at 1 mm from the lateral canal terminus. (d) Sonic agitation group; (i) residual biofilm at 2 mm from the canal terminus; (ii) residual biofilm at 1 mm from the canal terminus. (e) Ultrasonic agitation group; (i) residual biofilm at 2 mm from the canal terminus; (ii) residual biofilm at 1 mm from the canal terminus…....213

Figure 11.1: Images of DNA band of the 4 species used in the study on agarose gel stained with red gel stain. a) Bands of DNA ladder (L), *E. faecalis* positive control (efp), S*. mutans* positive control (smp), *E. faecalis* sample (ef), S. mutans sample (sm), *E. faecalis* negative control (efn), and S*. mutans* negative control (smn). b) Bands of DNA ladder (L), *fu. nucleatum* positive control (fnp), P*. intermedia* positive control (pip), *fu. nucleatum* sample (fn), P*. intermedia* sample (pi), *fu. nucleatum* negative control (fnn), and P*. intermedia* negative control (pin).……..……...263

Figure 11.2: SEM images of the Endo-Vu material surface. a. and b. before, c. and d. after autoclaving ……..……..….269

Figure 11.3: SEM images of the Polystyrene material surface. a. and b. before, c. and d. after autoclaving…….…….270

Figure 11.4: SEM images of the Photopolymer 3D material surface. a. and b. before, c. and d. after autoclaving……..……...270

Figure 11.5: SEM images of the Accura 3D material surface. a. and b. before, c. and d. after autoclaving……..……....271

Figure 11.6 SEM images of the Endo-VU material surface. a. and b. before, c. and d. after gas plasma sterilisation……..……..…….272

Figure 11.7: SEM images of the Polystyrene material surface. a. and b. before, c. and d. after gas plasma sterilisation……..……..…….272

Figure 11.8: SEM images of the Photopolymer 3D material surface. a. and b. before, c. and d. after gas plasma sterilisation…….……273

Figure 11.9: SEM images of the Accura 3D material surface. a. and b. before, c. and d. after gas plasma sterilisation……...…….273

List of tables

Table 2.1: Mean values (n = 3) of the zeta-potential of the dentine and substratum materials…….67

Table 2.2: One-Way ANOVA to compare the effect of water immersion on *E. faecalis* biofilm between dentine and biomaterial substrata (n=3 per group)…..……75

Table 3.1: Allocation of the root canal models……91

Table 3.2: ANOVA analyses compare the amount of residual biofilm or film (hydrogel, collagen) following 60 seconds irrigation (NaOCl, water) delivered into the root canal model (closed, open) (n = 3 per group)……..…103

Table 3.3: Generalized linear mixed models analyzing the effect of time on the area percentage of canal surface coverage with residual film or biofilm for each experimental group (n = 3 per group)……..……104

Table 3.4: Mean values of available chlorine (Total n = 18, n = 3 per group) of NaOCl before and after 60 seconds of irrigation of the organic film (hydrogel, collagen) or biofilm in the root canal models (closed, open)……...105

Table 3.5: Generalised linear mixed-model analysis for the effect of organic film or biofilm NaOCl irrigant interaction on the available chlorine of NaOCl (n = 3 per group)……..106

Table 3.6: Mean pH values (Total n = 18, n = 3 per subgroup) of NaOCl before and after 60 seconds of irrigation for organic film (hydrogel, collagen) or biofilm in root canal models (closed, open)……..……..….106

Table 3.7: Generalised linear mixed-model analysis for the effect of organic film or biofilm NaOCl irrigant interaction on the PH values of NaOCl (n = 3 per group)……..…..……107

Table 3.8: Number of samples required to achieve 90% power and 0.05 alpha per subgroups (biofilm, organic film) irrigated with NaOCl…….....107

Table 4.1: Repeated measure ANOVA analyzing the difference in the area percentage of slide surface coverage with residual material (biofilms, hydrogel, and collagen) over irrigation time (60 seconds) with irrigant (2.5% NaOCl, water) (n = 10 per group)……...……...120

Table 5.1: Mean values of the biofilm (%) covering the root canal surface before and after one-minute irrigation using different irrigants (5.25% NaOCl, 2.5% NaOCl, water) delivered using syringe and needle placed at 3mm or 2mm from the canal terminus at flow rate of 0.15 mL s-1 (n = 10 per group)…….……132

Table 5.2: Analysis of covariance (ANCOVA) comparing the mean amount of residual biofilm (%) remaining on the surface of the root canal, over time (1 to 60 seconds) of irrigation using three irrigants (5.25 % NaOCl, 2.5% NaOCl, and water) delivered by syringe and needle placed at 3 mm (group 1) from the canal terminus and at flow rate of 0.15 mL s^{-1} (Total n = 30, n = 10 per group)……133

Table 5.3: Analysis of covariance (ANCOVA) comparing the mean amount of residual biofilm (%) remaining on the surface of the root canal, over time (1 to 60 seconds) of irrigation using three irrigants (5.25% NaOCl, 2.5% NaOCl, and water) delivered by syringe and needle placed at 2 mm (group 1) from the canal terminus and at flow rate of 0.15 mL s^{-1} (Total n = 30, n = 10 per group)…….……...133

Table 6.1: Kruskal–Wallis analysis to compare the difference in the amount of residual biofilms covering the canal surface following passive or active irrigation time (30s) with 2.5% NaOCl irrigant (n = 10 per group)……..……147

Table 6.2: Generalized linear mixed model analysing the effect of time (second) on the amount of biofilm removed from the canal surface of each experimental group (n = 10 per group)……...……...148

Table 6.3: Kruskal–Wallis analysis analysing the effect of biofilm NaOCl irrigant interaction on the available chlorine (left) and pH (right) of NaOCl as dependent variables (n = 10 per group)……149

Table 7.1: Generalized linear mixed model analysis to compare the difference in the amount of residual biofilms (%) covering the lateral canal surface following passive or active irrigation time with 2.5 % NaOCl irrigant (n = 10 per group)…….……172

Table 7.2: Generalized linear mixed model analysing the effect of time (seconds) on the amount of biofilm removed from the lateral canal surface of each experimental group (n = 10 per group)……173

Table 8.1: Types of the bacterial strains used to create multi-species biofilm, their morphology, Gram staining and catalase reaction results……192

Table 8.2: Mean values of the biofilm (%) covering the root canal surface before and after one-minute of syringe irrigation followed by 30 seconds passive or active irrigation protocols (n = 10 per group)……..198

Table 8.3: Generalized linear mixed model analysis to compare the difference in the amount of residual multi-species biofilms (%) covering the canal surface following passive or active irrigation time with 2.5 % NaOCl irrigant (n = 10 per group)……..199

Table 8.4: Generalized linear mixed model analysing the effect of time (seconds) on the amount of multi-species biofilm removed from the canal surface of each experimental group (n = 10 per group)……..……..200

Table 8.5: Generalized linear mixed model analysis to compare the difference between single and multiple residual biofilms (%) covering the canal surface following passive or active irrigation with 2.5 % NaOCl irrigant (n = 10 per group)…..……..200

PUBLICATIONS

Saifalarab Mohmmed, Morgana E. Vianna, Matthew R. Penny, Stephen T. Hilton, Nicola Mordan, Jonathan C. Knowles (2016). A novel experimental approach to investigate the effect of different agitation methods using sodium hypochlorite as an irrigant on the rate of bacterial biofilm removal from the wall of a simulated root canal model. *Dental Material*, 32(10), 1289–1300.

Saifalarab Mohmmed, Morgana E. Vianna, Matthew R. Penny, Stephen T. Hilton, Nicola Mordan, Jonathan C. Knowles (2016). Investigation to test potential stereolithography materials for development of an *in vitro* root canal model. *Microscopy Research & Technique*, 80 (2), 202-210.

Saifalarab Mohmmed, Morgana E. Vianna, Matthew R. Penny, Stephen T. Hilton, Nicola Mordan, Jonathan C. Knowles (2017). Confocal laser scanning, scanning electron and transmission electron microscopy investigation of *Enterococcus faecalis* biofilm degradation using passive and active sodium hypochlorite irrigation within a simulated root canal model. *MicrobiologyOpen*, doi.org/10.1002/mbo3.455.

Saifalarab Mohmmed, Morgana E. Vianna, Matthew R. Penny, Stephen T. Hilton, Jonathan C. Knowles (2017). The effect of sodium hypochlorite concentration and irrigation needle extension on biofilm removal from a simulated root canal model. *Australian Endodontic Journal,* doi: 10.1111/aej.12203.

PRESENTATIONS

Saifalarab Mohmmed, Morgana E. Vianna, Jonathan C. Knowles. Investigation of the rate of bacterial biofilm or organic film removal by a sodium hypochlorite irrigant, delivered in open or closed simple anatomy root canal models. British Society of Dental Research Annual Conference 14th- 16th September 2015, Cardiff, UK.

Saifalarab Mohmmed, Morgana E. Vianna, Jonathan C. Knowles. Investigation into the effect of sodium hypochlorite irrigant concentration delivered by a syringe on the rate of bacterial biofilm removal from the wall of a simulated root canal model. 7th Global Dentists and Paediatric Dentistry Annual Meeting, March 31March – 01 April 2016, Valencia, Spain.

Saifalarab Mohmmed, Morgana E. Vianna, Jonathan C. Knowles. Investigations into the effect of sodium hypochlorite agitation on the rate of biofilm removal from a simulated root canal model. 15th Euro Congress on Dental & Oral Health Conference, 24 – 26 October 2016, Rome, Italy.

Saifalarab Mohmmed, Morgana E. Vianna, Jonathan C. Knowles. A comparative study of single and multi-species biofilm removal from the wall of a simulated root canal model by passive or active sodium hypochlorite irrigant. Research Away Day at UCL, 4th November 2016, London, UK.

Chapter 1
Introduction

1.1. Introduction

Apical periodontitis or periradicular periodontitis is an inflammatory lesion around the dental root caused mainly by bacteria (Nair, 1987). Bacteria adhere to solid surfaces (e.g. root canal) and rapidly form biofilms (Costerton *et al.*, 1999). Root canal treatment describes the dental procedure used to either prevent apical periodontitis by the treatment of diseased or infected soft tissue contained in the hollow space of the hard dental shell of the tooth, or the procedure used to resolve established apical periodontitis (European Society of Endodontology, 2006). Root canal treatment principally involves three subsequent steps: First, access opening preparation of the canal. Then the microbial control of the infected root canal system is achieved through chemo-mechanical debridement. Finally, the root canal system will be obturated (Cohen and Burns, 1998). Chemo-mechanical debridement includes instrumentation and irrigation. Instrumentation aims to give the canal system a shape that permits the delivery of locally used medications, as well as a root canal filling, which helps to trap remaining microbiota (Nair *et al.*, 2005).

The instruments used comprise conical wires (with sharp cutting edges) inserted into the canal orifice. From here, they penetrate the canal system, following a direction piloted by the tip. The pathway traversed by the instrument is clinically described as the “canal”. The parts of the canal system that do not come into contact with the instrument lie in the peripheral area of the pathway to varying extents. This peripherally placed anatomy may follow a pattern of direct continuity as a space that runs from the main canal or branch away from the pathway and

into the bounded but more restrictive blind-ending isthmi or lateral and accessory canals. As the instrument is rotated or reciprocated along its long axis to sculpt the inner canal surface with which it engages, the peripherally placed anatomy remains untouched (Peters *et al.*, 2001b). The peripherally placed surface can only be reached using a fluid that is delivered into the main canal, from where it may be introduced into the peripheral areas (Macedo *et al.*, 2014a). The use of a final irrigation regimen after the completion of chemo-mechanical canal preparation with high volumes of various chemically active solutions may contribute to improved debridement in the non-instrumented part of the root canal system (Ballal *et al.*, 2009).

The process of delivery for the irrigant introduced into the root canal system is called irrigation. Irrigation deals with how the irrigant flows, penetrates and its exchange with the stagnant body of fluid present in the root canal space. Irrigation aims to remove pathogenic microorganisms (microbiota) in the root canal system, especially in apical and peripherally placed anatomy (Macedo *et al.*, 2014a).

The irrigant is commonly delivered continually from a hand syringe through a needle. Sodium hypochlorite (NaOCl) is the most popular irrigating solution used worldwide (Baumgartner *et al.*, 1987) which showed antimicrobial activity against a broad spectrum of microorganisms (Harrison and Hand, 1981). However, the debridement action of an irrigant (e.g. NaOCl) within the root canal system may remain elusive when using a needle and syringe alone (Jiang *et al.*, 2012). This may be related to the low fluid velocity of irrigant delivered by the hand syringe. Consequently, there is little interaction between the irrigant and canal walls (Chen *et al.*, 2014). Attempts to improve the efficacy of irrigant penetration and irrigant mixing within the root canal system are therefore important (Druttman and Stock,

1989) since they may improve the removal of residual biofilm. Agitation may be applied to aid the dispersal of the irrigant into the root canal system (Macedo *et al.*, 2014a).

The outcome of the root canal treatment is dependent on the severity of the endodontic infection and size of periapical lesions (Sjögren *et al.*, 1997). However, it has been argued that disinfection of the root canal system by the irrigation procedure is the most crucial step of a successful root canal treatment, because it has a considerable effect on the complete elimination of root canal infection (Verhaagen *et al.*, 2012). Therefore, success of the root canal treatment may be enhanced by a better understanding of the nature of the interaction between the irrigant and bacterial biofilm within the root canal system.

In this chapter, a systematic insight into the literature that investigate some important aspects of the root canal treatment is presented, focusing on composition of the root canal microbiota, biofilm concept, fluid dynamics concept of irrigation, irrigant agitation, and models which have already been developed to investigate irrigant-bacterial biofilm interaction.

1.2. Literature review

1.2.1. Composition of the root canal microbiota and pathogenesis of apical periodontitis

It is well known that the microorganisms of the oral microbiota are present in a symbiotic balance with the human body (Fouad, 2009). When this relationship becomes altered, the bacteria colonise the tooth surface and rapidly form dental plaque, which is responsible for the development of caries and periodontal disease (McKee *et al.*, 1985). Microorganisms gain access to the root canal system through different routes (Bergenholtz TZ *et al.*, 1977): (1) through dentinal

tubules from a caries lesion; (2) through exposed pulp due to trauma or fracture; (3) through the apical foramen of a periodontal ligament. Initial pulp infection causes inflammation of the pulp tissue, which has been recognised as pulpitis which is either reversible or irreversible (Fouad, 2009). Both the innate and adaptive host immune systems will be operated to protect the pulp from microbial invasion. However, failure of the immune system to achieve complete clearance of the pulp from the microorganisms will cause pulp necrosis and development of apical periodontitis that is associated with bone destruction (Stashenko *et al.*, 1998). Although viruses (Li *et al.*, 2009) and fungi (Waltimo *et al.*, 1997) have been identified in the microbial community of root canal with periapical infection, bacteria are the most persistent microorganisms in endodontic disease (Siqueira and Rôças, 2008).

The causative relationship between bacteria and apical periodontitis was originally reported in relation to animal experimentation (Kakehashi *et al.*, 1965). Sundqvist (1976) consolidates the relation between bacteria and apical pathosis through human experimentation. He reported that bacteria could only be isolated from intact teeth with periapical pathosis and that infected root canal systems are dominated by obligate anaerobes. The number of bacterial species present in an infected root canal, identified using culture techniques, might vary from fewer than 10^2 to over 10^8 (Zavistoski *et al.*, 1980; Sundqvist, 1976). Commonly isolated species include *Streptococcus* spp. (facultative anaerobes), *Peptostreptococcus* spp. (anaerobes), *Fusobacterium nucleatum* spp. (anaerobes), *Eubacterium* spp. (anaerobes), *Lactobacillus* spp. (facultative anaerobes), *Actinomyces* spp. (facultative anaerobes), *Bacteroides* spp. (anaerobes) and *Prevotella* spp. (anaerobes) (Craig Baumgartner and Falkler, 1991; Sundqvist, 1976).

Microorganisms that initially invade and colonize the necrotic pulp tissue cause primary root canal infection, which is characterized as an opportunistic polymicrobial infection that predominantly comprises anaerobic bacteria. These observations have been made based on culture studies in humans (Sundqvist, 1976) and monkeys (Fabricius *et al.*, 1982). Möller (1966) showed in a human study that obligate anaerobes play an important role in root canal infection. In addition, he demonstrated the importance of antiseptic measures and transportation during sampling procedures in the root canals. It has been suggested that the reason for the higher proportion of anaerobes to facultative anaerobes is due to the fact that oxygen decreases when the blood supply in the infected root canal system is inhibited or suppressed (Sundqvist, 1994). It has been shown that anaerobes are more likely to be found in the apical third of the root canal system where they might be protected against salivary oxygen. This oxygen might either be consumed quickly by the facultative aerobes, which prevail in the coronal part, or simply fail to diffuse to the apex (Thilo *et al.*, 1986). The exact proportion of anaerobic to facultative species has been found to depend on the clinical environment of the teeth, as well as their position within the root canal system being microscopically examined or from which the sample was taken. It has been suggested that in carious teeth, about 70% of the infection in the apical 5 mm of the canal is predominantly anaerobic in nature (Craig Baumgartner and Falkler, 1991), whereas in intact teeth the infection is composed of 90% anaerobes (Sundqvist, 1992). The inconsistency in observation may be due to the variation in the condition of teeth examined as carious teeth that have been exposed to the oral environment, and may prefer the growth of facultative bacteria (Craig Baumgartner and Falkler, 1991).

Considering intact teeth, the closed environment may permit the growth of obligate anaerobes (Sundqvist, 1976). Nevertheless, Chugal *et al*. (2011) reported approximately the same results for the percentages of the obligate anaerobe bacteria, in carious (68.9%) and intact pulp teeth (68.5%).

Maintenance of asepsis using a combination of chemo-mechanical and optimal obturation, as well as coronal restoration, presents a favourable long-term treatment outcome. However, an unfavourable outcome can sometimes occur with the presence of persistent or secondary intraradicular infection (Siqueira *et al.*, 2002; Nair *et al.*, 2005). Microorganisms that survive in the canal after treatment can cause secondary infections of the root canal system. *Enterococcus faecalis* is an important pathogen in persistent root canal infections, for their presence in teeth with post-treatment infection (Mejare, 1974; Sedgley *et al.*, 2004). With the innovation of molecular techniques, investigations based on the polymerase chain reaction (PCR) have found that *E. faecalis* is again the dominant species in cases of root-filled teeth associated with periradicular lesions (Rôças *et al.*, 2004; Stojanović *et al.*, 2014). The PCR technique uses a specific Taq polymerase enzyme (thermostable DNA polymerase) to amplify a small fragment of DNA by approximately one million times, allowing the detection of bacteria (Mullis *et al.*, 1994). A possible explanation for the persistence of *E. faecalis* may be their capacity to endure prolonged periods of starvation (Figdor, 2004), high pH environment (Evans *et al.*, 2002), immune response of the host (Fabricius *et al.*, 1982), and ability to penetrate dentinal tubules (Love, 2001). More recently, a pyrosequencing method for high throughput DNA sequencing has been introduced. This is based on the detection of pyrophosphate (PPi) release during DNA synthesis (Ronaghi *et al.*, 1996). Based on this method, both

the unanticipated bacterial diversity and the most dominant microbial taxa have been examined in the apical part of the infected root canals. The findings demonstrate a marked inter-individual variability in the composition of apical bacterial communities (Siqueira Jr *et al.*, 2011).

In an infected root canal, bacterial species are present either as suspended (planktonic) cells (Costerton *et al.*, 1995) or as a community of condensed bacterial layers on the canal walls (Nair, 1987). These bacterial communities are known as a biofilm (Costerton *et al.*, 1999).

1.2.2. The biofilm concept

Biofilms contain colonies of aggregated bacterial cells attached to a solid substrate and each other, and which are embedded in an extracellular polymeric matrix (EPS) (Costerton *et al.*, 1995). This matrix is composed of highly hydrated polysaccharides and other molecular substances, mainly water, lipids, proteins, and nucleic and amino acids (Millward and Wilson, 1989; Wilson, 1996). Lawrence *et al*. (1991) identified the presence of water channels within the matrix that allow for the transportation of nutrients and waste products.

The first serious discussions and analyses of the communities embedded in an extracellular matrix of their origin, and attached to the surface of the dentinal tubules emerged by Nair (1987). These bacterial colonies are now known as endodontic biofilms. The author used a light microscope and a transmission electron microscope to examine the apical 5 mm of root canals of 31 carious teeth with periapical lesions. He suggested that the bacterial layers consisted of an aggregation of rods, cocci, spirochaetes, and filaments and its structure was similar to the dental plaque on human tooth surfaces. Richardson *et al*. (2009) examined the distribution of the root canal biofilm in extracted teeth associated

with apical periodontitis using three microscopy techniques (scanning electron microscope, light microscope, and transmission electron microscope). He reported the presence of bacterial biofilms in the form of patches that run along the length of the canal walls. It has been shown that biofilms in human extracted teeth that exhibit apical periodontitis consist of multiple layers of different bacterial cells and form in varying thicknesses, with thicker biofilms occurring on the coronal third and thinner biofilms on the apical third (Rojekar *et al.*, 2006).

1.2.3. Formation of biofilm

Microbial film formation comprises three stages whereby bacterial cells floating in a fluid medium attach to biomaterial (natural or synthetic) surfaces (Marshall *et al.*, 1971) (Figure 1.1). The first stage involves surface conditioning (Korber *et al.*, 1995). Here the adsorption on the solid surface of organic and inorganic molecules from tissue fluids such as saliva leads to the formation of a conditioning layer (Love, 2010). An example of this layer is that of the “acquired pellicle”, which develops on tooth enamel surfaces and enhances the attachment of *streptococcus* species which represent the primary colonising species (Diaz *et al.*, 2006). The conditioning layers serve as receptors for the bacterial cell, which may colonize pellicle-conditioned surfaces within hours since these layers alter the physical/chemical properties of the surface such as hydrophobicity (Gibbons and Van Houte, 1971). It has been urged that the conditioning layers play an important role in the initial attachment of the bacterial cell (Suwarno *et al.*, 2016) as these layers effectively reverse the charge of the surface to positively charged proteins and promote the attachment of planktonic microbial cells (Donlan, 2002). The second stage includes adhesion and co-adhesion of bacterial cells to the surface. The initial adhesive potential of microbial cells to natural (e.g. dentine)

or synthetic (for example; glass & plastic) includes a process of three-phases (Derjaguin and Landau, 1941). The initial phase of the bacteria–substrate interaction is determined by the physical and chemical properties (e.g. surface free energy. zeta-potential, hydrophobicity) of the substrate surfaces. This reversible interaction is followed by the second phase of molecular-level nonspecific interactions between the bacterial surface structures and the substrate (Verwey *et al.*, 1999). Surface structures of bacterial cells include fimbrae, pili, and flagella (Tomaras *et al.*, 2003).

In the final phase, a more specific bacterial adhesion to the substrate is established by producing polysaccharides that connect with surface materials and/or receptor-specific ligands located on surface structures.

The last stage includes bacterial cell growth and biofilm extension. The primary colonizing species stick to each other or different species (secondary colonizing species) forming aggregates on the substratum, and give rise to the final structure of biofilm. During this stage, microbial cells exhibit proliferation and detachment (Leung *et al.*, 1998).

In general, the initial bacterial adhesion can be illustrated by Derjaguin, Landau, Vervey, and Overbeek (DLVO) theory (Derjaguin and Landau, 1941) of calculating the interaction energy between cells and substrate as a function of separation distance (Doyle, 2000). Adhesion can be mediated by non-specific interactions, including Van der Waals forces, electrostatic forces, and acid-base interactions forces (Van Oss, 1995). As soon as microorganisms reach a surface, they are either attracted to, or repelled by it, depending on the sum of the different non-specific interactions (Fonseca *et al.*, 2001). Hydrophobic interactions and

surface free energy (SFE) are usually the strongest of all long-range forces (Teixeira and Oliveira, 1999).

After the attachment of bacterial cells to the root canal surface, inter-bacterial co-aggregation occurs among distinct bacteria cells. Co-aggregation is a specific cell-to-cell process that occurs between genetically distinct cell types. Co-aggregation alters the surface environment, offering additional binding sites to other potential members of the biofilm community (Blehert *et al.*, 2003).

An important aspect of biofilm development involves dynamic metabolic processes since the accumulation of microorganisms in the developing biofilm greatly depends on nutrition and oxygen. Microorganisms form a community when the resources of energy and oxygen are sufficient (Chalmers *et al.*, 2008). The sources of nutrition are derived from food (sugar), saliva, gingival crevicular fluid, and host tissue (for example, dead pulp tissue). The metabolic processes associated with biofilm development involve three stages. These are, first, the metabolism of the carbohydrates obtained, second, protein hydrolysis and the metabolism of any remaining carbohydrates, and finally, protein degradation, the fermentation of products derived from amino acids and the catabolism of complex host molecules (Ter Steeg and Van Der Hoeven, 1990).

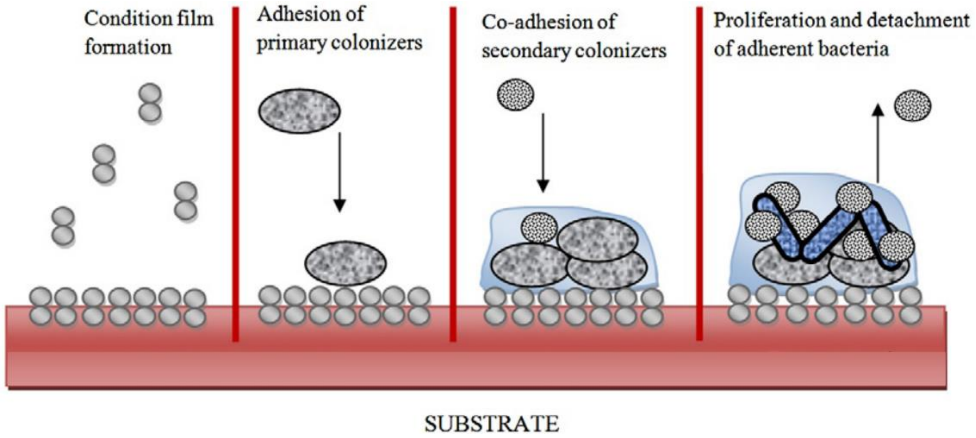

Figure 1.1: Schematic diagram illustrating the stages of biofilm formation. [Adapted from Kishen and Haapasalo (2010)].

1.2.4. Resistance of biofilm to antimicrobial agent

Compared to the development in planktonic form, a biofilm has its own mechanisms for resisting the antimicrobial agent (Brown and Gilbert, 1993). Biofilm resistance to antimicrobial agent has been recognised as a considerable hindrance to successful root canal treatment (Al-Ahmad *et al.*, 2014). This section describes a variety of mechanisms that are related to antimicrobial resistance of the biofilm.

1.2.4.1. Extracellular polymeric substance matrix

The protection role of the extracellular polymeric substance (ESP) is attributed as one of such mechanisms (Flemming *et al.*, 2007). Several studies have been performed that examine the diffusion of the antimicrobial agent through biofilms which showed that the EPS matrix has the ability to act as an impermeable barrier that limits antimicrobial penetration, thereby protecting the biofilm cells (Lawrence *et al.*, 1991; Donlan, 2002; Flemming *et al.*, 2007). This is known as the viscoelastic property of the EPS that acts as protection from chemical and mechanical stress (Stewart and Franklin, 2008). When placed under minor stress a biofilm can be deformed elastically, whereas when placed under intense stress it is able to flow viscously (Flemming *et al.*, 2007). In addition, with disinfectant action, the bacteria at the top of the liquid–biofilm interface die because of their direct exposure to the antimicrobial action, while the bacteria embedded deep inside the biofilm are capable of surviving. Such protection may be due to the direct binding of antibiotics by the EPS matrix, since the biofilm matrix can bind and isolate toxic antimicrobial peptides and positively charged antibiotics (for example, aminoglycosides) (Nichols *et al.*, 1988). However, for many antimicrobial agents the EPS matrix provides little or no barrier to penetration

.Therefore, the resistance mechanism of EPS to antibiotics might not present a general mechanism of protection (Donlan, 2002).

1.2.4.2. Extent of antimicrobial agent penetration

Another mechanism that gives a reason for biofilm resistance is the decline of the antimicrobial agent to penetrate the biofilm as a result of a reaction-diffusion interaction (Stewart and Franklin, 2008). The proportion of diffusing agent in the biofilm depends on its type (Anderl *et al.*, 2000), concentration, and time of exposure (Nichols *et al.*, 1988). Nonetheless, the diffusion reduction of the agent is not the only reason for biofilm resistance. For instance, ampicillin and ciprofloxacin penetrate *Klebsiella pneumoniae* biofilm, but fail to eradicate it. This demonstrates that other resistance mechanisms may be involved (Anderl *et al.*, 2000).

1.2.4.3. Mature biofilm

Resistance of generated biofilms over time has been intensively explored. For instance, Wang *et al.* (2012) compare the disinfectant effects of three agents (2% NaOCl, 6% sodium NaOCl, 2% chlorhexidine (CHX), and QMiX) on 1 day and 3 weeks old *E. faecalis* biofilms. The study showed that young biofilm was more sensitive to all medicaments, and bacteria were more easily killed than in old biofilm. It has been urged that the biofilms become increasingly resistant to antibacterial agents between 2 and 3 weeks (Stojicic *et al.*, 2013). However, another study suggested the biofilm resistance is inherent and it is possible to generate mature wild bacterial biofilm (*Pseudomonas aeruginosa*) after 5 days incubation (Klausen *et al.*, 2003).

1.2.4.4. Persister cells

The formation of persister cells is another mechanism of antibiotic resistance (Dufour *et al.*, 2010). Persister cells undergo delayed mitosis and therefore exhibit behaviour below the threshold of antimicrobial activity (Lewis, 2006). Persister cells are not antibiotic-resistant mutants but rather phenotypic variants of the bacterial population of genetically identical cells (Levin and Rozen, 2006). It has been reported that persister cells exhibited tolerance to disinfectant agents (Lewis, 2010).

1.2.4.5. Microbial diversity of the biofilm of infected root canals

The role of microbial diversity in enhancing the resistance of biofilms to antimicrobial agent has been identified in previous studies (Leriche *et al.*, 2003; Burmølle *et al.*, 2006; Kara *et al.*, 2006). For example, Burmølle *et al.* (2006) examine the difference in resistance to disinfectant between single species biofilms of four isolates (*Dokdonia donghaensis, Shewanella japonica, Microbacterium phyllosphaerae* and *Acinetobacter lwoffii*) and multi-species biofilm (different combinations). The result showed increased resistance to disinfectant agents of multi-species biofilm than of single species biofilm. This finding has been ascribed to the synergic behaviour of bacterial community of the biofilm permitting protection upon exposure to disinfectant. In comparison, Whiteley *et al.* (2001) reported that the synergic effect exhibited between bacteria of multi-species biofilm did not enabling survival upon exposure to antimicrobial agents. Therefore, cooperative behaviour does not necessarily increase the resistance of the biofilm. It seems that more investigations are required to explain the resistance of multi-species biofilm. Based on next-generation sequencing technique, which describe a DNA sequence mixtures, it has been identified the

heterogeneous aetiology and diversity of bacterial biofilms of the periapical disease (Siqueira Jr *et al.*, 2016).

Periapical disease is a biofilm-mediated inflammation and the elimination of bacterial biofilm from the root canal system remains the primary focus of its management (Ricucci *et al.*, 2009). The mechanism of biofilm removal depends on the effectiveness of endodontics treatment, which aims to eliminate the cause of inflammation (Torabinejad and Walton, 2009).

1.2.5. Role of root canal treatment in management of an intracanal biofilms

To maintain asepsis of the root canal system or to adequately disinfect it, three subsequent steps that comprise the root canal treatment should be effectively performed (European Society of Endodontology, 2006). The first step is mechanical intracanal preparation, which includes establishment of access opening through the occlusal surface of the tooth to the root canal system as well as the shaping of the canal wall surfaces using rigid metal instruments (Cohen and Burns, 1998). Traditionally, the intracanal preparation has been considered an essential means to reduce the bacterial load within the root canal system (Bystrom and Sundqvist, 1981; Stewart, 1955). Yet, it has been suggested that the role of mechanical intraradicular preparation is shifted away from debridement towards an extension to the access opening, which is known as radicular access (Gulabivala and Ng, 2014). This could be attributed to the complex anatomy of the root canal system where more than half of the canal walls may remain untouched by the metal instruments following mechanical preparation (Peters *et al.*, 2001b). Accordingly, the next step of the root canal treatment which is chemical intracanal preparation is regarded as a crucial stage

to achieve the maximum removal of biofilms from the root canal system (Siqueira *et al.*, 2000). This step is achieved by the irrigation procedure using an irrigant solution of antibacterial action with optimum concentration and volume to provide continued chemical efficacy (Kishen, 2010). To ensure degradation of the residual biofilm from the root canal system, inter-appointment use of chemical medication (e.g calcium hydroxide) has been recommended (Vera *et al.*, 2012). The final step following mechanical and chemical preparation is root canal obturation, which is achieved through sealing and obturation of the root canal system (Cohen and Burns, 1998). The purpose of this stage is to prevent the reinfection and promote the healing of the inflamed periapical tissue (Torabinejad and Walton, 2009).

1.2.6. Root canal irrigation solutions

The irrigation solution should provide optimum properties to fulfil the role of maximum cleaning efficacy and biofilm elimination from the root canal system along with minimum side effects. These properties are: (a) technically, provide lubrication of instruments used in mechanical preparation (Grossman, 1955); (b) chemically, inactivation of bacteria through a broad antimicrobial action against different species colonized in biofilms (Spratt *et al.*, 2001), and deactivation of bacterial endotoxin (Gomes *et al.*, 2009); (c) physically, allow the flow of the irrigant throughout the root canal system in order to detach the biofilm structures and loosen/flush out the debris from the said system (Kishen, 2010); (d) the irrigant should be biocompatible, not irritant, and non-toxic to periapical human tissues (Hülsmann *et al.*, 2003).

There is a myriad of research regarding investigations of the use of different solutions as root canal irrigants. Despite compatibility of both water and normal

saline, both solutions in conjunction with instrument debridement are not enough to render root canals free of pulp tissue, debris, and bacterial biofilm (Basrani and Haapasalo, 2012). A number of antibacterial agents were used as irrigants and their efficacy was tested. For example, Sodium hypochlorite (NaOCl) (Byström and Sunvqvist, 1985), chlorhexidine gluconate (CHX) (Ercan *et al.*, 2004; Abdullah *et al.*, 2005), Ethylenediaminetetraacetic acid (EDTA) (Bystrom and Sundqvist, 1981; Baumgartner *et al.*, 1987), a mixture of doxycycline, citric acid, and a detergent MTAD (Torabinejad and Walton, 2009), povidone iodide (Abdullah *et al.*, 2005). Although all antibacterial agents exhibit a variety of efficacy within the root canal system, NaOCl remains the most effective antimicrobial irrigant and fulfils most of the above mentioned properties of an ideal root canal irrigation solution (Estrela *et al.*, 2002). The mechanism of action of an irrigant (e.g. NaOCl) within the root canal system depends on its physical and chemical action during root canal irrigation (Kishen, 2010).

1.2.7. Physical and chemical efficacy of NaOCl in root canal treatment

Sodium hypochlorite is a non-specific oxidising agent (Siqueira *et al.*, 1997). In addition to the lubricant action for endodontic instruments, NaOCl has the merit of dissolving the capacity of the organic tissue, and the organic component of the smear layer (Estrela *et al.*, 2002). Another merit related to its antimicrobial action is through a wide-spectrum non-specific bactericidal and fungicidal ability (Akay *et al.*, 2016). Both these merits are related to both pH contributed by hydroxyl ions (OH^-) and available chlorine represented by hypochlorite ion (OCl^-) and hypochlorous acid ($HOCl^-$) (Estrela *et al.*, 2002).

Sodium hypochlorite was reported to exist in water in a dynamic equilibrium (Pecora *et al.*, 1998). This equilibrium is presented in the equation 1 below:

$$NaOCl + H_2O \leftrightarrow NaOH + HOCl \leftrightarrow Na^+ + OH^- + H^+ + OCl^- \quad \text{..... (1)}$$

The equation shows that Na^+ and the hypochlorite ions (OCl^-) are in an equilibrium with hypochlorous acid (HOCl) (Estrela *et al.*, 2002). Both OCl^- and $HOCl^-$ of the NaOCl are responsible for the antimicrobial action of NaOCl and they are called the active moieties because they are responsible for the inactivation of bacteria by chlorine releasing agents. The active chlorine gas (Cl_2) is a strong oxidizing agent that is responsible also for the antimicrobial action. It inhibits bacterial enzymes by irreversible oxidation of the sulfhydryl groups (–SH) of bacterial essential enzymes (cysteine), therefore disrupting the metabolic function of bacteria (Moorer and Wesselink, 1982; Siqueira *et al.*, 1997). In addition, the tissue-dissolving capacity of NaOCl is related to the available chlorine (de Macedo, 2013).

As soon as NaOCl contacts organic tissue, the following reactions occur, saponification, amino acid neutralisation, and chloramination (Kandaswamy and Venkateshbabu, 2010).

Sodium hypochlorite degenerates fatty acids (equation 2) into fatty acid salts (detergent) and glycerol (alcohol) (Estrela *et al.*, 2002) resulting in the dissolution of organic matter (Estrela *et al.*, 2002). Consequently, a reduction in the surface tension of the solution takes place, because of the detergent (Spanó *et al.*, 2001).

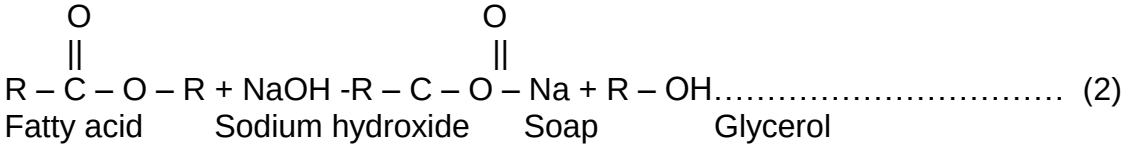

NaOCl neutralises the amino acids (equation 3), which results in the formation of salt and water. The reaction causes consumption of hydroxyl ions (OH^-) and therefore the pH is reduced (Spanó *et al.*, 2001; Estrela *et al.*, 2002).

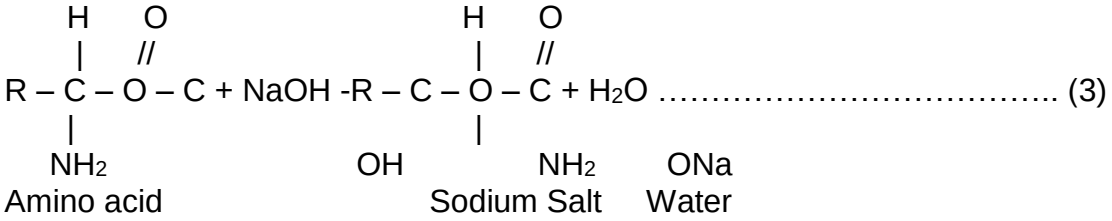

The available chlorine of NaOCl releases and combines with the amino group NH (equation 4) of the protein through chloramination reaction and forms chloramines (Spanó *et al.*, 2001). The degradation of protein interferes with cell metabolism.

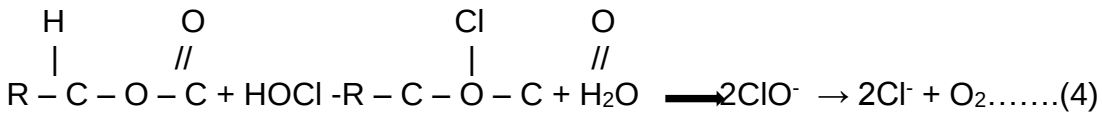

Bacterial destruction by the chemical effect of the NaOCl depends on its type and concentration (Macedo *et al.*, 2010), the surface area of contact (Moorer and Wesselink, 1982), and the duration of interaction between the irrigant and the infected material (Spratt *et al.*, 2001; Ragnarsson *et al.*, 2014). Once delivered into the root canal, NaOCl reacts with its organic content such as pulp, biofilm, or organic part of dentine (canal wall, smear layer, or debris). The protein degradation triggered by the active chlorine ions of NaOCl (Estrela *et al.*, 2002) causes depletion of freely available chlorine (Baker *et al.*, 1975) and changes in pH (Jungbluth *et al.*, 2011). Both the concentration and exposure time of NaOCl to organic content influence the chemical efficacy of NaOCl (Macedo *et al.*,

2014b). However, it has been shown that a 1% NaOCl irrigant can retain its chemical activity in the root canal for an extended period of between 10 and 100 minutes (Ragnarsson *et al.*, 2014).

The physical effect of the irrigant is to generate shear stress on the canal wall through fluid flow (Boutsioukis *et al.*, 2010a). Sodium hypochlorite provides a flushing capacity against the attached biofilm through the physical action that acts in synergy with the chemical action (Cunningham *et al.*, 1982). However, the dominated viscous environment of NaOCl as well as the confinement of the root canal system may hinder the flushing action of NaOCl (Verhaagen *et al.*, 2012).

An attempt has been made to increase NaOCl penetration by adding a surfactant, which enhances wetting properties (Abou-Rass and Patonai, 1982). Surfactants diffuse in liquid and adsorb at liquid/air interfaces, so that the surface energy of the liquid is reduced water and its wettability property is increased (Bukiet *et al.*, 2012). However, it has been reported that the addition of surfactant to NaOCl may accelerate the consumption of available chlorine of NaOCl solutions (Nouioua *et al.*, 2015).

It is also worth noting that effective delivery, mixing, and replacement of irrigant require a full understanding of the fluid dynamic of the irrigant within the confinement of the root canal system (Gulabivala *et al.*, 2010).

1.2.8. Fluid dynamics concept of irrigation

In fluid dynamics, two main types of flow exist: (1) laminar flow, characterized by smooth and constant fluid motion; and (2) turbulent flow which has chaotic eddies and vortices (Munson *et al.*, 1990). The type of flow is related to the Reynolds number (Re); a dimensionless number quantifying the relative importance of

inertial and viscous forces (Guyon, 2001). In the case of a root canal system, similar to a tube, Re is presented in the equation (5):

$Re=PVD/\mu$…….. (5)

Where: p is the fluid density (kg m^{-3}); v is the fluid velocity (m s^{-1}); D is the root canal diameter (mm); μ is the fluid dynamic viscosity (Pa s or kg s^{-1} m^{-1}).

As there is a relation between the Reynolds number (Re) and fluid viscosity, the Re factor must be taken into account when assessing the fluid dynamics of the irrigant in a root canal system. At low Reynolds numbers, viscous forces are dominant leading to laminar flow, whereas at high Reynolds number, inertial forces are dominant leading to turbulent flow (Holman, 2002). Theoretically, turbulent flow may be associated with higher wall shear stress, and possibly better biofilm disturbance.

During irrigation within the root canal system, fluid flow generated by injection via a needle and syringe tends to be laminar between the canal walls and needle (Boutsioukis *et al.*, 2009). The laminar flow may not exert enough shear stress and therefore be unlikely to affect biofilm removal (Gulabivala *et al.*, 2010). In addition, analysis of the fluid mechanics shows that fresh irrigant injected into the root displaces the resident irrigant just below the end of the point of injection (van der Sluis *et al.*, 2010).

Mixing of new irrigant and the liquid within a root canal can be achieved through two ways (Paz *et al.*, 2015). First, without flow that is called diffusion (the average of the random motions of molecules from high to low concentration of the fluid), which takes a long time of the active irrigant. Second, with flow that is called advection (constituent of the fluid is carried along with the fluid), which is confined only to the upper reaches of the main canal if only the injection is relied upon

(Gulabivala *et al.*, 2010). However, effective irrigant flow at the periphery of the root canal system (e.g. apical end, isthmi or lateral and accessory canals) may not be achieved by needle and syringe alone, which may be attributed to the effect of increased viscosity and canal confinement on fluid dynamics. Therefore, an attempt to increase the fluid flow within the root canal system is important, as this may improve the efficacy of irrigant flow and irrigant mixing within the root canal system (Gu *et al.*, 2009). Consequently, it may improve the removal of residual biofilm.

In previous studies on fluid dynamics of an irrigant within the root canal system, the extent of penetration was assessed using either digital radiograph and hypaque solution (Bronnec *et al.*, 2010), or thermal image analysis (Hsieh *et al.*, 2007). These methods may be considered as the initial attempts to develop our knowledge about irrigation flow. However, they have their own limitation that the evaluation was relatively difficult and the ability of radiographs to detect the exact penetration was poor (Salzgeber and Brilliant, 1977). In recent years, there has been an increasing interest in flow visualization using transparent root canal models and a high-speed camera combined with particle imaging velocimetry (PIV) (Matsumoto *et al.*, 2011; Layton *et al.*, 2015). Other researchers used computational fluid dynamics (CFD) (Gao *et al.*, 2009; Boutsioukis *et al.*, 2009; Shen *et al.*, 2010a), which is a branch of fluid dynamics that are utilised to solve and analyse various problems related to fluid flow by means of a computer simulation and mathematical modelling of the flow pattern (Anderson and Wendt, 1995). Based on high-speed imaging and CFD experiments, the irrigant flow at the apical part is reduced to a degree that it interferes with irrigant replacement (Boutsioukis *et al.*, 2010b; Verhaagen *et al.*, 2012). Although CFD represents a

powerful tool to measure the velocity, pressure, and flow rate of the irrigant solution, it has a limitation that it lacks the capability to examine the antimicrobial action of the irrigants (Layton *et al.*, 2015).

1.2.9. Factors influencing the penetration of an irrigant within the root canal system

Two phenomena are inherent to irrigant apical penetration in the confined space of a closed root canal system: (1) the stagnation of the irrigant flow beyond the irrigation needle tip (Ram, 1977; Goode *et al.*, 2013); and (2) the gas bubbles or vapour lock effect ahead of the advancing front of the irrigant (Tay *et al.*, 2010).

Ram (1977) identifies the stagnation plane of the irrigant beyond which the irrigant cannot penetrate and does not replace the radio-opaque solution in the apical half of most canals. The presence of this area beyond the needle, which cannot be replenished with fresh irrigant, also represents a constant finding, regardless of the different flow rates in a canal model (Boutsioukis *et al.*, 2009). The aim is therefore to move the stagnation plane to coincide with the level of instrumentation and allow for the optimal delivery of the irrigant at this level (Gulabivala *et al.*, 2010).

Recently, concern has been expressed about the possible presence of gas bubbles in the apical part of the root canal during irrigation (Parente *et al.*, 2010; de Gregorio *et al.*, 2010). These bubbles are described as the ‘vapour lock effect’. It has been reported that these bubbles are related to the closed channel behaviour of the root canal system, which results in gas entrapment at the apical third during the irrigation regimen and may interfere with irrigant penetration at the end of the root canal system (Tay *et al.*, 2010). However, such observations are unsatisfactory for an explanation of the effect of bubbles on the efficacy of

the irrigant to remove bacterial biofilm since the aforementioned study focuses on the removal of debris. The effect of a vapour lock can be reduced by the brief insertion of the needle to the working length while irrigating at a low flow rate without changing the needle's position (Boutsioukis *et al.*, 2014).

1.2.10. Overcoming the problems of irrigant penetration

Many factors have been considered with the aim of overcoming irrigant penetration. These factors include:

(1) The final taper and size of the prepared canal (Ram, 1977; Boutsioukis *et al.*, 2010a; Bronnec *et al.*, 2010);

(2) The size and design of the needle used for irrigation (Sedgley *et al.*, 2005);

(3) The flow rate of the irrigant (Q) (Boutsioukis *et al.*, 2007);

(4) The volume of irrigant (V) (Boutsioukis *et al.*, 2009).

During root canal irrigation, both the apical diameter and degree of the root canal taper facilitate the placement of the irrigation needle to within 1-2 mm of the end of the working length (Boutsioukis *et al.*, 2009).

Larger size preparations provide better apical exchange of the irrigant (Boutsioukis *et al.*, 2010a). Consequently, larger canal tapers allow for a better flushing action (Huang *et al.*, 2008). However, the disadvantages of a larger dimension and taper of the root canal system include an undesirable deviation from the original shape of the canal, a weakening of the root, and procedural complications such as ledge formation, transportation, and perforations (Adorno *et al.*, 2009). In addition, further enlargement does not provide any additional benefit during root canal treatment. Moreover, it has been suggested that enlarging small canals beyond an apical size of 30 with a 0.05/0.06 taper may not yield a higher probability of periapical healing (Ng *et al.*, 2011).

The apical penetration of an irrigant never exceeds a depth of 1 mm to 1.5 mm beyond the needle tip (Boutsioukis *et al.*, 2007). Thus, the use of a relatively small diameter needle (gauge 27, 30) during root canal irrigation is recommended since small gauge needles are able to penetrate deeper into the root canal system (Boutsioukis *et al.*, 2007). Consequently, irrigant penetration and biofilm removal are improved (De Moor *et al.*, 2014). However, the disadvantages of using small needles may include breakage or blockage (Walters *et al.*, 2002). In addition, finer needles require increased effort when injecting the irrigant. Consequently, the possibility of operator fatigue is higher in the delivery of optimal irrigation volume and duration when compared to a larger needle size (Shen *et al.*, 2010a). The side-opening needle has been found to improve flow and remove the hydrogel biofilm simulant in the area adjacent to the side hole (Verhaagen *et al.*, 2012). It has been shown that irrigant replacement in front of open-ended needles is greater than for close-ended needles, although higher apical pressure may be considered a disadvantage of open-ended needles (van der Sluis *et al.*, 2010).

A key variable during irrigation is the rate of irrigant delivery. The flow rate of the irrigant is determined by the pressure difference between the barrel of the syringe and the root canal. Flow rate rather than intra-barrel pressure should be regarded as the factor that influences flow beyond the tip of the needle (Boutsioukis and Kishen, 2012). A greater volume of irrigant has been reported to increase the debridement efficacy of the irrigant (Huang *et al.*, 2008).

The debridement action of an irrigant within the root canal system may remain elusive when using a needle and syringe alone (Jiang *et al.*, 2012). Agitation may be applied to aid the dispersal of the irrigant into the root canal system, especially into the peripheral area (Macedo *et al.*, 2014a). Agitation techniques for root canal

irrigants include either manual agitation (Cecic *et al.*, 1984; Druttman and Stock, 1989; Huang *et al.*, 2008) or automated agitation (Sabins *et al.*, 2003; Cunningham *et al.*, 1982).

1.2.11. Agitation of irrigant solution

Agitation techniques for root canal irrigants include either manual dynamic agitation (Cecic *et al.*, 1984; Druttman and Stock, 1989; Huang *et al.*, 2008; Sabins *et al.*, 2003; Cunningham *et al.*, 1982) or automated agitation (Cunningham *et al.*, 1982; Sabins *et al.*, 2003).

Manual dynamic agitation (MAD) of the irrigant could be achieved by using a file (Bronnec *et al.*, 2010) or a taper gutta-percha cone (Huang *et al.*, 2008). It is achieved by moving the master file or gutta-percha cone up and down in short strokes within an instrumented canal that cause the displacement of the irrigant apically and coronally (Jiang *et al.*, 2012). It has been suggested that MAD was more effective in removing stained collagen film (Huang *et al.*, 2008) than syringe irrigation and pulsating injection systems (RinsEndo) (McGill *et al.*, 2008). MAD has been recommended as a method of irrigant agitation for its simplicity and cost-effectiveness (Huang *et al.*, 2008). However, it has been argued that manual agitation might cause apical extrusion (Parente *et al.*, 2010). Furthermore, dentists might find this method needs both effort and time. Therefore, attempts have continually been made to develop faster agitation systems for root canal irrigation. For instance, sonic and ultrasonic agitation devices (Sabins *et al.*, 2003). These devices allow oscillation of their tips in a way which provides irrigant penetration throughout the root canal system (Verhaagen *et al.*, 2014b).

Sonically activated instruments are driven with a frequency range of 1-6 kHz (Tronstad *et al.*, 1985). The EndoActivator system is a sonic device with a

cordless electrically driven handpiece (Ruddle, 2007). The device has working frequencies of 160, 175, and 190 Hz, which are based on the measurement of the putative frequency of the device (Jiang *et al.*, 2010). The instrument was designed to use polymer tips of various sizes (ISO size 15, 25, 35) and tapers (0.02, 0.04) (Ruddle, 2007). Brito *et al* (2009) used colony-forming units (CFUs) to examine the reduction in bacterial load by conventional and EndoActivator irrigation protocols and they found no superiority of any of the protocols. Pasqualini *et al* (2010) apparently contradicted this observation, as they reported that EndoActivator was more effective than needle irrigation in reducing bacterial population. More recently, Chatterjee *et al* (2015) showed that sonic agitation with EndoActivator was more efficient than manual dynamic agitation and conventional needle irrigation in removing bacteria from the root canal system.

In ultrasonic agitation, a tip oscillates at frequencies of 25 to 30 kHz in a pattern of motion consisting of nodes and anti-nodes along its length (Weller *et al.*, 1980). A randomized controlled trial (RCT) by Liang *et al.* (2013) compared the outcomes of a root canal treatment of 86 single-rooted teeth using 5.25% NaOCl syringe irrigation with and without ultrasonic agitation. All selected teeth showed radiographic evidence of periapical lesion. The results indicated differences in the reduction and absence of apical lesion following the use of syringe irrigation with ultrasonic agitation (95.1%) compared to syringe irrigation alone (88.4%). However, the differences were statistically not significant. RCT is necessary for documentation of performance as it provides the clinician with evidence-based strategies for effectively treating root canal lesion. Nevertheless, the major limitations of this study are those related to the root canal treatment itself (Ng *et al.*, 2011). For instance, the difficulty to standardise the root canal anatomy,

structure of the bacterial biofilm, and the effect of instrumentation and root canal filling, which may interfere with the effect of the irrigation procedures.

The greatest effect of ultrasonic agitation on fluid dynamics that is associated with better biofilm removal in comparison to syringe and sonic irrigations has been identified (Layton *et al.*, 2015). In contrast, Khaord *et al.* (2015) reported that the efficacy of sonic and MDA was better than ultrasonic irrigation protocol. This inconsistency may be attributed to the difference in the outcome measure as the later study used the smear layer, which is different from biofilm in response to irrigation procedure.

1.2.12. Investigations of efficacy of irrigants against root canal microbiota

Both clinical and laboratory studies have been developed to examine the antimicrobial efficacy of root canal irrigants against bacteria and bacterial biofilm.

Taken collectively, clinical studies (*in vivo*) have attempted to investigate the antimicrobial efficacy of irrigants after the application of irrigation regimens to infected root canal systems. These human (Goldman and Pearson, 1969; Bystrom and Sundqvist, 1981; Ercan *et al.*, 2004; Paiva *et al.*, 2013) and animal (Tanomaru *et al.*, 2003; Silva *et al.*, 2004; Santos *et al.*, 2014) investigations measure the reduction of microbial counts and negative cultures as outcomes.

An assessment of irrigant efficacy through the use of an *in vivo* model could be considered standard protocol, since the materials and methods under investigation are considered relevant to the clinical scenario. For example, the efficacy of root canal irrigants in reducing the microbial load within the root canal system has been assessed using culture techniques and performing CFUs (Byström and Sundqvist, 1983). Counting the CFUs gives data about the viable

bacteria. However, the CFUs method detect bacteria that are capable of forming colonies through cell division (Paz *et al.*, 2015). Another technique includes radiographic assessment through periapical radiography and cone-beam computed tomography at first visit and at recall (Liang *et al.*, 2013; Kanagasingam *et al.*, 2016). Recently, molecular analysis techniques of endodontic infections have been used to quantify and identify the bacteria that remain in the root canal system after exposure to an irrigant (Paiva *et al.*, 2013; Zandi *et al.*, 2016).

Histological techniques have also been used to identify the remaining bacteria after root canal irrigation procedures for both single-visit (Nair *et al.*, 2005) and multiple-visit treatment protocols (Vera *et al.*, 2012; Neelakantan *et al.*, 2016). Based on histological investigations, Nair (1987) observed dense bacterial aggregates embedded in amorphous materials and attached to the dentinal wall while examining histological sections of the apical 5 mm of root canals using light and electron microscopy. Despite the usefulness of histological investigations to provide visual insight of endodontic biofilms, they suffer from risks related to surgical intervention or the extraction of the tooth sample under assessment (Paz *et al.*, 2015). In addition to, the risk of biofilm components disruption during sample sectioning and histological processing. Another potential problem is the limitation of microscopic examination of the histological samples in the identification of biofilm microbiota (Silva *et al.*, 2004).

An *in vivo* testing of root canal biofilms has many drawbacks. For instance, they are relatively labour-intensive to carry out and ethical issues and difficulties in patient recruitment may limit the ability to achieve adequate sample sizes (Spratt *et al.*, 2001). Furthermore, they are hampered by a lack of standardization in the biofilm in terms of composition, structure, maturity and thickness (Kishen and

Haapasalo, 2010). Consequently, multitudes of laboratory biofilm models have been used to examine the antimicrobial efficacy of irrigants. These models are useful to obtain standardized biofilm models with predictable structures and behaviours. However, many parameters need to be considered during the designing of the biofilm model (Kishen and Haapasalo, 2010), including the microbial type and concentration in the inoculum, incubation time and substratum properties. It is important that the bacterial type and concentration are representative of clinical isolates. In addition, it is important to provide sufficient bacteria–substrate interaction time and optimum environmental conditions since bacterial adherence to a substrate may occur over a period of a few hours or days, depending on the bacterial strain and environmental conditions (Dunne, 2002). Furthermore, the solid substratum should allow for bacterial attachment and the growth of bacterial cells (Donlan, 2002).

Laboratory biofilm models include *ex vivo* biofilm models, *in vitro* biofilm models, and simulant biofilm models (*ex vivo, in vitro*).

Ex vivo models are composed of extracted teeth of human or animal origin. The extracted teeth are infected with selected bacteria and then exposed to the test antimicrobial agents (Şen *et al.*, 1999; Bhuva *et al.*, 2010; Al Shahrani *et al.*, 2014; Niazi *et al.*, 2015; Malentacca *et al.*, 2017). The use of extracted teeth to investigate endodontic disinfection by an irrigant constitutes an effort to bring the experimental conditions much closer to those found in the clinical scenario. However, it is relatively time consuming and labour intensive to construct *ex vivo* models since the collection of teeth requires patient consent and involves ethical issues (Kishen and Haapasalo, 2010).

Multitudes of biofilm *in vitro* models have been used to test the efficacy of antimicrobial agents. These include test models (*in vitro*) for selected bacteria exposed to an antimicrobial agent (D'Arcangelo *et al.*, 1999; Vianna *et al.*, 2004; Ferraz *et al.*, 2007). Bacteria, collected in known concentrations, are incubated for varying durations in antimicrobial irrigants of various concentrations, sampled, diluted and cultured. This allows for a counting of the Colony Forming Units or a measuring of the growth inhibition zone after a period of growth. Although the design of the test models seems simple, the outcomes show variations as a result of the bacteria being subjected to non-standardised exposure conditions during the introduction of the irrigant (Shen *et al.*, 2012). Another *in vitro* model includes the growth of selected bacteria on a substratum surface and its subsequent exposure to the antimicrobial agent. The substrata used to grow biofilms include nitrocellulose filter membranes (Spratt *et al.*, 2001; Abdullah *et al.*, 2005; Bryce *et al.*, 2009), hydroxyapatite discs (Guggenheim *et al.*, 2001; Niazi *et al.*, 2014; Tawakoli *et al.*, 2017), sections of root apex (Clegg *et al.*, 2006), dentine discs (Savvides *et al.*, 2010; Stojicic *et al.*, 2012; Wu *et al.*, 2014; Arias-Moliz *et al.*, 2015; Yang *et al.*, 2016) and resin (Williamson *et al.*, 2009; Layton *et al.*, 2015).

Based on substratum-biofilm models, it has been shown that 2.5% NaOCl is the most effective chemical endodontic antimicrobial agent against *E. faecalis* biofilms when compared with other test agents (0.2% chlorhexidine and 10% povidone iodine) (Spratt *et al.*, 2001; Bryce *et al.*, 2009). Moreover, sodium hypochlorite is capable of rendering bacteria non-viable, in addition to degrading and removing the biofilm structure (Clegg *et al.*, 2006; Bryce *et al.*, 2009). Substratum-biofilm models provide information about the efficacy of antimicrobial irrigants on single and multi-species biofilms outside the root canal system.

However, approaches of this kind carry with them the limitation that the immersion of samples in the irrigant is different from exposure to irrigant flow within the confinement of a root canal system. Another *in vitro* model includes the use of organic films (hydrogel, collagen) as standardised test targets to represent biofilms and study their interactions with irrigants either in simulated root canal systems (Verhaagen *et al.*, 2012; Macedo *et al.*, 2014a) or in extracted teeth (Huang *et al.*, 2008; McGill *et al.*, 2008). The rationale for this is the use of films with similar mechanical, adhesive and degradation properties as bacterial biofilms to simplify the experimental set-up. Growing and controlling bacterial biofilms is infinitely more complicated and subject to variation. Although the results based on organic film models are interesting, they do not necessarily replicate the process of bacterial biofilm removal by irrigant.

In conclusion, the current biofilm models used to investigate the antimicrobial efficacy of irrigants involve the use of *in vivo*, *ex vivo* and *in vitro* models. It is possible to standardise the design of *in vitro* models to some extent, but it is not always possible to extrapolate results from these models to the clinical scenario. Ethical issues may hinder *in vivo* or *ex vivo* research options. It seems that no single and ideal biofilm model exists for all applications.

1.3. Statement of the problem

For most of the past century an interrelationship between microbial existence within the root canal system and periapical lesion development has been found (Kakehashi *et al.*, 1965; Sundqvist, 1976). It is likely that a completely bacteria-free environment and subsequent apical healing can be only achieved through effective steps of the endodontics treatment (Vera *et al.*, 2012). It is known that teeth that have a positive culture before the obturation have a lower success rate

than teeth with negative culture (Sjögren *et al.*, 1997). It has been argued that mechanical and chemical preparation represented by instrumentation and irrigation respectively play an important role in the root canal treatment (Stewart, 1955), and is responsible for the major microbial reduction (Vianna *et al.*, 2006). However, an *in vitro* study has shown that instrumentation of the canal is inadequate for complete eradication of the root canal surface from microorganisms, especially from the apical root canal third and infected dentinal tubules (Peters *et al.*, 2011). The presence of bacterial communities as a biofilm structure in the root canal systems and their resistance to antibacterial agents together with the complex anatomy of the root canal system poses challenges during root canal treatment (Ricucci *et al.*, 2009). This demonstrates the essential role of the irrigation in the root canal treatment to remove bacterial biofilm (Siqueira *et al.*, 2000). Sodium hypochlorite is the most popular irrigant for its capacity to kill bacteria when they are in intimate contact for sufficient time (Spratt *et al.*, 2001).

More recently, literature has emerged that offers important insights into strategies of irrigant delivery, mixing, and agitation. However, the real-time monitoring of bacterial biofilm removal by NaOCl, and the condition of residual biofilm in the root canal system are not completely understood. Furthermore, our knowledge regarding the effect of root canal complexity and the diversity of bacterial biofilm on the efficacy of NaOCl is not complete. Therefore, more knowledge of biofilm-NaOCl interaction within the root canal system is crucial to improve the outcomes of the root canal treatment.

1.4. Null hypothesis

The null hypothesis of the present study is that there exists no difference in the efficacy of passive and active sodium hypochlorite irrigation on the removal and destruction of single and multispecies bacterial biofilms from the walls of 3 mm of the apical third and lateral canal of the root canal system.

1.5. Aim of the study

- To investigate the effect of the position of the irrigation needle on irrigant replacement within the root canal system.
- To investigate the influence of the concentration of NaOCl irrigant (2.5% & 5.25%, canal design (closed, open), type of irrigation [passive and active (manual, sonic, and ultrasonic)], root canal anatomy [simple and complex anatomy (lateral canal)], type of biofilm (single and multi-species), on the removal rate of bacterial biofilm by NaOCl irrigant delivered into an *in vitro* test model;
- To examine the structure of the residual biofilm (single and multi-species) following NaOCl irrigation delivered into an *in vitro* root canal model.

Objectives:

- To test the potential of the model materials to create an *in vitro* infected root canal model.
- To develop and utilise the root canal models of different anatomy (simple and complex), to facilitate investigations into the removal patterns of bacterial biofilms by sodium hypochlorite irrigations.
- To investigate the outcomes of the interaction between a NaOCl irrigant and bacterial biofilm using composition of bubbles generated, available chlorine, and pH of outflow as outcome measures.

Chapter 2

Development and optimization of the materials used in the study

2.1. Introduction

A variety of laboratory (*in vitro*) biofilm models that simulate the clinical situation have been used for different investigations in endodontics. However, an approximation of the environment present in the clinical scenario and the well-controlled *in vitro* experiments are challenging (Kishen and Haapasalo, 2010). In addition, optimal models should allow a prediction of the outcomes of the clinical and *ex vivo* studies (Basrani, 2015). Therefore, many parameters are needed to be considered in the development of a biofilm model before its application in irrigation studies. For example, adhesion and generation of biofilm on the model surface, and the model should provide the same condition exist in the real clinical scenario.

This chapter consists of two parts:

1. Investigation to test potential substratum materials for development of an *in vitro* biofilm model.
2. Investigation using computational fluid dynamics to measure the velocity distribution of irrigant flow in the root canal system and the effect of needle position on the irrigant flow.

2.2. Investigation to test potential substratum materials for development of an *in vitro* biofilm model.

2.2.1. Justification of the investigation

It is well known that the crucial step in biofilm formation is bacterial cell adhesion to a solid surface (Costerton *et al.*, 1999). The three main elements implicated in biofilm development are fluid medium, bacterial cells, and a solid surface (Katsikogianni and Missirlis, 2004). However, formation of biofilm depends on bacteria-substratum interaction which is influenced by chemical composition of the substratum and the physicochemical properties of the components involved in the biofilm (Baumgartner *et al.*, 2008). These properties include wettability or hydrophobic interactions, surface free energy (SFE), and surface charge or the zeta potential (Baumgartner *et al.*, 2008).

Recently, approaches have been performed to inhibit bacterial adherence, growth, proliferation, and consequently reducing the possibility of biofilm formation on a solid surface by bacteria (Tran *et al.*, 2015). One approach includes the addition of bactericidal agent (e.g. nitric oxide, silver, gentamycin) to the polymers of the substratum material, which leach out and reduce the adhesion of the bacteria (Zhang *et al.*, 2008).

Previous investigations reported that the physicochemical properties could influence bacterial adhesion to solid substrata (Marshall *et al.*, 1971; Cerca *et al.*, 2005), and consequently play an important role in microbial infections (Doyle, 2000). The best method to determine bacterial wettability and SFE is by contact angle measurements (Doyle, 2000). The relation of physicochemical properties of substratum and bacterial adhesion has been critically discussed in the literature. For example, some authors reported that materials with low SFE result in less bacterial adherence (Liu and Zhao, 2005; Bürgers *et al.*, 2009); whilst

others suggested that bacterial adhesion decreased with increasing surface energy of substrata (Absolom *et al.*, 1983; McEldowney and Fletcher, 1986).

It seems justifiable that the first step for the development of an ideal biofilm *in vitro* model is the investigation of substratum antimicrobial activity and material properties concerning bacterial adhesion and growth as it is a crucial factor in the formation of biofilm (Donlan, 2002). Ideally, the substratum should be inert and exhibit properties similar to dentine with regards to bacterial adhesion. Materials that do not fulfill these characteristics affect negatively on microbial growth (Kishen and Haapasalo, 2010).

The aims of the present study were to compare the physical and chemical properties (zeta-potential, wettability, and surface free energy) of potential substrata (Endo-Vu block, Polystyrene, Photopolymer, Accura) to dentine, to determine if the substratum materials have antimicrobial activity, and to compare the attachment of bacterial biofilm (*Enterococcus. faecalis*) onto the surface of these substratum materials to dentine.

2.2.2. Materials and Methods

2.2.2.1. Preparation of the samples

2.2.2.1.1. Preparation of dentine samples

A total of twenty one single-rooted, mature apices, and caries-free adult teeth were obtained from the Biobank, UCL Eastman Dental Institute (study reference number 1310) (Appendix 1). The teeth were stored in sterile water after extraction. Under aseptic conditions, the crown part of each tooth was removed using a rotary diamond wheel (Abrasive Technology Inc., Westerville, USA), mounted on a straight air motor hand-piece (W&H UK Ltd, St Albans, UK) under water cooling. Pulp tissue in the root canal was removed using a barbed broach

(Dentsply Tulsa Dental Specialties, Tulsa, OK, USA). The cementum was ground using a grinding wheel (Struers Ltd, Solihull, UK). Each root dentine was sectioned and 1 mm thick standard squares (5 mm x 5 mm) were created using a diamond wheel. The method was based on a previous study (Sousa *et al.*, 2009) but with changes in the dimensions of samples.

2.2.2.1.2. Preparation of the substratum material samples

Four biomaterial substratum materials [Endo-Vu block, Polystyrene slide, and two stereolithography (STL) materials (Photopolymer, Accura)] were evaluated in this investigation. Endo-Vu block is a polymethyl methacrylate material (Richard W. Pacina, Waukegan, IL, USA). It is designed for training dentists in instrumentation and obturation skills. Polystyrene is a synthetic aromatic polymer made from a styrene monomer (Fisher scientific, Rochester, NY, USA). The Polystyrene slide used in the flow cell device is designed to allow visual observation of biofilm growth and development. The two STL materials were manufactured by 3D printing technique, and delivered in the form of sheets of different dimensions. Photopolymer is an acrylic base clear™ material (AZoNetwork Ltd., Cheshire, UK), which is composed of a mixture of methacrylic acid esters and a photo-initiator. Accura is an epoxy based material (3D Systems, Inc., Rock Hill, South Carolina, USA), which is composed of Bisphenol-A epoxy resin.

A total of twenty one sheets of each substratum material were sectioned using a diamond wheel to create 1 mm thick standard squares (5 mm x 5 mm). All samples were smoothed by using grinder discs for 3 minutes (1200 µm, Struers Ltd, Solihull, UK).

2.2.2.2. Measurements of the zeta-potential of dentine and the substratum materials

The surface charge (positive or negative) of the dentine and the substratum materials were determined using a nano-Zetasizer device (Malvern Instruments Ltd, London, UK), which use the Laser Doppler Micro-electrophoresis technique to measure the charge. An electric field was applied to a solution of particles, which then moved with a velocity related to their charge. This velocity was measured, which enabled the calculation of the particles charge (Hsu *et al.*, 2013).

A total of three (n = 3) samples of each test material (Dentine, Endo-Vu b, Polystyrene, Photopolymer, Accura) were ground using a Retsch grinding machine (Retsch Gmbh, Hanna, Germany). This produced powder with particles with a maximum size of 5 μm, which was achieved using sieves (Endecotts, London, UK). A total of 10 g of each material powder was mixed with 10 mL Brain Heart infusion broth (Sigma-Aldrich, St. Louis, Montana, USA), which was gently vortexed at maximum speed for 30 seconds using a Vortex (IKA, Chiltern Scientific, Leighton, UK). One mL of each mixture was added individually into the cuvette of the Nano-Zetasizer device using 1 mL sterile pipettes (Alpha Laboratories Ltd, Winchester, UK). The DTS Nano version 5.03 software of the device was used to control the measurement of the zeta-potential of each sample. Measurements were taken in triplicate for each sample.

2.2.2.3. Comparison of contact angle and solid surface free energy between dentine and the substratum materials

The measurements of contact angle (θ) and surface free energy (*Y*) were achieved by the sessile drop method using a goniometer device equipped with a video camera (KSV instruments, Fairfield, Connecticut, USA) and an image analyser (Fletcher and Marshall, 1982; Hsieh *et al.*, 2007). Three different liquids

that included non-polar [diiodomethane (Y=50.8 mN/m)] and polar [glycerol (Y=64 mN/m), water (Y=72.8 mN/m)] were used with each sample. A total of nine samples (n = 9) of each test material (Dentine, Endo-Vue block, Polystyrene, Accura, and Photopolymer) were examined, with three samples per liquid. Each sample was placed on the stage of the goniometer and the contact angle of one drop of the designated liquid was measured. With each liquid droplet, five measurements were made. A manually controlled micrometre syringe was used to push liquid droplets onto the solid surface from above. The video signal of the sessile drop on the solid surface was acquired by use of a CCD camera connected to a digital video processor, which performed the digitization of the image. Attension Theta software (Biolin scientific, Staffordshire, UK) was used to measure the contact angle. The surface free energy of the sample was calculated from the contact angle according to Owrk/ Extended Fowkes (1964) method. The polar and dispersive values for the tested liquids was taken from the literature (Good and van Oss, 1992).

2.2.2.4. Evaluation of the antimicrobial activity of the substratum materials

2.2.2.4.1. Sterilisation of the samples

A total of nine square samples of each test material were placed individually into packaging bags (Sterrad 100S, ASP®, Irvine, CA, USA) and then sterilised using gas plasma with hydrogen peroxide vapour (Sterrad 100S, ASP®, Irvine, CA, USA) for fifty minutes (Precautions and Flush, 2008).

2.2.2.4.2. Preparation of microbial strain and determination of the standard inoculum (CFU/mL)

Biofilms were grown from a single bacterial strain (*Enterococcus faecalis;* ATCC 19433). The strain was supplied in the form of frozen stock in a brain-heart infusion broth (BHI) (Sigma-Aldrich, St. Louis, Montana, USA) and 30% glycerol

(Merck, Poole, UK) stored at -70 °C. The strain was thawed to a temperature of 37 °C for 10 minutes and swirled for 30 seconds using a Vortex (IKA, Chiltern Scientific, Leighton, UK) (Siqueira *et al.*, 2002). After thawing, 100 µL of the strain were taken and plated onto a BHI agar plate (Sigma-Aldrich, St. Louis, Montana, USA) with 5% defibrinated horse blood (E&O Laboratories, Scotland, UK) and incubated at 37 °C in a 5% CO_2 incubator (LEEC, Nottingham, UK) for 24 hours. Bacterial morphology and catalase activity were confirmed prior to the generation of the biofilms. For this, two colonies of the strain were separately removed using a sterile inoculating loop (VWR, Leicester, UK), and catalase test using 3% H_2O_2 (Sigma-Aldrich Ltd, Dorset, UK) and Gram staining test (BD Ltd., Oxford, UK), were performed. In addition, the identification of the strain was achieved by performing 16S rRNA gene sequencing and analysis (Appendix 2).

A standard inoculum of 10^8 CFU/mL concentration was used, which was adapted from a previous study (Al Shahrani *et al.*, 2014). For this, six colonies were removed from the agar plate, placed into 20 mL of BHI broth with 5% defibrinated horse blood, and incubated at 37 °C in a 5% CO_2 incubator for 24 hours. BHI containing *E. faecalis* was adjusted to 0.5 absorbance at a wavelength of 600 nm using a spectrophotometer (NanoDrop™ Spectrophotometer ND-100, Wilmington, USA) (Al Shahrani *et al.*, 2014). Inoculum concentration was confirmed by determining the colony forming units per millilitre (CFUs/mL) using six ten-fold serial dilutions (Peters *et al.*, 2001a). This was performed by mixing aliquots of 100 µL bacterial inoculum into 900 µL of reduced transport fluid in 1.5 mL mini tubes (Sarstedt Ltd, Nümbrecht, Germany). From these dilutions, aliquots of 20 µL were plated on BHI agar plates with 5% defibrinated horse blood and then incubated at 37 °C in the 5 % CO_2 incubator for a period of 24 hours.

The colony forming units per millilitre (CFUs/mL) corresponding was 1.1×10^8 CFU/mL.

2.2.2.4.3. Kirby-Bauer antibiotic testing

A total of three samples (n = 3) of each substratum material were used to perform Kirby-Bauer antibiotic testing to examine the antimicrobial activity of the test materials, which was adapted from Gopikrishna *et al.* (2006). The inoculum of *E. faecalis* strain was prepared by taking six colonies of the strain from a BHI agar plate and placed into 20 mL of BHI broth and incubated for 24 hours at 37 °C in a 5% CO_2 incubator. One hundred microlitres of each bacterial strain were taken and plated onto a Mueller-Hinton agar (Sigma-Aldrich, St. Louis, Montana, USA) containing 5% defibrinated horse blood. Each sample was placed onto the Mueller-Hinton agar, and then the plates were incubated at 37 °C in a 5% CO_2 incubator for two days. The zone of inhibition around each material was measured and recorded at 2 time intervals (24, 48 hours) (Siqueira *et al.*, 2002).

2.2.2.5. Comparison between bacterial biofilm growth and attachment on dentine and biomaterial substrata

2.2.2.5.1. Generation and staining of E. faecalis biofilm on the substratum material surfaces

Each sample was incubated with 1 mL of *E. faecalis* inoculum, which was delivered into a sterile 7 mL plastic bijou bottle (Sarstedt Ltd, Nümbrecht, Germany), containing the samples, using a sterile syringe (BD Plastipak™, Franklin Lakes, NJ, USA) and a 21-gauge needle (BD Microlance™, Franklin Lakes, NJ, USA). The samples were then incubated at 37 °C in a 5% CO_2 incubator (LEEC) for 10 days. Every two days, half of the inoculum that surrounded the sample was discarded using a syringe and a 30G needle and replaced with fresh BHI broth using a sterile syringe and needle (De-Deus *et al.*, 2007).

After incubation, all samples with biofilms were removed from the plastic bottle and the biofilm on the surface of three samples (n = 3) of each material was observed using scanning electron microscope (SEM) (FEI XL30 FEG SEM, FEI, Eindhoven, Netherlands). For this, the sample was fixed in 3% glutaraldehyde (Agar Scientific, Stansted, UK) in 0.1 M sodium cacodylate buffer (Agar Scientific, Stansted, UK) at 4 ˚C overnight. Then, they were dehydrated in a graded series of alcohol (50, 70, 90, and 100%) (Sigma Aldrich, Dorset, UK), placed in hexamethyldisilazane (Agar Scientific, Stansted, UK) for 5 minutes and air-dried. Samples were mounted onto aluminum pin stubs (Agar Scientific, Stansted, UK), and sputter coated with gold/palladium (Polaron E5000, QUORUM Technology, UK) before examination using SEM.

The other three samples (n = 3) were placed onto a slide and rinsed with 1 mL sterile distilled water (Roebuck, London, UK) for 1 minute using a sterile 10 mL syringe (Plastipak, Franklin Lakes, New Jersey, USA) to remove loosely attached cells. Using a micropipette, 1 µL of crystal violet (CV) stain (Merck, Darmstadt, Germany) was applied to the biofilm and left for 1 minute for staining. Each sample was subsequently washed with 3 mL of sterile distilled water for 1 minute to remove excess stain (Izano *et al.*, 2007).

2.2.2.5.2. Assessment of bacterial growth and attachment

To quantify the surface coverage by biofilm, each sample was placed on the stage of an optical microscope coupled to a recording CCD camera (BX51, Olympus Optical Co., Ltd., Tokyo, Japan), and viewed using an objective lens (Cerca *et al.*, 2005). For standardisation of measurement, a template was created using AutoCAD® software (Autodesk, Inc., San Rafael, CA, USA). The template was printed on transparency printer paper of the same size as the sample (5 mm × 5 mm) to provide a grid of 25 squares each of 1 mm^2. The template was placed

over the sample and five squares of one mm^2 were imaged, the first square was located in the centre of the template and the other four at each corner of the centre square. The surface area coverage with bacterial biofilm onto the surface of the five squares of each sample was quantified, using Image-pro plus 4.5 (MediaCybernetics®, Silver Spring, USA).

The method used to assess the attached biofilm was based on Cerca *et al.* (2005) study. Each sample was grasped in the horizontal plane using tweezers, and immersed slowly for 10 seconds in 100 mL distilled water in a sterilised 100 mL glass tube (Sarstedt Ltd, Nümbrecht, Germany). The immersion cycle was repeated three times. The sample was then dried for 3 minutes at room temperature. The sample surface with bacterial biofilm was imaged and the difference in percentage surface area of substratum coverage with bacteria biofilm attached to the samples before and after water immersion was quantified.

2.2.2.6. Statistical analysis

All data were analysed using SPSS (BM Corp. Released 2013. IBM SPSS Statistics for Windows, Version 22.0. Armonk, NY: IBM Corp). For evaluating differences in physico-chemical properties, means and standard deviations were calculated and a descriptive analysis and bar chart were used to compare the differences in the zeta potential, contact angle, and surface free energy between the dentine and the substratum materials. The mean values of the percentage surface area of dentine versus the substratum surfaces coverage with *E. faecalis* biofilm before immersion experiments were plotted using bar chart. Because the data were normally distributed, they were compared using one-way ANOVA with Dunnett *post-hoc* test. The same test was used for the comparison of the mean difference in percentage surface area coverage with biofilm before and after

immersion between dentine and the substratum surfaces. All tests were performed at a level of significance $p \leq 0.05$ with a confidence level of 95%.

2.2.3. Results

2.2.3.1. Measurement of the zeta-potential

Mean values and standard deviations of the zeta-potential of the dentine and the substratum materials are presented in Table 2.1. The distributions of zeta potential of the test materials are presented in Appendix 3.

Table 2.1: Mean values (n = 3) of the zeta-potential of the dentine and substratum materials.

Type of measurement	Substratum	Zeta Potential (mV) (±SD)
zeta-potential	Dentine	-9.11(±4.1)
zeta-potential	Polystyrene	-29.1(±6.51)
zeta-potential	Endo-VU	9.05(±6.7)
zeta-potential	Accura	-23.7(±6.9)
zeta-potential	Photopolymer	-18.8(±3.5)

SD = Standard deviation

The results indicated that root dentine had a negative charge [-9.11 mV (±4.1)] (. Only one substratum material (Endo-Vu) had a positive charge [9.05 mV (±6.7)]. In comparison, other materials (Polystyrene, Accura, Photopolymer) have a negative charge [-29.1mV (±6.51)], [-23.7 mV (±6.9)], [-18.8 mV (±3.5)] respectively). However, the concentration of anionic electrolytes of dentine was less than the substratum materials with negative charge surfaces.

2.2.3.2. Measurement of the contact angle (wettability and surface free energy measurements)

Substratum physico-chemical characteristics presented by the contact angle and surface free energy parameters were obtained using the three liquids tested and are given in Figures 2.1 & 2.2 respectively.

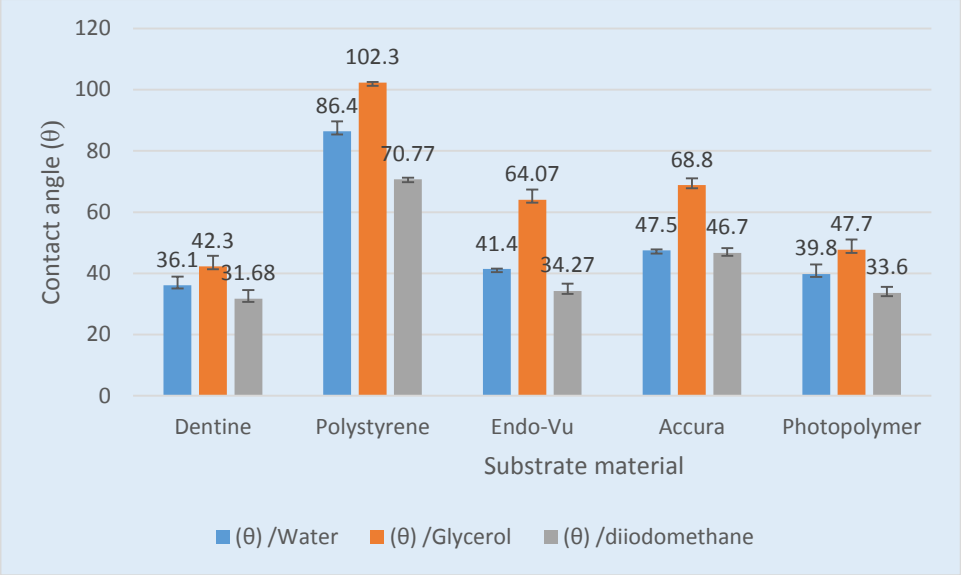

Figure 2.1: Mean values and standard deviation of the contact angle (θ) at the interface between the substratum and polar (water, glycerol), and non polar (diiodomethan) liquids.

Measurement of the contact angle showed that all test materials were hydrophilic (θ < 90°), with the exception of polystyrene substratum that presented a hydrophobic contact angle (θ =102°) using glycerol liquid. Dentine had the lowest water contact angle (more hydrophilic) [θ = 36.1° (±2.8°)]. Similarly, photopolymer material had hydrophilic properties [θ = 39.8° (±3.1°)], which was closer to dentine followed by Endo-Vu [θ = 41.4° (±0.1°)], Accura [θ = 47.5° (±0.3°)], and Polystyrene [θ = 86.4° (±3.2°)] respectively.

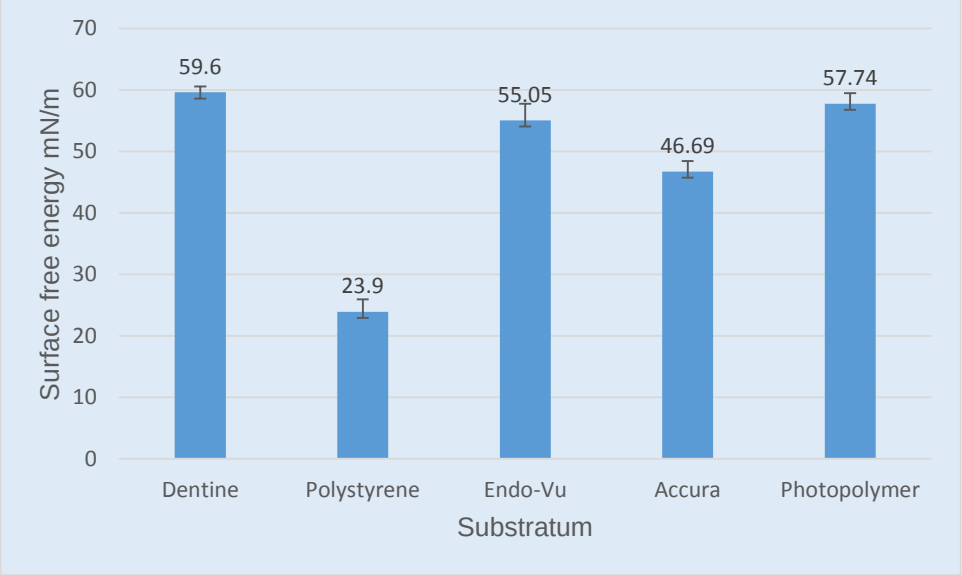

Figure 2.2: Mean and standard deviation values of the surface free energy of the biofilm model stratified by the type of the substratum.

On the other hand, the surface free energy showed a variation consistent with the size of the standard deviations. The highest SFE was associated with dentine [59.6(±0.9) mN/m] followed by Photopolymer [57.74(±1.7) mN/m], Endo-Vu [55.05(±1.7) mN/m], Accura [46.69(±1.7) mN/m], while the lowest SFE was associated with Polystyrene [23.9(±2.04) mN/m].

2.2.3.3. Assessment of antimicrobial activity of the substratum materials

Images of the substratum materials, which were placed on a Mueller-Hinton agar surface smeared with *E. faecalis* are presented in Figure 2.3.

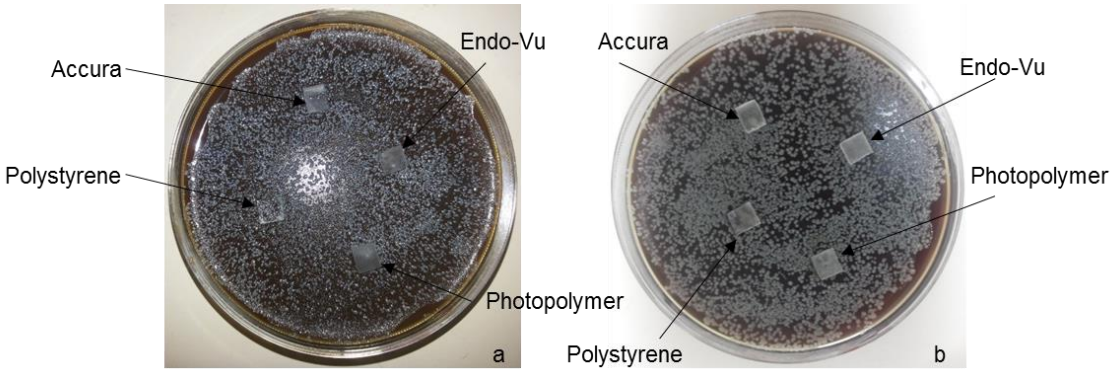

Figure 2.3: Images depict the lack of antibacterial activity of the substrata materials against *E. faecalis* bacteria after 24 (a) and 48 (b) hours incubation in Mueller-Hinton agar.

The images do not show any signs of a zone of bacterial inhibition developing around the samples of the substrata after 24 and 48 hours incubation with *E. faecalis* species. Accordingly, the substratum materials did not exert any antibacterial activity against the test strain.

2.2.3.4. Assessment of biofilm growth and attachment

2.2.3.4.1. Observations assessment

Representative SEM images of the biofilm onto the surface of the dentine and the substratum materials are presented in Figure 2.4.

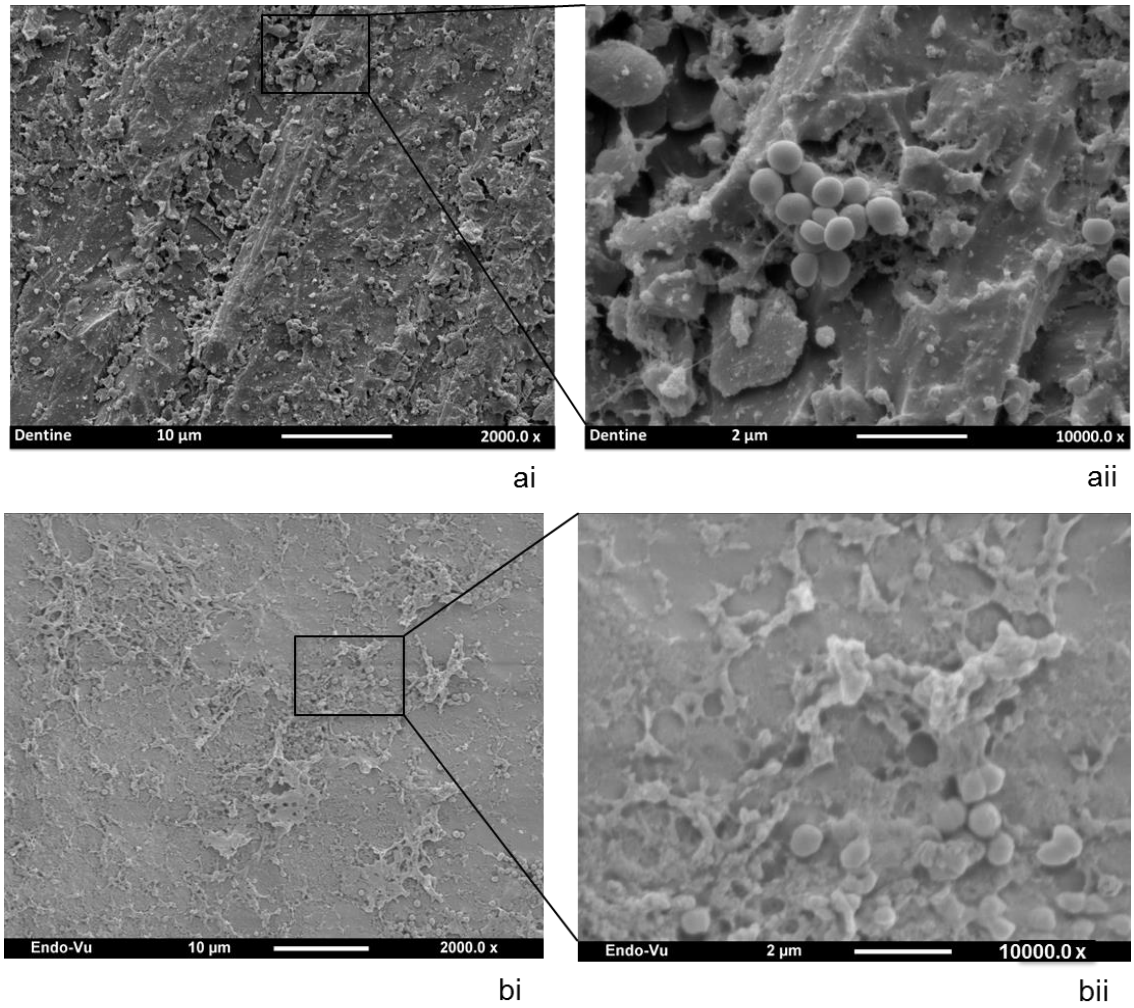

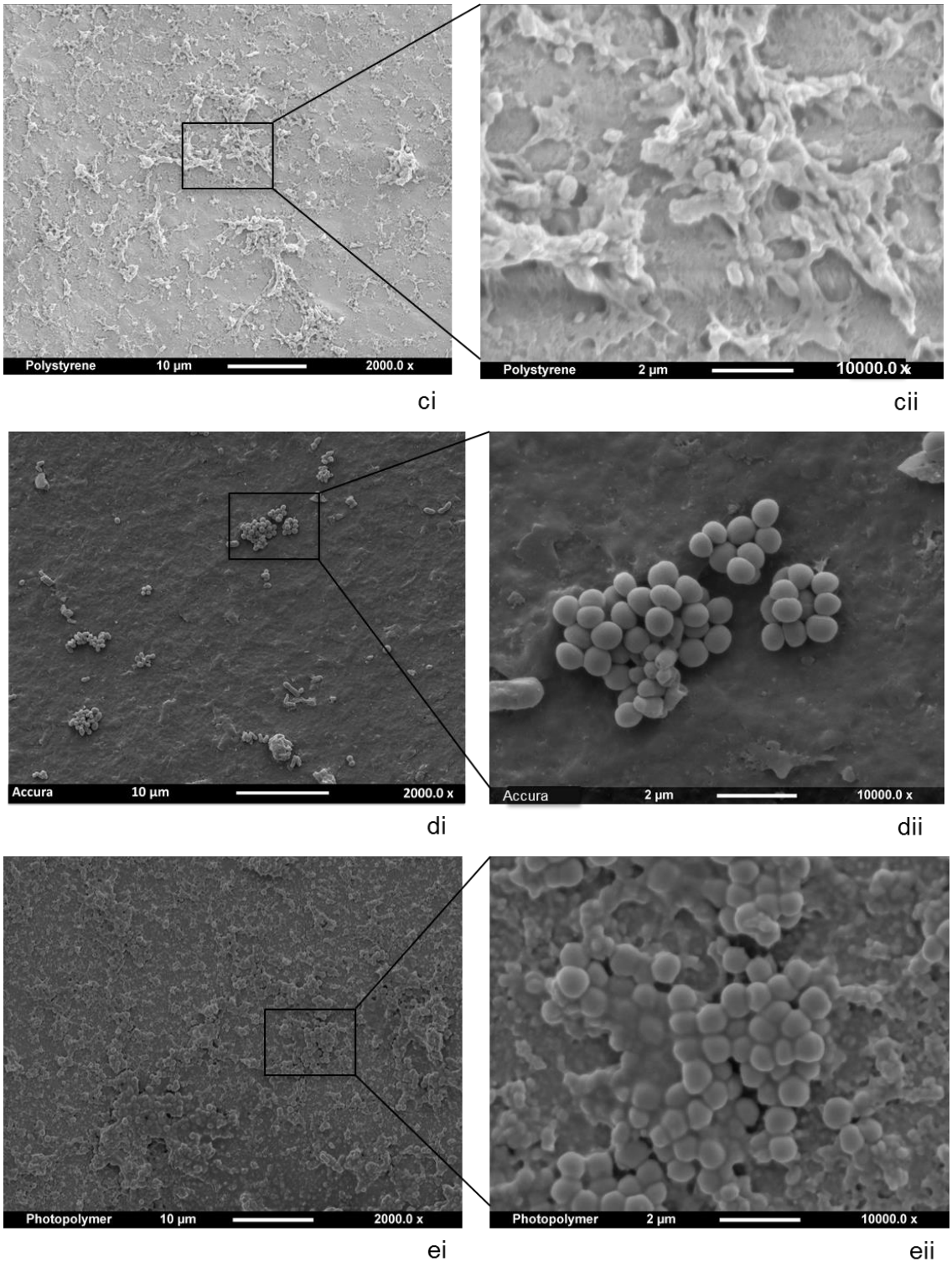

Figure 2.4: SEM images illustrate that the *E. faecalis* biofilm grown onto the surface of the dentine (a1, aii), Endo-Vu (b1, bii), Polystyrene (ci, cii), Accura (di, dii), and Photopolymer (ei, eii) after ten-day incubation.

The images reveal the extracellular polymeric substance of the bacterial biofilm and a cluster organization of *E. faecalis* cells in the biofilms. This demonstrates

that biofilm grew on the surface of the dentine (a1, aii), Endo-Vu (b1, bii), Polystyrene (ci, cii), Accura (di, dii), and Photopolymer (ei, eii).

Further identification of the biofilm growth on the substratum surface is depicted in optical microscopy images (Figure 2.5).

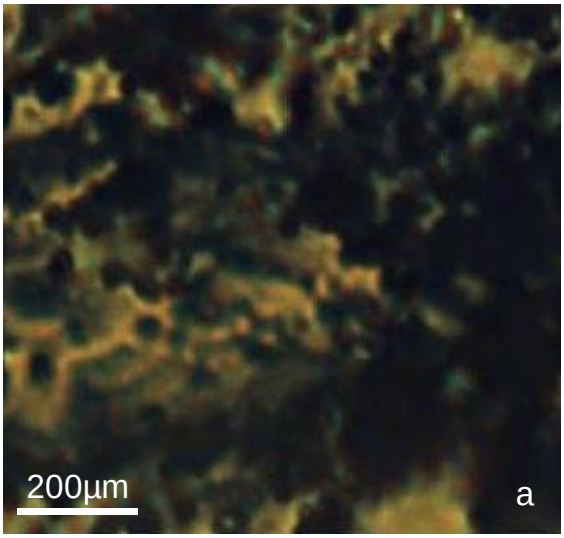

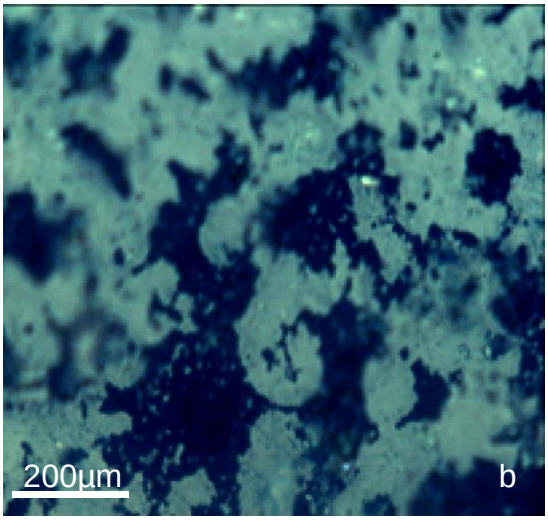

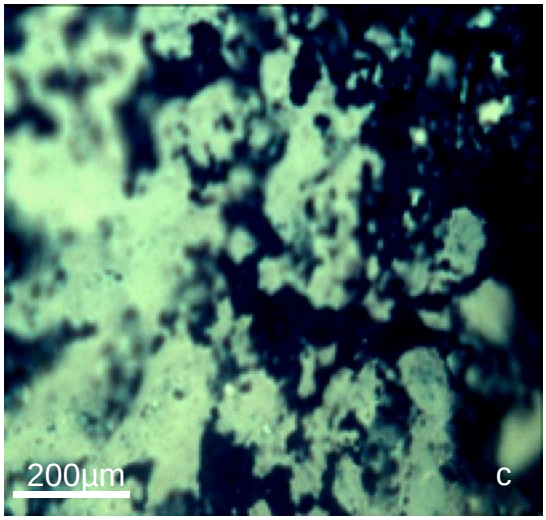

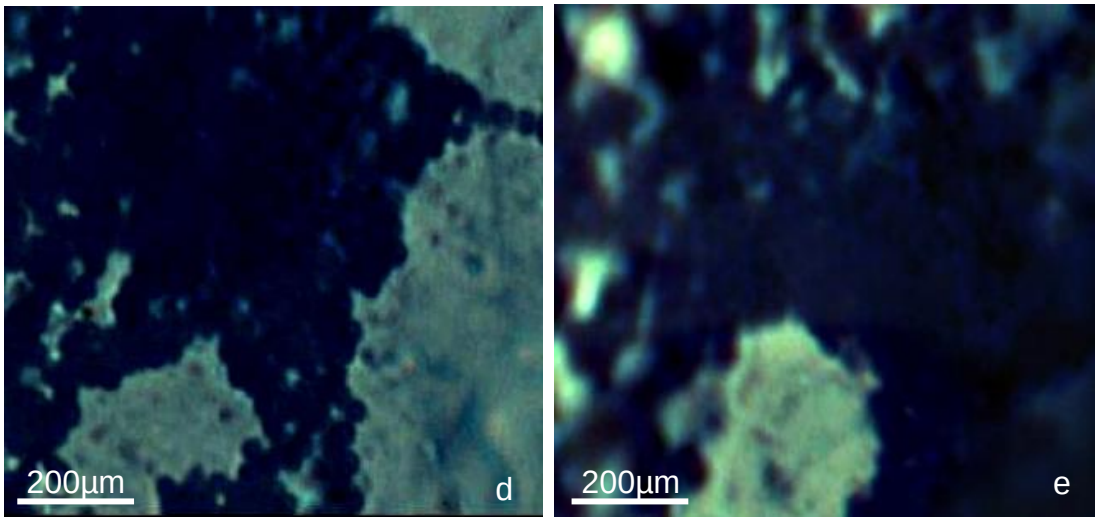

Figure 2.5: Microscopy images of crystal violet stained *E. faecalis* biofilm on one of the (a) dentine, (b) Endo-Vu, (c) Polystyrene, (d) Accura, and (e) Photopolymer sample surfaces.

It is apparent from the images that the abundant bacterial biofilm grew on the dentine surface (a) followed by Photopolymer (e), Accura (d), Polystyrene (c), and Endo-Vu (b) materials respectively. In addition, the spatial distribution of the biofilm on the surface of dentine and the substratum materials is obviously different.

2.2.3.4.2. Statistical analysis

The mean values of percentage surface area coverage with *E. faecalis* biofilm attached to dentine *versus* the substratum materials before 3 cycles of immersion in water are presented in Figure 2.6.

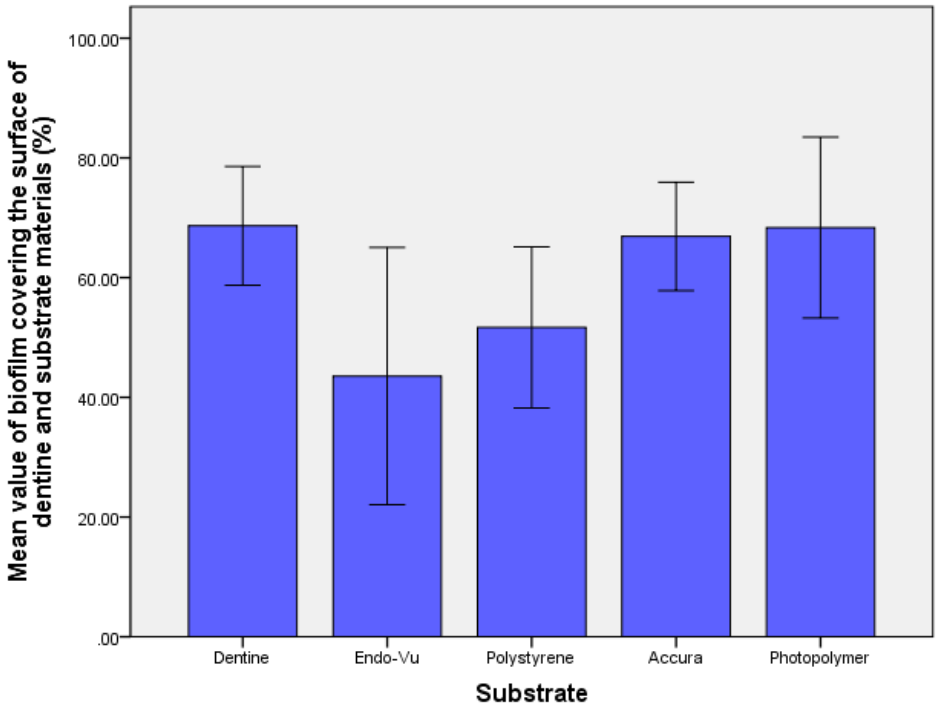

Figure 2.6: Mean and standard deviation values of percentage area of surface coverage with biofilm, stratified by substratum material (dentine, Endo-Vu, Polystyrene, Accura, and Photopolymer).

The mean value of percentage surface area coverage with biofilm was the highest on the dentine [68.7%, (±4.96)], followed by Photopolymer [64.2%, (±7.55)], Accura [63.89%, (±4.35)], Polystyrene [51.68%, (±6.73)], and Endo-Vu [43.55%, (±7.75)]; however, there was no statistically significant difference between the experimental groups (p = 1.00).

The 3 cycles of immersion in water of all experimental groups had a minimal effect on the removal of attached biofilm from the surface of the substrata. The mean difference of biofilm percentages before and after immersion in water is shown in Table 2.2.

Table 2.2: One-Way ANOVA to compare the effect of water immersion on *E. faecalis* biofilm between dentine and biomaterial substrata (n=3 per group).

Substratum (reference category)	Mean difference (%) (±SD)	95% CI	P value
Endo-Vu block (Dentine)	0.1 (±0.7)	-0.8, 0.9	1.0
Polystyrene (Dentine)	0.5 (±0.7)	-0.27, 1.3	0.3
Accura (Dentine)	0.1 (±0.7)	-0.8, 0.9	0.9
Photopolymer (Dentine)	0.3 (±0.7)	-0.5, 1.2	0.7

SD= Standard deviation, CI = Confidence interval.

The results revealed that there was no statistically significant difference between biofilm grown on the dentine surface and that on the substratum materials.

2.2.4. Discussion

The present chapter aimed to compare the physico-chemical properties (zeta-potential, wettability, surface free energy) of the potential substratum materials (Endo- Vu block, Polystyrene, Photopolymer, Accura) and to evaluate the substratum potential to develop *Enterococcus faecalis* biofilm. The biomaterial substrata showed similar physico-chemical properties (except the positive charge of the Endo-Vu material) to that of dentine, and they were suitable for growth and attachment of single species biofilm (*E. faecalis*).

The selection of the relevant materials was related for their excellence in terms of optical transparency, which will enable direct and real-time imaging of biofilm removal by antibacterial agents (e.g. NaOCl).

In the present study, the substrata samples were sterilised using the gas plasma method as it has been demonstrated that the gas plasma method was capable of destruction and inactivation of bacterial biofilms (Lloyd *et al.*, 2010). One criticism that can be made in relation to the sterilisation method is that the surface

characteristic of the substrata materials may be affected by the sterilisation technique. In this regard, a pilot experiment (appendix 4) to compare the effect of two sterilisation methods (autoclave, gas plasma) showed that gas plasma procedure had no effect on the substrata materials.

The biofilms on the surface of the test materials were observed using scanning electron microscope, which provided information about the structure and components of the single species biofilm formed on the test materials. However, the study did not measure the thickness of the biofilm. The reason for this is related to the effect of dehydration procedure during SEM sample preparation, which may cause shrinkage of biofilm and subsequently affect the thickness of biofilm (Paz *et al.*, 2015).

Optical microscope and image processing software were used to image biofilm grown onto dentine and each substratum surface. This type of microscope has previously been used to assess oral biofilms growth (Wang *et al.*, 2014), and attachment to substratum (Cerca *et al.*, 2005). One major advantage of this technique is that it allows a direct visualisation of the samples, without need for fixation, dehydration or the disturbing of the biofilm structures. Nevertheless, one limitation associated with the microscopy images was the presence of images surrounded by "halos" around the outlines of details. These are optical artifacts, which may obscure the boundaries of details. This may be related to thickness of samples, which can interfere with light illumination (Wilson and Bacic, 2012).

For standardisation purposes and to reduce chances of bias, the same areas of all samples were examined; five fields of view were selected in the central area of the sample. Although the areas measured may not represent the whole surface

area of the sample, literature suggests that measurements from a regular array of points is more accurate than random assessment (Loebl, 1985).

In order to obtain an alternative *in vitro* model to dentine that allows microbial growth, it is important that these materials exhibit comparable properties to dentine. The physicochemical properties of the test materials were shown to be similar to that of dentine. In the case where the surface charge of the substratum (Endo-VU) was positive, an attraction to the negatively charged surface of the bacterial cell may be responsible for the bacterial adhesion and biofilm formation (Jucker *et al.*, 1996). The negatively charged property of the material may be explained by the aqueous environments applied during measurement that result in more cations that can be solvated in comparison to anions on the surface (Shaw *et al.*, 1988). According to DLVO theory, the negative charges of the bacterial cell (*E. faecalis*) and the substratum materials hinder bacterial adhesion due to charge-charge repulsions (Doyle, 2000). However, the findings of the present study showed that biofilm was able to attach and grow on the materials and dentine. It could be also due to the formation of a conditioning layer over the model's surface by direct proteins adsorption that present within the BHI broth (Lehner *et al.*, 2005). This layer may reverse the charge of the substratum surfaces to positively charge and promote the adhesion of planktonic microbial cells to the solid surface (Donlan, 2002). A second possible reason for the abovementioned bacterial attachment may be related to the hydrophilic properties of the test materials, which serve to overcome the repulsive force that exists between the negatively charged surfaces of both bacterial cells and test materials (Donlan, 2002). The hydrophilic property of the materials could be

related to the hydrophilic hydroxyl groups in the molecules of resin materials (Wang *et al.*, 2010).

The findings of the present study are consistent with other studies that had shown more bacterial attachment on hydrophilic solid surfaces (Absolom *et al.*, 1983; Almaguer-Flores *et al.*, 2012). Nevertheless, another study has failed to identify a correlation between surface hydrophobicity and the attachment of bacteria to a solid surface (Espersen *et al.*, 1994).

Although the distribution of biofilm on the dentine and substratum materials was different, the results showed no significant difference between the surface area coverage with biofilm onto the surface of all substrata and that of dentine. Some factors could explain these results: (a) the level of charges could play a role in the bacterial adhesion, as dentine presented lower negative charges which could reduce the repulsion charges; (b) the roughness of dentine favoured biofilm attachment and subsequent growth, (c) the presence of type I collagen in the dentine could provide extra nutrition for bacterial growth (Kishen *et al.*, 2008). Therefore, the type of substratum can influence the distribution of the grown biofilm.

The results of the physico-chemical properties measured and bacterial adhesion demonstrate that the test materials are an exciting option for the development of a biofilm model to be used for *in vitro* experiments with the advantages of direct visualisation and the development of a biofilm somewhat the same as in the natural environment. This is particularly important to study the outcomes of the interaction between an irrigant (and/or irrigation method) and bacterial biofilm

within the root canal system. In addition, the mechanics of fluids within the root canal could be investigated in real-time.

Overall, the test materials proved to be potential materials to create an *in vitro* biofilm model to study irrigation. However, the adhesion mechanism to the substratum remains to be explored in future investigations.

2.2.5. Conclusion

Within the limitations of the present study, the physical and chemical properties of the test materials (Endo-Vu, Polystyrene, Photopolymer, and Accura) were shown to be comparable to those of dentine, except for the positive charge of Endo-Vu material. Furthermore, they allowed the attachment and growth of *E. faecalis* biofilm onto their surface to a similar extent to that of dentine. The test materials had no antibacterial activity. The tested materials demonstrated good potential for use in *in vitro* tests that require microbial colonization with the advantage of transparency when compared to dentine. This could be applied to the study of root canal disinfection strategies using artificially infected models, in order to evaluate the fluid dynamics of biofilm removal during root canal irrigation.

2.3. The effect of needle position on the velocity distribution of irrigant in the root canal system

2.3.1. Justification of the investigation

Recent evidence suggests that continual replacement of the irrigant solution within the root canal system is an essential factor for maximum chemical action (Basrani, 2015). It has been argued that the confinement of the root canal has an effect on the fluid dynamics of the irrigant by reducing the velocity of irrigation and consequently reducing the irrigant refreshment (Verhaagen *et al.*, 2012). In addition, preparation of the root canal to apical size 25, and taper 0.06 was not adequate for an optimum irrigant flow and penetration (Hsieh *et al.*, 2007; Boutsioukis *et al.*, 2010a). This demonstrates that an effective penetration of irrigant could be achieved in the apical part of at least size 30 and taper 0.06 root canal (Boutsioukis *et al.*, 2010b).

It has been reported that reducing the distance between the end of the irrigation needle and the apical end of the working length result in an improvement of the irrigant replacement during irrigation (Boutsioukis *et al.*, 2010c). However, this conclusion is based on a study using a computational fluid dynamics (CFD) model simulating irrigation delivered from a needle of 30 gauge into a root canal of size 45 and taper 0.06. With such parameters, the space between the canal wall and the needle was adequate for the irrigant flow toward the coronal part of the canal. Hence, there are no data on the flow pattern in a smaller size canal when a decision on the apical enlargement takes into account the possibility of weakening of the root canal structure.

Computational fluid dynamics is a computer-based technique recently used to analyse a system involving flow dynamics by computer simulation and

mathematical modelling of the relevant system (Versteeg and Malalasekera, 2007). The simulation geometry is subdivided into cells (elements), creating a grid on which the equations describing the real physical condition are solved using finite element methods (Dick, 2009).

CFD models have been considered as powerful tools to simulate physical conditions related to the fluid flow within the root canal system and provided details on the fluid dynamics in situations where an experimental measurement is difficult to be achieved (Boutsioukis *et al.*, 2010d).

In this study, CFD was utilized to investigate the effect of needle placement (3 and 2 mm) from the apical terminus on the flow pattern, velocity distribution of irrigant in the root canal system and irrigant replacement.

2.3.2. Materials and methods

A CFD model simulating the root canal was manufactured using ANSYS software version 15.0, (2013) (ANSYS, Inc., Washington, Pennsylvania, USA). The model was created as a frustum of a cone with 18 mm length, 0.06 taper. The cone diameter at the wider orifice was 1.38 mm, and 0.30 mm (ISO size 30) at the most apical terminus that was simulated as an impermeable and rigid wall. A 27-gauge side-cut open-ended needle (Monoject, Sherwood Medical, St. Louis, MO, USA) was used as a reference to create a model of the irrigation needle. The external and internal diameter and the length of all needles was standardized ($D_{external}$ = 0.420 mm, $D_{internal}$ = 0.184 mm, length = 31 mm) (Figure 2.7). The needle was centred within the CFD model of the root canal. A 2.5% NaOCl irrigant was modelled as Newtonian incompressible fluid (Tilton, 2008), with a viscosity μ = 0.001073 Pa. s, density = 1.06 g/cm3 and temperature= 22 ºC (Guerisoli *et al.*,

1998). The irrigant delivered at a flow rate of 0.15 mL s^{-1} using a needle, which was modelled at 2 levels (3 mm & 2 mm) short of the apical terminus (0.3 mm).

ANSYS Fluent Meshing (Pre-processing) software (ANSYS, Inc., Washington, Pennsylvania, USA) was used to construct the computational cells required for building of a hexahedral mesh of the model. No-slip boundary conditions were performed to the walls of the root canal and needle models. Irrigation at a flow rate of 0.15 mL s^{-1} was imposed at the needle inlet. The package of commercial ANSYS software was used to analyse the outcomes of the irrigation procedure. The simulation was performed for 10-step time of 0.001 second interval. The flow patterns computed for the two cases (3 mm & 2 mm) were compared in terms of fluid flow, velocity magnitude, and replacement throughout irrigation after delivery from the outlet of the irrigation needle.

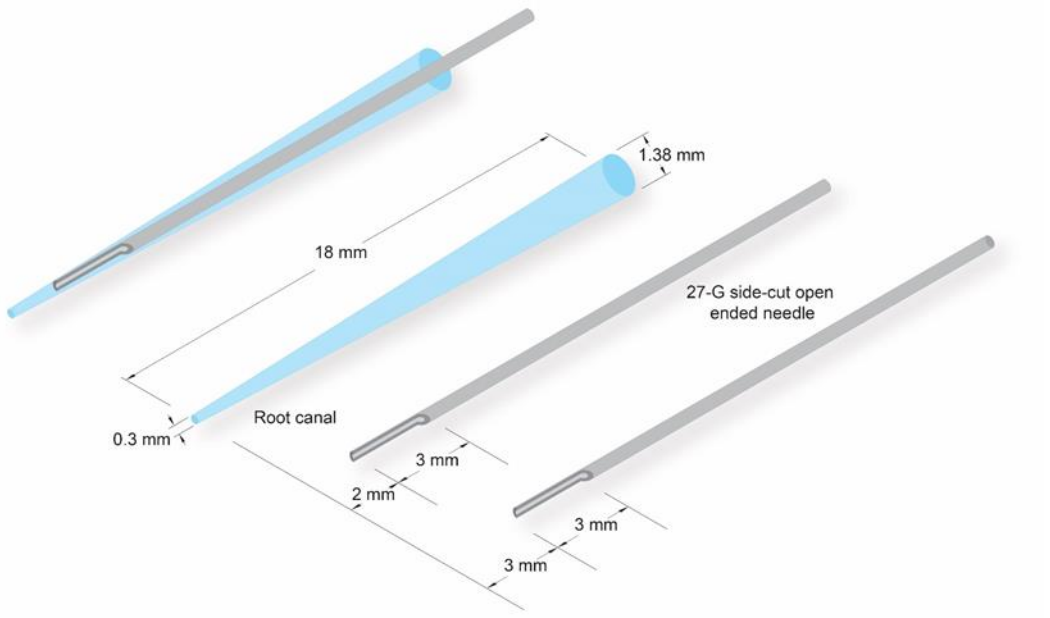

Figure 2.7: Sketch of the design of the computational fluid dynamics model.

2.3.3. Results

The CFD simulations of the velocity magnitude of irrigation during 10-step times along a specific part of the root canal geometry just apical to the tip of the irrigation needle placed at 3 and 2 mm from the apical terminus are presented in Figure 2.8 and 2.9 respectively.

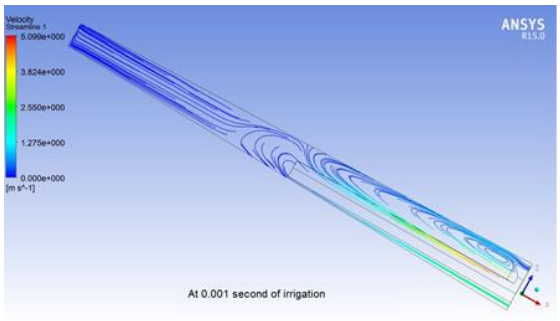

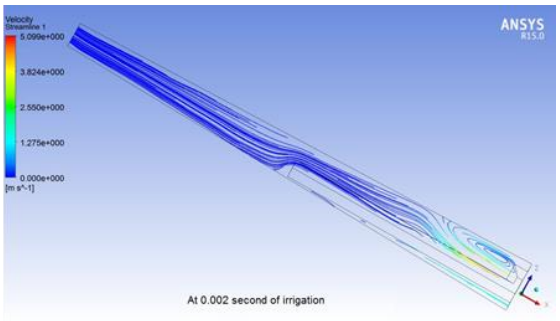

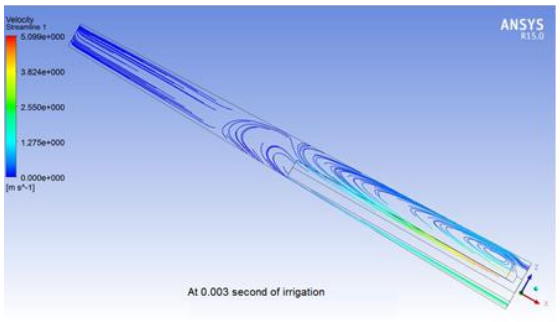

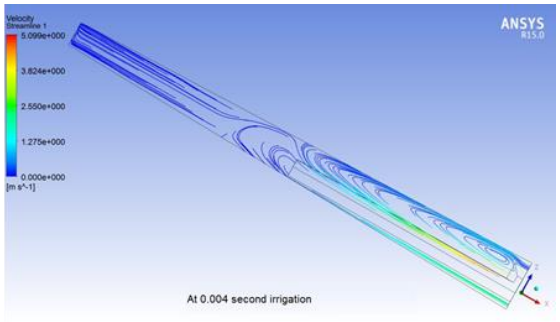

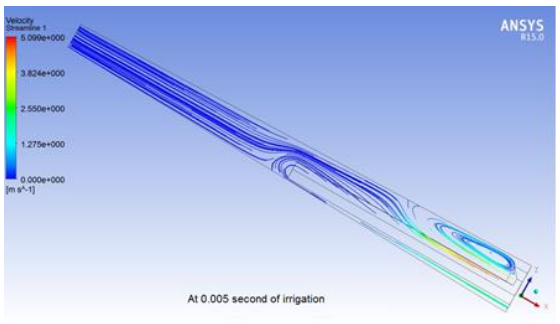

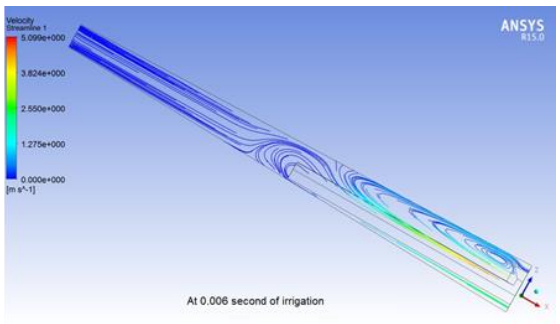

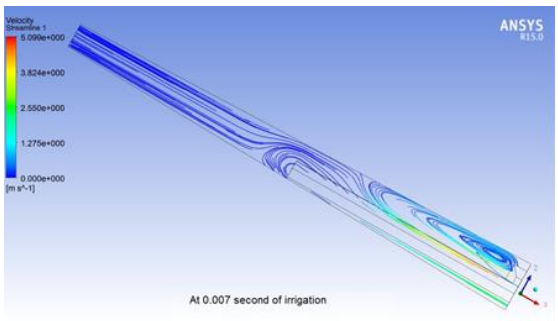

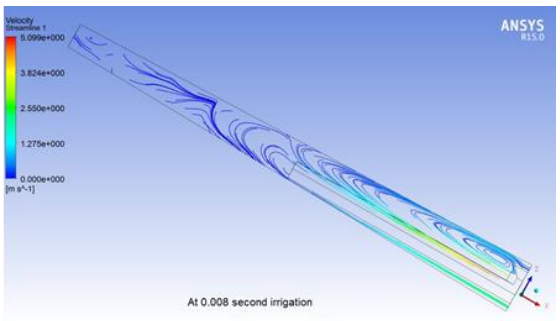

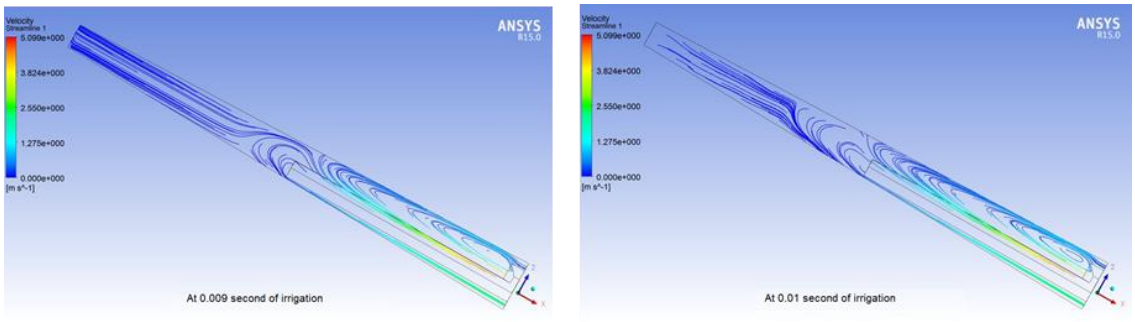

Figure 2.8: CFD images illustrate the velocity magnitude of irrigation during 10-step times (0.001 – 0.01 seconds) in the root canal geometry just apical to the tip of the irrigation needle place at 3 mm from the apical terminus.

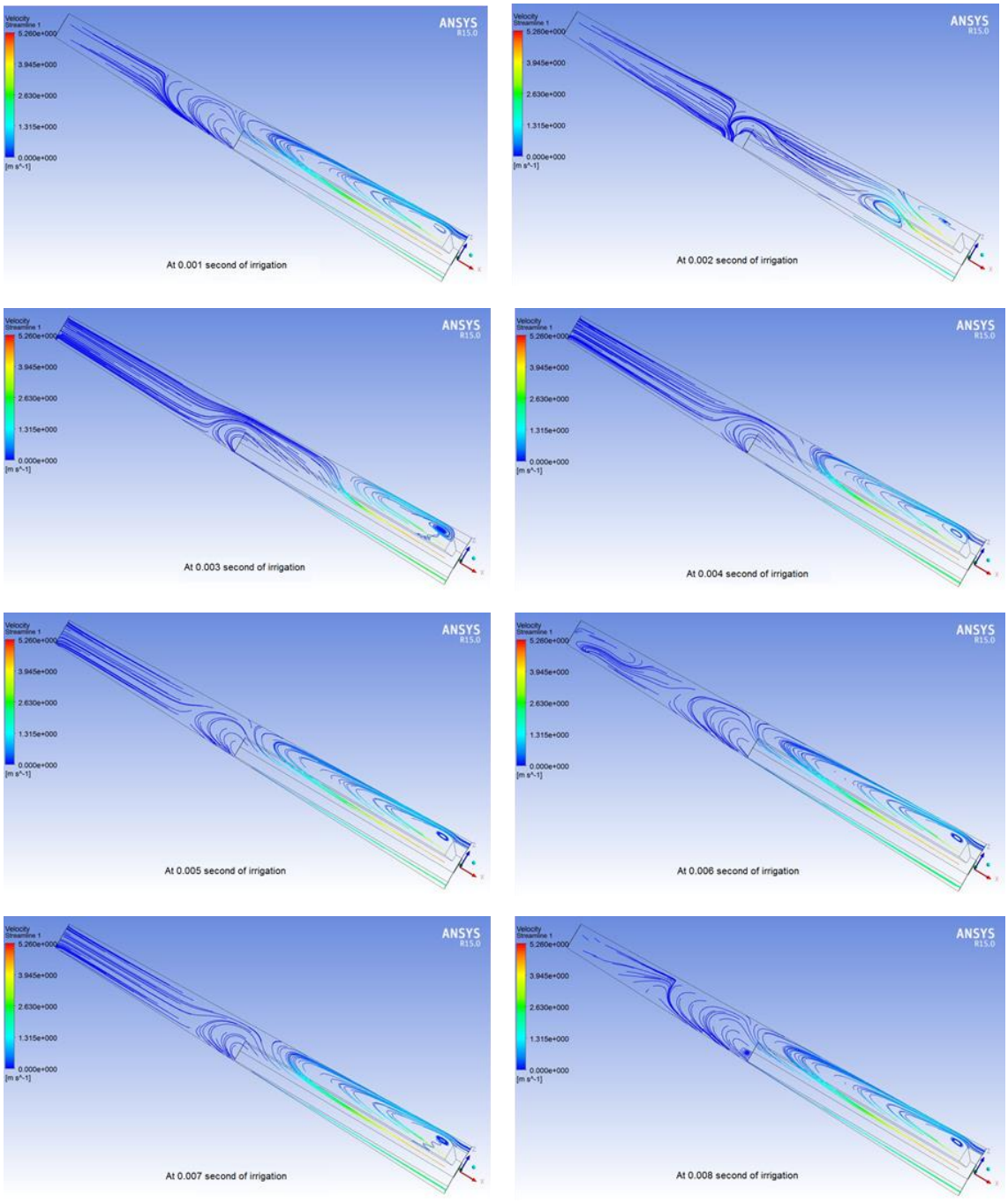

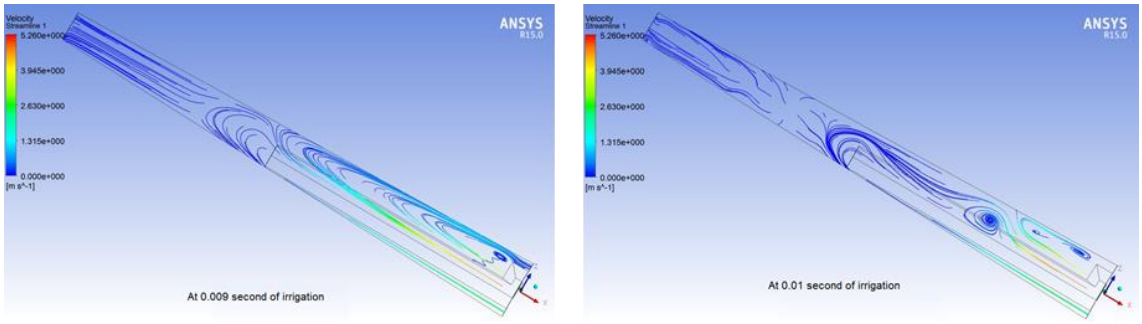

Figure 2.9: CFD images illustrate the velocity magnitude of irrigation during 10-step times (0.001 – 0.01 seconds) in the root canal geometry just apical to the tip of the irrigation needle place at 2 mm from the apical terminus.

Regardless of the needle position, the CFD outcomes showed that the irrigant flow was unsteady non-uniform as the velocity magnitude was not the same at every point along the apical part of the root canal. The velocity streamline of the irrigant flow delivered at flow rate 0.15 mL s^{-1} demonstrated considerably high velocity magnitude at the needle outlet (5.099 m s^{-1} & 5.260 m s^{-1} from needle tip positioned at 3 mm and 2 mm from the canal terminus). Then the velocity magnitude was drastically decreased to zero at the apical terminus. This demonstrates that irrigant flow movement towards the canal terminus was weak.

Once the irrigation protocol was established, the irrigation fluid flowed in a circular pattern and a series of vortices formed just apically to the side-cut end open-ended needle. The size of vortices increased as needle was placed closer to the canal terminus (2 mm). However, the needle placed at 3 mm allowed more irrigant replacement than the needle at 2 mm.

2.3.4. Discussion

The present study was designed to investigate the effect of the needle tip position from the canal terminus (3 mm & 2 mm) on irrigant flow within the root canal. The finding revealed that the two needle levels appeared to have a limited influence on the flow pattern generated within the apical part of the tapered canal. In

addition, extending the needle toward the apical terminus did not result in significant increase in flow and replacement of irrigant.

In the present study, computational fluid dynamics simulation of the root canal and irrigation procedure was conducted to explore the aims as the set of CFD model has been used in a previous study to provide quantitative data regarding the fluid dynamic of irrigation protocols within the confinement of the root canal system. (Boutsioukis *et al.*, 2010a; Boutsioukis *et al.*, 2010b; Shen *et al.*, 2010a). However, CFD simulation does not account for the chemical action of an irrigation solution as well as the effect of intracanal biofilm on the irrigant efficacy (Versiani *et al.*, 2015).

In the current study, the observed eddies at the tip of the side-cut open-ended needle may be attributed to the fluid circulation between the side-cut of the needle and the canal walls (Boutsioukis *et al.*, 2010b). However, the size of eddies was reduced as the velocity decreases toward the apical end. A possible explanation for this might be related to the effect of taper confinement of the canal (Verhaagen *et al.*, 2012). Some degree of irrigant replacement was noted in case the needle was placed 3 mm away from the canal end. This could be attributed to the space between the needle and canal walls (0.02 mm) (Boutsioukis *et al.*, 2010a). In comparison, extending the needle deeper to the canal end (2 mm) resulted in the reduction in irrigant replacement because at this point there was no clearance between the needle and root canal.

These findings may help us to understand the flow pattern of irrigant within the root canal. However, at present it is not known what the maximum efficacy of

irrigation is to remove bacterial biofilm by its chemical action. Thus, a further study with more focus on irrigant-bacterial biofilm interaction is therefore suggested.

2.3.5. Conclusion

Within the limitation of the present study, the position of the irrigation needle from the canal terminus had no effect on the flow pattern. Maximum velocity was identified at the needle tip, which followed vortices pattern. The fluid velocity decreased toward the terminal end. Although inserting the needle toward the canal terminus resulted in vortices closer to the canal terminus, the irrigant replacement reduced.

Chapter 3

Investigations into the effect of root canal design (closed, open) on the efficacy of 2.5% NaOCl to remove bacterial biofilms or organic films

3.1. Introduction

It has previously been reported that the fluid dynamics of liquid within closed end conical channels is reduced because of air entrapment (Dovgyallo *et al.*, 1989). The tapered confinement of the root canal system and periapical tissue enclosing the root apex causes the root canal to behave as a closed canal system (Adcock *et al.*, 2011). Studies investigating the debridement efficacy of irrigant delivered into a closed and an open canal system have been carried out (Tay *et al.*, 2010; Parente *et al.*, 2010). Conclusions derived from such investigations suggested the adverse effect of apical vapour lock on the efficacy of irrigation within the closed root canal system when compared with the open canal system that exhibited no restriction to the fluid flow. However, these studies have only assessed debris removal by irrigation and lacked any information about bacterial biofilm removal, which is the crucial aim of the root canal treatment (Siqueira *et al.*, 2002). Therefore, the efficacy of irrigation protocol to remove bacterial biofilm from a closed and an open root canal system has not been assessed in a single study.

In laboratory experiments, two organic molecule films have been used in test models to represent biofilms to study their interaction with irrigants within the root canal system. The simulant biofilm includes the collagen film (Huang *et al.*, 2008) and hydrogel film (de Macedo, 2013). The rationale is to use films with similar mechanical, adhesive and degradation properties similar to bacterial biofilms to eliminate the complications associated with live bacterial systems (Verhaagen *et*

al., 2012). Standardized growing and controlling of bacterial biofilms is infinitely complicated and subject to variation (Gulabivala *et al.*, 2005). Nevertheless, the simulant films must meet certain basic requirements to act as representative substitutes (Kishen and Haapasalo, 2010).

The present investigation was therefore carried out to:

- Develop and utilise simple and transparent test models to facilitate the assessment of the removal amount of *Enterococcus faecalis* biofilm and organic films (hydrogel, collagen) during irrigation procedure using 2.5% NaOCl delivered into a closed and an open root canal models,
- To investigate the effect of root canal design (closed, open) on the efficacy of 2.5% NaOCl to remove bacterial biofilms or organic films (hydrogel, collagen),
- Compare the difference in response to NaOCl irrigation between biofilm and organic films (hydrogel, collagen) using the removal rate, available chlorine, and pH of the outflow NaOCl, as outcome measures.

3.2. Material and methods

3.2.1. Preparation of simple anatomy canal models

Thirty-six Endo-Vu blocks were used to create the root canal models used herein. The Endo-Vu blocks, which are made of polymethyl methacrylate (Richard W. Pacina, Waukegan, Illinois, USA) with straight simple canals. Each canal was enlarged to apical size 30 with a 0.06 taper using nickel titanium rotary instruments (Profile system, Dentsply, Maillefer, Ballaigues, Switzerland) in a crown-down sequence; specifically, with a low-speed (300 rpm) and 70:1 controlled-torque rotary hand piece. During the instrumentation process, all

canals were irrigated with demineralized water (Roebuck, London, UK). The working length was set at the apical canal terminus in all models.

3.2.2. Longitudinal sectioning of the canal models

Before sectioning the canal models into two equal longitudinal halves, four holes were drilled on either side of the Endo-Vu blocks using a size-63 drill bit (Dormer, Sheffield, UK) attached to a mini grinder (Marksman, Birmingham, UK). The block was then sectioned transversely just apical to the end of the canal using a diamond disk (75 × 0.15 × 12.7 mm) (Struers, Ballerup, Denmark). This disk was attached to a precision cutting machine (Struers Accutom 50, Copenhagen, Denmark) with a 1000 rpm wheel speed, low force limit and 200 mm/s feed speed. The portion containing the prepared canal was then sectioned longitudinally using a diamond disc. During cutting, the block was fixed to the specimen holder and its position was set using the step motor of the machine (Figure 3.1).

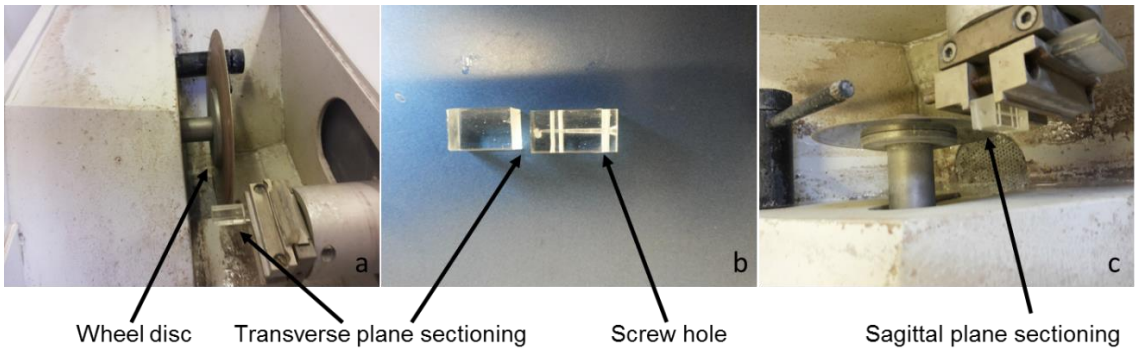

Figure 3.1: Photographic images illustrate the sectioning procedure of an Endo-Vu block into two sagittal halves: (a) sample and wheel position; (b) transverse sectioning of the model; (c) sagittal sectioning of the model.

3.2.3. Allocation of models to experimental groups

The models were divided into two main groups (A, B) (Table 3.1), with the closed canal models comprising group A (n = 18) and the open canal models comprising group B (n = 18). The models within each group were randomly subdivided into

three equal subgroups for the application of a hydrogel (subgroup 1) (n = 6) or collagen (subgroup 2) (n = 6), or the generation of a bacterial biofilm (*Enterococcus faecalis*) (subgroup 3) (n = 6). After the application of the organic film or generation of a biofilm, the models were then randomly allocated for irrigation with either 2.5% NaOCl (n = 3) or demineralized water (control group) (n = 3).

Table 3.1: Allocation of the root canal models

Group	Subgroups (1-3)	
A (closed canal models) (n = 18)	(1) Hydrogel (n = 6)	2.5% NaOCl (n = 3)
		Demineralized water (n = 3)
	(2) Collagen (n = 6)	2.5% NaOCl (n = 3)
		Demineralized water (n = 3)
	(3) Biofilm (n = 6)	2.5% NaOCl (n = 3)
		Demineralized water (n = 3)
B (open canal models) (n = 18)	(1) Hydrogel (n = 6)	2.5% NaOCl (n = 3)
		Demineralized water (n = 3)
	(2) Collagen (n = 6)	2.5% NaOCl (n = 3)
		Demineralized water (n = 3)
	(3) Biofilm (n = 6)	2.5% NaOCl (n = 3)
		Demineralized water (n = 3)

3.2.4. Preparation and application of stained organic films (hydrogel, collagen) on the canal wall (subgroups 1, 2)

A hydrogel was prepared by dissolving 3 g of gelatine (Merck, Whitehouse Station, NJ, USA) and 0.06 g of hyaluronan (sodium hyaluronate 95%, Fisher, Waltham, MA, USA) in 45 mL of distilled water at 50 ºC on a stirrer (Popa *et al.*, 2011). The collagen (Type I rat tail collagen) was used exactly as received,

without any modifications (First Link Ltd., West Midlands, UK). Japanese orange ink (Guanghwa, London, UK) (0.2 mL) was mixed with 15 mL of hydrogel or collagen on a stirrer (Bibby Scientific Ltd, Stone, UK). Four layers of the designated organic film (hydrogel for subgroup 1, collagen for subgroup 2) were applied along the most apical 3 mm of one root canal half using a nylon detail brush (Blodmere, Wakefield, UK), a process adapted from Huang *et al.* (2008).

3.2.5. Generation of single species biofilm (*Enterococcus faecalis*) on the surface of the root canal models (subgroup 3)

3.2.5.1. Preparation of microbial strain and determination of the standard inoculum (CFU/mL)

The preparation of microbial strain (*E. faecalis*) and standard inoculum determination were performed as described in section 2.2.2.4.2.

3.2.5.2. Sterilisation of Endo-Vu block canal model

Each half of the model was sterilised separately in empty 7 mL plastic bottles (Sarstedt Ltd, Nümbrecht, Germany). A silicone gasket (Biosurface Technologies Corporation, Bozeman, Montana, USA) was placed in a plastic bottle with the model half for which no biofilm would be generated. For the other model half, the apical 3 mm length of the canal was marked using a black waterproof pen (Sarstedt Ltd, Nümbrecht, Germany). The coronal 3 mm of this half was inserted into 1.5 mL Eppendorf tubes (Eppendorf, Hamburg, Germany). This apparatus (Figure 3.2) was then placed in another plastic bottle. A total of twenty-four halves of twelve canal models from subgroup 3 were sterilised in a steam autoclave (Ascot Autoclaves Ltd, Berkshire, UK) (121°C, 103.421 kpa, 30 minutes) (Farrugia *et al.*, 2015).

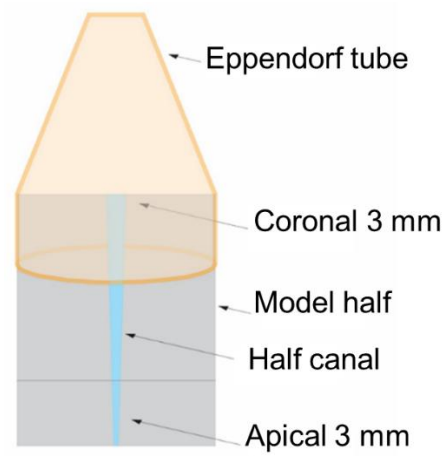

Figure 3.2: Schematic diagram illustrating the set-up of the apparatus.

3.2.5.3. Generation of single species biofilm on the canal surface of the model

One mL of standard *E. faecalis* inoculum (1.1×10^8 CFU/mL) was delivered into a sterilised 7 mL plastic bijou bottle that contained the sterilised half model. The apparatus incubated at 37 °C in a 5% CO_2 incubator (LEEC, Nottingham, UK) for 7 days. A sterile syringe (BD Plastipak™, Franklin Lakes, NJ, USA) and a 21-gauge needle (BD Microlance™, Franklin Lakes, NJ, USA) were used to immerse the 3 mm apical portion of the half model (Figure 3.3). Every three days, half of the inoculum that surrounded the model was discarded and replaced with fresh BHI broth (De-Deus *et al.*, 2007).

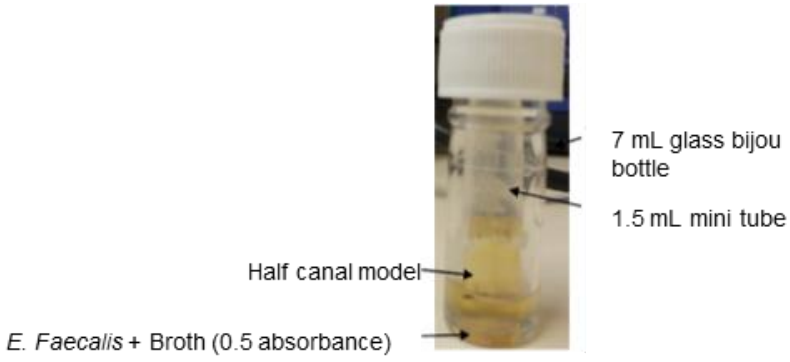

Figure 3.3: Photographic image illustrates the set-up of the apparatus used to generate single species biofilm (*E. faecalis*) on the canal model.

3.2.5.4. Staining of biofilms grown on the surface of the models

After one week of incubation all model halves with biofilms were removed from the plastic bottle and prepared for staining with a crystal violet (CV) stain in order to reveal any relevant changes as a result of the irrigation experiments. Each model half with a biofilm was placed on a microscopic slide. The model was rinsed with distilled water (Roebuck, London, UK) to remove loosely attached cells. Using a pipette (Alpha Laboratories Ltd, Eastleigh, Winchester, UK), 2 µL of CV stain (Merck, Darmstadt, Germany) was applied to the part of the canal half where the biofilm had been generated (3 mm) and left for 1 minute for staining. It was subsequently washed with distilled water (Izano *et al.*, 2007).

3.2.6. Re-apposition of the model halves

Before reassembling the two model halves, the silicone gasket was positioned on the half coated with organic film or biofilm. Any part of the gasket that overhung the canal boundary was removed using a surgical blade (Swann-Morton, Sheffield, UK) without disturbing the film or biofilm. The two halves of the model were then held in position using four brass bolts (size 16 BA) and nuts (Clerkenwell Screws, London, UK) (Figure 3.4).

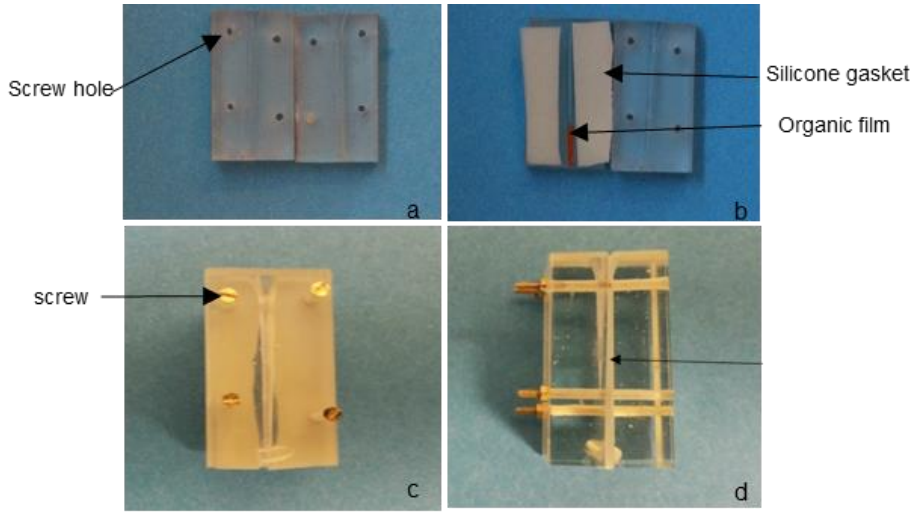

Figure 3.4: Photographic images illustrating the re-assembling of the two halves of the canal model: (a) sagittal halves of the canal model; (b) silicone gasket and organic film positions; (c) front view of the model; (d) side view of the model.

3.2.7. Irrigation experiments

3.2.7.1. Experimental set-up

For the closed canal models (Group A), the apical end of each canal was blocked using sticky wax (Associated Dental Product Ltd, Swindon, UK). Each model was fixed to a plastic microscopic slide (75×25×1.2 mm) (Fisher Scientific Ltd, Rochester, NY, USA) using a custom-fabricated clamp. The half with the organic film or biofilm faced the slide. The microscopic slide was placed on the stage of an inverted fluorescent microscope (Leica DMIRB, London, UK). A total of 9 mL of irrigant (NaOCl or water) was used as an intracanal irrigant. Concentration of available chlorine in the NaOCl (Teepol® bleach, Teepol products, Egham, UK) was verified before experiments using iodometric titration (British Pharmacopoeia 1973) and adjusted to 2.5% (Appendix 5). The irrigant was delivered using a 10 mL syringe (Plastipak, Franklin Lakes, New Jersey, USA) with a 27-gauge side-cut open-ended needle (Monoject, Sherwood Medical, St. Louis, MO, USA). The needle was inserted into the canal just coronal to the organic film or biofilm. The port opening of the needle always faced the model half containing the organic

film or biofilm. The syringe was attached to a programmable precision syringe pump (NE-1010; New Era Pump Systems, Wantagh, NY, USA) in order to deliver the irrigant at a flow rate of 0.15 mL s^{-1}. For each canal, a total of 9 mL of irrigant was delivered during a period of 1 minute. The outflow irrigant was collected in a 15 mL plastic tube (TPP, Switzerland), using a vacuum pump (Neuberger, London, UK).

3.2.7.2. Recording of organic film or biofilm removal by the irrigant

The rate of film or biofilm removal was recorded using a high-resolution CCD camera (QICAM Fast 1479, Toronto, Canada). The camera was connected to a 2.5× magnification lens of the fluorescent microscope. During the time-lapse recording of interactions between the irrigant and the organic film or biofilm, both fluorescing (red filter) and non-fluorescing (intensity of 2.5 W/m^2) light was used to achieve a better resolution (Figure 3.5).

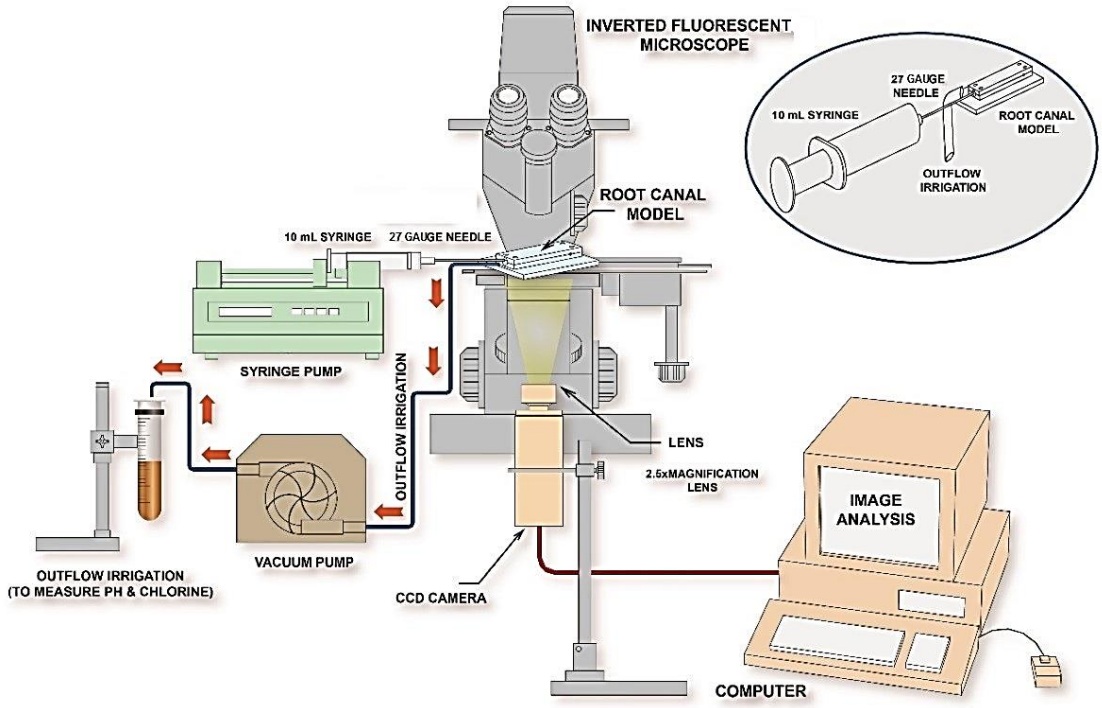

Figure 3.5: Sketch illustrating the set-up of equipment for recording of the organic film or biofilm removal by NaOCl irrigation protocol using a camera connected to a 2.5× lens of an inverted fluorescent microscope. The irrigant was delivered using a syringe with a 27-gauge side-cut open-ended needle, which was attached to a programmable precision syringe pump. The residual biofilm was quantified using computer software (Image-pro Plus 4.5). Outflow irrigant was collected in a plastic tube using a vacuum pump. The amount of available chlorine (%) and pH were measured using iodometric titration and a pH calibration meter respectively.

3.2.8. Image analysis

The video-captured recording was separated into sixty images according to each second of footage using Image J 1.4 and micro-imaging software 1.4 (Media Cybernetics Inc., Rockville, MD, USA). The images were analysed using Image-pro Plus 4.5 and ipWin4 software (MediaCybernetics®, Silver Spring, Maryland, USA). Canal surface coverage by residual organic film or biofilm present after every second of irrigation (0.15 mL) was quantified.

3.2.9. Measurement of available chlorine and pH of outflow NaOCl

After one minute of the irrigation protocol the amount of available chlorine (%) and pH of the outflow NaOCl were measured using iodometric titration (British

Pharmacopoeia 1973) and a pH calibration meter (HANNA pH 211, Hanna Instrument, UK) respectively.

3.2.10. Data analysis

The data representing the mean percentages of residual biofilm or residual stained film (hydrogel, collagen) covering the root canal surface present at the baseline and after every second of the 9 mL/minute irrigation protocol were first entered into an Excel spread sheet (Microsoft®, Redmond, Washington, USA) and then into an SPSS database (BM Corp. Released 2013. IBM SPSS Statistics for Windows, Version 22.0. Armonk, NY: IBM Corp).

The residual organic film (hydrogel, collagen) or biofilm present during irrigation with an irrigant (NaOCl or water) delivered into the root canal model (closed or open) were observed using line plots. The data representing the percentages of canal surface coverage by a residual organic film or biofilm in the root canal model were compared using analysis of variance (ANOVA). The effects of irrigation duration on the percentage of residual biofilm or film (hydrogel, collagen) covering the root canal surface were analysed by type of test target [film (hydrogel, collagen) or biofilm], type of canal model (closed or open) and type of irrigant (NaOCl or water) using generalised linear mixed models (GLMMs). Robust standard errors were used to account for the clustering effects of repeated measurements taken from the canal surfaces.

A GLMM was also used to analyse the effects of the type of organic film or biofilm on the available chlorine and pH of outflow NaOCl. A significance level of 0.05 was used throughout. Based on the data analysis, an estimation was calculated for the sample size using Stata software version 12 (STATA Corporation®, Texas

2011) in order to determine the exact sample size required to obtain robust statistical results of the study.

3.3. Results

3.3.1. Observations of irrigation experiments

Interesting observations were made during the experimental procedures:

The removal of an organic film (hydrogel or collagen) (Figures 3.6 and 3.7) or biofilm (Figure 3.8) by intracanal irrigation was more extensive in the open canal model than in the closed canal model. Independent of canal model, the removal of the biofilm was less effective than the removal of the organic films.

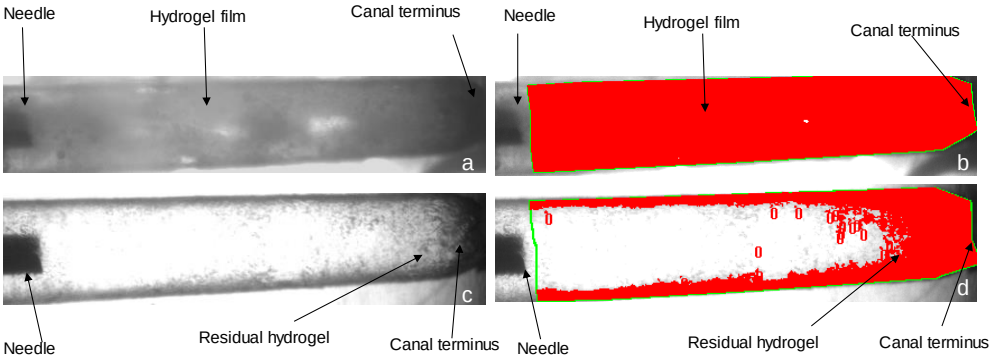

Figure 3.6: Images illustrate the stained hydrogel film on the canal surface of the open canal model: (a) before and (c) after 60 seconds of irrigation using NaOCl in an open canal model. Image-pro plus 4.5 software depicts the respective stained organic film in red (b, d).

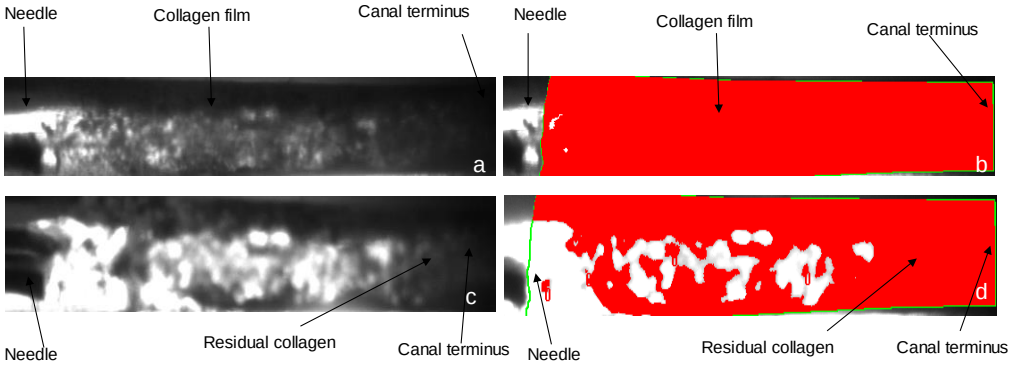

Figure 3.7: Images illustrate stained collagen film on the canal surface of the open canal model (a) before and (c) after 60 seconds of irrigation using NaOCl in an open canal model. Image-pro plus 4.5 software depicts the respective stained organic film in red (b, d).

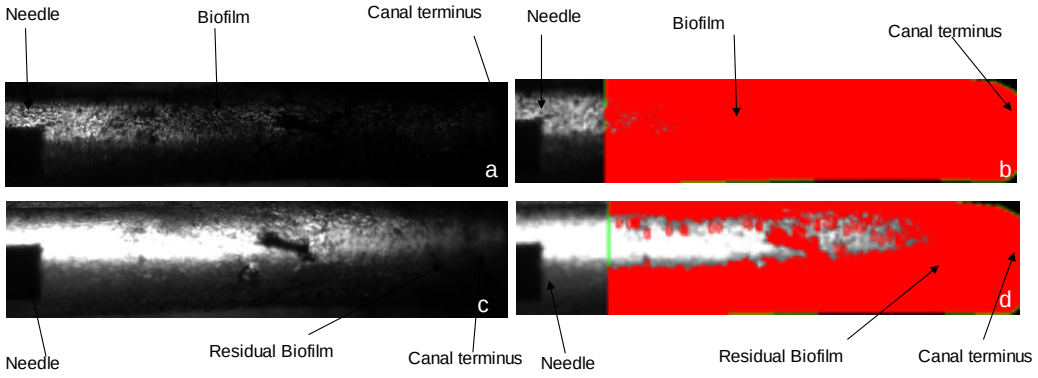

Figure 3.8: Images illustrate stained *E. faecalis* biofilm on the canal surface of the open canal model (a) before and (c) after 60 seconds of irrigation using NaOCl in an open canal model. Image-pro plus 4.5 software depicts the respective stained biofilm in red (b, d).

The removal of the organic films (hydrogel or collagen) or biofilm using a NaOCl irrigant was more effective than removal by water during the irrigation of the root canal models (closed or open) (Figure 3.9).

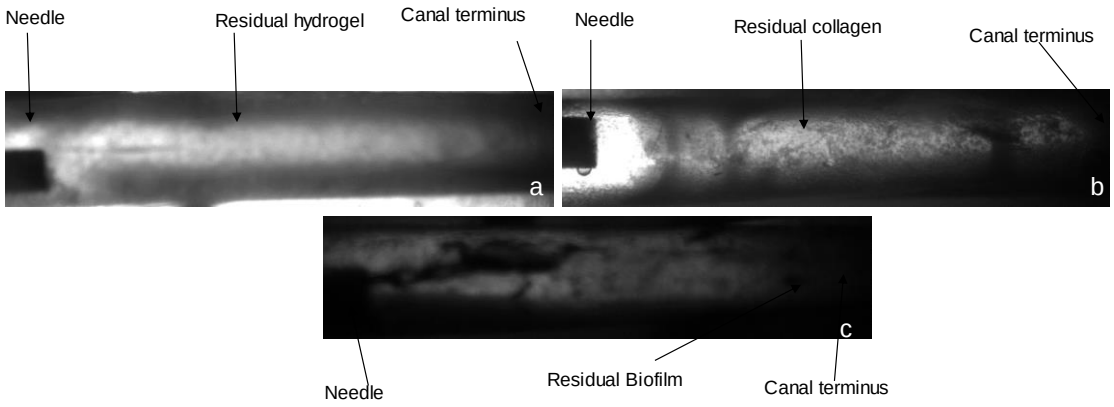

Figure 3.9: Images depict residual stained (a) hydrogel, (b) collagen film, and (c) biofilm on the canal surface of an open canal model after 60 seconds of irrigation with water.

Air bubbles were only detected in the closed canal models during the NaOCL irrigation protocol for the organic films (hydrogel, collagen) or biofilm (Figure 3.10).

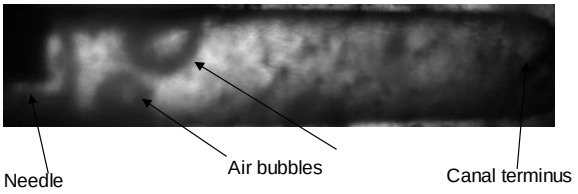

Figure 3.10: Image showing the presence of air bubbles after 25 seconds of irrigation for the biofilm removal using NaOCl in a closed canal model.

3.3.2. Results of statistical analyses

3.3.2.1. Organic film (hydrogel or collagen) or biofilm (*E. faecalis*) removal by irrigant (NaOCl or water) in the root canal model (open or closed)

Using plot graphs of the data, initial investigations were carried out to understand trends in biofilm or organic film removal by irrigants during the period of irrigation. The mean (95% confidence intervals) percentages of the canal surface-area coverage with residual organic film (hydrogel or collagen) or biofilm against duration of irrigation(s), stratified by canal model (closed or open) and irrigant (NaOCl or water) are presented in Figure 3.11.

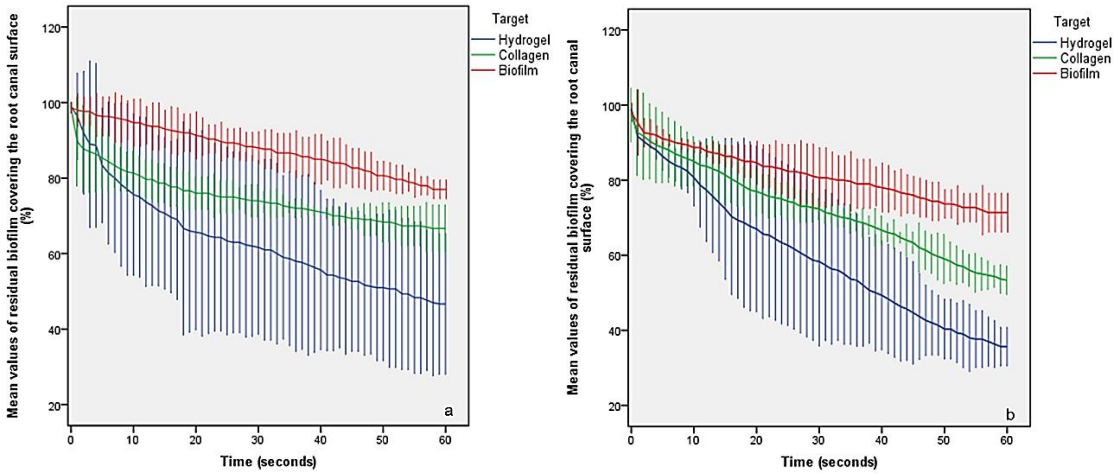

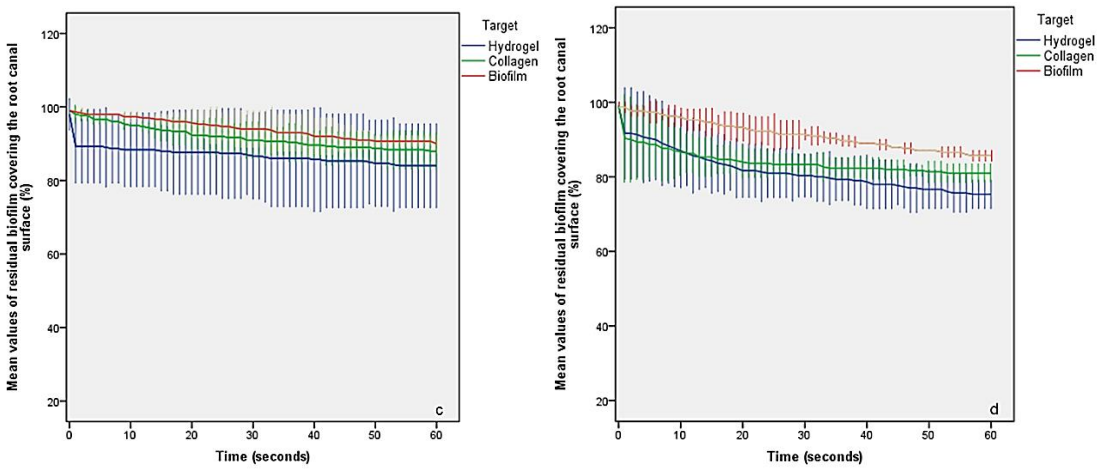

Figure 3.11: Mean percentages (95% confidence intervals) of residual biofilm or residual stained film (hydrogel, collagen) covering the root canal surface over duration (s) of irrigation. (a) NaOCl irrigation delivered into closed canal, (b) NaOCl irrigation delivered into open canal, (c) Water irrigation delivered into closed canal, (d) Water irrigation delivered into open canal.

The data revealed a consistent pattern, with the rate of removal being the lowest for *E. faecalis* biofilm and greatest for hydrogel, regardless of open or closed canal status or type of irrigant. NaOCl irrigation was associated with a substantially higher rate of removal than water irrigation. There was a small but observably greater rate of removal of organic film or biofilm existed in open canals when compared to that of closed canals.

3.3.2.2. Comparison of final residual biofilm or residual stained film (hydrogel, collagen) covering the root canal model

The results of ANOVA analyses (Table 3.2) showed that there was a statistically significant difference following NaOCl irrigation in the closed model groups between the residual biofilm on the canal surface and the hydrogel film ($p = 0.001$).

Regarding NaOCl irrigation in the open model groups, the difference was statistically significant between the residual biofilm and both hydrogel and collagen films ($p = 0.001$). In addition, it is apparent from the table that the difference was statistically significant between the collagen and hydrogel film following NaOCl irrigation and regardless of canal type ($p \leq 0.05$).

In comparison, following a 60-second irrigation of open canals, the difference was statistically significant between the residual biofilm and both hydrogel and collagen films (p = 0.001). Likewise, the difference was significant between the hydrogel film and the collagen film (p = 0.002).

Table 3.2: ANOVA analyses compare the amount of residual biofilm or film (hydrogel, collagen) following 60 seconds irrigation (NaOCl, water) delivered into the root canal model (closed, open) (n = 3 per group).

Experimental groups	Irrigation	Model	Mean difference (%) (±SE)	95% CI	P value
Biofilm vs hydrogel	NaOCl	closed	30.3 (±3.8)	17.9, 42.7	**0.001**
Biofilm vs collagen	NaOCl	closed	10.3 (±3.8)	-2.0, 22.7	0.100
Collagen vs hydrogel	NaOCl	closed	20.0 (±3.8)	7.6, 32.3	**0.005**
Biofilm vs hydrogel	NaOCl	open	35.7 (±1.7)	30.5, 40.8	**0.001**
Biofilm vs collagen	NaOCl	open	18.0 (±1.7)	12.9, 23.1	**0.001**
Collagen vs hydrogel	NaOCl	open	17.7 (±1.7)	12.5, 22.8	**0.001**
Biofilm vs hydrogel	water	closed	6.0 (±2.4)	-1.9, 13.9	0.140
Biofilm vs collagen	water	closed	2.0 (±2.4)	-5.9, 9.9	1.000
Collagen vs hydrogel	water	closed	4.0 (±2.4)	-3.9, 11.9	0.441
Biofilm vs hydrogel	water	open	10.3 (±0.9)	7.4, 13.3	**0.001**
Biofilm vs collagen	water	open	4.7 (±0.9)	1.7, 7.6	**0.001**
Collagen vs hydrogel	water	open	5.7 (±0.9)	2.7, 8.6	**0.002**

SE= standard error, CI = Confidence interval.

3.3.2.3. The removal rate of biofilm or stained film (hydrogel, collagen) covering the root canal model (closed, open)

The results from the GLMM analysis (Table 3.3) revealed that the duration of irrigation had an influence on the mean percentages of biofilm or stained films covering the root canal surface of the experimental subgroups. This was statistically significant (p = 0.001), with the exception of those with closed canals that contained hydrogel (p = 0.1) or collagen (p = 0.7) which were irrigated with water. Among those canals irrigated with NaOCl, the rate of hydrogel removal

was higher than the rate of collagen and biofilm removal, regardless of whether the canals were closed or open.

Table 3.3: Generalized linear mixed models analyzing the effect of time on the area percentage of canal surface coverage with residual film or biofilm for each experimental group (n = 3 per group).

Experimental groups	*Coefficient for removal rate (% s^{-1})	95% CI	P value
Hydrogel film, closed canal, NaOCl irrigant	-0.8	-1.01, -0.6	**0.001**
Hydrogel film, closed canal, water irrigant	-0.1	-0.2, 0.01	0.1
Hydrogel film, open canal, NaOCl irrigant	-0.9	-1.09, -0.9	**0.001**
Hydrogel film, open canal, water irrigant	-0.3	-0.3, -0.2	**0.001**
Collagen film, closed canal, NaOCl irrigant	-0.5	-0.5, -0.4	**0.001**
Collagen film, closed canal, water irrigant	-0.01	-0.05, 0.07	0.7
Collagen film, open canal, NaOCl irrigant	-0.6	-0.7, -0.5	**0.001**
Collagen film, open canal, water irrigant	-0.2	-0.2, -0.1	**0.001**
Biofilm, closed canal, NaOCl irrigant	-0.4	-0.4, -0.3	**0.001**
Biofilm, closed canal, water irrigant	-0.2	-0.2, -0.1	**0.001**
Biofilm, open canal, NaOCl irrigant	-0.4	-0.4, -0.3	**0.001**
Biofilm, open canal, water irrigant	-0.2	-0.2, -0.1	**0.001**

*Coefficient for removal rate represents the rate of organic film or biofilm removal, CI = Confidence interval.

3.3.2.4. Comparison of available chlorine in outflow NaOCl following irrigation to remove biofilm or films (collagen, hydrogel) from the root canal model (closed, open)

The mean values of the available chlorine present in the outflow NaOCl are presented in Table 3.4.

Table 3.4: Mean values of available chlorine (Total n = 18, n = 3 per group) of NaOCl before and after 60 seconds of irrigation of the organic film (hydrogel, collagen) or biofilm in the root canal models (closed, open).

Experimental subgroups (n = 3)	% of chlorine of NaOCl before irrigation (time = 0 seconds)	% of chlorine of NaOCl after irrigation (time = 60 seconds) (±SD)
Biofilm, closed canal, NaOCl	2.5	2.2(±0.1)
Biofilm, open canal, NaOCl	2.5	1.9(±0.3)
Collagen, closed canal, NaOCl	2.5	1.9(±0.3)
Collagen, open canal, NaOCl	2.5	1.7(±0.4)
Hydrogel, closed canal, NaOCl	2.5	1.6(±0.4)
Hydrogel, open canal, NaOCl	2.5	1.5(±0.5)

SD= Standard deviation

The results (Table 3.5) showed that the reduction of available chorine in the outflow solution was minimal for all subgroups. The results obtained from GLMMs analysis (Table 7) revealed that the chlorine available in the outflow solution collected from the canals containing biofilm was 0.2% (95% CI: 0.1, 0.3) more than the chlorine available in the outflow solution collected from canals containing hydrogel or collagen. This was statistically significant (p = 0.001). On the other hand, the available chlorine available in the outflow solution collected from the canals containing collagen was 0.03% (95% CI: -0.1, 0.2) more than the chlorine available in the outflow solution collected from canals containing hydrogel. This was statistically not significant (p = 0.6). The chlorine available in the outflow solution from closed canals was 0.2% (95% CI: 0.01, 0.09) more than that available in the outflow solution from the open canals. This was statistically significant (p = 0.001).

Table 3.5: Generalised linear mixed-model analysis for the effect of organic film or biofilm NaOCl irrigant interaction on the available chlorine of NaOCl (n = 3 per group).

Experimental groups	Coefficient (±SD)	95% CI	P value
Hydrogel vs biofilm	0.2 (±0.1)	0.1, 0.3	**0.001**
Collagen vs biofilm	0.2 (±0.1)	0.1, 0.3	**0.001**
Hydrogel vs collagen Film	0.03 (±0.1)	-0.1, 0.2	0.6
Open canal vs closed canal	0.2 (±0.2)	0.01, 0.09	**0.001**

SD= Standard deviation, CI = Confidence interval.

3.3.2.5. Comparison of pH values of outflow NaOCl following irrigation to remove biofilm or films (collagen, hydrogel) from the root canal model (closed, open)

The mean pH values of the outflow NaOCl are presented in table 3.6.

Table 3.6: Mean pH values (Total n = 18, n = 3 per subgroup) of NaOCl before and after 60 seconds of irrigation for organic film (hydrogel, collagen) or biofilm in root canal models (closed, open).

Experimental subgroups (n = 3)	pH of NaOCl before irrigation (time =0 second)	pH of NaOCl after irrigation (time 60 seconds) (±SD)
Biofilm, closed canal, NaOCl	14.0	12.8(±1.6)
Biofilm, open canal, NaOCl	14.0	11.9(±1.7)
Collagen, closed canal, NaOCl	14.0	11.9(±1.1)
Collagen, open canal, NaOCl	14.0	11.2(±1.2)
Hydrogel, closed canal, NaOCl	14.0	10.9(±1.9)
Hydrogel, open canal, NaOCl	14.0	10.3(±2.1)

SD= Standard deviation

As can be seen in Table 3.6, the NaOCl solution showed a minimal reduction in pH value for all subgroups. The results (Table 3.7) showed that the mean values of pH in the outflow NaOCl collected from the canals containing biofilm was 0.9 (95% CI: 0.8, 1.1) more than mean values of pH in the outflow solution collected from canals containing hydrogel or collagen. This was statistically significant (p = 0.001). However, the mean values of pH in the outflow solution collected from the canals containing collagen was 0.3 (95% CI: -1.1, 1.7) more than the mean values of pH in the outflow solution collected from canals containing hydrogel. This was

statistically not significant (p = 0.82). The mean values of pH in the outflow solution from closed canals was 0.2 (95% CI: 0.02, 0.3) greater than that in the outflow solution from the open canals. This was statistically significant (p = 0.001).

Table 3.7: Generalised linear mixed-model analysis for the effect of organic film or biofilm NaOCl irrigant interaction on the PH values of NaOCl (n = 3 per group).

Independent variables (test vs reference category)	*Coefficient (±SD)	95% CI	P value
Hydrogel vs biofilm	0.9 (±0.3)	0.8, 1.1	**0.001**
Hydrogel vs collagen Film	0.5 (±0.3)	0.3, 0.6	**0.001**
Collagen vs biofilm	0.3 (±0.3)	-1.1, 1.7	0.82
Closed canal vs open canal	0.2 (±0.6)	0.02, 0.3	**0.001**

SD = standard deviation, CI = Confidence interval.

3.3.2.6. Calculation of the sample size

The number of samples was determined using Stata software, which depended on a comparison of the mean and standard deviation for the biofilm and organic film (hydrogel, collagen) subgroups irrigated with NaOCl. The data used for this purpose are presented below in Table 3.8.

Table 3.8: Number of samples required to achieve 90% power and 0.05 alpha per subgroups (biofilm, organic film) irrigated with NaOCl.

Subgroups	Power = 90%, alpha = 0.05			
	Mean	**Standard deviation**	**sample size/subgroup**	**Total sample size**
Biofilm, open canal, NaOCl	81.48	±7.004	n = 9	n = 108
Hydrogel, open canal, NaOCl	59.90	±18.011	n = 9	
Biofilm, open canal, NaOCl	81.48	±7.004	n = 10	n = 120
Collagen, open canal, NaOCl	72.19	±11.698	n = 10	
Biofilm, closed canal, NaOCl	87.87	±6.474	n = 5	n = 60
Hydrogel, closed canal, NaOCl	63.44	±14.811	n = 5	
Biofilm, closed canal, NaOCl	87.87	±6.474	n = 6	n = 72
Collagen, closed canal, NaOCl	74.90	±6.932	n = 6	

Based on the 20% relevant removal difference between the biofilm and organic films that were found by this study in relation to NaOCl, the ideal sample size for the present study should be 10 per subgroup. This sample size provides sufficient power (power= 90%, alpha = 0.05) to detect a significant difference in the outcomes of the study.

3.4. Discussion

The *in vitro* investigation presented herein was conducted to examine the rate of bacterial biofilm (*E. faecalis*) or simulant biofilm (hydrogel, collagen) removal using either sodium hypochlorite or distilled water (control) irrigant. Following NaOCl irrigation in the closed canal, the model displayed statistically more residual biofilm than both collagen and hydrogel film. The removal rate of biofilm was less than simulant biofilms (collagen, hydrogel). The model design (closed or open) had a significant influence on the amount of biofilm or simulant biofilms covering the root canal surface. The available chlorine and pH of outflow NaOCl collected from the canals containing biofilm was significantly more than the solution collected from canals containing hydrogel or collagen.

For the purpose of this study, Endo-Vu blocks made of transparent plastics (polymethyl methacrylate) were selected to create the test root canal models. Although the use of plastic canal models is recommended in other studies (Weller *et al.*, 1980; Lee *et al.*, 2004), a limitation of this model is that the sectioning of Endo-Vu blocks did not result in two identical canal halves. Another potential limitation is that the model used in this study does not account for root canal complexities such as the lateral canal, isthmus area and accessory canals.

It seems essential to develop an *in vitro* model that allows the generation of multiple samples with the same anatomical features. 3D printing with

stereolithography materials is a technique used to convert digital data created in computer-aided design (CAD) software or Three-dimensional imaging into models with details of much finer resolution (Melchels *et al.*, 2010). Hence, 3D printing with stereolithography materials may hold the possibilities to create test models with simple or complex root canal anatomies.

In the study presented herein, 36 (n = 3 per subgroup) model samples were used, which is a relatively small number. Although statistically significant differences were indeed found, indicating that the model is sensitive enough, such statistical significance does not tell us how big the difference is. This is important in clinical terms since it may alter the clinical approach of the irrigation procedure (Trope *et al.*, 1999). A robust calculation of the optimal sample size for the study is crucial for the minimization of the risk of type I or II errors (Schuurs *et al.*, 1993). To compensate for this issue, power statistic tests were performed on the preliminary data in order to determine the necessary sample size at which the effect of clinical significance could be achieved for the observed difference. In general, a total sample size of 120 will be considered in future work in order to make the results of this study more reliable and robust.

The findings of the present study showed that both an *E. faecalis* biofilm and simulant biofilms (organic films) were susceptible, in varying degrees, to the irrigant agents under consideration (NaOCl and water). In general, NaOCl seems to be more effective than distilled water in biofilm or organic film (hydrogel, collagen) removal from the walls of closed or open canal models. Nevertheless, conventional syringe irrigation with a 2.5% NaOCl solution and a contact time of 60 seconds is insufficient for 100% removal of either *E. faecalis* biofilm or simulant biofilms. *E. faecalis* provided more resistance than simulant biofilms. It

is difficult to compare the results of this study with those of other studies because of the small samples used in each group (n = 3), a result of which is the fact that the available data are not robust enough. However, based on the different models used, a useful comparison can be made to assess the efficacy of NaOCl.

The results of this investigation are consistent with those of previous studies that showed the incomplete removal of a biofilm after the application of a NaOCl irrigant to the root canal system (Byström and Sunvqvist, 1985; Estrela *et al.*, 2004; Nair *et al.*, 2005; Krause *et al.*, 2007). The subjective observations and data analyses in this study showed that 9 mL of 2.5% NaOCl were insufficient for the removal of a biofilm or organic films from the walls of the root canal models (closed, open). In closed canals, this incomplete removal may be explained by a lack of adequate contact between the antimicrobial agent and the biofilm or organic films due to the stagnation of the irrigant at the apical level of the canal (Ram, 1977), or because of the formation of air bubbles during irrigation (Tay *et al.*, 2010). These two phenomena are related to the closed nature of the root canal system, which interferes with the fluid dynamic, flushing, and replacement of the irrigant as well as limiting its dissolving action (Tay *et al.*, 2010). The difference in response between biofilm and organic films may be related to the EPS of the biofilm that may hinder irrigant penetration into the biofilm structure and thus decrease the rate of removal (Costerton *et al.*, 1999). In open canals, the results proved surprising. Although irrigant stagnation and air bubble entrapment did not occur, the test targets were not completely removed. This may be related to the limited time of irrigation (60 seconds) for the irrigant used in this study, which was ultimately insufficient (Macedo *et al.*, 2010; Ragnarsson *et al.*, 2014).

Interesting findings relate to a small reduction in the total remaining amount of available chlorine and pH of NaOCl. Although significant differences between the available chlorine and pH values of NaOCl between the closed and open canal models were presented, the reduction was less than originally expected. This indicates that the interactions between the irrigant and the test targets were short. This may be due to the small area of contact on the surface between the irrigant and the test targets (Moorer and Wesselink, 1982) or due to the short duration of the irrigant process (Ragnarsson *et al.*, 2014).

In the present study, organic films (hydrogel, collagen) were used as a simulant to the bacterial biofilm. The simulant biofilms showed relatively similar trends of removal as those of the bacterial biofilm when the NaOCl irrigant was used. However, the removal rate did differ to some extent since the former exhibited a greater removal rate than the latter, with increased removal evident for hydrogel. This may be attributed to the fact that organic films were not grown on but applied to the surface of the canal models, meaning that their attachment to the canal wall was generally weaker than that of the biofilm. More specifically, this can be ascribed to a reliance on physicochemical interactions between the model surface and the film layer alone (Sagvolden *et al.*, 1998). In addition, hydrogel is less stable and more hydrophilic than collagen (Otake *et al.*, 1989) and as thus, its dissolution by NaOCl was greater than that for collagen and biofilm.

Further research is essential for an understanding of ways to improve NaOCl efficacy and the apical penetration of NaOCl within the root canal system (e.g. increase irrigant concentration, irrigant agitation). It should be kept in mind that the major factor that contributes to successful irrigation is that of correctly understanding the properties of irrigant agents and the effects of confinement of

the small root canal system on irrigant efficacy. Several questions remain unanswered at present. These include whether irrigant activity will be enough to remove the biofilm from the most apical part of the canal. In addition, what is the extent of the complexity of the root canal system effect on the outcomes of the irrigation regimen?

3.5. Conclusion

Within the limitations of the current study, removal was greatest for a hydrogel and collagen organic film than for an *E. faecalis* biofilm. The closed canal models adversely affect the debridement efficacy of NaOCl. The debridement efficacy of 2.5% NaOCl, delivered via an irrigation syringe into a simple root canal model, was insufficient for the removal of the test targets (biofilm, films) from the most apical part of the root canal system. It can be stated that the use of a 2.5% NaOCl irrigant is better for organic film and biofilm removal than water.

Chapter 4

Investigations into the efficacy of sodium hypochlorite to remove bacterial biofilm or organic film simulating biofilm from a slide surface of a flow cell

4.1. Introduction

As highlighted in the introduction chapter, the close contact between NaOCl and bacterial biofilm for a sufficient time was essential for the optimum killing effect (Spratt *et al.*, 2001). Several attempts have been made to investigate the biofilm disrupting, dissolution, and removing capacity of root canal irrigants. For example, Ordinola-Zapata *et al.* (2012) used dentine specimens of bovine teeth for biofilm development, which were immersed separately in different irrigant solutions (1% NaOCl, 2% chlorhexidine, 17% EDTA, 10% citric acid, and distilled water) for 5 minutes. They reported that NaOCl had a significant killing effect on *Enterococcus faecalis*. Another study suggested that dissolution of multi-species biofilm required the infected bovine dentine to be immersed in NaOCl of different concentration (1%, 2.5%, 5.25%) for 30 minutes contact times (del Carpio-Perochena *et al.*, 2011). The killing effectiveness of NaOCl has been exemplified in an *in vitro* study by Retamozo *et al.* (2010) who reported that long exposure and high concentration were crucial for complete elimination of *E. faecalis* bacteria.

Although these studies provided information about the efficacy of irrigation, their results were based upon a technique of immersing the biofilm model into a static irrigant. In such conditions, the efficacy of irrigation was related to its chemical action as well as diffusion. Thus, what is not yet clear is the impact of irrigant flow (mechanical effect) together with its chemical effect.

A flow cell is a device that allows real time imaging of surfaces and/or cells and their interaction in a dynamic environment (Stoodley *et al.*, 2002). It may be possible to create a single species biofilm model that provides a method to understand the nature of interaction between irrigant and biofilm without the effect of root canal confinement.

This chapter aimed to investigate the real-time efficacy of 2.5% NaOCl to remove *Enterococcus faecalis* biofilm or organic film (hydrogel, collagen) grown or applied onto a slide of a flow cell model using the residual biofilm, and composition of the generated bubbles as the outcome measures. It also aimed to investigate the mimic behaviour of organic films in comparison to bacterial biofilm.

4.2. Materials and Methods

4.2.1. Allocation of the flow cell slides to experimental groups

Sixty polystyrene microscopic slides (75 × 25 × 1.2 mm) (Fisher scientific, Rochester, NY, USA) were used as substrata for generation of bacterial biofilm or application of organic films (hydrogel, collagen). The slides were divided to three groups. In-group 1, *E. faecalis* biofilm was generated onto the slide surface (n = 20). In-group 2, the hydrogel film was applied (n = 20). In-group 3, the collagen film was applied (n = 20). Each group was subdivided according to the irrigant regimen. Subgroup A received treatment with 2.5 % NaOCl (n = 10), and subgroup B was treated with sterile demineralized water (n = 10).

4.2.2. Preparation and application of stained organic films (hydrogel, collagen) on the slide (groups 1, 2)

The preparation of and application of stained organic films were performed as described in section 3.2.4.

4.2.3. Preparation of microbial strain and determination of the standard inoculum

This step was performed as described in section 2.2.2.4.2.

4.2.4. Generation and staining of single species *E. faecalis* biofilm on slide surface

Each plastic slide (group 3; n = 20) was placed inside an empty 60 mL plastic Bottle (Fisher Scientific, London, UK), and sterilised in a steam autoclave (121°C, 103.421 kpa, 30 minutes) (Farrugia *et al.*, 2015). A total of 16.5 mL of standard *E .faecalis* inoculum (10^8 CFU/mL) was delivered into the sterilised plastic bottle containing the sterilised plastic slide using a sterile syringe (BD Plastipak™, Franklin Lakes, NJ, USA) and a 21-gauge needle (BD Microlance™, Franklin Lakes, NJ, USA), until 18 mm of the slide was immersed. These were incubated at 37 °C in a 5% CO_2 incubator for 10 days. Every two days, half inoculum was aseptically discarded and replaced with fresh BHI broth using pipettes (Alpha Laboratories Ltd, Eastleigh, Winchester, UK) (De-Deus *et al.*, 2007). After incubation, the slide containing the biofilms were removed from the tubes, placed in a horizontal stand, and stained with crystal violet dye (CV) (Merck, Darmstadt, Germany). Each slide was rinsed with 3 mL sterile distilled water for 1min using a sterile 10 mL syringe (Plastipak, Franklin Lakes, New Jersey, USA) to remove loosely attached cells. Using a micropipette, 2 µL of CV stain was applied to the biofilm (18 mm of the plastic slide) and left for one minute. The slide was subsequently washed with 3 mL sterile distilled water for one minute to remove excess stain (Izano *et al.*, 2007).

4.2.5. Irrigation experiments

The slide coated with hydrogel, collagen or biofilm was placed onto the mounting base of the flow-cell model FC 71 (Friedrich & Dimmock Inc., Millville, NJ, USA) with a flow channel (0.2 mm deep, 11 mm wide, 40 mm long) (Figure 4.1a & b).

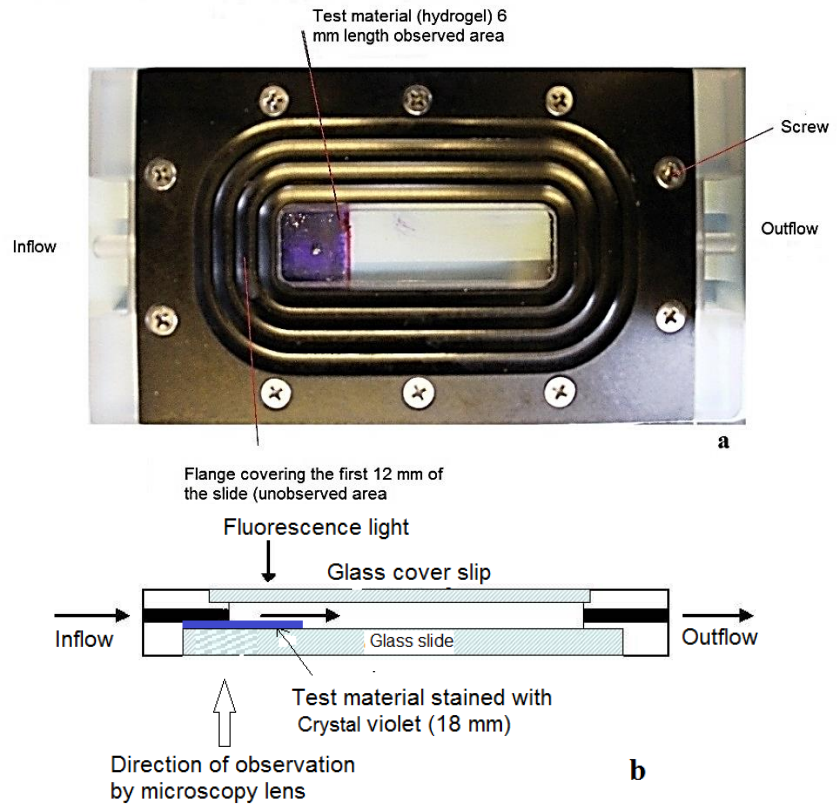

Figure 4.1: (a) Image of flow cell with test material (hydrogel) applied on slide surface, and (b) schematic diagram of the direction of irrigant (2.5% NaOCl) delivery into the flow cell.

The flow cell was placed on the stage of an inverted fluorescent microscope (Leica DMIRB, London, UK). Test irrigants used in the experiment were 2.5% NaOCl (Teepol® bleach, Egham, UK) and demineralized water (Roebuck, London, UK). A total of 9 mL of irrigant (NaOCl or water) were delivered using a 10 mL syringe (Plastipak, Franklin Lakes, NJ, USA) for 1-minute. The syringe was attached to a programmable precision syringe pump (NE-1010; New Era Pump Systems, Wantagh, NY, USA) to deliver the irrigant at a flow rate of 0.15

mL s^{-1}. The outflow irrigant was collected in a 15 mL plastic tube (TPP, Schaffhausen, Switzerland).

4.2.6. Recording of organic film or biofilm removal by the irrigant

This step was performed as described in section 3.2.7.2.

4.2.7. Image analysis

Image analysis was performed as described in section 3.2.8.

4.2.8. Assessment of composition of bubbles between NaOCl and bacterial biofilm film (collagen, hydrogel)

A total of three mL of the outflow irrigant were collected separately from flow cells containing bacterial biofilm (*E.faecalis*), hydrogel film, or collagen film and then delivered separately into vials of a Gas Chromatograph-Mass spectrometry machine (GC-MS) (Thermo Scientific™, TRACE™ 1310, UK) using 10 mL syringe. Three samples of each target material (biofilm, hydrogel film or collagen film) were prepared (n = 3). Mass spectra were generated for composition of NaOCl using Thermo Scientific™ TargetQuan 3 software (Thermo Scientific™, TRACE™, UK) and then analysed to identify different substances within a test sample. Mass spectra were taken in triplicate for each sample.

4.2.9. Data analyses

Separately for NaOCl and water, a repeated measure ANOVA was used to compare the residual remaining in the target material (biofilm, hydrogel, and collagen) over time (1 to 60 seconds). If there was no significant interaction between target material and time, Dunnett's *post-hoc* test was used to compare biofilm with each of the other target materials. Because there was a significant

interaction with time, the analysis was repeated for relevant time periods. A two-sample *t*-test was used to compare the mean residual biofilm between NaOCl and water at the end of irrigation (i.e. at 60 seconds). The assumptions of each ANOVA were checked by a study of the statistical residuals and of the *t*-test by confirming normality and constant variance. A significance level of 0.05 was used throughout. The data were analysed by SPSS (BM Corp. Released 2013. IBM SPSS Statistics for Windows, Version 22.0. Armonk, NY: IBM Corp).

4.3. Results

4.3.1. Results of statistical analysis

The results obtained from the repeated measures ANOVA (Table 4.1) revealed that during the first 12 seconds of irrigation, the mean amount of residual biofilm was 3.4% s^{-1} and 1% s^{-1} more than residual hydrogel and collagen respectively. This was statistically significant ($p = 0.001$). Between 13 and 30 seconds of irrigation, the difference in residual material had increased between the biofilm and film groups because residual biofilm was 11.2% s^{-1} and 9.4% s^{-1} more than that of hydrogel and collagen respectively. This was statistically significant ($p = 0.001$). From 31 to 40 seconds, the differences were increased as the residual biofilm was 17% s^{-1} 11.4% s^{-1} more than that of hydrogel and collagen groups respectively ($p = 0.001$). From 41 to 60 seconds, the differences showed a further increase between the residual biofilm and film groups. The residual biofilm was 21.4% s^{-1} and 10.5% s^{-1} more than residual hydrogel and collagen respectively. This was statistically significant ($p = 0.001$). In comparison, the residual biofilm was 0.5% s^{-1} and 0.2% s^{-1} more than hydrogel and collagen groups respectively during the first four seconds of water irrigation time. This was statistically not significant ($p > 0.05$). Between 5 and 12 seconds of irrigation, the residual biofilm

was 2.6% s^{-1} and 2.9% s^{-1} greater than hydrogel and collagen groups respectively. This was statistically significant ($p = 0.001$). Between 13 and 20 seconds of irrigation, the differences in residual materials were increased, as the residual biofilm was 7.3% s^{-1} and 5.5 % s^{-1} more than residual hydrogel and collagen respectively. This was statistically significant ($p = 0.001$). Between 21 and 30 seconds of irrigation, the residual biofilm was 15% s^{-1} and 6.5% s^{-1} greater than residual hydrogel and collagen respectively. This was statistically significant ($p = 0.001$). From 31 to 60 seconds, the residual biofilm was 22.6% s^{-1} 9.1% s^{-1} greater than residual hydrogel and collagen respectively. This was statistically significant ($p = 0.001$).

Table 4.1: Repeated measure ANOVA analyzing the difference in the area percentage of slide surface coverage with residual material (biofilms, hydrogel, and collagen) over irrigation time (60 seconds) with irrigant (2.5% NaOCl, water) (n = 10 per group).

Experimental variable (reference category)	Type of irrigant	Duration of irrigation (second)	*Mean difference in residual material (% s^{-1})	95 % CI for mean difference	p value
Hydrogel (biofilm)	2.5% NaOCl	1- 12	3.4	2.4, 4.3	**0.001**
Collagen (biofilm)			1	0.01, 1.9	**0.05**
Hydrogel (biofilm)	2.5% NaOCl	13- 30	11.2	10, 12.4	**0.001**
Collagen (biofilm)			9.4	8.2, 10.6	**0.001**
Hydrogel (biofilm)	2.5 % NaOCl	31- 40	17	16, 19	**0.001**
Collagen (biofilm)			11.4	9.9, 12.9	**0.001**
Hydrogel (biofilm)	2.5% NaOCl	41- 60	21.4	20.6, 22.1	**0.001**
Collagen (biofilm)			10.5	9.7, 11.2	**0.001**
Hydrogel (biofilm)	Water	1- 4	0.75	-0.2, 1,1	0.17
Collagen (biofilm)			0.1	-0.5, 0.8	0.79
Hydrogel (biofilm)	Water	5- 12	2.6	-3.3, 1.8	**0.001**
Collagen (biofilm)			2.9	2.1, 3.6	**0.001**
Hydrogel (biofilm)	Water	13- 20	7.3	6.1, 8.5	**0.001**
Collagen (biofilm)			5.5	4.3, 6.7	**0.001**
Hydrogel (biofilm)	Water	21- 30	15	13.7, 16.2	**0.001**
Collagen (biofilm)			6.5	5.2, 7.8	**0.001**
Hydrogel (biofilm)	Water	31- 60	22.6	21.9, 23.2	**0.001**
Collagen (biofilm)			9.1	8.4, 9.7	**0.001**

* The mean difference is significant at the 0.05 level, CI = Confidence interval.

4.3.2. Results of GC-MS analysis of the outflow NaOCl

Mass spectra of the experimental groups using Gas Chromatograph- mass spectrometry are presented in Figure 4.2. Although the main volatile compound in the vials containing NaOCl (control group) was hypochlorous acid ($HClO^-$) (68%) and hypochlorite (ClO^-) (5%), the most abundant (%) compounds of bubbles in the other groups were related to carbon dioxide (CO_2) and chloroform

compounds [Trichloromethane ($CHCl_3$), Dichloromethane (CH_2Cl_2), Acetyl chloride (CH_3COCl)] which were the lowest with biofilm (47%), then with collagen (97%) and the highest with hydrogel (98%).

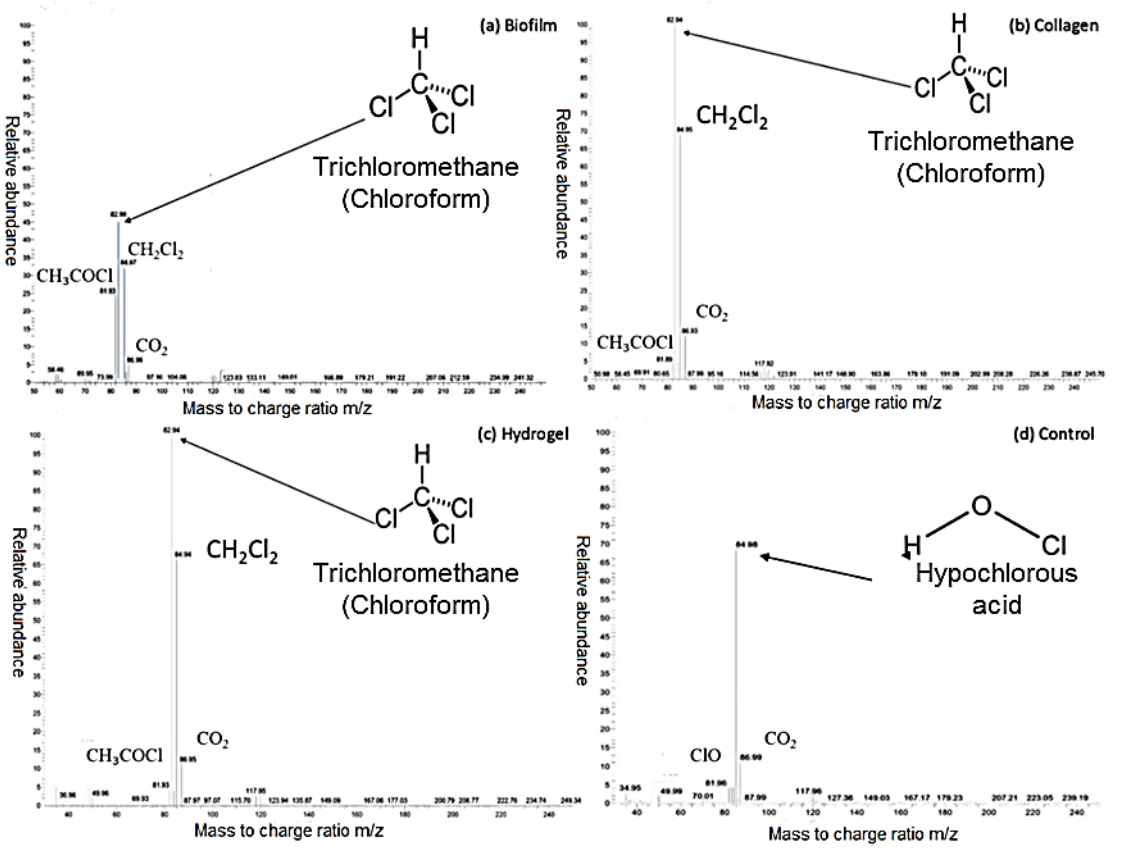

Figure 4.2: Spectra of Gas Chromatography mass spectrometry of the experimental groups. (a) Biofilm group; (b) collagen group; (c) hydrogel group; and (d) control group.

4.4. Discussion

In the present chapter, a flow cell slide was used to investigate the visual changes in the biofilm-irrigant reaction by measuring the removal rate of bacterial biofilm (*E. faecalis*) or simulant biofilm (hydrogel, collagen) using sodium hypochlorite (NaOCl) or water (control) irrigant. The result showed that the removal action of NaOCl was effective throughout the irrigation (one-minute). The results showed that NaOCl was more efficient in organic film removal than biofilm. The content of the generated bubbles was mainly of carbon dioxide (CO_2) and chloroform compounds.

The biofilm model proposed in this study did not take into account the representation of root canal geometry that may interfere with the chemo-mechanical action of the irrigant (Verhaagen *et al.*, 2012). However, it still represents the direct interaction of irrigant and biofilm grown on a flat slide without inclusion of other variables. The first 12 mm of the slide length was not in the observation area of the lens as aluminium flanges cover it. In addition, it was difficult to control the bacterial growth only on the observed area (24 mm^2). For standardisation purposes, 18 mm of slide length was chosen to apply film or generate biofilm.

Gas chromatography was used to determine the composition of bubbles because it allowed the separation of the mixture of gases or volatile liquids into components in a reasonable time that would require hours by any alternative methods i.e. fractional distillation (Basrani *et al.*, 2010).

The findings of the present study showed that NaOCl irrigant was more effective than distilled water in biofilm removal from the slides of flow cell models. This may be related to the organic tissue dissolution capacity of NaOCl (chemical action) (Estrela *et al.*, 2002) that increased due to flow dynamics (mechanical action) (Shen *et al.*, 2010b). Nevertheless, a 2.5% NaOCl solution and a contact time of 60 seconds was insufficient to remove 100% of *E. faecalis* biofilm which proved to be more resistant than simulated biofilms. The results of the present study are consistent with those of previous studies that show the incomplete removal of a biofilm after the application of a NaOCl irrigant to the root canal system (George and Kishen, 2007; Ordinola-Zapata *et al.*, 2013).

Bubbles that formed during the reactions of NaOCl with biofilm or organic film were chloroform (mainly $CHCL_3$) as the major products in the outflow NaOCl. This

may be attributed to the composition of the target materials. Biofilm consists of polysaccharide $(C_6H_{10}O_5)_n$ and peptidoglycan ($C_{40}H_{67}N_9O_{21}$) of the bacterial cell wall (Macfarlane and Macfarlane, 2006). For the organic film, Collagen film ($C_2H_5NOC_5H_9$) contains three polypeptide chains that are held together by inter-chain hydrogen bonds (Rich *et al.*, 2014), while hydrogel consists of gelatine ($C_6H_7O_2OH_2COONa$) which is an irreversibly hydrolysed form of collagen and sodium hyaluronate ($C_{28}H_{44}N_2NaO_{23}$) (Popa *et al.*, 2011). The chloroform may result from the oxidation of peptide and protein compounds of the test materials by hypochlorous acid ($HOCl^-$)of NaOCl (Hawkins *et al.*, 2003).

In the present study, the simulant biofilms and biofilm showed a reduction throughout the irrigation procedure. However, the removal rate differed to some extent since the former exhibited a greater removal rate than the latter, with increased removal evident for hydrogel. This finding confirms the result in chapter 3 and therefore suggests that organic films cannot be used as a simulant for biofilms in the study of irrigant-biofilm interactions within the root canal system. Further studies into current organic films are therefore recommended in order to improve their mimic behaviours in relation to natural biofilms (for example, by changing their composition or thickness).

These findings provide information about the nature of interaction between NaOCl irrigant and biofilm during the time of irrigation. This may support the importance of intracanal irrigation with optimal antimicrobial efficacy to improve the prognosis of the infected root canal. Further research is essential for the understanding of removal efficacy of bacterial biofilm by different concentrations of irrigant and irrigant activation within the root canal system.

4.5. Conclusion

Within the limitations of the present study, a plastic slide mounted in a flow cell chamber was a method to visualise and examine the efficacy of root canal irrigants during irrigation regimen. It also allowed optimisation of some of the measurement methods utilised in later studies. This study showed that debridement efficacy of 2.5% NaOCl was insufficient for the complete removal of the test targets (biofilm, films). Removal was greatest for a hydrogel rather than a collagen film and least for an *E. faecalis* biofilm. Use of NaOCl irrigant was more efficient in biofilm removal than water.

Chapter 5

The effect of sodium hypochlorite concentration and irrigation needle extension on *Enterococcus faecalis* biofilm removal from a simulated root canal model

5.1. Introduction

As stated previously, the efficacy of NaOCl is enhanced by an increase in its concentration (de Macedo, 2013), and frequent application or replenishment (Sirtes *et al.*, 2005). However, there is no consensus about the optimum concentration. Several studies recommended the use of 5.25% NaOCl (Ragnarsson *et al.*, 2014). In contrast, others suggested a concentration of 2.5% which still provided antibacterial activity (Byström and Sundqvist, 1983), as well as reducing the risks of physical damage to dentine (Hu *et al.*, 2010). Measurement of the rate of biofilm removal during irrigation by NaOCl in the root canal system may help to identify the factors that may interfere with the efficacy of NaOCl irrigant within the root canal system that are likely to improve and affect the clinical outcomes.

This chapter aimed to compare between the *in-situ* biofilm removal by 5.25% and 2.5% NaOCl delivered into an *in vitro* root canal model using a syringe and needle. The percentage of canal wall coverage with residual biofilm, needle extension, and the values of available chlorine and pH of outflow NaOCl were used as the outcome measures.

5.2. Materials and Methods

5.2.1. Construction of transparent root canal models and distribution to experimental groups

A solid computer representation of the root canal model was created using AutoCAD® software (Autodesk, Inc., San Rafael, CA, USA). The design of the

model consisted of two equal rectangular moulds (18 mm × 6 mm × 1 mm) (Figure 1). Each mould contained four holes on either side, as well as a longitudinal half canal. When the two moulds were reassembled, a straight simple canal of 18 mm length, apical size 30, and a 0.06 taper was created. The AutoCAD format of the model was converted into stereo-lithography format (STL format). Forty root canal models were manufactured using PreForm Software 1.9.1 of Formlabs 3D printer (Formlabs Inc., Somerville, MA, USA). Side and top views of the model are represented in Figure 5.1.

The material used to create the model was a clear liquid photopolymer material (AZoNetwork Ltd., Cheshire, UK), which is composed of a mixture of methacrylates and a photo-initiator. The process of fabrication started by conversion of a digital geometric data of the model into a series of layers that were physically constructed layer-by-layer of 25 µm thickness. Each layer was fabricated by exposing the liquid photopolymer material to a laser light source from the printer causing the liquid to cure into a transparent solid state (printed canal model) as presented in Figure 5.1.

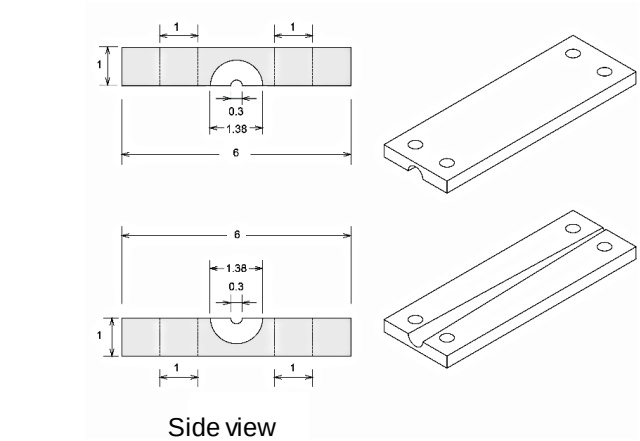

Figure 5.1: Image illustrates the design of the root canal model. Each half of a simulated canal is of 18 mm length with 1.38 mm diameter at the coronal portion and 0.3 mm diameter at the apical portion. The lower view shows the printed two halves and when they are reassembled, a straight simple canal of 18 mm length, apical size 30, and a 0.06 taper is created.

The root canal models (n = 60) were then divided into two main groups. The models where the irrigation needle was placed at 3 mm from the canal terminus (smallest diameter of the canal) comprised group 1 (n = 30) and those where the irrigation needle was placed at 2 mm comprised group 2 (n = 30). The models within each group were subdivided into three subgroups (n = 10) (A, B, and C) according to the type of irrigant (5.25%, 2.5%, Demineralized water respectively).

5.2.2. Preparation of microbial strain and determination of the standard inoculum

The preparation microbial strain and determination of the standard inoculum were performed as described in section 2.2.2.4.2.

5.2.3. Generation of single species biofilm (*E. faecalis*) on the surface of the apical 3 mm of the canal model

This step was performed as described in section 3.2.5.3, but the sterilisation method of the model was different as the models halves were packed individually in packaging bags (Sterrad 100S, ASP®, Irvine, CA, USA) and then sterilised using gas plasma with hydrogen peroxide vapor (Sterrad 100S, ASP®, Irvine, CA, USA) for 50 min (Precautions and Flush, 2008). The model was then incubated at 37 °C in a 5% CO_2 incubator for ten days.

5.2.4. Staining of biofilms grown on the surface of the models

The staining procedure was performed as mentioned in section 3.2.5.4.

5.2.5. Re-apposition of the model halves

Before reassembling the two model halves, a polyester seal film of 0.05 mm thickness (UnisealTM, Buckingham, UK) was positioned on the half coated with biofilm. Any part of the film that overhung the canal boundary was removed using a surgical blade (Swann-Morton, Sheffield, UK) without disturbing the biofilm. The two halves of the model were then held in position using four brass bolts (size 16 BA) and nuts (Clerkenwell Screws, London, UK).

5.2.6. Irrigation experiments

The apical end of each canal was blocked using a sticky wax. Each model was fixed to a plastic microscopic slide. The model half with the biofilm faced the slide. The microscopic slide was placed on the stage of an inverted fluorescent microscope (Leica, UK). Commercial NaOCl (Sigma–Aldrich, Germany) irrigant without surfactants was used. Nine mL per-minute of NaOCl irrigant (5.25% or 2.5%) were delivered using a 10 mL syringe with a 27-gauge side-cut open-ended

needle. In-group (1), the needle was inserted 3 mm from the canal terminus, and in group (2) the needle was inserted 2 mm from the canal terminus. The port opening of the needle always faced the model half containing the biofilm. The syringe was attached to a programmable precision syringe pump (NE-1010) to deliver the irrigant at a flow rate of 0.15 mL s^{-1}. Outflow irrigant was collected in a 15 mL plastic tube (Figure 5.2).

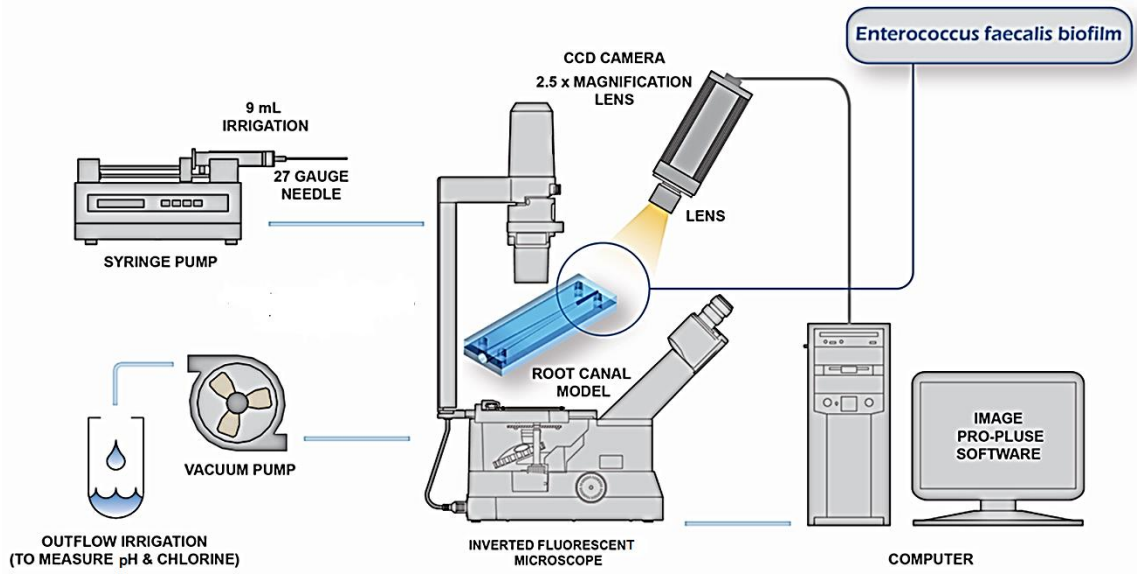

Figure 5.2: Schematic diagram illustrating the set-up of the equipment for recording residual biofilm by irrigant delivered at flow rate of 0.15 mL s^{-1} using an inverted fluorescent microscope.

5.2.7. Recording of biofilm removal by the irrigant

This step was performed as described in section 3.2.7.2.

5.2.8. Image analysis

Image analysis was performed as described in section 3.2.8.

5.2.9. Measurement of available chlorine and pH of outflow NaOCl

This step was performed as described in section 3.2.9.

5.2.10. Data analyses

The amount of residual *E. faecalis* biofilm after one-minute irrigation using three irrigants was assessed using line plots. An assumption concerning a normal distribution of data for the residual biofilm was checked using a visual inspection of the box and whisker plots. The data representing the percentages of residual biofilm covering the canal surface area were normally distributed and therefore the parametric analysis of covariance (ANCOVA) tests followed by Bonferroni *post-hoc* comparisons were performed to examine the effect of concertation and needle extent (2 & 3 mm) from the canal terminus on the area percentage of canal covered with residual biofilm. A two-sample t-test was used to compare the mean difference in available chlorine and pH of the outflow NaOCl before and at the end of irrigation. A significance level of 0.05 was used throughout. The data were analysed by SPSS (BM Corp. Released 2013. IBM SPSS Statistics for Windows, Version 22.0. Armonk, NY: IBM Corp).

5.3. Results

The mean (95% Confidence interval) percentages of the canal surface area covered with residual bacterial biofilm against duration of irrigation(s) are presented in Figure 5.3.

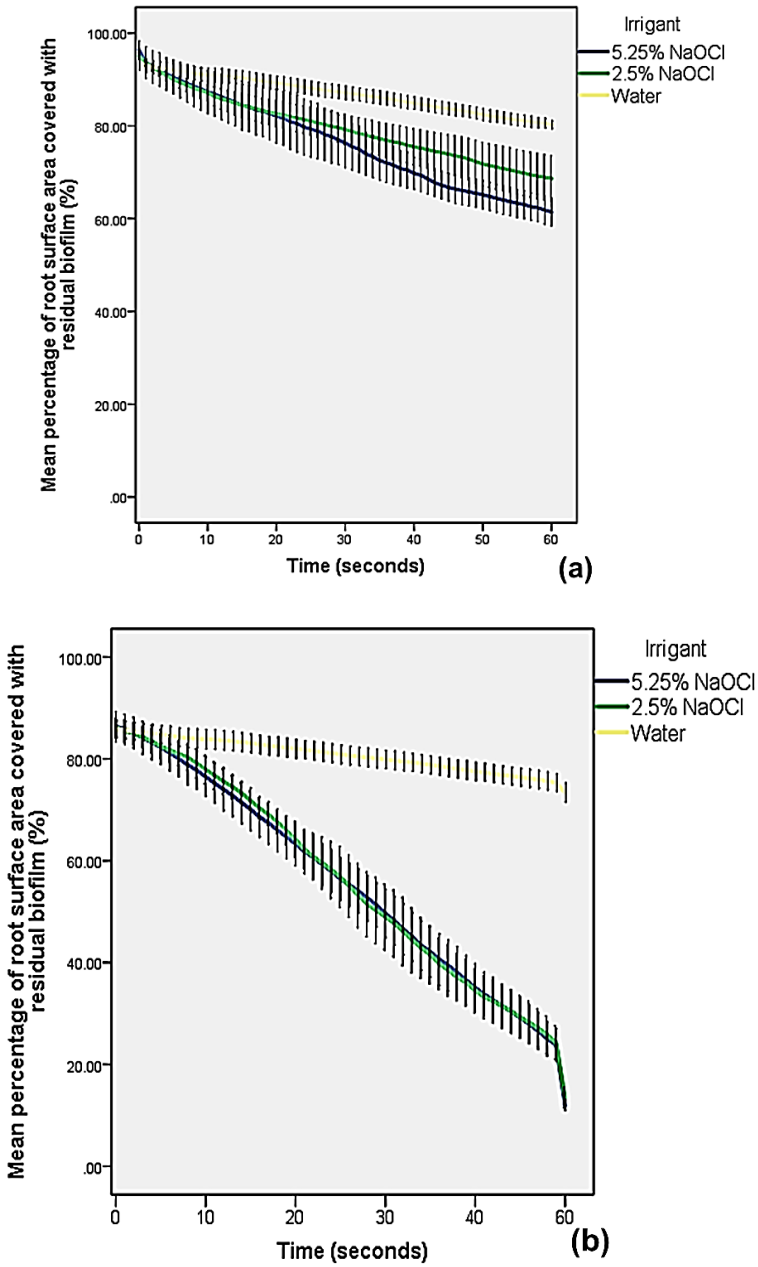

Figure 5.3: Mean percentages (95% CI) for root canal surface-area coverage with biofilm over duration (s) of canal irrigation using needle place at (a) 3 mm or (b) 2 mm from the canal terminus and delivered at flow rate of 0.15 mL s-1 for each group, stratified by type of irrigant (Total n = 60, n = 10 per group).

The data showed that in a canal where the needle was placed at 3 mm from the canal terminus (Figure 5.3a), the interaction of both NaOCl concentrations with biofilm was highest during the first 22 seconds. From then on, the removal declined, but with greater removal associated with 5.25% than that with 2.5%. The greatest residual biofilm was associated with water irrigant. However, in a canal where the needle was placed at 2 mm from the canal terminus (Figure

5.3b), the interaction was consistent throughout the irrigation procedure and was maximum during the first 31 seconds.

Regardless of needle position, the results showed (Table 5.1) that the difference between the amount of biofilm before and after irrigation was greater in the group where 5.25% NaOCl irrigant was used than the group using 2.5% NaOCl irrigant.

In general, one-minute irrigation was insufficient for complete removal of bacterial biofilm.

Table 5.1: Mean values of the biofilm (%) covering the root canal surface before and after one-minute irrigation using different irrigants (5.25% NaOCl, 2.5% NaOCl, water) delivered using syringe and needle placed at 3mm or 2mm from the canal terminus at flow rate of 0.15 mL s^{-1} (n = 10 per group).

Group	Type of irrigant	Mean (%) Before irrigation (±SD)	Mean (%) after irrigation (±SD)	Difference (Range) (%)
Group (1) Irrigation needle at 3 mm from the canal terminus (n = 30)	5.25% NaOCl (n = 10)	99.08 (±11.47)	54.58 (±11.47)	44.50
	2.5% NaOCl (n = 10)	97.04 (±8.34)	60.04 (±8.34)	37.00
	Water (n = 10)	96.80 (±4.22)	78.91 (±4.22)	17.89
Group (2) Irrigation needle at 2 mm from the canal terminus (n = 30)	5.25% NaOCl (n = 10)	98.08 (±22.63)	10.05 (±22.63)	88.03
	2.5% NaOCl (n = 10)	97.04 (±22.98)	11.05 (±22.98)	85.99
	Water (n = 10)	96.80 (±5.60)	70.02 (±5.60)	26.78

SD= Standard deviation.

When the needle was placed at 3 mm, the results (Table 5.2) revealed that the concentration of irrigant had an influence on the percentage of surface-area of the canal covered with biofilm. The residual biofilm after a 60-second irrigation protocol using 5.25% NaOCl irrigant was 10.8% (±0.3) less than that using water irrigant. This was statistically significant (p = 0.001). Furthermore, the residual biofilm after using 2.5% NaOCl irrigant was 7.5% (±0.3) less than that using water. This was statistically significant (p = 0.001). Moreover, the residual biofilm

using 5.25% NaOCl irrigant was 3.3% (±0.3) less than that using 2.5% NaOCl. This was statistically significant (p = 0.001).

Table 5.2: Analysis of covariance (ANCOVA) comparing the mean amount of residual biofilm (%) remaining on the surface of the root canal, over time (1 to 60 seconds) of irrigation using three irrigants (5.25 % NaOCl, 2.5% NaOCl, and water) delivered by syringe and needle placed at 3 mm (group 1) from the canal terminus and at flow rate of 0.15 mL s^{-1} (Total n = 30, n = 10 per group).

Experimental variable	*Mean difference in residual biofilm (%) (SE)	95% CI for mean difference	p value
5.25% NaOCl vs water	10.8 (±0.3)	10.2, 11.4	**0.001**
2.5% NaOCl vs water	7.5 (±0.3)	6.9, 8.1	**0.001**
5.25% vs 2.5% NaOCl	3.3 (±0.3)	2.7, 3.9	**0.001**

The mean difference is significant at the 0.05 level, SE = standard Error, CI = Confidence interval.

At 2 mm, the results (Table 5.3) revealed that the NaOCl action was increased as residual biofilm using 5.25% NaOCl irrigant was 29.7% (±0.3) less than that using water irrigant. This was statistically significant (p = 0.001). Whilst, when using 2.5% NaOCl, it was 29.4% (±0.3) less than that using water. This was statistically significant (p = 0.001). Moreover, the residual biofilm using 5.25% NaOCl irrigant was 0.3% (±0.3) less than that using 2.5% NaOCl. This was statistically not significant (p = 0.3).

Table 5.3: Analysis of covariance (ANCOVA) comparing the mean amount of residual biofilm (%) remaining on the surface of the root canal, over time (1 to 60 seconds) of irrigation using three irrigants (5.25% NaOCl, 2.5% NaOCl, and water) delivered by syringe and needle placed at 2 mm (group 1) from the canal terminus and at flow rate of 0.15 mL s^{-1} (Total n = 30, n = 10 per group).

Experimental variable	*Mean difference in residual biofilm (%) (SE)	95% CI for mean difference	p value
5.25% NaOCl vs water	29.7 (±0.3)	29.1, 30.3	**0.001**
2.5% NaOCl vs water	29.4 (±0.3)	28.8, 30.1	**0.001**
5.25% vs 2.5% NaOCl	0.3 (±0.3)	0.4, 0.9	0.3

The mean difference is significant at the 0.05 level, SE = standard Error, CI = Confidence interval.

The results of the ANCOVA test showed that there was a correlation between the extent of the irrigation needle and the percentages of residual biofilm. At 3 mm (group 1) the residual biofilm after irrigation using 5.25% and 2.5% NaOCl were (28.9%, 95% CI: 28.4, 29.5) and (25.9%, 95% CI: 25.3, 26.9) more than that where the needle was placed at 2 mm (group 2) respectively. This was statistically significant ($p = 0.001$). However, none of the needle positions examined could completely remove the bacterial biofilm.

The results of two-sample t-tests revealed the mean difference (before and after irrigation) in values of available chlorine of 5.25% NaOCl were 0.3% (95% CI: 0.1, 0.5) and 0.2% (95% CI: 0.1, 0.2) more than that that of 2.5% NaOCl respectively. This was statistically significant ($p < 0.001$). Regarding the pH values, the mean difference in values of pH of 5.25% NaOCl were 0.06% (95% CI: 0.1, 0.01) and 0.04% (95% CI: 0.03, 0.05) more than that of 2.5% NaOCl respectively. This was statistically significant ($p < 0.001$).

5.4. Discussion

This chapter has compared the real-time *E. faecalis* biofilm removal by 5.25% and 2.5% NaOCl irrigant delivered by a syringe into the root canal system, and how the position of the irrigation needle affects NaOCl action. Furthermore, the differences in available chlorine and pH of NaOCl have been evaluated. The findings show a clear improvement in removal efficacy when using higher concentration or extending the needle further apically However, One-minute syringe irrigation protocol using NaOCl was insufficient for complete biofilm removal.

For the objective of this investigation, the model proposed herein was made from transparent resin materials (acrylic), and created using 3D printing. The selection

of this material was due to its excellent optical transparency, which enabled direct and real-time imaging of biofilm removal by antibacterial agents (e.g., NaOCl), as well as the 3D printing technique which provided an accurate representation of the simple root canal anatomy and allowed numerous variables to be tested (Layton *et al.*, 2015).

The model proposed herein relied upon an adequate seal between the two model halves in order to minimize leakage of the irrigant during the irrigation procedure. This was achieved by using a seal film between the two halves as recommended in another study that assesses the efficacy of the antimicrobial agent in flow chambers (Chin *et al.*, 2006). Indeed, a pilot experiment to compare between models (n = 3) with the seal film and other models (n = 3) without the film showed that the leakage was minimal in models with film. For this, the placement of the seal film between the model halves, and the holding of this construction in position using nuts and bolts, is important in that it provides a seal and thus facilitates the irrigation and minimizes irrigant leakage from the canal model.

The findings showed that NaOCl was more effective than distilled water in biofilm removal from the walls of the canal models. This may be related to the organic tissue dissolution capacity of NaOCl (chemical action) (Estrela *et al.*, 2002) that increased by flow dynamics (mechanical action) (Kishen, 2010). Nevertheless, the subjective observations and data analyses showed that both 9 mL/min of 5.25% and 2.5% NaOCl were insufficient for the elimination of *E. faecalis* biofilm from the apical 3 mm of the root canal models. Although the residual biofilm was less with higher concentration NaOCl (5.25%), the possible reason for incomplete removal may be related to the inadequate NaOCl replacement, which became progressively weak towards the apical terminus (Druttman and Stock, 1989) as a

result of the canal confinement effect on the irrigant flow (Gulabivala *et al.*, 2010; Verhaagen *et al.*, 2012).

The results suggest that the efficacy of the chemical action of NaOCl was enhanced by increasing its concentration due to its higher level of available chlorine (Macedo *et al.*, 2010). However, the slow fluid flow allows fresh NaOCl to move apically through diffusion (Paz *et al.*, 2015). This may be the result of incomplete removal even with higher NaOCl concentration. Another possible explanation for the difference in biofilm removal is the significant difference ($p < 0.001$) in the values of the available chlorine and pH of NaOCl between the two concentrations. However, it has been argued that the pH value had no effect on the efficacy of NaOCl (Macedo *et al.*, 2010).

Although extending the needle apically was associated with less residual biofilm, both concentrations failed to achieve complete biofilm removal. A probable explanation is that when the irrigation needle was placed at 2 mm from the canal terminal, there was no space between the needle and the canal wall (refer to part 2 of chapter 2) and therefore the replacement of irrigant was minimum. Another explanation for incomplete removal is the extracellular substance of the biofilm, which hindered the penetration of depleted NaOCl irrigant (Flemming and Wingender, 2010).

The results of this investigation are consistent with Sena *et al.* (2006) that showed 5.25% NaOCl destroyed *E. faecalis* more rapidly than 2.5% NaOCl. However, the complete eradication of an *E. faecalis* biofilm has been demonstrated by Rossi-Fedele *et al.* (2010) in bovine models. This difference in efficacy may be related to a difference in volume, since a greater irrigant volume was used twice in the latter study. Estrela *et al.* (2007) reported that the use of 2.5% NaOCl for 20

minutes was not completely effective against *E. faecalis* after 60 days of incubation. It appears that a 60-day period was enough to render the biofilm more resistant.

Further research is essential for an understanding of ways to improve the apical penetration of irrigants within the root canal system (for example, irrigant agitation).

5.5. Conclusion

Within the limitation of the present study, both the concentration and the position of the irrigation needle affect the efficacy of NaOCl to remove *E. faecalis* biofilm. Although 5.25% NaOCl was more effective than 2.5%, one-minute irrigation using higher concentration was not enough for complete biofilm removal.

Chapter 6

Investigations into the effect of different agitation methods using sodium hypochlorite as an irrigant on the rate of bacterial biofilm removal from the wall of a simulated root canal model

6.1. Introduction

The topic of the effect of an agitation method on the process of bacterial biofilm disruption by an irrigant has received considerable critical attention. A number of researchers have reported the important role of agitation for delivering the irrigant in to the most apical part of the canal as well as its mixing and replacement within the root canal system (Townsend and Maki, 2009; Paragliola *et al.*, 2010; Sáinz-Pardo *et al.*, 2014). However, the challenge is not only fluid penetration into the complex root anatomy, but it also includes the effective overcoming of the protection structure of the biofilm community, which renders bacteria more resistant to the antimicrobial agents (Jhajharia *et al.*, 2015). Data about the real-time effect of agitation on the efficacy of irrigant, and the condition of the residual biofilm within the root canal are therefore essential for understanding the antimicrobial mechanism of active irrigation.

This chapter aimed to compare the residual biofilm and removal rate of biofilm when subjected to passive (stagnant) and active irrigation (2.5% NaOCl). The structure of the residual biofilm was also examined. Finally, the outcomes of chemical interaction between a NaOCl irrigant and bacterial biofilm were represented by the available chlorine and pH of outflow irrigant, as outcome measures were assessed.

6.2. Materials and Methods

6.2.1. Construction of transparent root canal models and distribution to experimental groups

The root canal models (n = 40) were created as described in section 5.2.1 and then divided into four groups (n = 10 per group) according to the type of irrigation protocol. In-group 1 (the passive irrigation group), no agitation was applied. In-group 2 (the manual agitation group), the irrigant was agitated using a gutta-percha cone (GP) (SybronEndo, Buffalo, New York, USA). In-group 3 (the sonic agitation group), the irrigant was agitated using the EndoActivator® device (Dentsply Tulsa Dental Specialties, Tulsa, OK, USA). In group-4 (the ultrasonic agitation group), the irrigant was agitated using a Satelec® P5 ultra-sonic device (Satelec, Acteon, Equipment, Merignac, France).

6.2.2. Preparation of microbial strain and determination of the standard inoculum

The preparation microbial strain and determination of the standard inoculum were performed as described in section 2.2.2.4.2.

6.2.3. Generation of single species biofilm (*E. faecalis*) on the surface of the apical 3 mm of the canal model

This step was performed as described in section 5.2.3.

6.2.4. Staining of biofilms grown on the surface of the models

The staining procedure was performed as mentioned in section 3.2.5.4.

6.2.5. Re-apposition of the model halves

This step was performed as described in section 5.2.5.

6.2.6. Irrigation experiments

In all groups, sodium hypochlorite (NaOCl) of 2.5% available chlorine and 12.78 pH was used as the irrigating solution. 9 mL of the NaOCl were delivered using a 10 mL syringe (Plastipak, Franklin Lakes, New Jersey, USA) with a 27-gauge side-cut open-ended needle (Monoject, Sherwood Medical, St. Louis, MO, USA). NaOCl was delivered at a flow rate of 0.15 mL s^{-1} in the same manner as described in section 3.2.7.1. In group 1, followed the 60 s irrigation using a syringe and needle, the irrigant was kept stagnant (passive irrigation) in the canal for 30 s. in the other groups (2 - 4), the irrigating solution was agitated using manual (group 2) , sonic (group 3) and ultrasonic methods (group 4) .

In the manual agitation group, the irrigant was delivered as in the previous group. Following that, a gutta-percha cone with an apical ISO size 30 and 0.02 taper was placed 2 mm coronal to the canal terminus which was used to agitate the irrigant in the root canal system with a push–pull amplitude of approximately 3 – 5 mm at a frequency of 50 strokes per 30 s (Huang *et al.*, 2008). A new GP cone was used with each canal model.

For the sonic agitation group, the irrigant was delivered as in described in group 1. Following that, the agitation was carried out using an EndoActivator® device by placing the polymer tip of an EndoActivator® device with size 25 and 0.04 taper at 2 mm from the canal terminus, and then the agitation was continued for 30 s with a high power-setting (Ruddle, 2007). A new tip was used with each canal model.

For the ultrasonic agitation group, the irrigant was delivered as in the previous group. Following that, the agitation was carried out by placing a stainless steel

instrument size and taper 20/02 (IrriSafe; Satelec Acteon, Merignac, France) of Satelec® P5 Newtron piezon unit at 2 mm from the canal terminus, then the agitation was continued for 30 s. The file was energized at power setting 7 as recommended by the manufacturer. A new instrument was used with each canal model.

Outflow irrigant was collected individually for each sample in a 15 mL plastic tube (TPP,Schaffhausen, Switzerland) using a vacuum pump (Neuberger,London, UK) (Figure 6.1).

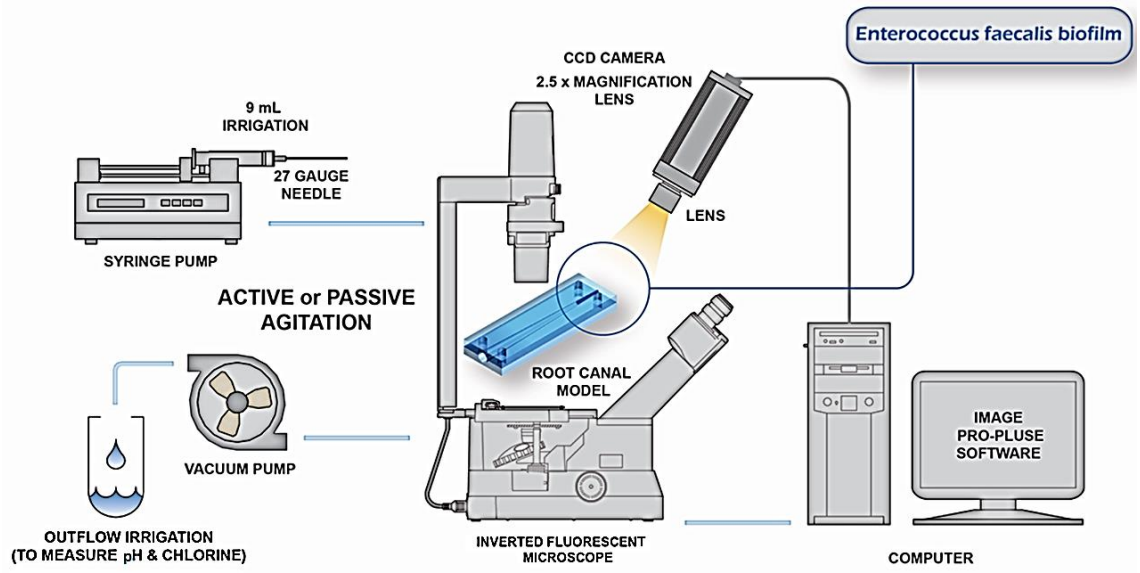

Figure 6.1: Sketch illustrating the set-up of equipment for recording of the biofilm (biofilm was generated on the apical portion (3 mm) of the canal model) removal by active or passive NaOCl irrigation protocol using a camera connected to a 2.5× lens of an inverted fluorescent microscope. The irrigant was delivered using a syringe with a 27-gauge side-cut open-ended needle, which was attached to a programmable precision syringe pump for 60 s. Following that, the irrigant was kept either stagnant or agitated using manual, sonic, or ultrasonic agitation methods for 30 s. The residual biofilm was quantified using computer software (Image-pro Plus 4.5). Outflow irrigant was collected in a plastic tube using a vacuum pump. The amount of available chlorine (%) and pH were measured using iodometric titration and a pH calibration meter respectively.

Following irrigation protocols, the residual NaOCl on the model surface was immediately neutralised by immersing the models in 2 mL of 5% sodium thiosulphate solution (Sigma-Aldrich Co Ltd., Gillingham, UK) for 5 minutes. This

reduces the active ingredient of NaOCl (hypochlorite), which becomes oxidized to sulphate (Hegde *et al.*, 2012).

The models in each group were then randomly divided in to three subgroups for investigation with CLSM, SEM, and TEM microscopy techniques (n = 3 per subgroup).

6.2.7. Recording of biofilm removal by the irrigant

This step was performed as described in section 3.2.7.2.

6.2.8. Image analysis

Image analysis was performed as described in section 3.2.8.

6.2.9. Measurement of available chlorine and pH of outflow NaOCl

This step was performed as described in section 3.2.9.

6.2.10. Preparation of the samples for confocal laser scanning microscope (CLSM)

Three models from each group were examined to assess the viability of bacterial cells in the residual surface biofilm using the Live/Dead® viability stain (LIVE/DEAD BacLight; Invitrogen, Paisley, UK) and CLSM (BioRad Radiance2100, Zeiss, Welwyn Garden City, Herts, UK) along with its designated software for documentation of results. The stain was prepared by mixing 3 µL each of Syto 9 and propidium iodide compounds. The models were removed from the incubator and the stain mixture was pipetted directly onto the surface of each sample. The samples were then placed in a sealed dark box and left to incubate for 15 minutes at room temperature (Defives *et al.*, 1999). Each sample was then placed onto the microscope stage of the CLSM and imaged with an x20 lens using both a fluorescent and laser light source. The canal surface was imaged at

3, 2, and 1 mm from the canal terminus with the green channel indicating live cells and the red channel showing the dead bacteria. For imaging, the pixel definition was set at 1024×1024 pixels with no digital zoom. The representative portion was scanned at ×1 digital zoom in a simple x y two-dimensional plane. The images were then constructed and manipulated using ImageJ® software. For standardisation of measurement, a template was created using AutoCAD® software (Autodesk, Inc., San Rafael, CA, USA). The template was printed on transparency printer paper to provide a grid of squares each of 0.3 mm^2. The template was placed over the sample and three squares were imaged. For each area (1 mm^2) of the 3 mm from the canal terminus, the sample was tested to obtain representative images of the live/dead cells by viewing 3 fields of 0.3 mm^2 from within the root canal. The fields were located in the top, middle, and bottom of the tested area (Figure 6.2).

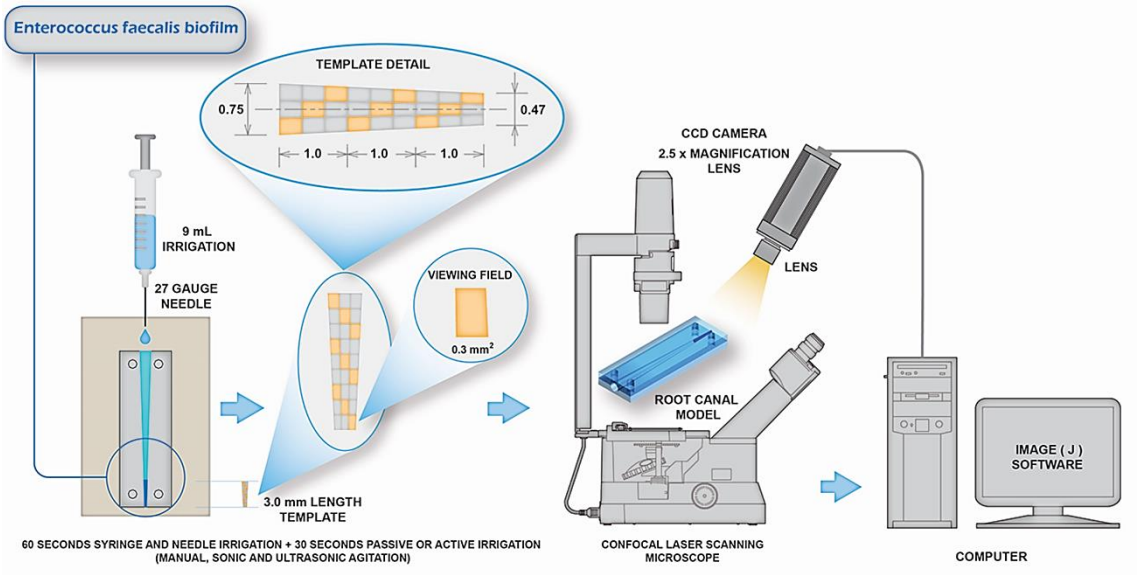

Figure 6.2: Image illustrates the set-up of the equipment to examine the residual biofilm. Confocal laser scanning microscope was used to observe and record images of the live/dead cells within the residual biofilm. A template was used to control the viewing fields (0.3 mm^2) which were located in the top, middle, and bottom of the tested area. The areas were imaged manipulated using ImageJ® software.

6.2.11. Preparation of the samples for scanning electron microscope (SEM)

Three models from each group were examined to assess the effect of 2.5% NaOCl irrigant on the residual surface biofilm using SEM. The samples were prepared in the same manner as described in the second paragraph of section 2.2.2.5.1. The residual biofilm on the canal surface was imaged at 3, 2, and 1 mm from the canal terminus.

6.2.12. Preparation of the samples for transmission electron microscope (TEM)

Three models from each group were examined using TEM to further assess the effect of 2.5% NaOCl on the residual biofilm and individual cells. Following fixation in 3% glutaraldehyde (Agar Scientific, Stansted, UK) in 0.1 M cacodylate buffer (Agar Scientific, Stansted, UK), samples were dehydrated in a graded series of alcohol (50%, 70%, and 3 × 90% for 10 minutes each) (Sigma Aldrich, Dorset, UK). They were then infiltrated with LR White resin (LR White (Hard grade), (Agar Scientific, Stansted, UK) by immersion in LR White resin and 90% alcohol (ratio of 1:1) for 2 hours at 4 ˚C, followed by a change to pure fresh LR White for 30 minutes, another change to fresh LR White overnight at 4 ˚C. The following day, the models were embedded in foil tins containing 20 ml of LR White and 30 µl LR White accelerator at room temperature. Air was excluded from the setting process by placing a piece of parafilm cut to size over the surface of the exposed resin mix in the foil tin. The resin mixture was stored overnight in the freezer for polymerisation and then removed and left to warm up to room temperature.

Semi-thin sections of the canal (80 – 90) nm were cut with a Diatom diamond knife (Duatome, TAAB, Aldermaston, UK) on an ultra-microtome (Ultracut E, Reichert Jung, Munich, Germany) and collected on gold 200 mesh grids (Agar Scientific, Stansted, UK). The models were then stained on the grid with 0.4% (w/v) uranyl acetate (Agar Scientific, Stansted, UK) in absolute alcohol for 5 minutes; models were examined on a TEM (Philips CM12, FEI, Eindhoven, Netherlands) operating at 80 kV.

6.2.13. Data analyses

The residual biofilm (%) at each second over a 90 s irrigation period with passive and active NaOCl irrigation was analysed using line plots. An assumption concerning a normal distribution of data for the residual biofilm was checked using a visual inspection of the box and whisker plots. The data representing the percentages of residual biofilm covering the canal surface area were not normally distributed and therefore the non-parametric Kruskal–Wallis test, followed by Bonferroni *post-hoc* comparisons were performed to compare their distributions in the four experimental groups. The effects of irrigant agitation duration on the percentage of residual biofilm covering the canal surface area were analysed by the type of irrigation (passive or manual, sonic, and ultrasonic active irrigation) using a generalized linear mixed model. The differences in median of chlorine and pH values of the outflow NaOCl of the four groups before and after irrigation were compared using the Kruskal–Wallis test. A significance level of 0.05 was used throughout. The data were analysed by SPSS (BM Corp. Released 2013. IBM SPSS Statistics for Windows, Version 22.0.Armonk, New York, IBM Corp.).

6.3. Results

6.3.1 Statistical analysis

The median values of the residual biofilm (%) covering the canal surface-area against duration of irrigation(s), stratified by the type of irrigation are presented in Figure. 6.3. The data show that the greatest removal was associated with the ultrasonic group (90.13%) followed by the sonic (88.72%), the manual (80.59%), and the passive irrigation groups (control) (43.67%) respectively.

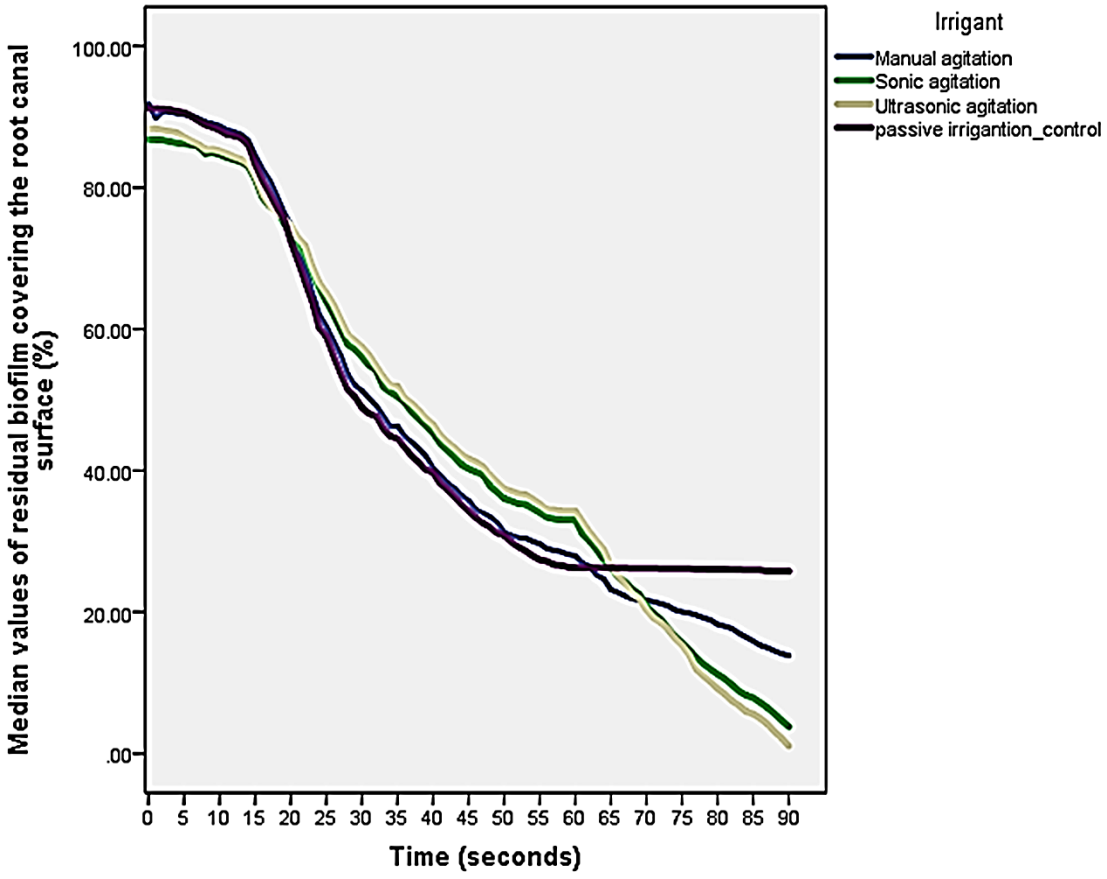

Figure 6.3: Median values of the residual biofilm (%) covering the root canal surface-area over duration (s) of syringe irrigation followed by passive or active irrigation protocols, stratified by type of irrigation (n = 10 per group).

The results of the Kruskal–Wallis test (Table 6.2) revealed that there was a statistically significant difference between the residual biofilm on the canal surface area in the ultrasonic agitation group and both manual (p = 0.002) and passive irrigation groups (p = 0.001). The difference was statistically significant between the sonic agitation group and the passive syringe group (p = 0.001).

Table 6.1: Kruskal–Wallis analysis to compare the difference in the amount of residual biofilms covering the canal surface following passive or active irrigation time (30s) with 2.5% NaOCl irrigant (n = 10 per group).

Comparable groups		*Median (minimum, maximum) (%)		p
Group 1	Group 2	Group 1	Group 2	value
Ultrasonic	manual	1.09 (0, 5.25)	13.85 (12.51, 15.18)	**0.002**
Ultrasonic	passive irrigation	1.09 (0, 5.25)	25.76 (20.23, 29.30)	**0.001**
Ultrasonic	sonic	1.09 (0, 5.25)	3.82 (1.63, 5.25)	0.78
Sonic	manual	3.82 (1.63, 5.25)	13.85 (12.51, 15.18)	0.21
Sonic	passive irrigation	3.82 (1.63, 5.25)	25.76 (20.23, 29.30)	**0.001**
Manual	passive irrigation	13.85 (12.51, 15.18)	25.76 (20.23, 29.30)	0.34

* The median difference is significant at the 0.05 level.

The data of the generalized linear mixed model analysis (Table 6.2) revealed that the biofilm removal using passive irrigation was [5.35% s^{-1} (±1.1), 6.66% s^{-1} (±1.1), 7.52% s^{-1} (±1.1)] less than the biofilm removal using active manual, sonic, and ultrasonic irrigation respectively. This was statistically significant (p = 0.001). For the active irrigation groups, the biofilm removal using ultrasonic agitation was [2.18% s^{-1} (±1.1)], more than the biofilm removal using the manual agitation. This was statistically significant (p = 0.047).

Table 6.2: Generalized linear mixed model analysing the effect of time (second) on the amount of biofilm removed from the canal surface of each experimental group (n = 10 per group).

Experimental groups	*Coefficient for time effect (±SE)	95% CI for coefficient	p value
Manual agitation vs passive irrigation	-5.35 (±1.1)	-7.49, -3.19	**0.001**
Sonic agitation vs passive irrigation	-6.66 (±1.1)	-8.81, -4.51	**0.001**
Ultrasonic agitation vs passive irrigation	-7.52 (±1.1)	-9.67, -5.37	**0.001**
Manual agitation vs ultrasonic agitation	2.18 (±1.1)	0.03, 4.323	**0.047**
sonic agitation vs ultrasonic agitation	0.86 (±1.1)	-1.29, 3.01	0.43
sonic agitation vs manual agitation	-1.32 (±1.1)	-3.47, 0.83	0.23

*Coefficient for time effect represents the rate of biofilm removal, SE= standard error, CI = Confidence interval.

The results of the Kruskal–Wallis tests (Table 6.3) revealed that there was a relation between available chlorine reduction and irrigant agitation because there was a statistically significant difference between the available chlorine in the passive group and both the ultrasonic group (p = 0.001) and sonic group (p = 0.016). Among the active irrigation groups, it was revealed that there was a statistically significant difference between the level of available chlorine in the ultrasonic group and the manual group (p = 0.006).

The data from the right half of the table indicated that there was a strong evidence of pH reduction when NaOCl was activated, as statistically significant differences between the pH in passive irrigation group and active irrigation groups were shown (ultrasonic; p = 0.001, sonic; p = 0.021, and manual; p = 0.029). Comparing the active irrigation groups, there was a statistically significant difference between the pH in ultrasonic group and both sonic (p = 0.029), and manual groups (p = 0.021).

Table 6.3: Kruskal–Wallis analysis analysing the effect of biofilm NaOCl irrigant interaction on the available chlorine (left) and pH (right) of NaOCl as dependent variables (n = 10 per group).

Comparable groups		*Median available chlorine (minimum, maximum) (%)		p value	*Median pH (minimum, maximum)		p value
Group 1	Group 2	Group 1	Group 2		Group 1	Group 2	
Passive	US	0.43 (0.29, 0.61)	1.35 (1.26, 1.52)	**0.001**	0.56 (0.41, 0.68)	3 (2.15, 4.39)	**0.001**
Passive	sonic	0.43 (0.29, 0.61)	0.89 (0.52, 1.12)	**0.016**	0.56 (0.41, 0.68)	1.71 (1.56, 1.88)	**0.021**
Passive	manual	0.43 (0.29, 0.61)	0.69 (0.53, 0.81)	0.127	0.56 (0.41, 0.68)	0.69 (0.53, 0.81)	**0.029**
US	sonic	1.35 (1.26, 1.52)	0.89 (0.52, 1.12)	0.057	3 (2.15, 4.39)	1.71 (1.56, 1.88)	**0.029**
US	manual	1.35 (1.26, 1.52)	0.69 (0.53, 0.81)	**0.006**	3 (2.15, 4.39)	0.69 (0.53, 0.81)	**0.021**
Sonic	manual	0.89 (0.52, 1.12)	0.69 (0.53, 0.81)	1	1.71 (1.56, 1.88)	0.69 (0.53, 0.81)	1

* The median difference is significant at the 0.05 level. US =ultrasonic.

6.3.2. Microscopic images analysis

The CLSM images of the biofilm on the surface of the root canal models before and after irrigation are presented in Figure 6.4.

In the untreated model (control group), observations of the CLSM images of the biofilm (Fig. 6.4ai) demonstrated more live cells (green) than dead cells (red). The dark background of these images indicates the non-fluorescent property of the model materials.

In the treated groups, the CLSM images exhibited no residual biofilm at the 3 mm level from the canal terminus in all groups (Fig. 6.4aii). At the 2 mm level, the images showed no viable cells in all groups. However, dispersed clusters of residual dead biofilm (red) were more abundant in the passive irrigation group (Fig. 6.4bi) than manual agitation group (Fig. 6.4ci). Complete removal of biofilm was associated with the automated groups (sonic, ultrasonic) (Figs. 6.4di & ei respectively).

At 1 mm, the images demonstrated both viable and dead cells in the passive irrigation group (Fig. 6.4bii) and manual (Fig. 6.4cii) groups with greater live cells than dead cells in the former group. Regarding the automated groups, it was

notable that no viable cells were detected. Moreover, the scanty clusters of the residual dead cells in the sonic (Fig. 6.4dii) group were more than that of the ultrasonic group (Fig. 6.4eii).

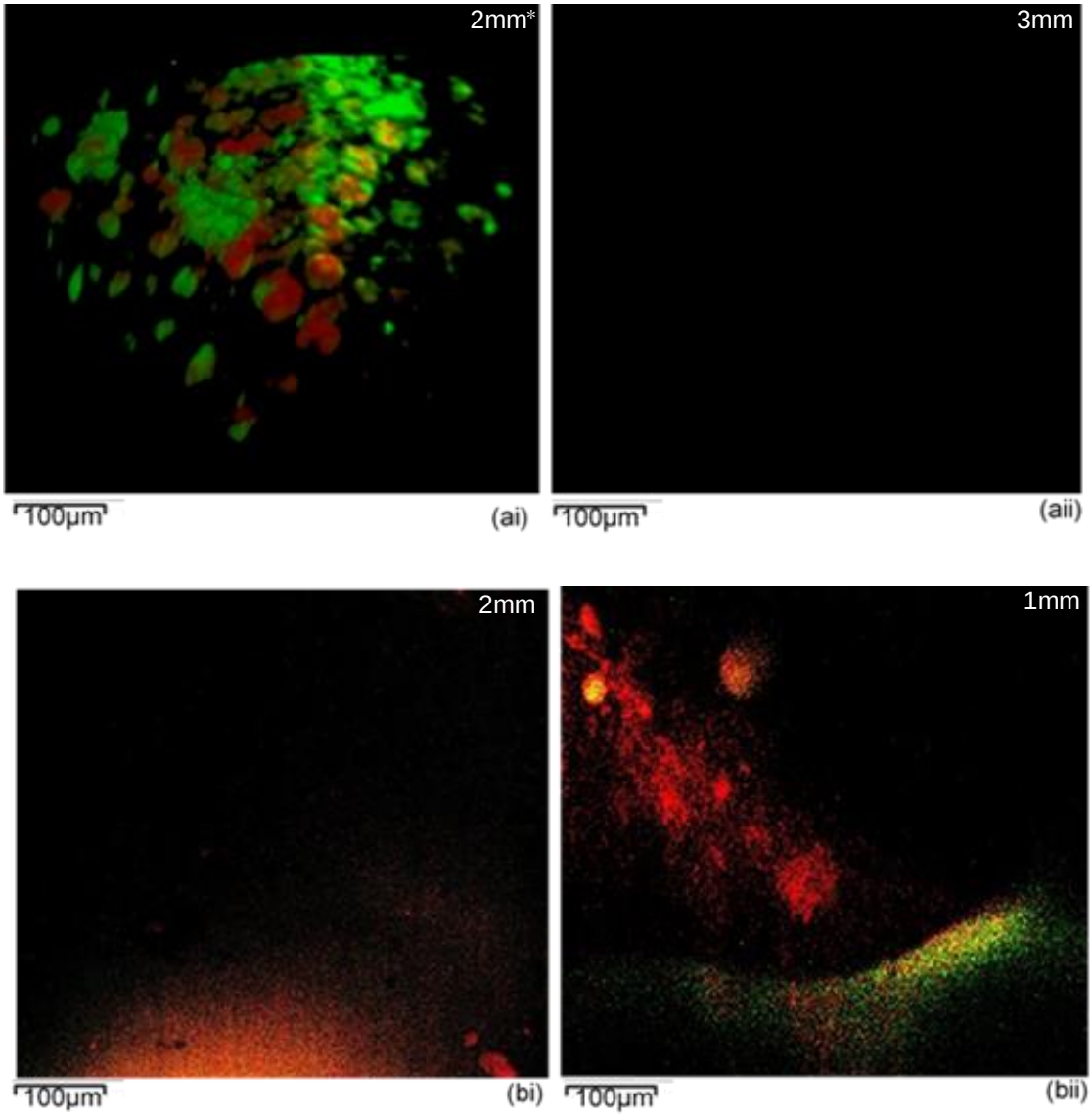

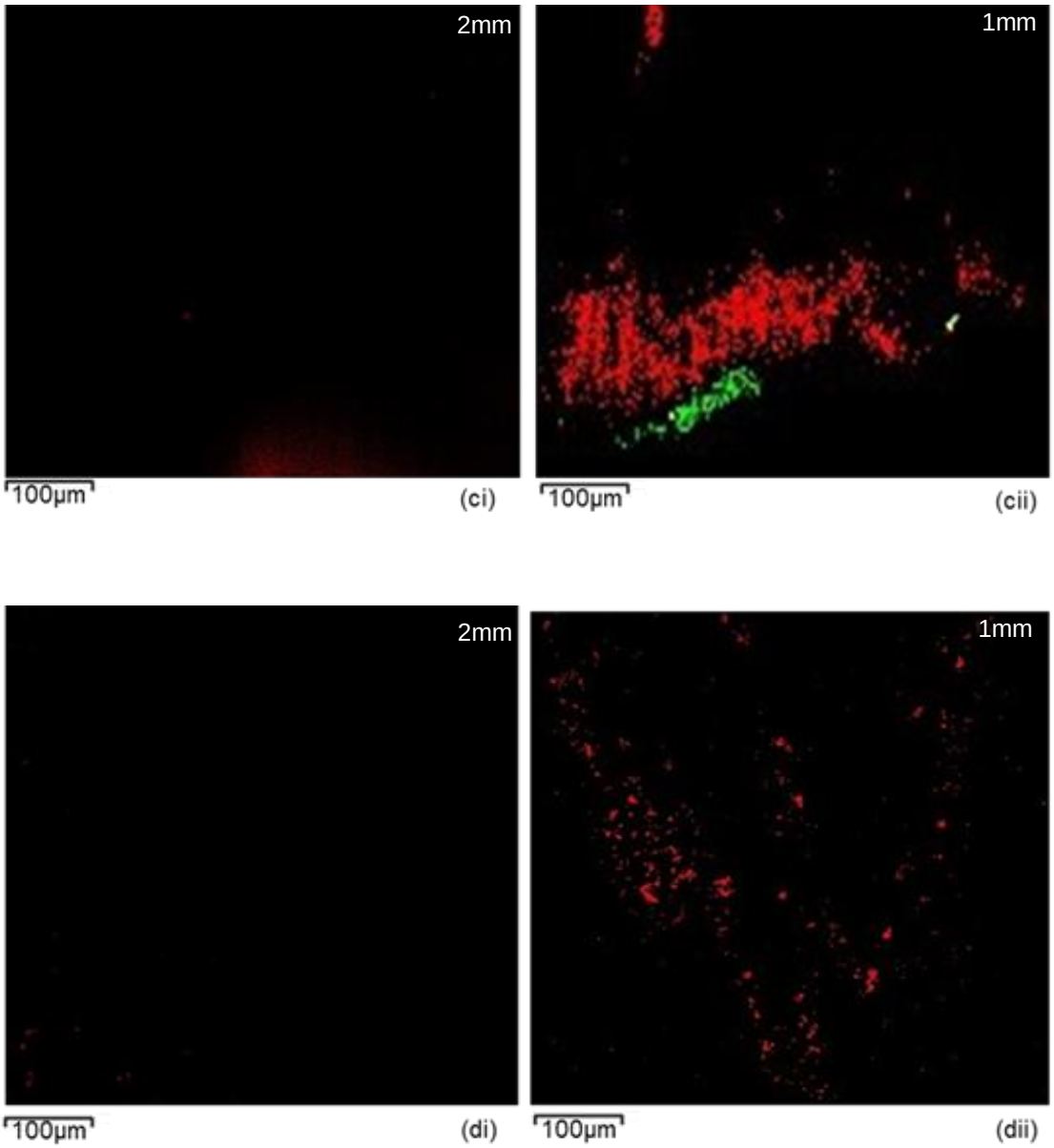
2mm
1mm
100µm
(ci)
100µm
(cii)
2mm
1mm
100µm
(di)
100µm
(dii)

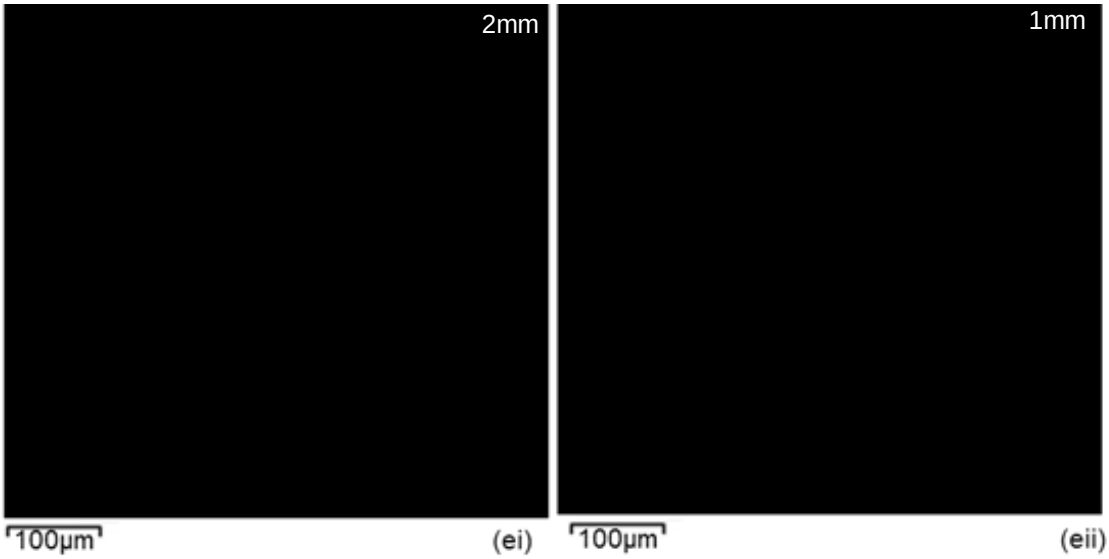

*The information at the upper right of each image indicates the level of the root canal (in mm) from the canal terminus where the residual biofilm was captured.

Figure 6.4: CLSM images (0.3 mm^2) from within the root canal to illustrate (a) *E. faecalis* biofilm grown for 10 days and stained using Live/Dead® viability stain with the green colour indicating live cells and the red colour showing the dead bacteria (control). (ai) residual biofilm at 3 mm from the canal terminus after passive irrigation protocol. (b) Passive irrigation group; (i) residual biofilm at 2 mm from the canal terminus; (ii) residual biofilm at 1 mm from the canal terminus. (c) manual-agitation group; (i) residual biofilm at 2 mm from the canal terminus; (ii) residual biofilm at 1 mm from the canal terminus. (d) Sonic agitation group; (i) residual biofilm at 2 mm from the canal terminus; (ii) residual biofilm at 1 mm from the canal terminus. (e) Ultrasonic agitation group; (i) residual biofilm at 2 mm from the canal terminus; (ii) residual biofilm at 1 mm from the canal terminus.

SEM images of the biofilm on the surface of the root canal models before and after irrigation are presented in Figure 6.5.

SEM assessment of the untreated biofilm (Fig. 6.5ai) illustrated typical biofilm growth with many small and larger colonies often embedded within a layer of extracellular polymeric substance.

After 2.5% NaOCl irrigation, SEM images exhibited no residual biofilm detected at the 3 mm level of all groups (Fig. 6.5aii). SEM images of the biofilm at 2 mm showed that the least extracellular polymeric substance (EPS) and cells destruction was associated with the passive irrigation group (Fig. 6.5bi) followed by manual (Fig. 6.5ci), sonic (Fig. 6.5di), and ultrasonic (Fig. 6.5ei) groups respectively. At 1 mm, SEM images illustrated that the biofilm appeared intact

with the least bacterial cell destruction and deformation in the passive irrigation group (Fig. 6.5bii), followed by manual (Fig. 6.5cii), sonic (Fig. 6.5dii) groups respectively. Complete biofilm removal and cell damage were associated with the ultrasonic group.

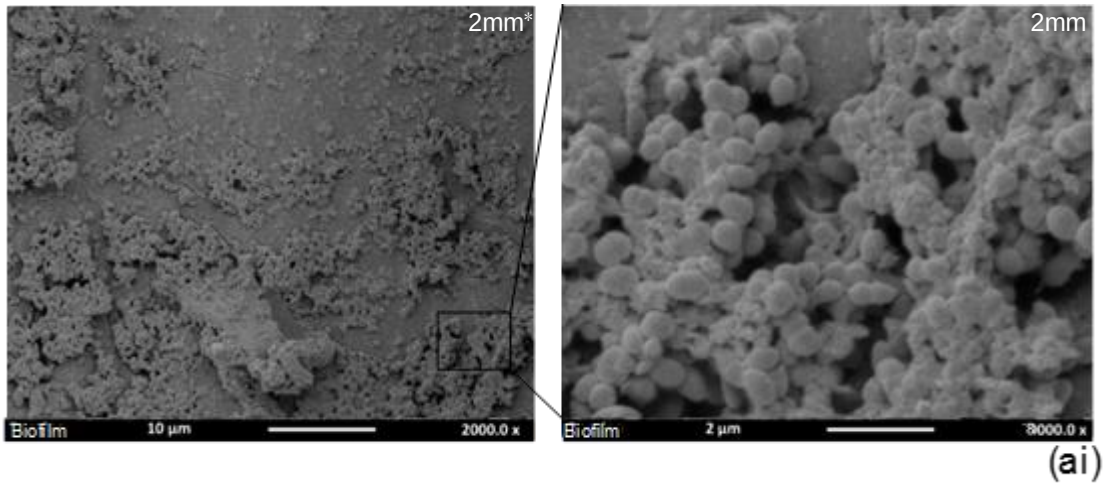

(ai)

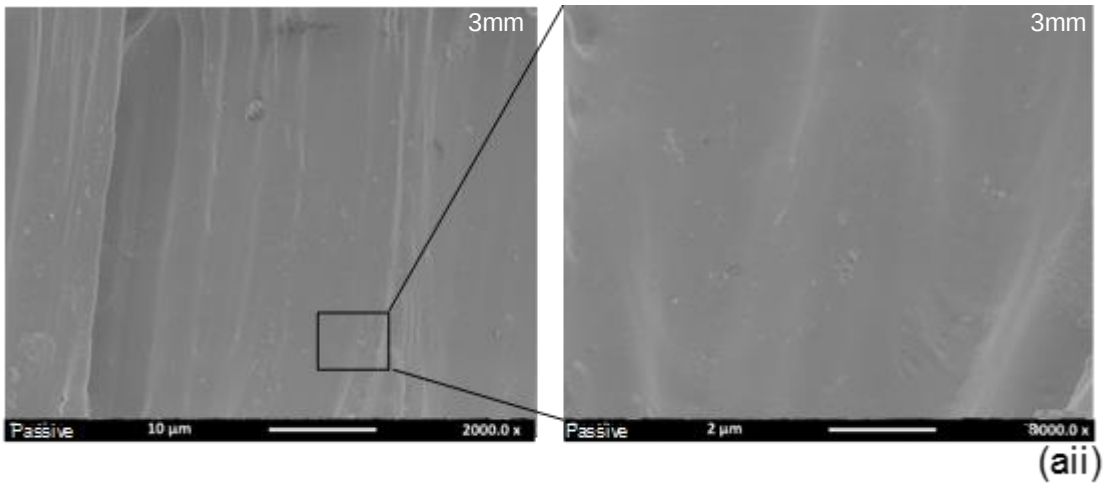

(aii)

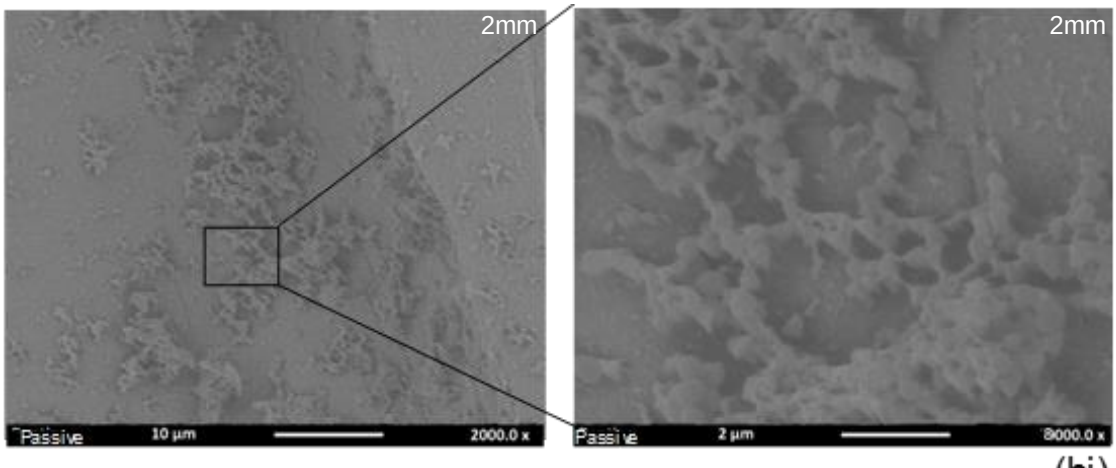

(bi)

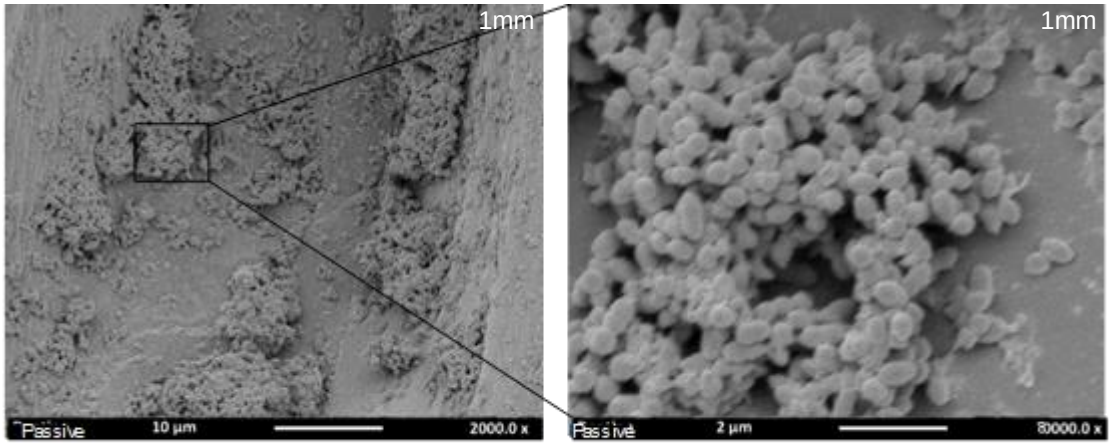
1mm
1mm
Passive
10 µm
2000.0 x
Passive
2 µm
8000.0 x

(bii)

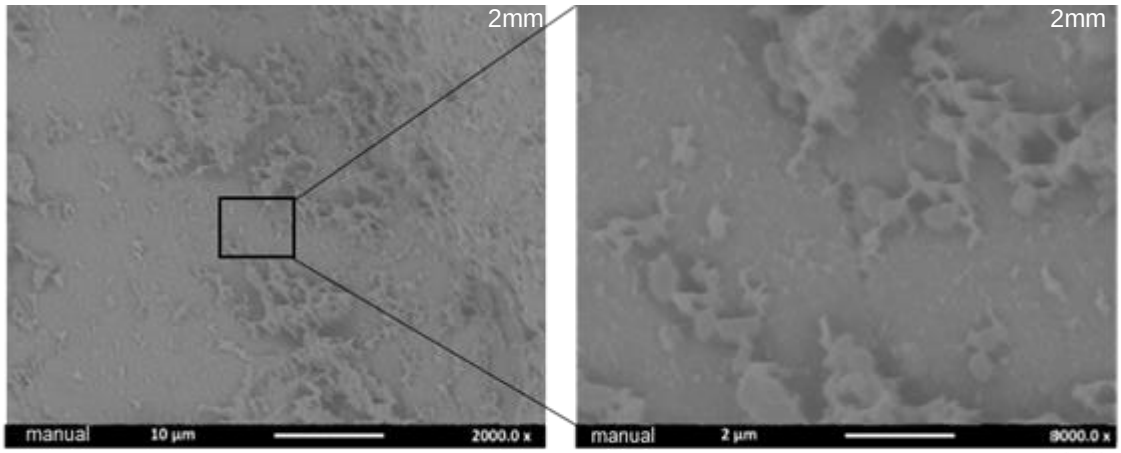
2mm
2mm
manual
10 µm
2000.0 x
manual
2 µm
8000.0 x

(ci)

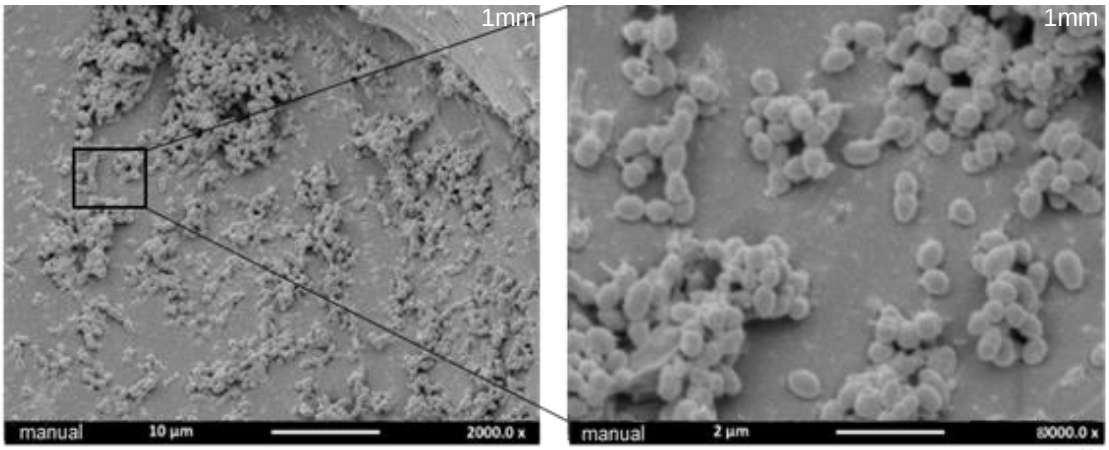
1mm
1mm
manual
10 µm
2000.0 x
manual
2 µm
8000.0 x

(cii)

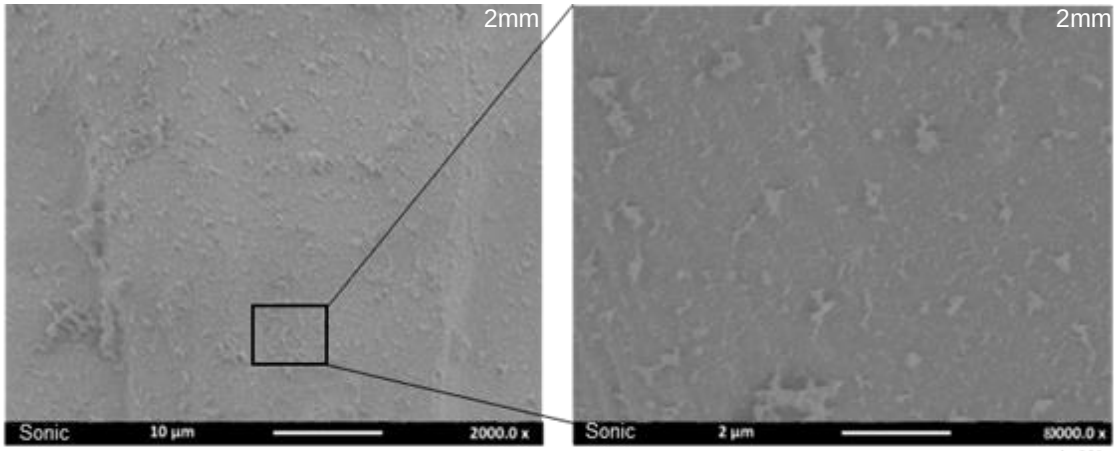
2mm
2mm
Sonic
10 µm
2000.0 x
Sonic
2 µm
80000.0 x

(di)

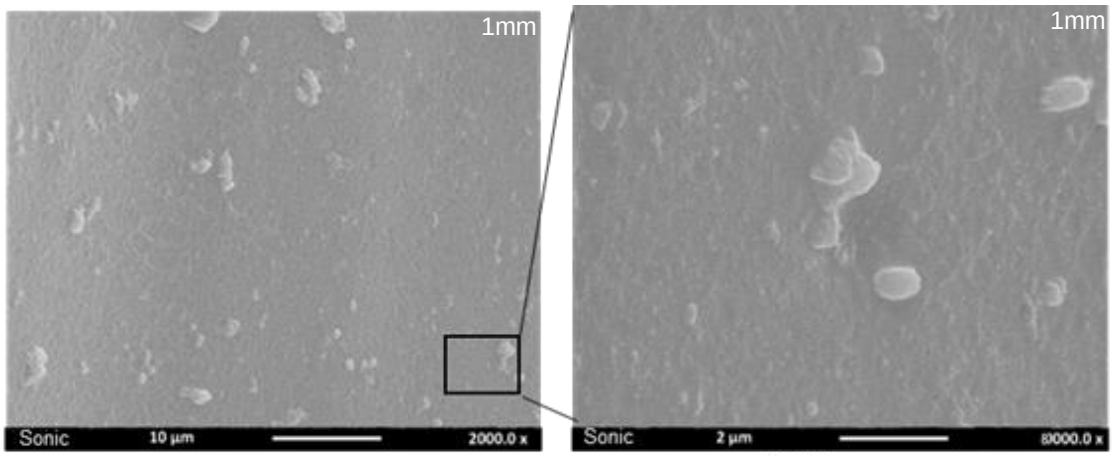
1mm
1mm
Sonic
10 µm
2000.0 x
Sonic
2 µm
80000.0 x

(dii)

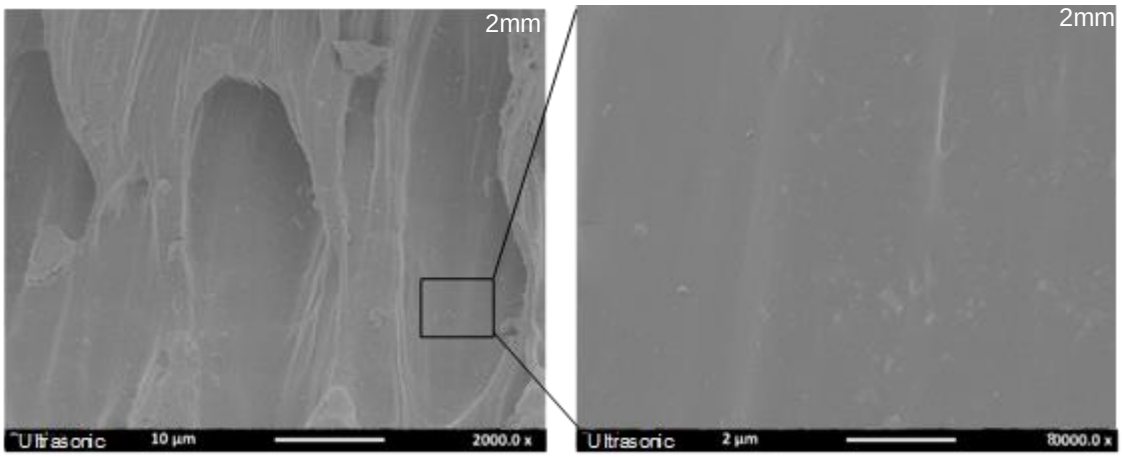
2mm
2mm
Ultrasonic
10 µm
2000.0 x
Ultrasonic
2 µm
80000.0 x

(ei)

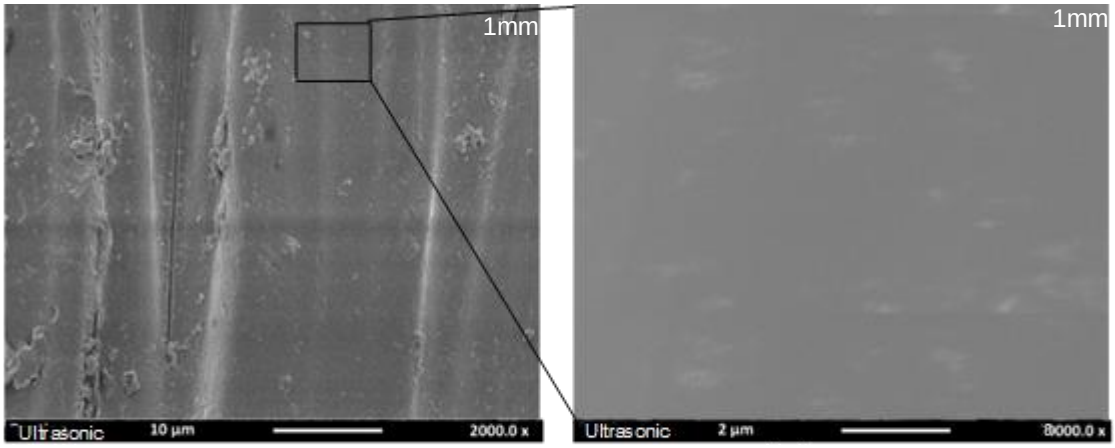

*The information at the upper right of each image indicates the level of the root canal (in mm) from the canal terminus where the residual biofilm was captured.

Figure 6.5: SEM images illustrate (ai) *E. faecalis* biofilm grown for 10 days onto the surface of the root canal model (control). (aii) residual biofilm at 3 mm from the canal terminus after passive irrigation protocol. (b) Passive irrigation group; (i) residual biofilm at 2 mm from the canal terminus; (ii) residual biofilm at 1 mm from the canal terminus. (c) manual-agitation group; (i) residual biofilm at 2 mm from the canal terminus; (ii) residual biofilm at 1 mm from the canal terminus. (d) Sonic agitation group; (i) residual biofilm at 2 mm from the canal terminus; (ii) residual biofilm at 1 mm from the canal terminus. (e) Ultrasonic agitation group; (i) residual biofilm at 2 mm from the canal terminus; (ii) residual biofilm at 1 mm from the canal terminus.

The TEM images of the biofilm on the surface of the root canal models before and after irrigation using passive irrigation, manual, and automated agitation protocols are presented in Figure 6.6.

TEM assessment of the untreated biofilm on the root canal model (Fig. 6.6ai) showed that it consisted of bacterial cells surrounded by EPS. At higher magnification, the bacterial cells exhibited a distinct coccoid appearance, a smooth and intact outer cell wall, a cell membrane surrounding the cytoplasm, and electron-dense irregularly shaped areas within the cell,

After 2.5% NaOCl irrigation, TEM images exhibiting no residual biofilm was detected at the 3 mm level of all groups (Fig. 6.6aii). The TEM images of the residual biofilm at 2 mm demonstrated extensive biofilm destruction, bacterial cell deformations/perforations, and apparent removal of EPS in passive irrigation

(Fig. 6.6bi) and manual (Fig. 6.6ci) groups. In comparison, complete biofilm destruction, removal, and cell damage were associated with Sonic (Fig. 6.6di) and ultrasonic (Fig. 6.6ei) groups. At 1 mm, bacterial cells in the residual biofilm seemed to maintain their cell wall and structural integrity in both passive irrigation (Fig. 6.6bii) and manual (Fig. 6.6cii) groups. In comparison, damaged cells of the residual biofilm were abundant in the sonic (Fig. 6.6dii) group, whilst, complete biofilm disintegration was associated with the ultrasonic (Fig. 6.6eii) groups.

Generally, passive irrigation with NaOCl resulted in more residual biofilm than NaOCl agitated by manual or automated (sonic, ultrasonic) method. Total biofilm destruction and non-viable cells were associated with automated groups.

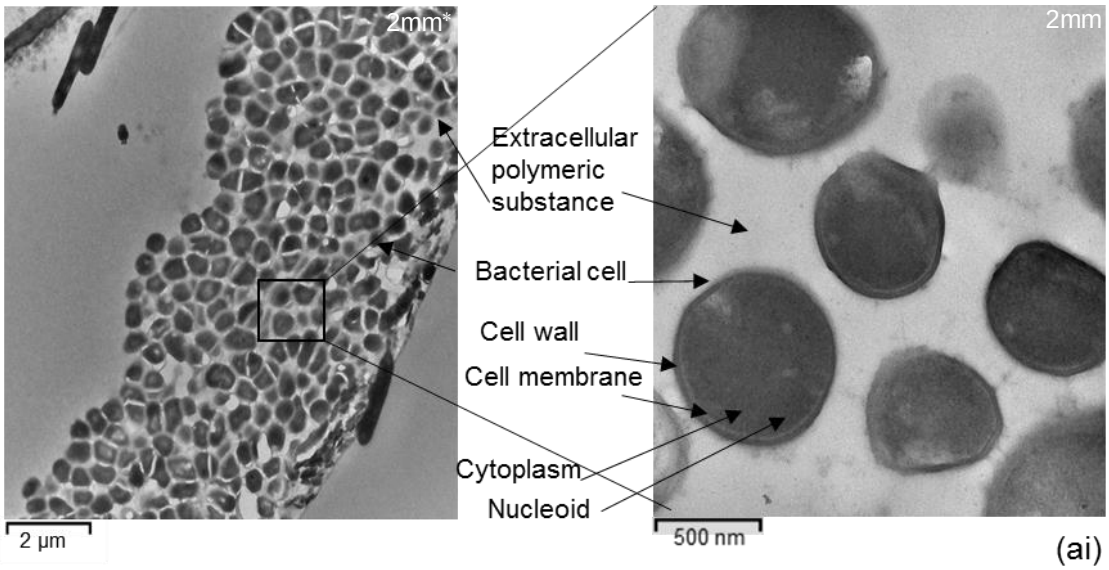

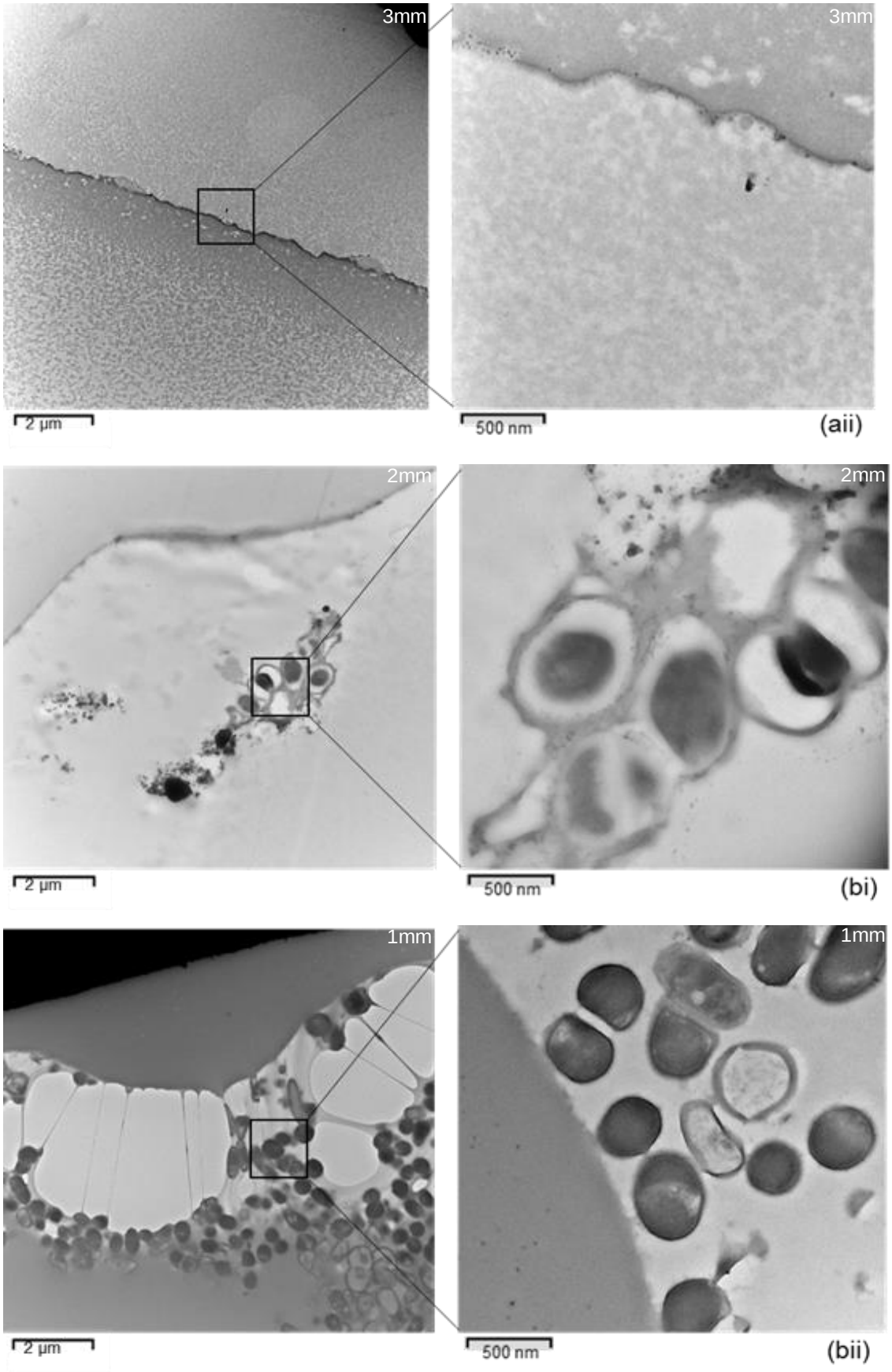
3mm
3mm
2 µm
500 nm
(aii)
2mm
2mm
2 µm
500 nm
(bi)
1mm
1mm
2 µm
500 nm
(bii)

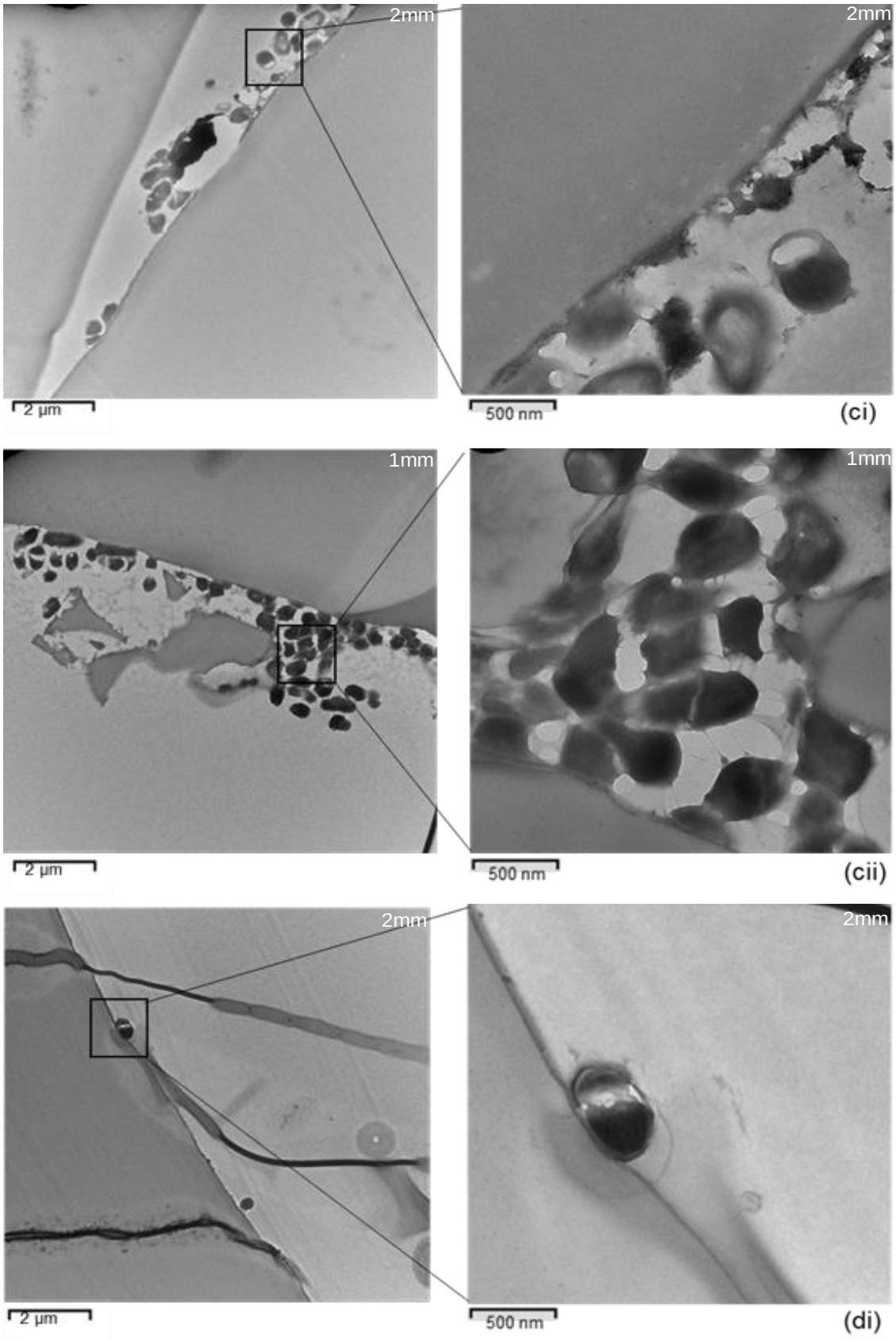
2mm
2mm
2 µm
500 nm
(ci)
1mm
1mm
2 µm
500 nm
(cii)
2mm
2mm
2 µm
500 nm
(di)

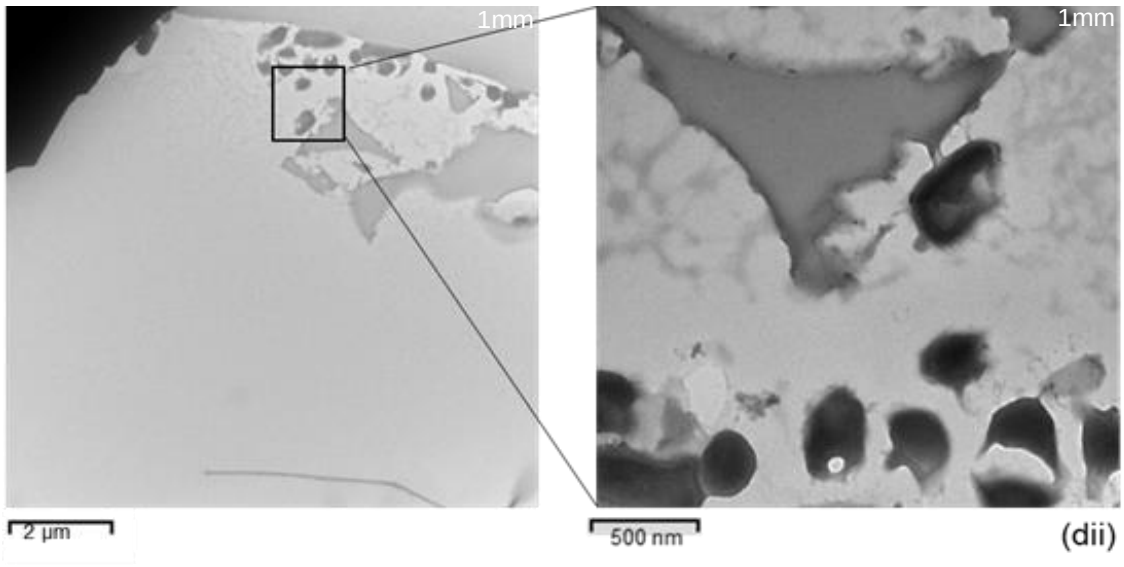

(dii)

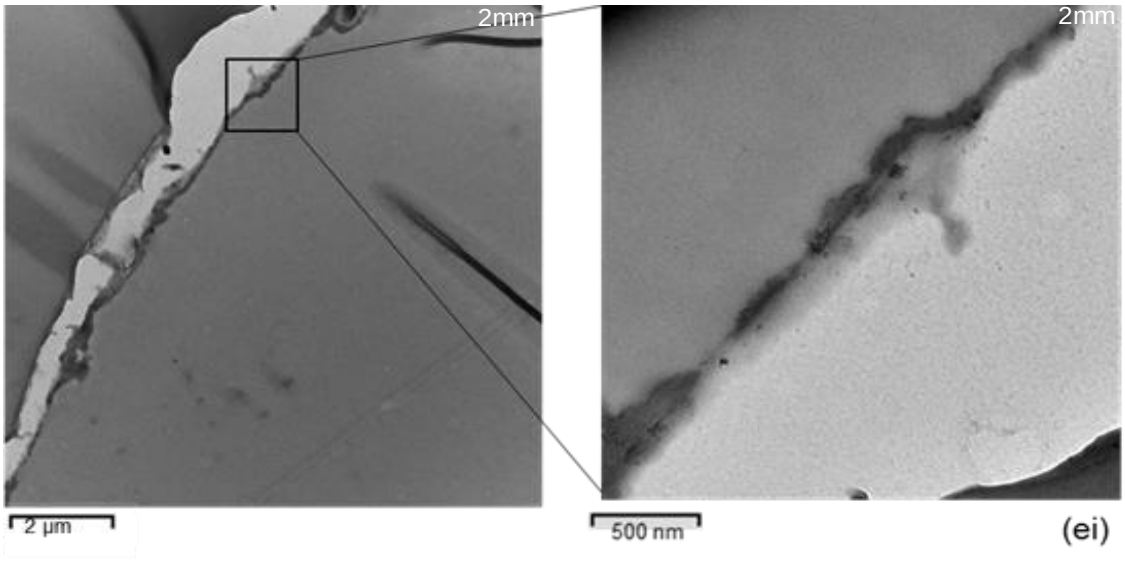

(ei)

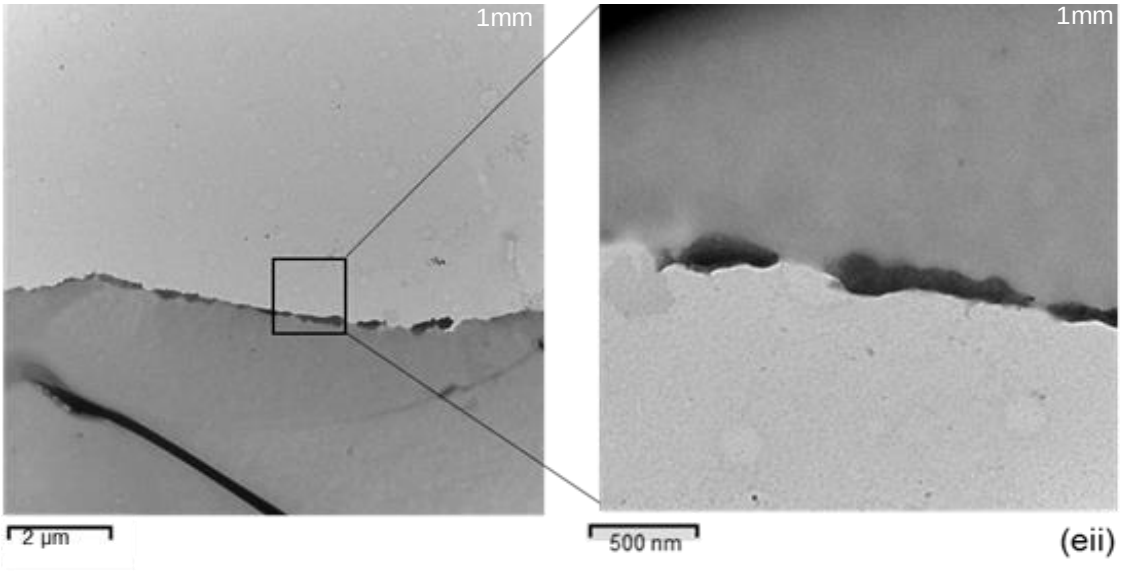

*The information at the upper right of each image indicates the level of the root canal (in mm) from the canal terminus where the residual biofilm was captured.

Figure 6.6: TEM images illustrate (ai) *E. faecalis* biofilm grown for 10 days onto the surface of the root canal model (control). (aii) residual biofilm at 3 mm from the canal terminus after passive irrigation protocol. (b) Passive irrigation group; (i) residual biofilm at 2 mm from the canal terminus; (ii) residual biofilm at 1 mm from the canal terminus. (c) manual-agitation group; (i) residual biofilm at 2 mm from the canal terminus; (ii) residual biofilm at 1 mm from the canal terminus. (d) Sonic agitation group; (i) residual biofilm at 2 mm from the canal terminus; (ii) residual biofilm at 1 mm from the canal terminus. (e) Ultrasonic agitation group; (i) residual biofilm at 2 mm from the canal terminus; (ii) residual biofilm at 1 mm from the canal terminus.

6.4. Discussion

The key attributions of this chapter were to investigate the rate of *E.faecalis* biofilm removal using passive or activated 2.5% NaOCl irrigant delivered into a simulated root canal model, and to compare the efficacy of passive irrigation and three different irrigation protocols (manual, sonic, and ultrasonic) in the biofilm removal. In addition, the effect of biofilm–irrigant interaction on available chlorine and pH was also examined. The findings indicated that the type of irrigation protocol used could be crucial to achieve complete loss of cell viability (killing), destruction, and removal of the bacterial biofilm. Overall, passive irrigation was ineffective, whilst ultrasonic agitation of 2.5% NaOCl seemed the most effective followed by sonic and manual agitation protocols.

The amount of residual biofilm in the canal models in active irrigation groups (manual, sonic, and ultrasonic) decreased from the passive irrigation group (control). The results of the data analysis were confirmed by microscopic image evaluation. Analysis of the microscopic images (CLSM, SEM, and TEM) of the one mm^2 surface area of the root canals at 3 mm showed no marked differences in the biofilm layer, in terms of killing, cell wall destruction and complete removal of biofilm. A possible explanation for these results may be related to fluid dynamics around the tip of the side cut needle, that creates an eddy with a diameter of approximately 1 mm in the area around to the needle tip (Verhaagen *et al.*, 2012), as well as, the chemical action, which related to the oxidizing effect of the OCl^- /$HOCl^-$ of the NaOCl (de Macedo, 2013). In comparison, the greater biofilm destruction and cell killing in active irrigation groups may be related to the impact of agitation on the dissolving capacity of NaOCl (Moorer and Wesselink, 1982). Furthermore, agitation enhances the mixing of fresh irrigant with the stagnant, used fluid in the apical part of the canal (Bronnec *et al.*, 2010). However, the difference in effectiveness of the techniques used to agitate NaOCl inside the root canal may be related to space restrictions of the root canal that interfere with the agitation method. The same abovementioned reasons may once again be responsible for the important finding that the reduction in the total remaining amount of available chlorine and pH of NaOCl was obvious in agitation groups in comparison to the passive syringe group. This suggests that it may be impossible to achieve complete removal of biofilm using passive irrigation in the apical part of the canal.

The difference between the manual, sonic, and ultrasonic agitation may be attributed to the fact that the manual push–pull motion of gutta-percha point

generated frequency is less efficient than the automated methods (Macedo *et al.*, 2014a). The difference between EndoActivator® sonic and ultrasonic agitation can be due to the driving frequency of the ultrasonic device being higher than that of the sonic device (Layton *et al.*, 2015). A higher frequency results in a higher flow velocity of NaOCl irrigant (Ahmad *et al.*, 1988). This may be the result of more biofilm removal by ultrasonic than EndoActivator® irrigation.

The results of this study are broadly consistent with the earlier study of Halford *et al.* (2012) who showed that the ultra-sonic agitation of NaOCl effectively reduces viable *E. faecalis* bacteria in root canal models when compared to syringe and sonic agitation. In contrast, the reduced efficacy of manual agitation compared to sonic and ultrasonic agitation, presented in this study, is not consistent with the results of the Townsend and Maki (2009) study, who suggested that manual agitation, sonic, and ultrasonic were similar in their ability to remove bacteria from the canal walls. These differences can be explained in part by the differences in canal preparation as Townsend and Maki used a size and taper 40/0.10 and 35/0.08; size 30 and taper 0.06 was used herein. For that, the larger apical sizes and taper may enhance irrigant exchange and the hydrodynamic forces generated by manual agitation. Based on the findings, the efficacy of passive irrigation using 2.5% NaOCl was less than that achieved by active irrigation protocols using 2.5% NaOCl. Manual agitation was associated with greater residual biofilm than the automated agitation (sonic & ultrasonic). Hence, the automated agitation increases the efficacy of 2.5% NaOCl within the root canal system. Although the difference between the sonic and ultrasonic agitation groups was not statistically significant ($p > 0.05$), total biofilm destruction and non-viable cells were associated with ultrasonic group. It could conceivably be

hypothesized that the ultrasonic activation provides optimum efficacy of 2.5% NaOCl within the root canal system.

Despite these promising results, there are still many unanswered questions about the efficacy of activated NaOCl on multi-species biofilms in a simple and complex root canal system. Further studies, which take these variables into account, will need to be undertaken.

6.5. Conclusion

Within the limitation of the present study, this study shows that the agitation of NaOCl irrigant is essential for increasing the efficacy of 2.5% NaOCl to remove biofilm. In addition, the use of automated agitation (sonic & ultrasonic) is better when compared to manual agitation. Ultrasonic agitation is recommended to achieve total biofilm destruction and non-viable cells.

Chapter 7

Investigations into the *in situ Enterococcus faecalis* biofilm removal and destruction efficacies of passive and active sodium hypochlorite irrigant delivered into lateral canal of a simulated root canal model

7.1. Introduction

The root canal system is one of the most widely used terms to describe the root canal space because of its complex anatomy that consists of main canals, accessory canal, isthmus, and lateral canals (Paz *et al.*, 2015). The location of bacteria that exist in biofilm form in such complex areas makes their disinfection and cleaning difficult (Ricucci *et al.*, 2009).

Based on radiologic and histologic investigations, Barthel *et al.* (2004) reported no relationship between the situation of the lateral canals being cleaned or infected and the persistence of periodontitis. On the contrary, Seltzer *et al.* (1963) illustrated the association between infected lateral canals and periradicular lesions. This indicates that understanding the irrigation outcomes of the root canal system with complex anatomy (e.g. lateral canal) using different irrigation protocols is important to shine new light on the irrigant action and fate of bacterial biofilm within the root canal system.

The current chapter investigated the effect of different agitation techniques on the efficacy of 2.5% NaOCl to eliminate the biofilm from the surface of the lateral canal using the residual biofilm, removal rate of biofilm, and the extent of destruction of the residual biofilm, as outcome measures. The effect of canal complexity (lateral canal) on the efficacy of the irrigation procedure was also assessed.

7.2. Materials and Methods

7.2.1. Construction of transparent root canal models with lateral canal and distribution to experimental groups

The root canal models (n = 40) were created as described in section 5.2.1 and then divided into four groups (n = 10 per group) in the same manner as described in section 6.2.1. The design of the model used herein consisted of a main canal of 18 mm length, apical size 30, a 0.06 taper, and a lateral canal of 3 mm length, 0.3 mm diameter located at 3 mm from the apical terminus (Figure 7.1).

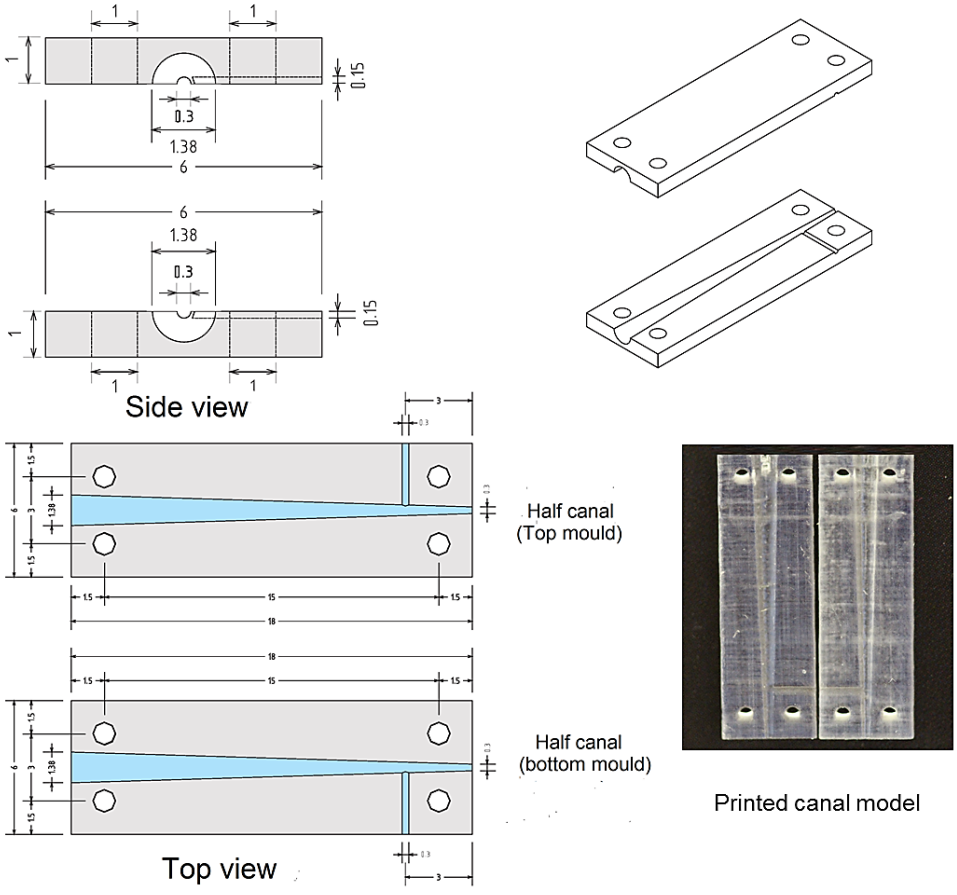

Figure 7.1: Image illustrates the design of the complex root canal mode (main and lateral canals. Each half of a simulated canal is of 18 mm length with 1.38 mm diameter at the coronal portion and 0.3 mm diameter at the apical portion. The lower view shows the printed two halves and when they are reassembled, a straight simple canal of 18 mm length, apical size 30, and a 0.06 taper is created with lateral canal of 3 mm length, 0.3 mm diameter.

7.2.2. Preparation of microbial strain and determination of the standard inoculum

The preparation microbial strain and determination of the standard inoculum were performed as described in section 2.2.2.4.2.

7.2.3. Generation of single species biofilm (*E. faecalis*) on the surface of the apical 3 mm of the canal model

This step was performed as described in section 5.2.3.

7.2.4. Staining of biofilms grown on the surface of the models

The staining procedure was performed as mentioned in section 3.2.5.4.

7.2.5. Re-apposition of the model halves

This step was performed as described in section 5.2.5.

7.2.6. Irrigation experiments

This step is illustrated in Figure 7.2 and it was performed as described in section 6.2.6.

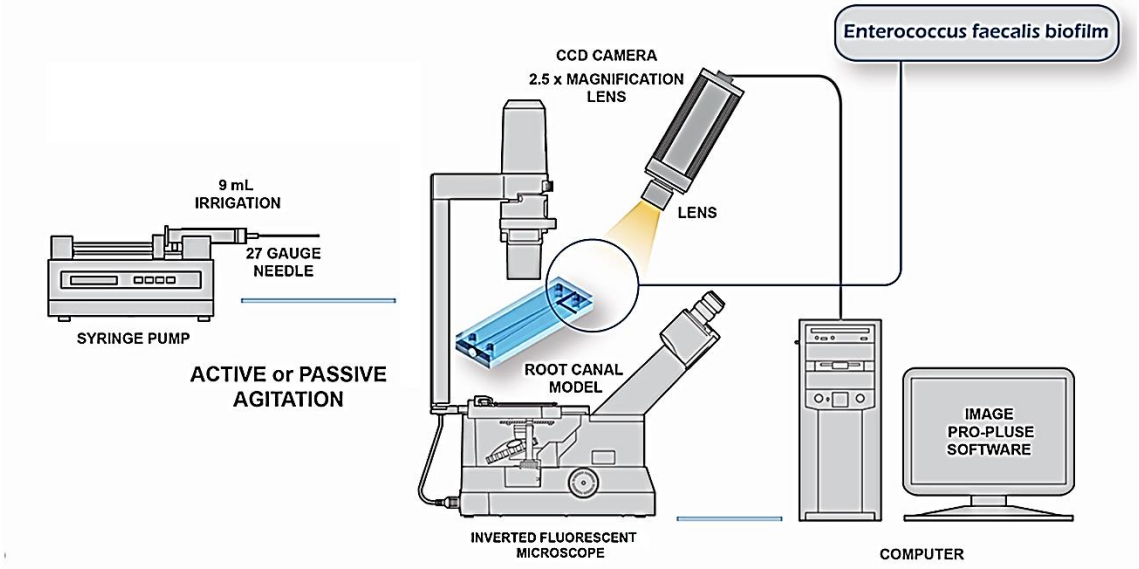

Figure 7.2: Sketch illustrating the set-up of equipment for recording of the biofilm (biofilm was generated on the apical portion (3 mm) of the main and lateral (3 mm) canals model) removal by active or passive NaOCl irrigation protocol using a camera connected to a 2.5× lens of an inverted fluorescent microscope. The irrigant was delivered using a syringe with a 27-gauge side-cut open-ended needle, which was attached to a programmable precision syringe pump. The residual biofilm was quantified using computer software (Image-pro Plus 4.5).

Following irrigation protocols, the residual NaOCl on the model surface was immediately neutralised by immersing the models in 2 mL of 5% sodium thiosulphate solution (Sigma-Aldrich Co Ltd., Gillingham, UK) for 5 minutes. This reduces the active ingredient of NaOCl (hypochlorite), which becomes oxidized to sulphate (Hegde *et al.*, 2012).

The models in each group were then randomly divided in to three subgroups for investigation with CLSM, SEM, and TEM microscopy techniques (n = 3 per subgroup).

7.2.7. Recording of biofilm removal by the irrigant

This step was performed as described in section 3.2.7.2.

7.2.8. Image analysis

Image analysis was performed as described in section 3.2.8.

7.2.9. Preparation of the samples for confocal laser scanning microscope (CLSM)

The illustration of this step is described in Figure 7.3. Sample were prepared as mentioned in section 6.2.10.

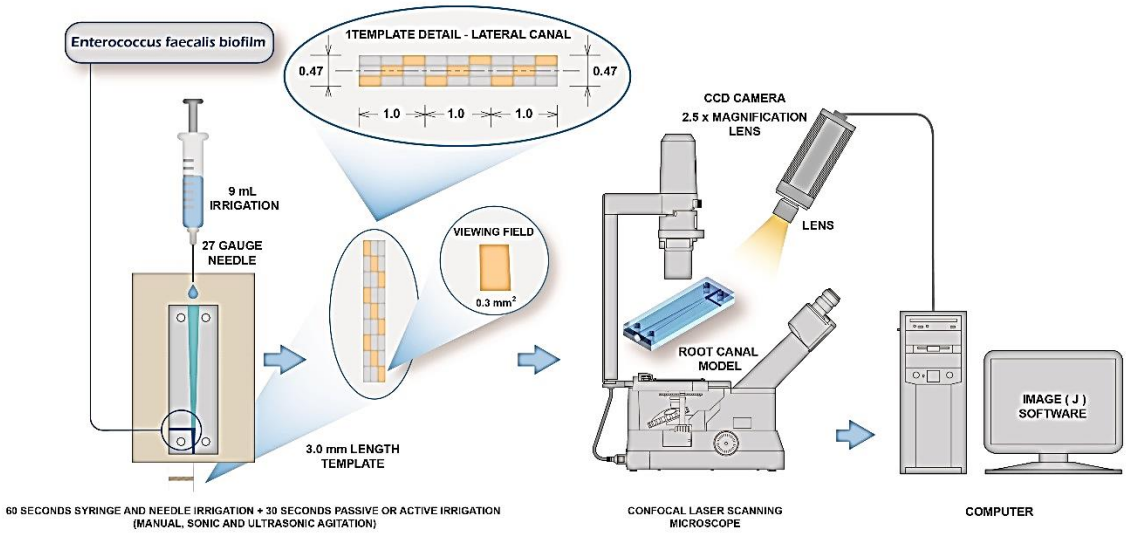

Figure 7.3: Image illustrates the set-up of the equipment to examine the residual biofilm in the lateral canal. Confocal laser scanning microscope was used to observe and record images of the live/dead cells within the residual biofilm. A template was used to control the viewing fields (0.3 mm^2) which were located in the top, middle, and bottom of the tested area. The areas were imaged manipulated using ImageJ® software.

7.2.10. Preparation of the samples for scanning electron microscope (SEM)

The samples were prepared as mentioned in section 6.2.11.

7.2.11. Preparation of the samples for transmission electron microscope (TEM)

The samples were prepared as described in section 6.2.12.

7.2.12. Data analyses

The residual biofilm (%) on the surface of the root canal model with a lateral canal anatomy at each second of 90 seconds irrigation with passive and active 2.5% NaOCl irrigant was analysed using line plots. An assumption concerning a normal distribution of data for the residual biofilm was checked using a visual inspection of the box and whisker plots. The data representing the percentages of residual biofilm covering the lateral canal surface area were normally distributed and therefore the generalised linear mixed models, followed by Dunnett *post-hoc* comparisons were performed to compare their distributions in the four

experimental groups. A similar analysis was performed to analyse the effects of irrigant agitation duration (time) and experimental group (passive or manual, sonic, and ultrasonic active irrigation) on the percentage of residual biofilm covering the lateral canal surface area. A comparison of the effect of the two-model designs used in this study (simple, complex anatomy) on the removal efficacy of NaOCl was performed using the same statistic model. A significance level of 0.05 was used throughout. The data were analysed by SPSS (BM Corp. Released 2013. IBM SPSS Statistics for Windows, Version 22.0. Armonk, New York, IBM Corp).

7.3. Results

7.3.1 Statistical analysis

The mean (95% Confidence interval) percentages of the lateral canal surface area coverage with residual bacterial biofilm against duration of irrigation(s) stratified by type of irrigation are presented in Figure 7.4. The data show that the greatest removal was associated with the ultrasonic agitation group (66.76%) followed by sonic agitation (45.49%), manual agitation (43.97%), and passive irrigation groups (control) (38.67%) respectively.

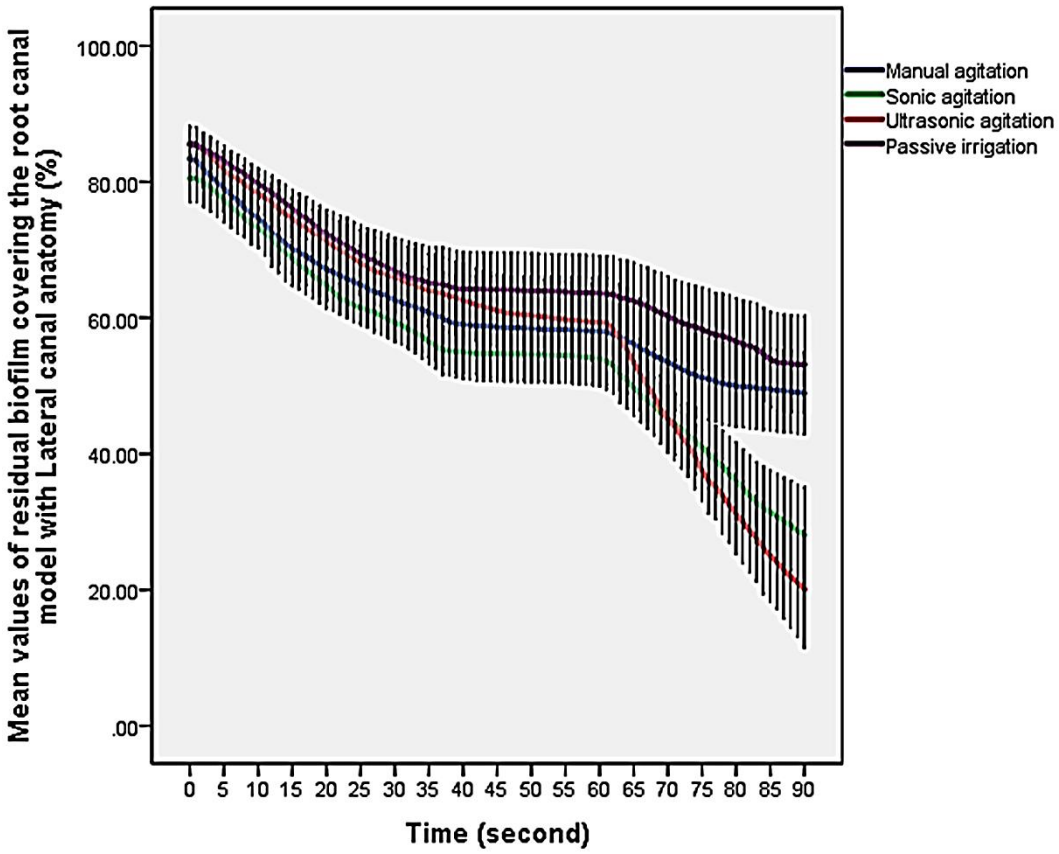

Figure 7.4: Mean (95% CI) percentages values of the residual biofilm (%) covering the root lateral canal surface-area over duration (s) of syringe irrigation followed by passive or active irrigation protocols, stratified by type of irrigation (n = 10 per group).

The results from the linear mixed model (Table 7.1) indicated that there was a statistically significant difference between the residual biofilm on the lateral canal surface area in the passive irrigation group and the automated groups (sonic & ultrasonic) ($p = 0.001$). Amongst the agitation groups, strong evidence of less residual biofilm was found in the ultrasonic agitation group than those in the sonic and manual agitation groups ($p = 0.011$).

Table 7.1: Generalized linear mixed model analysis to compare the difference in the amount of residual biofilms (%) covering the lateral canal surface following passive or active irrigation time with 2.5 % NaOCl irrigant (n = 10 per group).

Experimental groups	*Coefficient (±SE)	95% CI	p value
Manual agitation vs passive irrigation	10.78 (±5.9)	0.81, 22.36	0.068
Sonic agitation vs passive irrigation	21.04 (±5.9)	9.46, 32.63	**0.001**
Ultrasonic agitation vs passive irrigation	56.08 (±5.9)	44.49, 67.67	**0.001**
Manual agitation vs ultrasonic agitation	-66.88 (±5.9)	-78.46, -55.29	**0.011**
Sonic agitation vs ultrasonic agitation	-34.91 (±5.9)	-46.49, 23.33	**0.011**
Manual agitation vs sonic agitation	-32.31 (±8.1)	-43.89, 20.72	**0.011**

*Coefficient for the residual biofilm, SE= standard error, CI = Confidence interval.

Another important finding of the generalized linear mixed model analysis (Table 7.2) was that the interval of irrigant agitation had an influence on the amount of biofilm removed. The amount of biofilm removed using passive irrigation group was [0.51%/s; (±0.08), 1.01%/s; (±0.08)] less than the amount of biofilm removed using sonic, and ultrasonic agitation groups respectively. This was statistically significant (p = 0.001). For the agitation groups, the amount of biofilm removed using the ultrasonic agitation group was [0.07%/s; (±0.06), 0.49%/s; (±0.06)] more than that using the manual and sonic agitation group respectively. This was statistically significant (p = 0.001).

Regardless of the flushing protocols, a comparison of the two-model design (simple, complex anatomy model) revealing no marked reduction in the efficiency of NaOCl to remove biofilm from the main canal was found between the simple and complex anatomy models, as the difference in the residual biofilms was not significant (p = 0.098).

Table 7.2: Generalized linear mixed model analysing the effect of time (seconds) on the amount of biofilm removed from the lateral canal surface of each experimental group (n = 10 per group).

Experimental groups	*Coefficient (±SE)	95% CI	p value
Manual agitation vs passive irrigation	-0.06 (±0.08)	-0.22, 0.09	0.428
Sonic agitation vs passive irrigation	-0.51(±0.08)	-0.66, 0.36	**0.001**
Ultrasonic agitation vs passive irrigation	-1.01 (±0.08)	-1.12, -0.85	**0.001**
Manual agitation vs ultrasonic agitation	0.07 (±0.08)	0.91, 1.22	**0.001**
Sonic agitation vs ultrasonic agitation	0.49 (±0.08)	0.34, 0.65	**0.001**
Sonic agitation vs manual agitation	0.58 (±0.08)	0.43, 0.74	**0.001**

*Coefficient for time effect represents the rate of biofilm removal, SE= standard error, CI = Confidence interval.

7.3.2. Microscopic images analysis

The CLSM images of the biofilm on the surface of the lateral canal of the root canal models before and after irrigation are presented in Figure 7.5.

The CLSM image of the root canal model, which received no treatment (control group), (Fig. 7.5.ai) showed more live cell clusters (green) than the dead cell clusters (red). The black background of the image indicates the no fluorescent property of the model materials.

At the 3 mm level from the lateral canal terminus of the models treated with 2.5% NaOCl, the CLSM images illustrated more dead cell clusters in the passive irrigation group (Fig. 7.5.aii) than the manual agitation group (Fig.7.5. aiii). Notwithstanding, full biofilm destruction was detected in the automated group (sonic & ultrasonic) (Fig. 7.5.aiv). The CLSM images of the biofilm at the 2 mm level indicated the presence of residual biofilm with viable cells in the passive irrigation group (Fig. 7.5.bi) and manual agitation group (Fig. 7.5.ci). However, only dead cell clusters of residual biofilm were noted in the automated groups (sonic & ultrasonic), which were plenteous in the former (Fig. 7.5.di) than the later (Fig. 7.5.ei) group.

Again, an abundance of viable cell clusters was observed at the 1 mm level in both passive irrigation (Fig. 7.5.bii) and manual agitation (Fig. 7.5.cii) groups. With reference to the automated groups, the viable cell clusters were more prevalent than the dead cell clusters. Yet, the dead cell clusters in the sonic (Fig. 7.5.dii) group were sparse compared to that of the ultrasonic group (Fig. 7.5.eii).

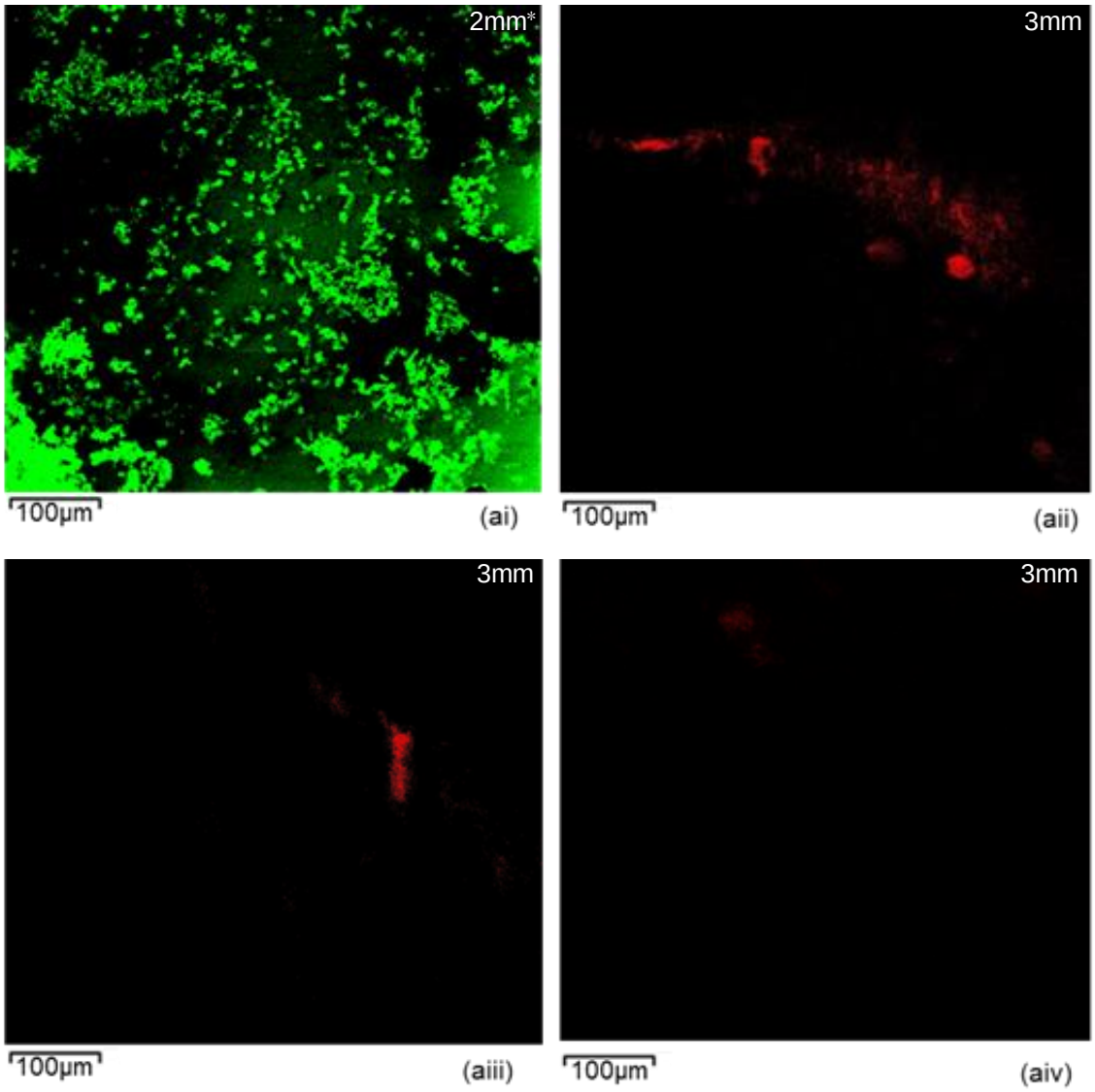

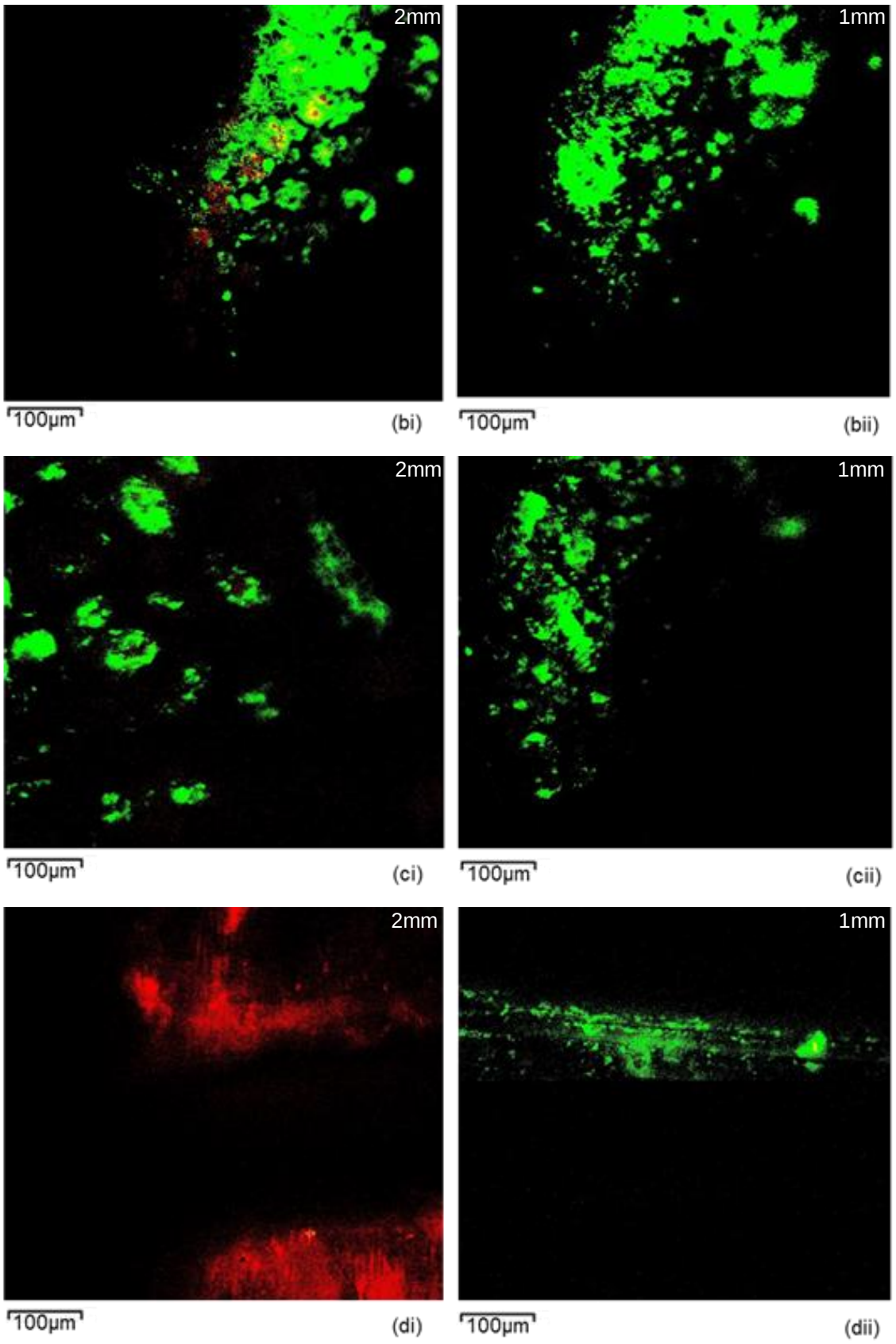
2mm
1mm
100µm
(bi)
100µm
(bii)
2mm
1mm
100µm
(ci)
100µm
(cii)
2mm
1mm
100µm
(di)
100µm
(dii)

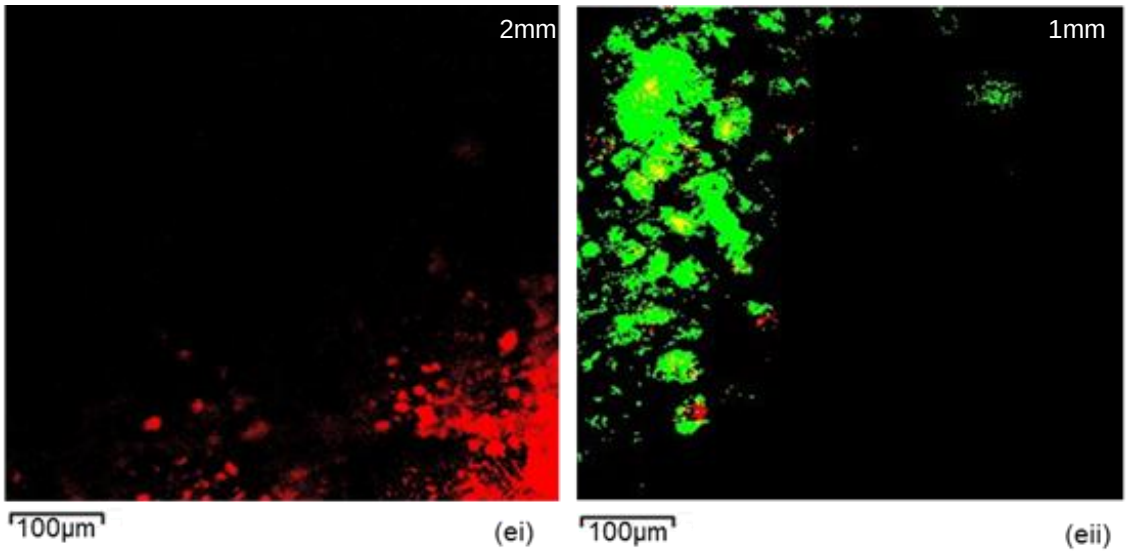

*The information at the upper right of each image indicates the level of the root canal (in mm) from the canal terminus where the residual biofilm was captured.

Figure 7.5: CLSM images (0.3 mm^2) from within the lateral canal to illustrate (ai) *E. faecalis* biofilm grown for 10 days and stained using Live/Dead® viability stain with the green colour indicating live cells and the red colour showing the dead bacteria (control). (aii, aiii, and aiv) residual biofilm at 3 mm from the lateral canal after passive irrigation, manual, sonic protocols respectively. (b) Passive irrigation group; (i) residual biofilm at 2 mm from the lateral canal terminus; (ii) residual biofilm at 1 mm from the lateral canal terminus. (c) manual-agitation group; (i) residual biofilm at 2 mm from the lateral canal terminus; (ii) residual biofilm at 1 mm from the lateral canal terminus. (d) Sonic agitation group; (i) residual biofilm at 2 mm from the lateral canal terminus; (ii) residual biofilm at 1 mm from the lateral canal terminus. (e) Ultrasonic agitation group; (i) residual biofilm at 2 mm from the lateral canal terminus; (ii) residual biofilm at 1 mm from the lateral canal terminus.

SEM images of the biofilm on the surface of the lateral canal models before and after irrigation are presented in Figure 7.6.

Taking the biofilm structure of the untreated model into account, SEM images (Fig. 7.6ai) showed cocci morphology of the bacteria cell. Bacterial cells were often gathered in colonies, and held together by a matrix of extracellular polymeric substance. Complete encapsulation of bacterial cells by the matrix could be observed.

The influences of 2.5% NaOCl irrigation on biofilm at the 3 mm level from the canal terminus are presented in Figure 7.6 (aii, aiii, aiv). Although SEM images of passive irrigation (Fig. 7.6aii) and manual agitation (Fig. 7.6aiii) groups showed residual biofilm with obvious ESP destruction and a damaged cell membrane;

some bacteria cells appeared flawless. Entire biofilm elimination was associated with automated groups (Fig. 7.6aiv).

At the 2 mm level, reduction in removal and destruction effect were evident in the passive irrigation (Fig. 7.6bi) and manual (Fig. 7.6ci) groups, and communities of bacterial cells held by EPS matrix were noted. This effect was more distinct in the former group. Regarding the automated groups, the greatest biofilm deformation and removal was associated with the ultrasonic group (Fig. 7.6ei) followed by the sonic group (Fig. 7.6di).

At 1 mm from the canal terminus, both passive irrigation (Fig. 7.6bii) and manual (Fig. 7.6cii) groups showed no effect and this pattern was reflected in the intact form and structure of the biofilm. The destruction effect of biofilm by NaOCl was noticed in the sonic (Fig. 7.6dii) and ultrasonic (Fig. 7.6eii) groups. This effect was superior in the latter group. However, unharmed bacterial cells that are enclosed in an extracellular polymeric substance was identified.

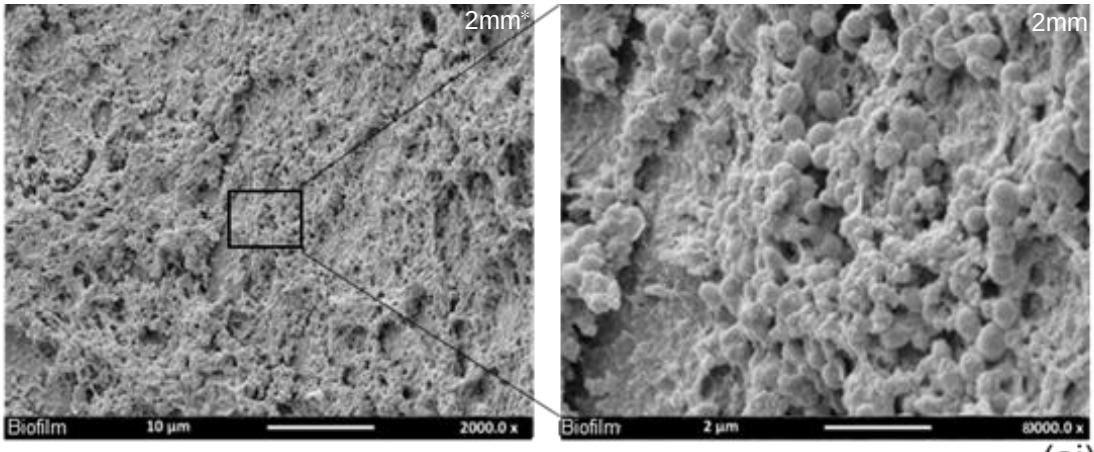

(ai)

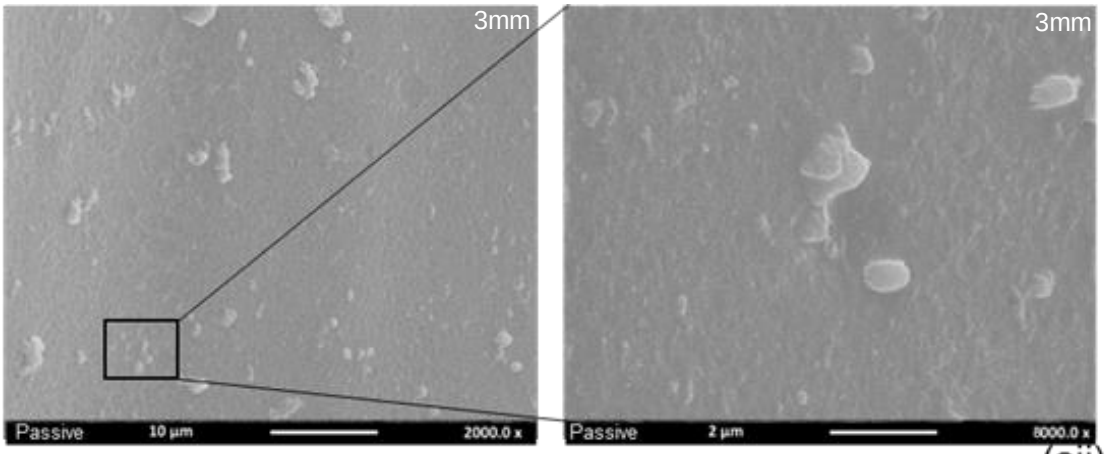
3mm
3mm
Passive
10 µm
2000.0 x
Passive
2 µm
8000.0 x

(aii)

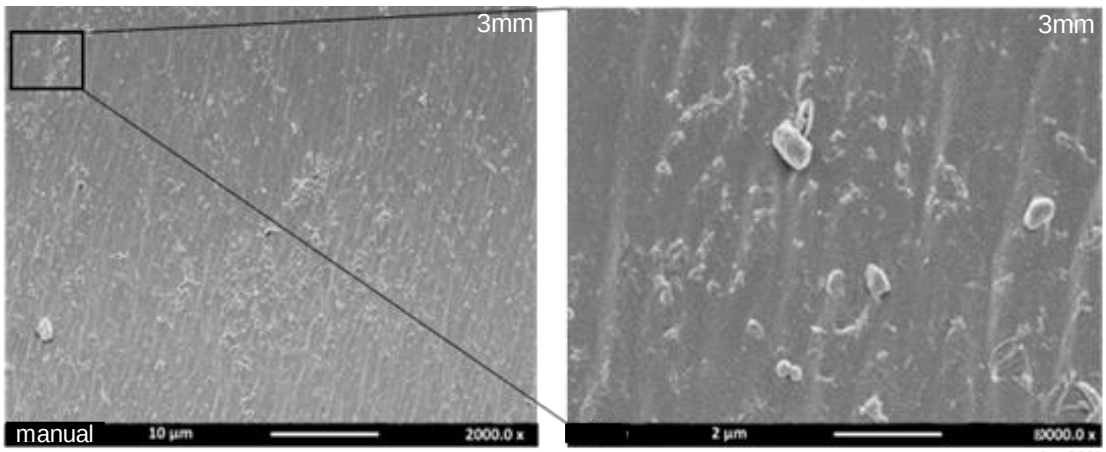
3mm
3mm
manual
10 µm
2000.0 x
2 µm
8000.0 x

(aiii)

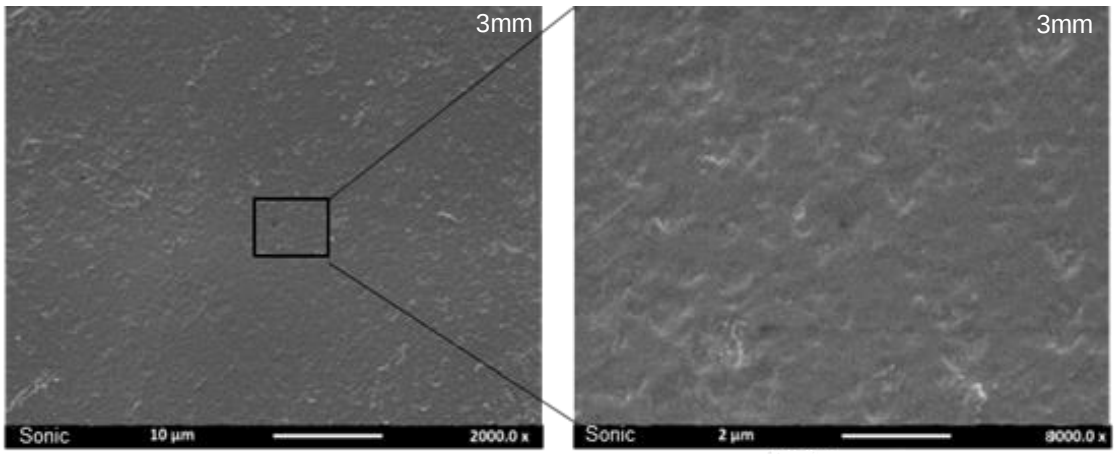
3mm
3mm
Sonic
10 µm
2000.0 x
Sonic
2 µm
8000.0 x

(aiv)

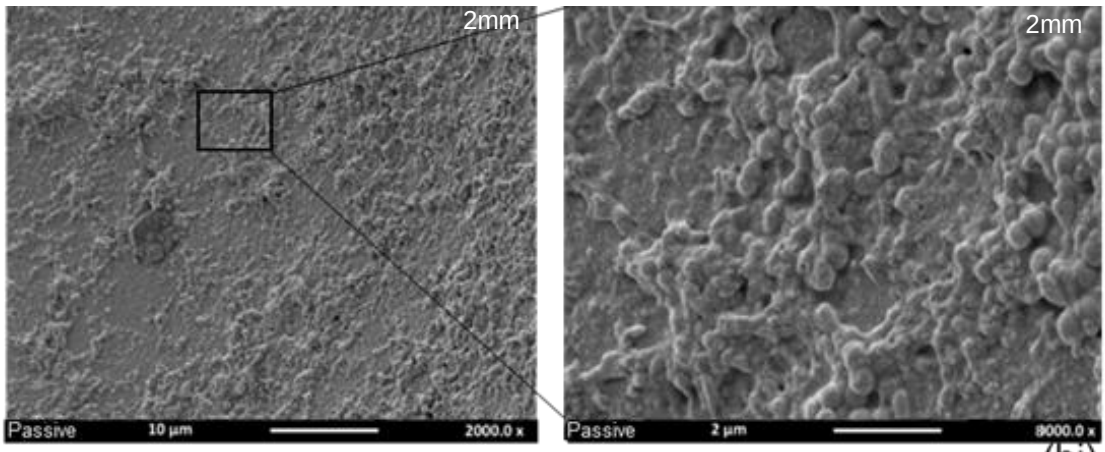
2mm
2mm
Passive
10 µm
2000.0 x
Passive
2 µm
8000.0 x

(bi)

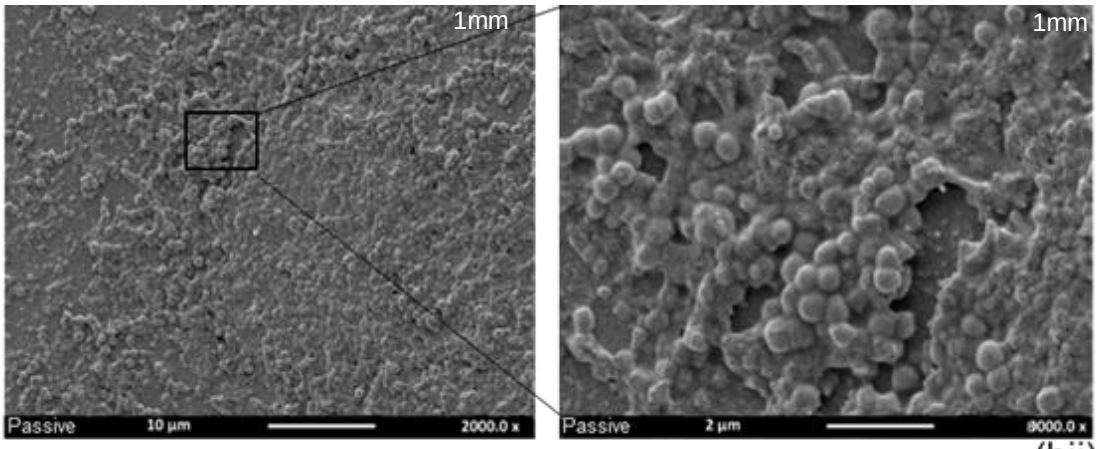
1mm
1mm
Passive
10 µm
2000.0 x
Passive
2 µm
8000.0 x

(bii)

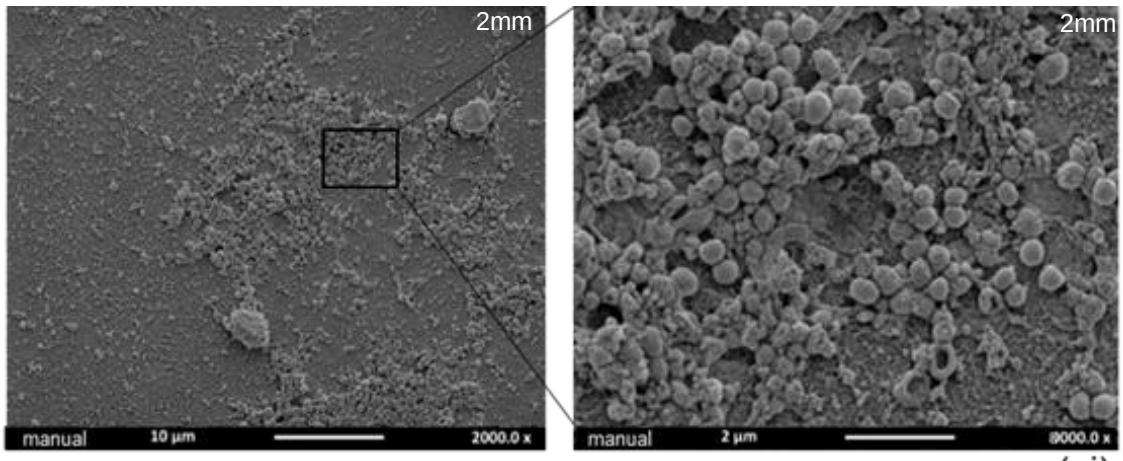
2mm
2mm
manual
10 µm
2000.0 x
manual
2 µm
8000.0 x

(ci)

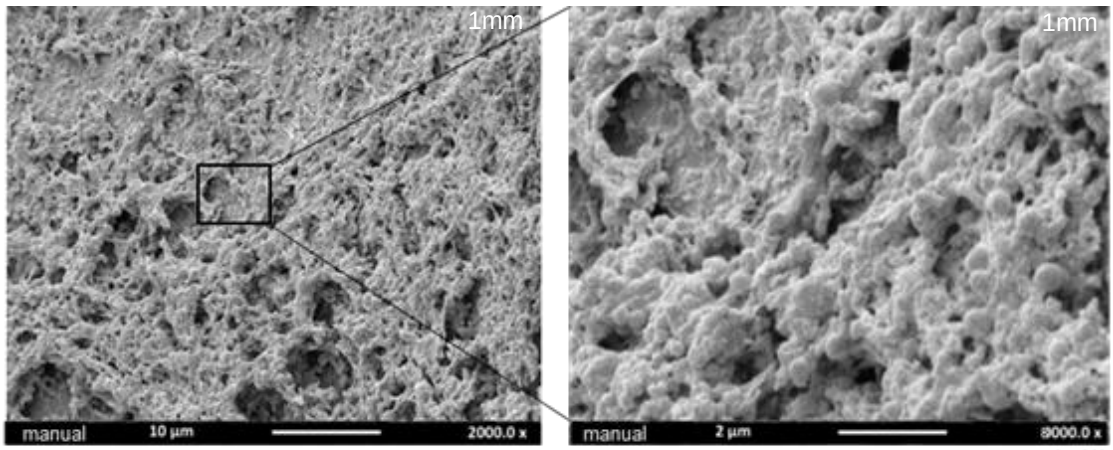
1mm
manual
10 µm
2000.0 x
1mm
manual
2 µm
8000.0 x

(cii)

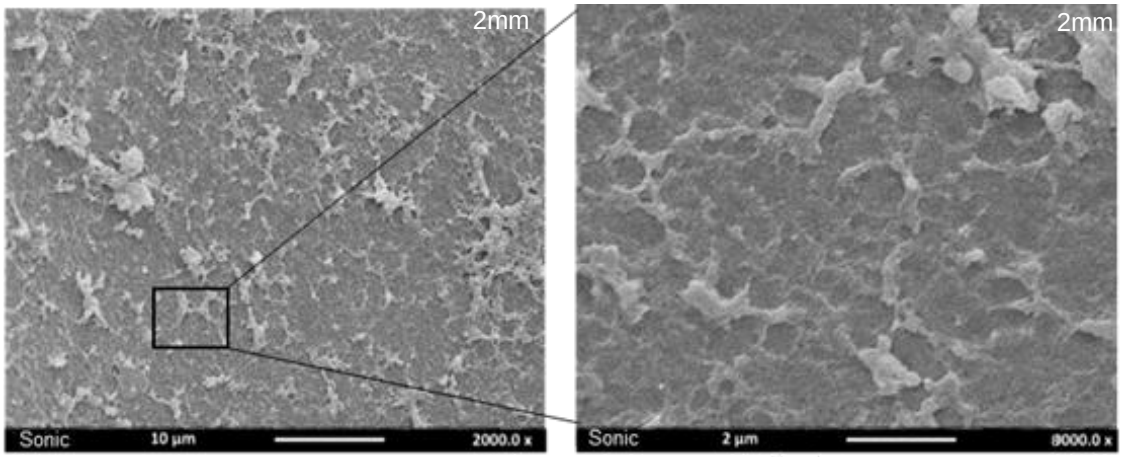
2mm
Sonic
10 µm
2000.0 x
2mm
Sonic
2 µm
8000.0 x

(di)

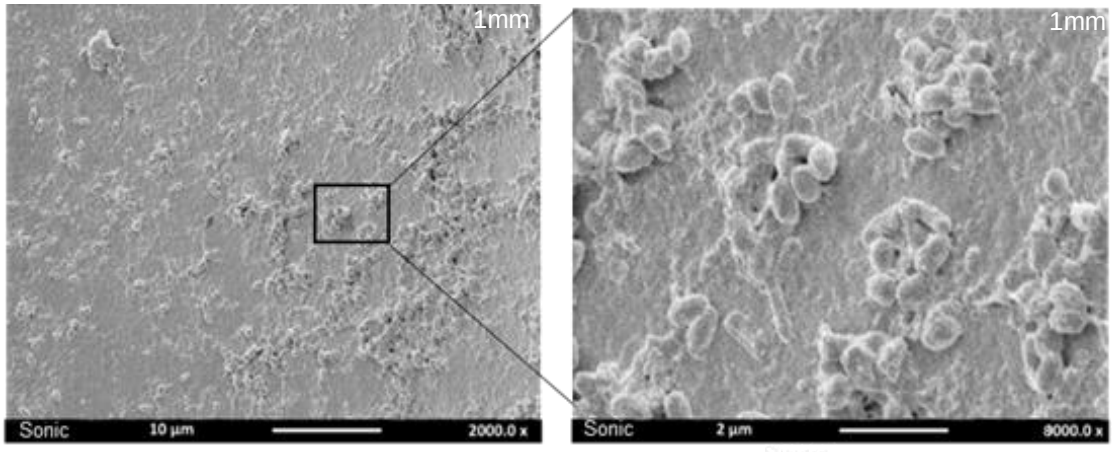
1mm
Sonic
10 µm
2000.0 x
1mm
Sonic
2 µm
8000.0 x

(dii)

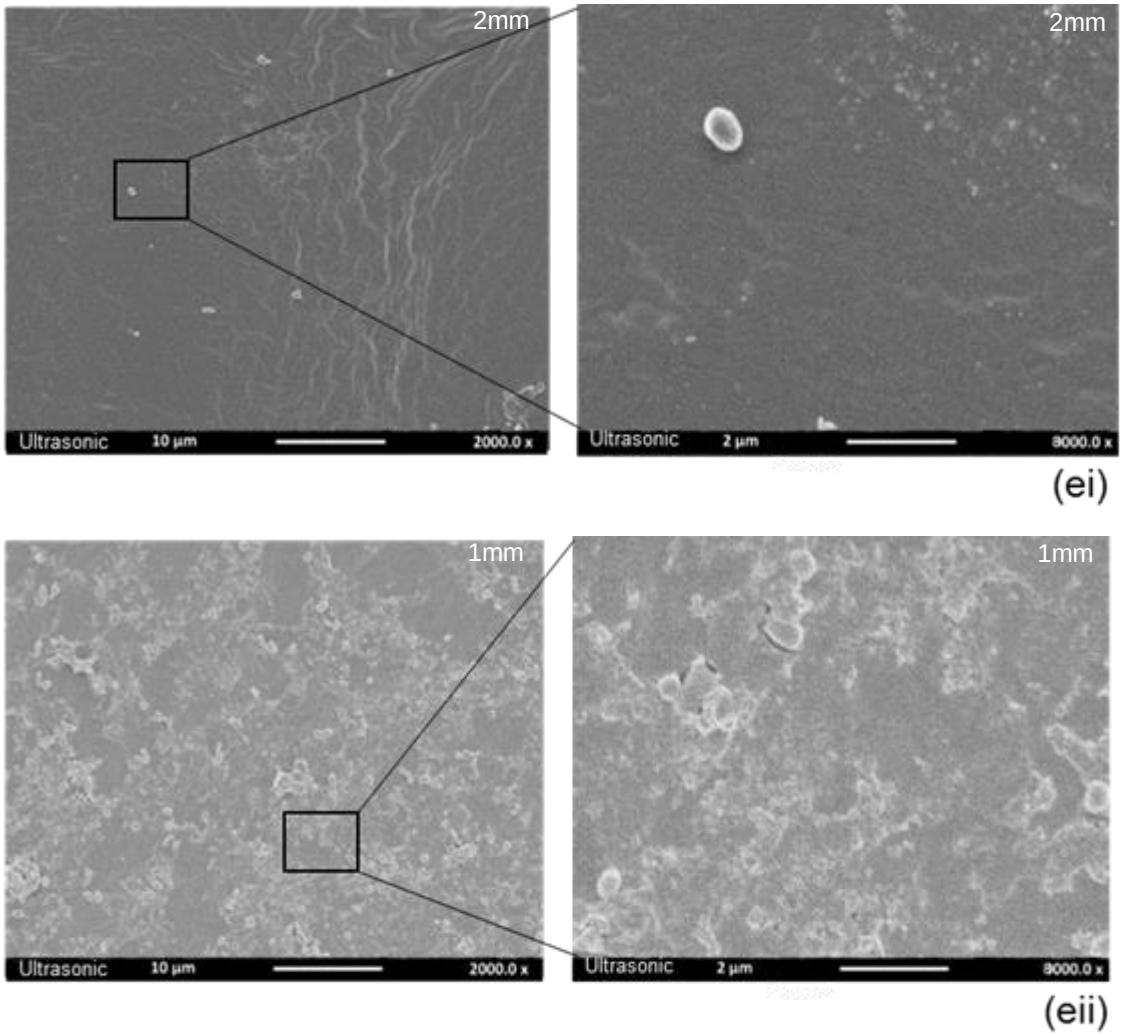

*The information at the upper right of each image indicates the level of the root canal (in mm) from the canal terminus where the residual biofilm was captured.

Figure 7.6: SEM images illustrate (ai) *E. faecalis* biofilm grown for 10 days. (aii, aiii, and aiv) residual biofilm at 3 mm from the lateral canal after passive irrigation, manual, sonic protocols respectively. (b) Passive irrigation group; (i) residual biofilm at 2 mm from the lateral canal terminus; (ii) residual biofilm at 1 mm from the lateral canal terminus. (c) manual-agitation group; (i) residual biofilm at 2 mm from the lateral canal terminus; (ii) residual biofilm at 1 mm from the lateral canal terminus. (d) Sonic agitation group; (i) residual biofilm at 2 mm from the lateral canal terminus; (ii) residual biofilm at 1 mm from the lateral canal terminus. (e) Ultrasonic agitation group; (i) residual biofilm at 2 mm from the lateral canal terminus; (ii) residual biofilm at 1 mm from the lateral canal terminus.

The TEM images of the biofilm on the surface of the lateral canal models before and after irrigation using passive irrigation, manual and automated agitation protocols are presented in Figure 7.7.

TEM images of the untreated multi-species biofilm on the root canal model (Fig. 7.7ai) displayed a group of cocci shape cell enclosed by an extracellular matrix. At higher magnification, the bacterial cells consisted of cytoplasm enveloped by cytoplasmic membrane and unblemished cell wall.

At the 3 mm level from the canal terminus, the impact of 2.5% NaOCl irrigation on the biofilm was indisputable in all groups. Yet, the impact was comparably lesser in passive irrigation (Fig. 7.7aii) and manual (Fig. 7.7aiii) groups. This is because cells with a damaged cell wall, as well as ghost cells (empty cells) were recognised. In contrast, residual biofilm was roughly eradicated in the automated groups (Fig. 7.7aiv).

At the 2 mm level, a high proportion of the bacterial cells in the passive irrigation (Fig. 7.7bi) and manual (Fig. 7.7ci) were surrounded by intact EPS with the majority having an unbroken cell wall. In relation to the automated groups, the bulk of the residual biofilm consisted of ghost cell, cells with a perforated cell wall, and a smashed cell. This was more evident in the ultrasonic group (Fig. 7.7ei) than the sonic group (Fig. 7.7di). A few intact bacterial cells were identified in the latter group.

At 1 mm, a lack of an irrigant destruction effect was notified in both passive irrigation (Fig. 7.7bii) and manual (Fig. 7.7cii) groups, as components of the residual biofilm was undamaged. In comparison, the destructive effect of NaOCl was evident in the sonic (Fig. 7.7dii) and ultrasonic (Fig. 7.7eii) groups. This effect was greater in the latter group. However, this effect was generally not severe, since the biofilm with cocci morphology cells, which were enclosed by the matrix was detected.

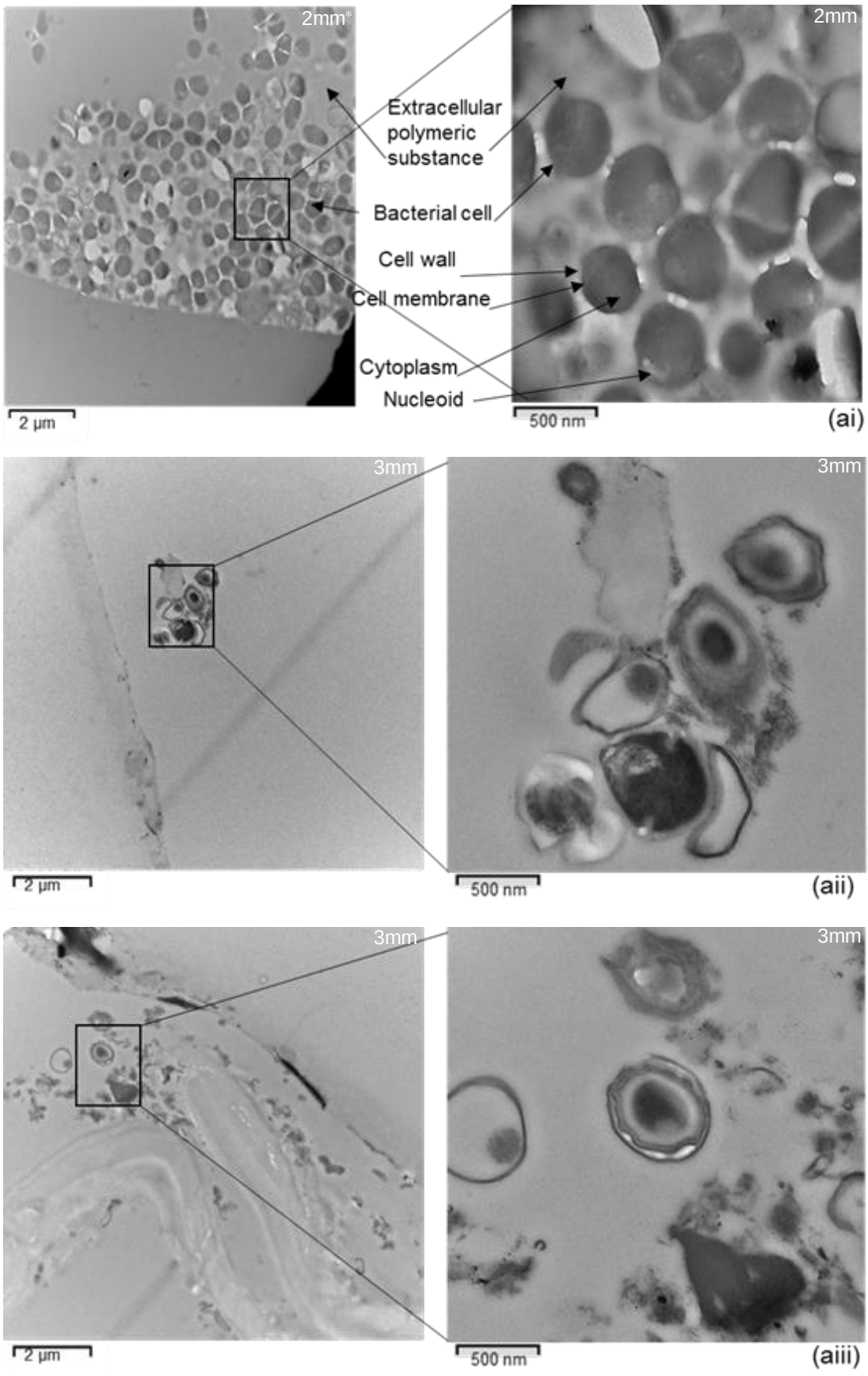
2mm*
2mm
Extracellular polymeric substance
Bacterial cell
Cell wall
Cell membrane
Cytoplasm
Nucleoid
2 µm
500 nm
(ai)
3mm
3mm
2 µm
500 nm
(aii)
3mm
3mm
2 µm
500 nm
(aiii)

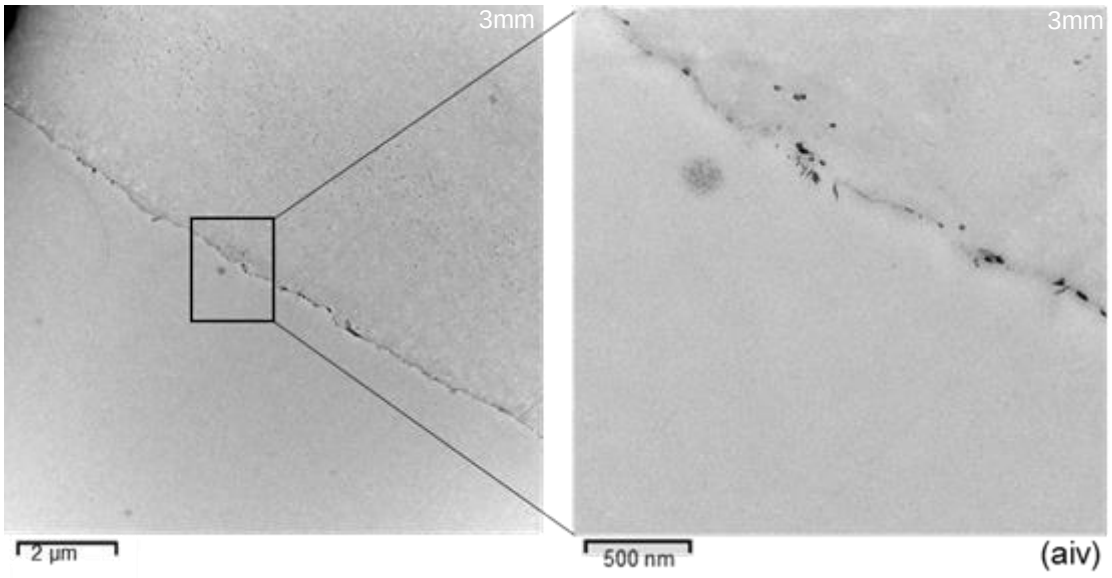
3mm
3mm
2 µm
500 nm
(aiv)

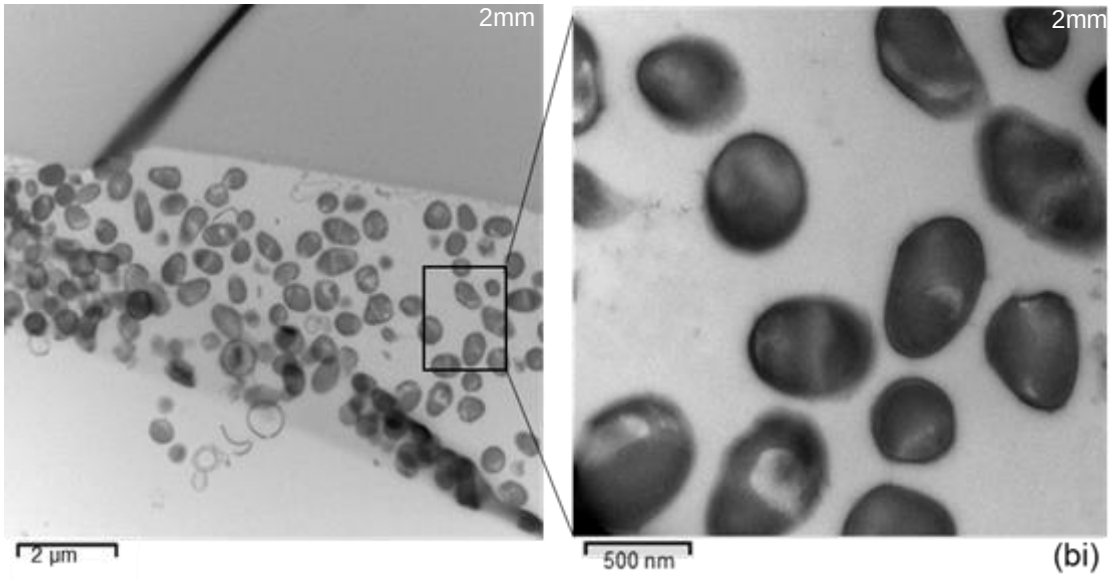
2mm
2mm
2 µm
500 nm
(bi)

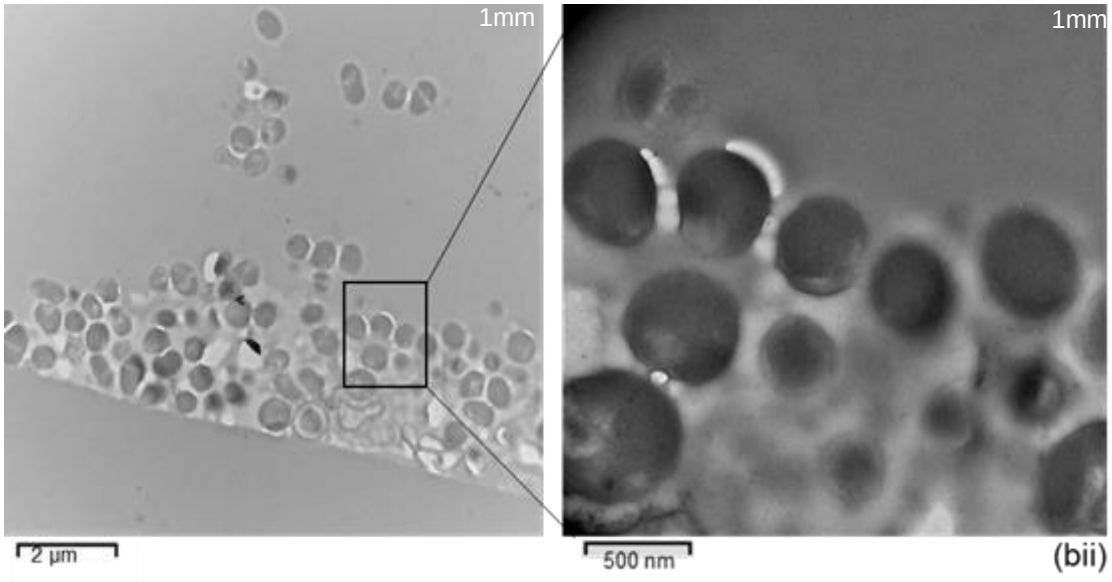
1mm
1mm
2 µm
500 nm
(bii)

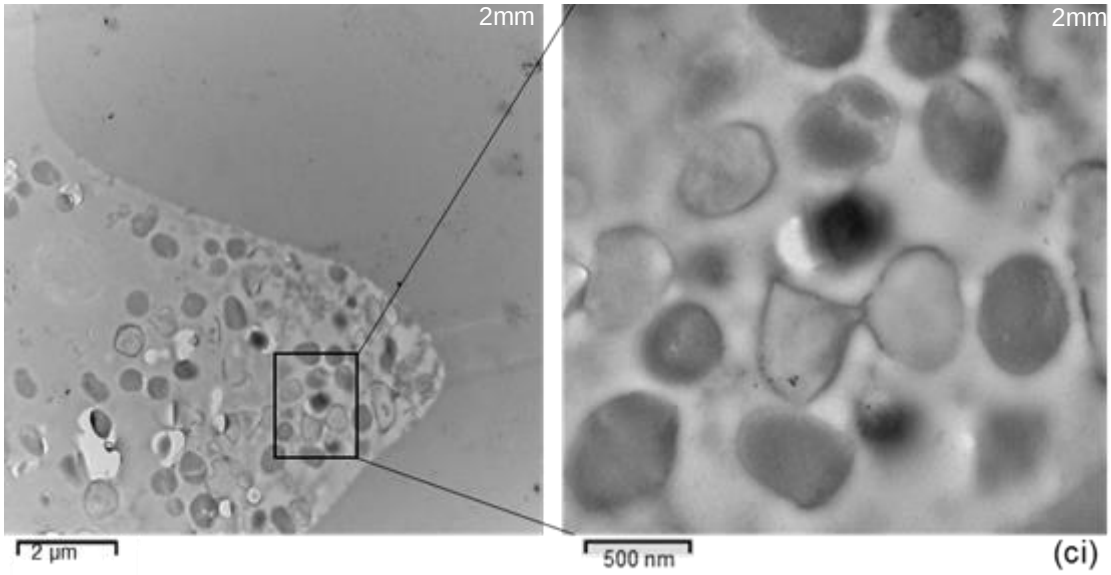
2mm
2mm
2 µm
500 nm
(ci)

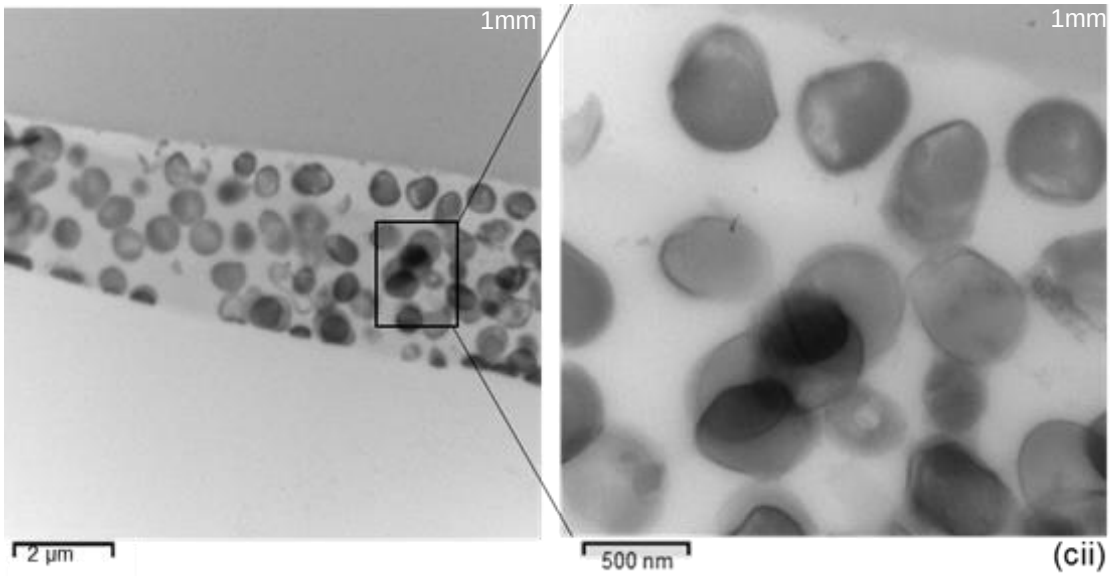
1mm
1mm
2 µm
500 nm
(cii)

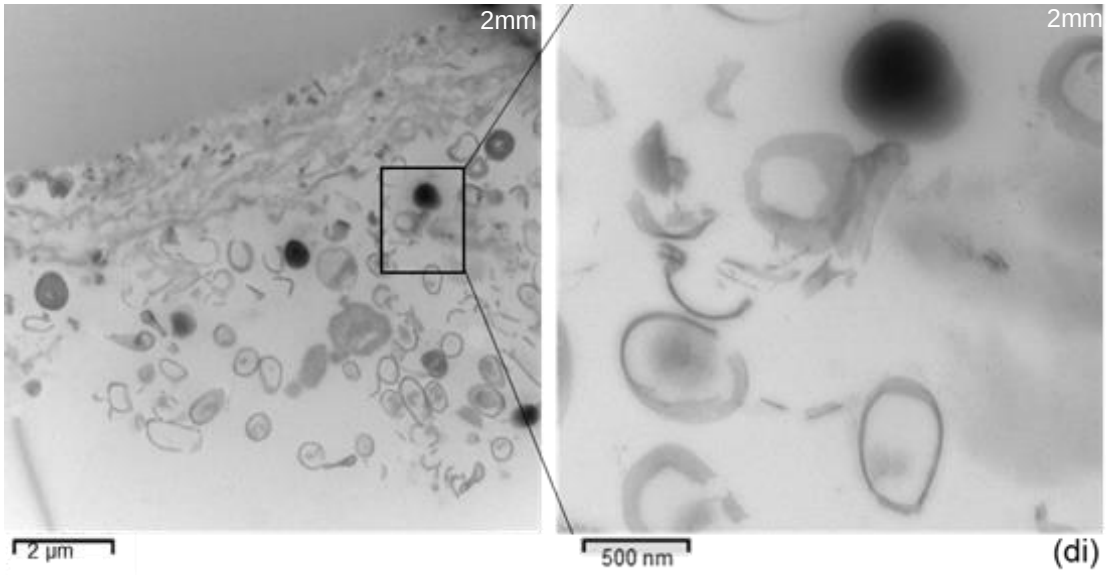
2mm
2mm
2 µm
500 nm
(di)

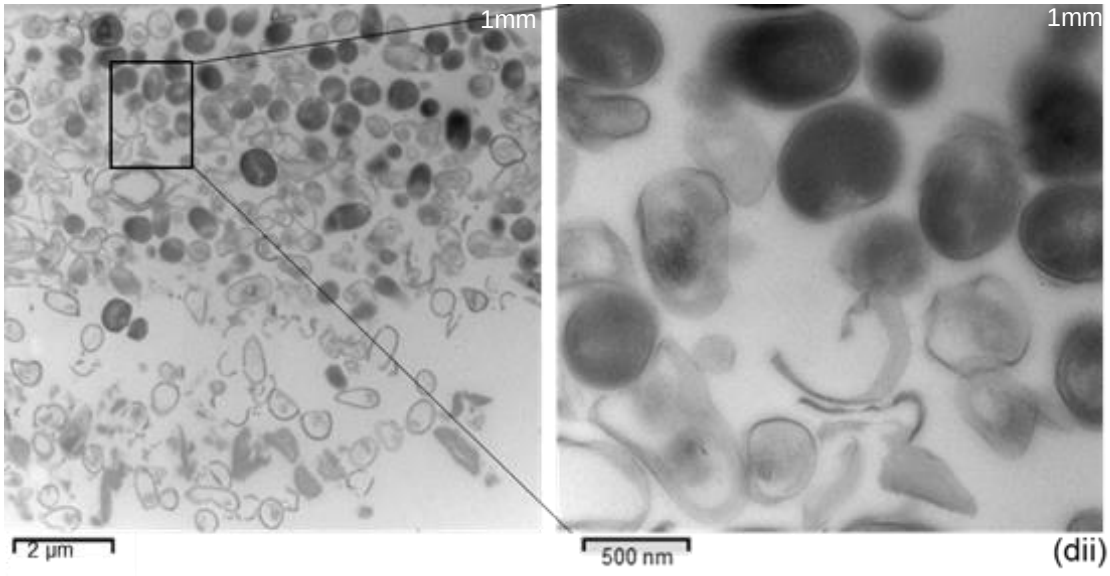
1mm
1mm
2 µm
500 nm
(dii)

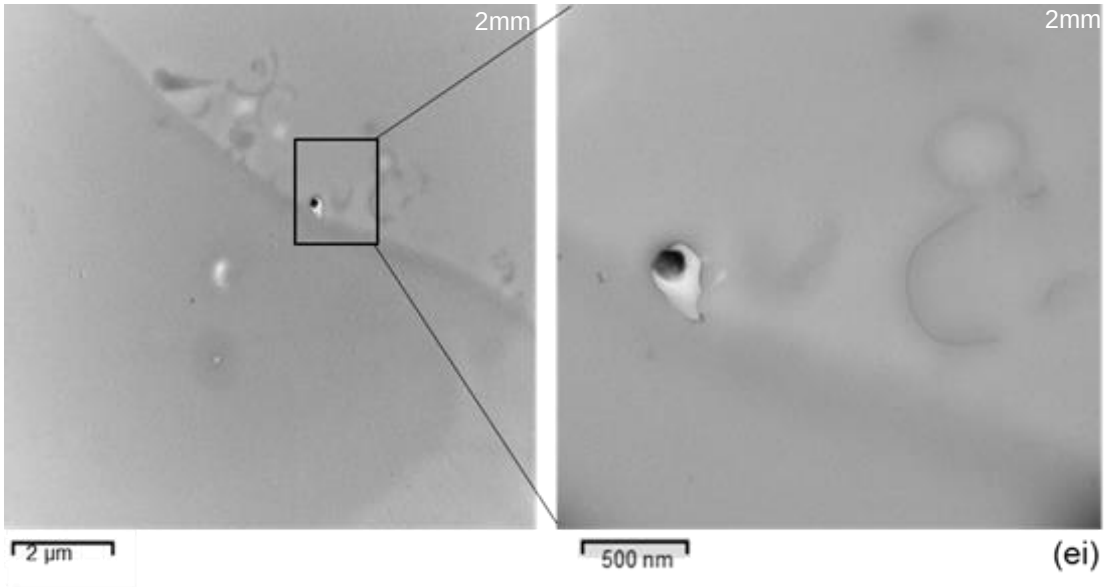
2mm
2mm
2 µm
500 nm
(ei)

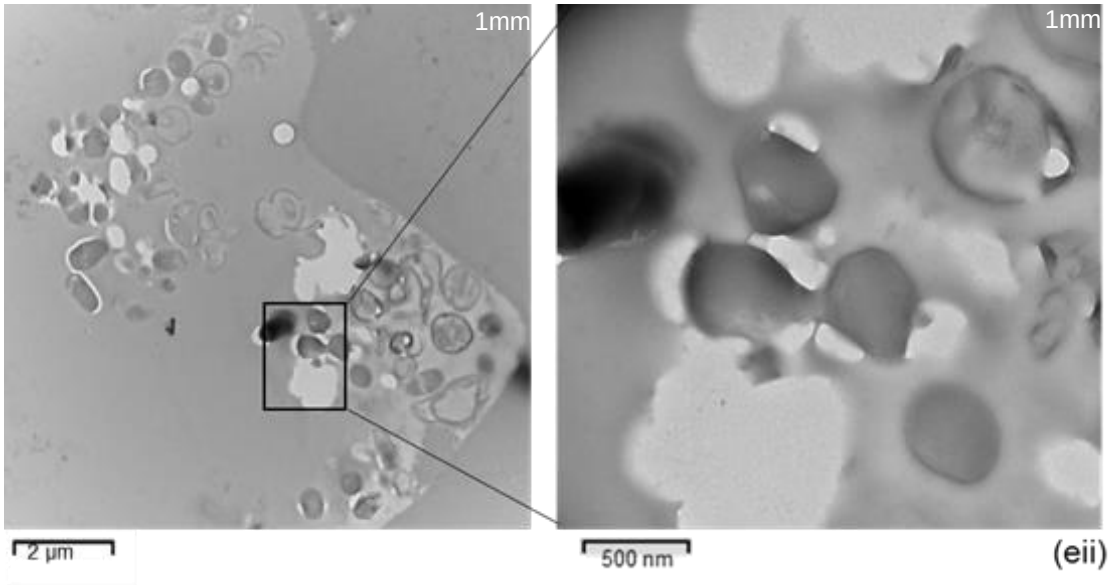

*The information at the upper right of each image indicates the level of the root canal (in mm) from the canal terminus where the residual biofilm was captured.

Figure 7.7: TEM images illustrate (ai) *E. faecalis* biofilm grown for 10 days. (aii, aiii, and aiv) residual biofilm at 3 mm from the lateral canal after passive irrigation, manual, sonic protocols respectively. (b) Passive irrigation group; (i) residual biofilm at 2 mm from the lateral canal terminus; (ii) residual biofilm at 1 mm from the lateral canal terminus. (c) manual-agitation group; (i) residual biofilm at 2 mm from the lateral canal terminus; (ii) residual biofilm at 1 mm from the lateral canal terminus. (d) Sonic agitation group; (i) residual biofilm at 2 mm from the lateral canal terminus; (ii) residual biofilm at 1 mm from the lateral canal terminus. (e) Ultrasonic agitation group; (i) residual biofilm at 2 mm from the lateral canal terminus; (ii) residual biofilm at 1 mm from the lateral canal terminus.

7.4. Discussion

This chapter set out with the aim of comparing the impact of passive and active irrigation protocols (manual, sonic, and ultrasonic agitation) and time of irrigation on the efficacy of 2.5% NaOCl irrigant to remove and destroy the structure of bacterial biofilm from the wall of a simulated lateral canal of the root canal system. In addition, another aim of the project was to identify the effect of canal complexity on the efficacy of NaOCl to remove biofilm from the apical part of the main root canal (3 mm). The results of this study did not show any significant increase in the efficacy of NaOCl during manual agitation. Although a greater removal and eradication effect of NaOCl on the *E. faecalis* biofilm was associated with the ultrasonic activation group, it was not enough for complete biofilm removal and dissolution from the lateral canal anatomy. Another important finding was that the

canal complexity represented by one lateral canal had no effect on the removal action of NaOCl in the main canal.

The diameter of the lateral canal of the root canal model used herein was 0.3 mm (300 μm). This may be considered as a limitation as it lies beyond the range of the lateral canals (10 - 200 μm) reported in previous studies using scanning electron microscope (Dammaschke *et al.*, 2004) and microcomputer tomography (Al-Jadaa *et al.*, 2009) of human teeth. However, this width was selected, as it was adequate for recording the *in-situ* removal of the bacterial biofilm. In addition, based on our observations on the printing of lateral canal models with a smaller diameter, the inner surface of the canal was incompletely polymerised. Furthermore, the lateral canal of diameter 250 μm, which is larger than the abovementioned range, was used in a previous study to investigate the removal of simulated biofilms from the lateral canals (Macedo *et al.*, 2014a).

The results which emerge from the statistical analysis and microscopic observations were that NaOCl is necessary to be in direct contact with the *E. faecalis* biofilm to perform total removal and killing of the bacterial cell (Moorer and Wesselink, 1982). This was achieved in all groups at the 3 mm level from the lateral canal terminus, as the port opening of the needle was facing the lateral canal, which may yield a jet with high velocity fluid flow (Boutsioukis *et al.*, 2010d; Verhaagen *et al.*, 2012).

The agitation of the NaOCl could enhance a lateral flow component, and improve irrigant penetration into the side canal (Castelo-Baz *et al.*, 2012). However, no complete eradication of biofilm was evident in the passive and manual agitation groups. The possible explanation for this might be that the rate of irrigant

refreshment as the irrigant diffused was decreased (van der Sluis *et al.*, 2010). As the irrigation procedure continued, the irrigant penetration into the terminus of the lateral canals was enhanced with automated groups (sonic and ultrasonic). This was demonstrated by the non-viable cells of the residual biofilm in the relevant groups. These results may be related to the acoustic streaming and cavitation effects that were created by the tip oscillation of the sonic and ultrasonic device within the main root canal (Van der Sluis *et al.*, 2005). Nevertheless, NaOCl efficacy was insufficient for complete destruction of the residual biofilm. This could be due to fact that the effective diffusion of NaOCl was restricted to the top layers of the biofilm (Renslow *et al.*, 2010). Another possible explanation for this is the rapid consumption of OCl^- ions of NaOCl during its reaction with biofilm (Moorer and Wesselink, 1982). The efficacy of NaOCl was reduced at 1 mm from the lateral canal terminus in all irrigation groups. This observation could be attributed to the reduction in both fluid convection (Verhaagen *et al.*, 2014a) and irrigant replacement (Wang *et al.*, 2014).

The findings are in agreement with de Gregorio *et al.* (2009) findings, who showed that the efficacy of the automated groups (sonic & ultrasonic) was greater than that of the passive irrigation group. However, the findings of the current study do not support the abovementioned study, which reported that there was no difference between the sonic and ultrasonic agitation groups. This inconsistency may be due to the structure of biofilm exhibiting resistance to antimicrobial agents (Roberts and Mullany, 2010) when compared to the contrast media used in the de Gregorio *et al.* study.

Further studies, which take the multi-species biofilm variable into account, will need to be undertaken.

7.5. Conclusion

Within the limitation of the present study, the removal and killing effect of NaOCl on the bacterial cell was limited to the 3 mm level from the lateral canal terminus. The agitation of NaOCl resulted in better penetration of the irrigant into the lateral canals. Ultrasonic agitation of NaOCl improved the destruction of bacterial biofilm.

Chapter 8

Investigations into the removal of multi-species biofilm and biofilm destructive efficacy of passive and active NaOCl irrigant delivered into a simulated root canal model

8.1. Introduction

Different bacterial species comprising the community of multi-species biofilm may have the potential for interspecies interactions, which include synergistic and antagonistic interactions that increase their pathogenicity and enhance biofilm resistance to antimicrobial agents (Burmølle *et al.*, 2006). Sundqvist (1976) observed the correlation between the severity of periapical disease and the number of bacterial species isolated from infected root canals, as he observed that infection with mixed species was associated with larger periapical radiolucency. Furthermore, it has been argued that the diversity of bacteria cells may be the main factor that defines their survival and maintains apical inflammation (Sjögren *et al.*, 1997).

Several attempts have been made to evaluate the role of antimicrobial agents in eliminating multi-species biofilms (Fimple *et al.*, 2008; Bryce *et al.*, 2009; Yang *et al.*, 2016). However, the real-time removal of multi-species biofilm from the root canal by the most popular irrigation solution (NaOCl), and the fate of residual biofilm is yet to be known. Research is also needed to determine the role of the irrigant agitation method on its efficacy to remove multi-species biofilm within the root canal system. Therefore, this chapter aimed to investigate the effect of different agitation techniques (manual, sonic, and ultrasonic) on the efficacy of 2.5% NaOCl to eliminate multi-species biofilm from the apical part (3mm) of the root canal using the residual biofilm, removal rate of biofilm, and extent of

destruction of the residual biofilm, as outcome measures. The difference between the removal of single and multi-species biofilms by the effect of the NaOCl irrigation procedure was also assessed.

8.2. Materials and Methods

8.2.1. Construction of transparent root canal models and distribution to experimental groups

The root canal models (n = 40) were created as described in section 5.2.1 and then divided into four groups (n = 10 per group) in the same manner as described in section 6.2.1.

8.2.2. Preparation of microbial strains and determination of the standard inoculum

Multi-species biofilms were grown from four bacterial strains (Table 8.1).

Table 8.1: Types of the bacterial strains used to create multi-species biofilm, their morphology, Gram staining and catalase reaction results.

Bacterial strains		Morphology	Gram staining	Catalase test
Facultative anaerobes	*Streptococcus mutans* (ATCC 700610)	Coccus	+	-
	Enterococcus faecalis (ATCC 19433)	Coccus	+	-
Obligate anaerobes	*Fusobacterium nucleatum* (ATCC 25586)	Spindle-shaped rod	-	+
	Prevotella intermedia (DSM 20706)	Rod shaped	-	+

ATCC American Type Culture Collection
DSM Diagnostic Services Manitoba

The facultative (*Enterococcus faecalis, Streptococcus mutans*) strains were supplied in the form of frozen stock in a brain-heart infusion broth (BHI) (BHI; Sigma-Aldrich, St. Louis, Montana, USA) and 30% glycerol (Merck, Poole, UK) stored at -70 °C. The obligate anaerobes (*Fusobacterium nucleatum, Prevotella intermedia*) strains were supplied in the form of frozen stock in fastidious anaerobe Broth (FAB) (FAB; Lab M Ltd., Heywood, UK) and 30% glycerol stored

at -70 °C. Each strain was thawed to a temperature of 37 °C for 10 minutes and swirled for 30 seconds using a Vortex (IKA, Chiltern Scientific, Leighton, UK) (Siqueira *et al.*, 2002). After thawing, 100 µL of each facultative strain were taken and plated separately onto BHI agar plates (Sigma-Aldrich, St. Louis, Montana, USA) with 5% defibrinated horse blood (E&O Laboratories, Scotland, UK) and incubated at 37 °C in a 5% CO_2 incubator (LEEC, Nottingham, UK) for 24 hours. Whilst, 100 µL of each obligate anaerobes strain were taken and plated separately onto fastidious anaerobe agar plates (Lab M Ltd., Lancashire, UK) with 5% defibrinated horse blood and incubated for 48 hours in an anaerobic chamber (MACSMG-1000 Anaerobic Workstation, Don Whitley Scientific, Skipton, UK), in an atmosphere of 10% hydrogen, 10% carbon dioxide and 80% nitrogen (Williams *et al.*, 1983). Bacterial morphology and catalase activity were confirmed prior to the generation of the biofilms. For this, two colonies of each strain were separately removed using a sterile inoculating loop (VWR, Leicester, UK), and catalase test using 3% H_2O_2 (Sigma-Aldrich Ltd, Dorset, UK) and Gram staining test (BD Ltd., Oxford, UK), were performed. In addition, the identification of the strain was achieved by performing 16S rRNA gene sequencing and analysis (Appendix 2).

A standard inoculum of 10^7 CFU/mL concentration was used (Shen *et al.*, 2010b). For this, six colonies of each facultative and obligate anaerobes strain were removed from the agar plate, and placed into 20 mL of tryptic soya broth (TSB) (Sigma-Aldrich, St. Louis, Montana, USA) with 5% defibrinated horse blood, 2.5 µL Menadione, 50 µL Haemin, and incubated either at 37 °C in a 5% CO_2 incubator for 24 hours or at an anaerobic chamber for 48 hours depending on the type of the strain. TSB containing facultative bacteria were adjusted to 0.25

absorbance, while TBS containing obligate anaerobes were adjusted to 1 absorbance at a wavelength of 600 nm using a spectrophotometer (NanoDrop™ Spectrophotometer ND-100, Wilmington, USA) (Al Shahrani *et al.*, 2014). Inoculum concentration was confirmed by determining the colony forming units per millilitre (CFUs/mL) using six ten-fold serial dilutions (Peters *et al.*, 2001a). This was performed by mixing aliquots of 100 µL bacterial inoculum into 900 µL of reduced transport fluid in 1.5 mL mini tubes (Sarstedt Ltd, Nümbrecht, Germany). From these dilutions, aliquots of 20 µL were plated on tryptic soya agar (Sigma-Aldrich, St. Louis, Montana, USA) plates with 5% defibrinated horse blood and then incubated either at 37 °C in a 5% CO_2 incubator for 24 hours or at an anaerobic chamber for 48 hours. The colony forming units per millilitre (CFUs/mL) corresponding was 10^7 CFU/mL. Equal amounts of each strain (1 mL) were mixed to create the multi-species baseline inoculum, which were then vortexed for 30s using a Vortex (IKA, Chiltern Scientific, Leighton, UK) to disperse the bacterial cells.

8.2.3. Generation of multi-species biofilm on the surface of the apical 3 mm of the canal model

This step was performed as described in section 5.2.3, with exception of incubation condition and growth time as the models were incubated in an anaerobic chamber (10% hydrogen, 10% carbon dioxide and 80% nitrogen) for ten days.

8.2.4. Staining of biofilms grown on the surface of the models

The staining procedure was performed as mentioned in section 3.2.5.4.

8.2.5. Re-apposition of the model halves

This step was performed as described in section 5.2.5.

8.2.6. Irrigation experiments

This step is illustrated in Figure 8.1 and it was performed as described in section 6.2.6.

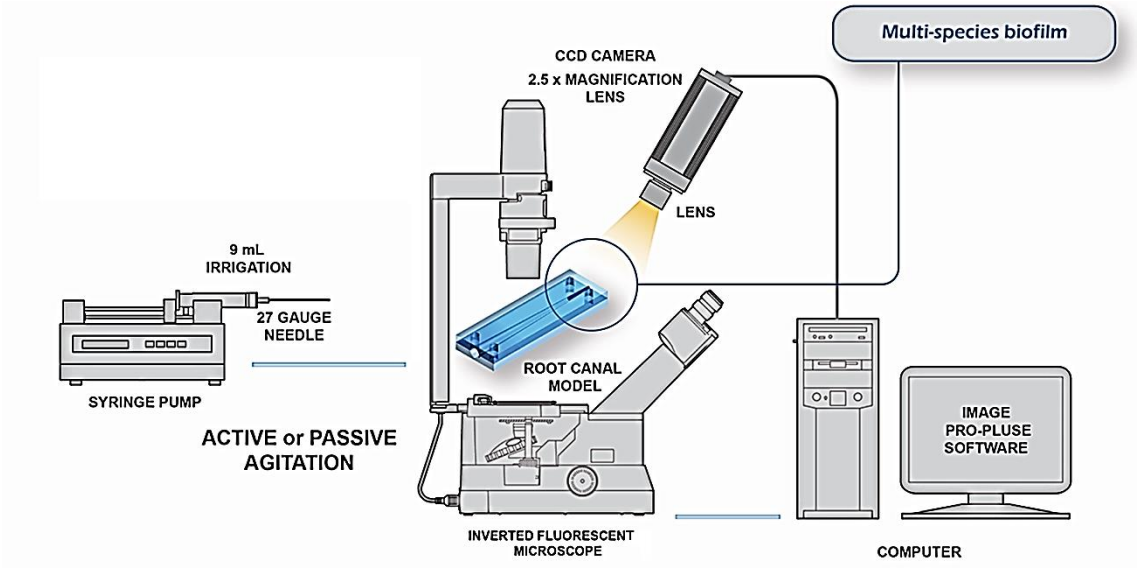

Figure 8.1: Sketch illustrating the set-up of equipment for recording of the multi-species biofilm (biofilm was generated on the apical portion (3 mm) of the canals model) removal by active or passive NaOCl irrigation protocol using a camera connected to a 2.5× lens of an inverted fluorescent microscope. The irrigant was delivered using a syringe with a 27-gauge side-cut open-ended needle, which was attached to a programmable precision syringe pump. The residual biofilm was quantified using computer software (Image-pro Plus 4.5).

Following irrigation protocols, the residual NaOCl on the model surface was immediately neutralised by immersing the models in 2 mL of 5% sodium thiosulphate solution (Sigma-Aldrich Co Ltd., Gillingham, UK) for 5 minutes. This reduces the active ingredient of NaOCl (hypochlorite), which becomes oxidized to sulphate (Hegde *et al.*, 2012).

The models in each group were then randomly divided in to three subgroups for investigation with CLSM, SEM, and TEM microscopy techniques (n = 3 per subgroup).

8.2.7. Recording of biofilm removal by the irrigant

This step was performed as described in section 3.2.7.2.

8.2.8. Image analysis

Image analysis was performed as described in section 3.2.8.

8.2.9. Preparation of the samples for confocal laser scanning microscope (CLSM)

The illustration of this step is described in Figure 8.2. Sample were prepared as mentioned in section 6.2.10.

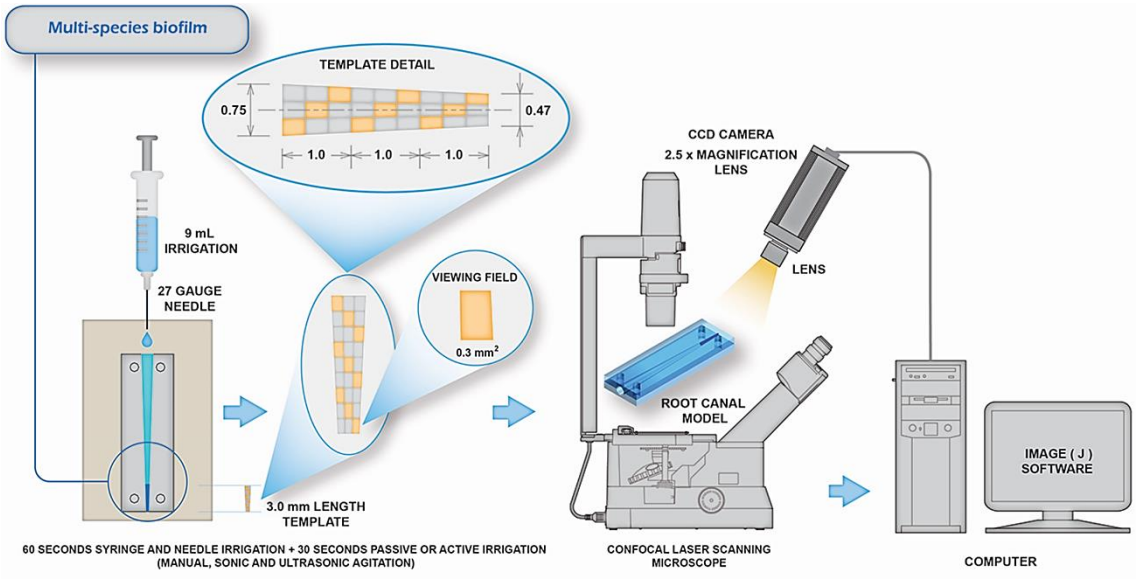

Figure 8.2: Image illustrates the set-up of the equipment to examine the residual multi-species biofilm. Confocal laser scanning microscope was used to observe and record images of the live/dead cells within the residual biofilm. A template was used to control the viewing fields (0.3 mm^2) which were located in the top, middle, and bottom of the tested area. The areas were imaged manipulated using ImageJ® software.

8.2.10. Preparation of the samples for scanning electron microscope (SEM)

The samples were prepared as mentioned in section 6.2.11.

8.2.11. Preparation of the samples for transmission electron microscope (TEM)

The samples were prepared as described in section 6.2.12.

8.2.12. Data analyses

The residual multi-species biofilm (%) at each second of 90 seconds irrigation with passive and active 2.5% NaOCl irrigant was analysed using line plots. An assumption concerning a normal distribution of data for the residual multi-species biofilm was checked using a visual inspection of the box and whisker plots. The data representing the percentages of residual multi-species biofilm covering the canal surface area were normally distributed and therefore the linear mixed models, followed by Dunnett *post-hoc* comparisons were performed to compare their distributions in the four experimental groups. A similar analysis was performed to analyse the effects of irrigant agitation duration (time) and experimental group (passive or GP, sonic, and ultrasonic active irrigation) on the percentage of residual multi-species biofilm covering the canal surface area. The non-linear aspect was accommodated by including time^2 as an additional variable. A comparison between the resistance of single (data from chapter 6) and multi-species biofilms to the removal efficacy of NaOCl was performed using the same statistic model. A significance level of 0.05 was used throughout. The data were analysed by SPSS (BM Corp. Released 2013. IBM SPSS Statistics for Windows, Version 22.0. Armonk, New York, IBM Corp).

8.3. Results

8.3.1 Statistical analysis

The mean (95% Confidence interval) percentages of the lateral canal surface area coverage with residual bacterial biofilm against duration of irrigation(s), stratified by type of irrigation, are presented in Figure 8.3. The data (Table 8.2) showed that the greatest removal was associated with the ultrasonic group

(91.53%) followed by sonic (78.32%), manual (70.65%), and passive irrigation group (control) (59.48%) respectively.

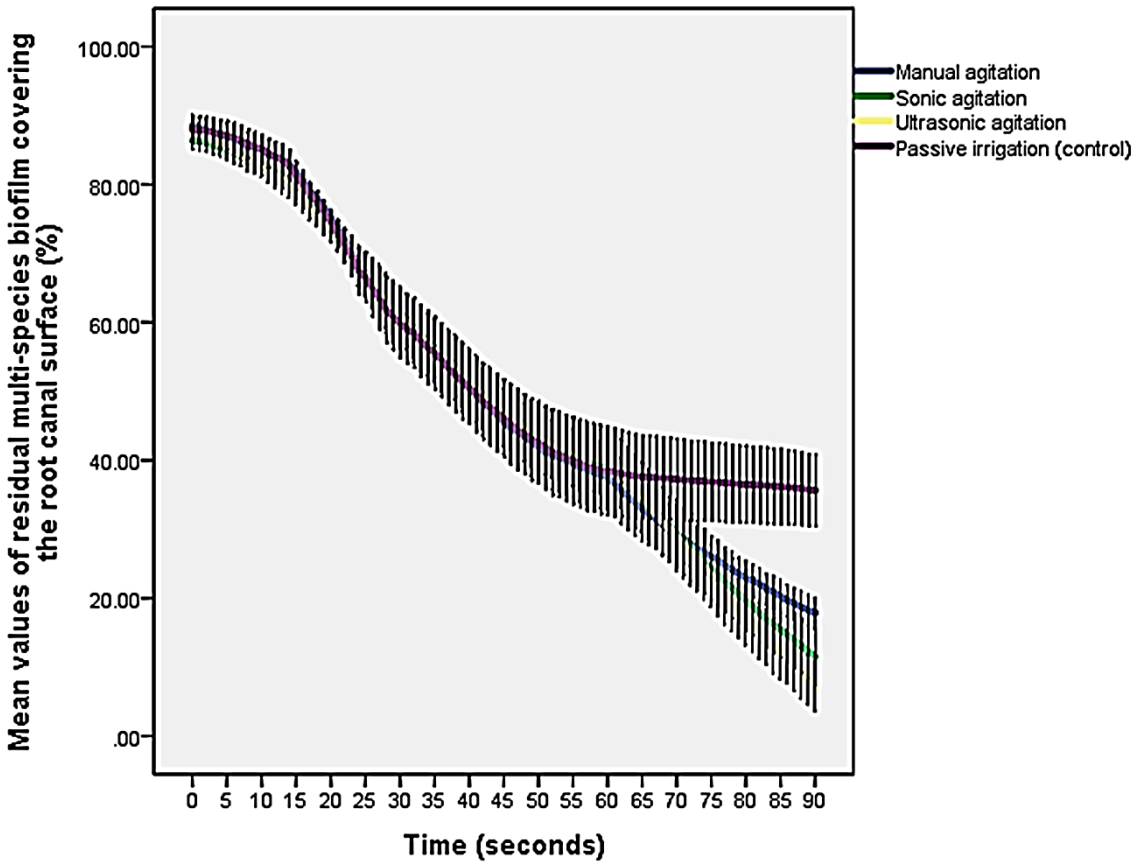

Figure 8.3: Mean (95% CI) percentages values of the residual biofilm (%) covering the root lateral canal surface-area over duration (s) of syringe irrigation followed by passive or active irrigation protocols, stratified by type of irrigation (n = 10 per group).

Table 8.2: Mean values of the biofilm (%) covering the root canal surface before and after one-minute of syringe irrigation followed by 30 seconds passive or active irrigation protocols (n = 10 per group).

Type of irrigant	Mean (%) Before irrigation (±SD)	Mean (%) after irrigation (±SD)	Difference (Range) (%)
Manual agitation	89.44 (±19.95)	18.79 (±19.95)	70.65
Sonic agitation	92.81(±19.58)	14.49(±19.58)	78.32
Ultrasonic agitation	93.02 (±20.87)	1.49 (±20.87)	91.53
passive irrigation	90,55 (±14.55)	31.07 (±14.55)	59.48

The results from the linear mixed model (Table 8.3) indicated that there was a statistically significant difference between the residual multi-species biofilm on the canal surface area in the passive irrigation group and all activation groups (manual, sonic, and ultrasonic agitation groups) (p = 0.001). Amongst the active irrigation groups, strong evidence of less residual multi-species biofilm was found in the automated groups (ultrasonic & sonic) than those in the manual agitation group. However, this difference was only statistically significant between the ultrasonic agitation and manual agitation groups (p = 0.011).

Table 8.3: Generalized linear mixed model analysis to compare the difference in the amount of residual multi-species biofilms (%) covering the canal surface following passive or active irrigation time with 2.5 % NaOCl irrigant (n = 10 per group).

Experimental groups	*Coefficient (±SE)	95% CI	p value
Manual agitation vs passive irrigation	38.40 (±2.3)	33.89, 42.91	**0.001**
Sonic agitation vs passive irrigation	54.28 (±2.3)	49.77, 58.79	**0.001**
Ultrasonic agitation vs passive irrigation	63.18 (±2.3)	63.67, 72.69	**0.001**
Manual agitation vs ultrasonic agitation	-24.39 (±8.9)	-42.81, -5.98	**0.011**
Sonic agitation vs ultrasonic agitation	-13.41 (±8.9)	-31.82, 4.99	0.147
Manual agitation n vs sonic agitation	-9.71 (±8.1)	-26.68, 7.26	0.245

*Coefficient for the residual multi-species biofilm, SE= standard error, CI = Confidence interval.

Another important finding of the generalized linear mixed model analysis (Table 8.4) was that the amount of biofilm removed using passive irrigation was [0.72%/s; (±0.02), 0.91%/s; (±0.02), 1.12%/s; (±0.02)] less than the amount of multi-species biofilm removed using active manual, sonic, and ultrasonic irrigation respectively. This was statistically significant (p = 0.001). For the active irrigation groups, the amount of multi-species biofilm removed using ultrasonic agitation was [0.34%/s; (±0.1)] more than that using the manual agitation. This was statistically significant (p = 0.011).

Table 8.4: Generalized linear mixed model analysing the effect of time (seconds) on the amount of multi-species biofilm removed from the canal surface of each experimental group (n = 10 per group).

Experimental groups	*Coefficient (±SE)	95% CI	p value
Manual agitation vs passive irrigation	-0.72 (±0.02)	-0.76, -0.68	**0.001**
Sonic agitation vs passive irrigation	-0.91(±0.02)	-0.95, -0.85	**0.001**
Ultrasonic agitation vs passive irrigation	-1.12 (±0.02)	-1.16, -1.09	**0.001**
Manual agitation vs ultrasonic agitation	0.34 (±0.1)	0.09, 0.59	**0.011**
Sonic agitation vs ultrasonic agitation	0.21 (±0.1)	-0.05, 0.46	0.108
Sonic agitation vs manual agitation	0.12 (±0.1)	-0.10, 0.33	0.282

*Coefficient for the time effect represents the rate of biofilm removal, SE= standard error, CI = Confidence interval.

Regardless of the flushing protocols, the results (Table 8.5) indicated evidence on the resistance of different biofilm types (single, multi-species) to the effect of NaOCl irrigation as there was more residual multi-species biofilm than single species biofilm. This difference was statistically significant (p = 0.001).

Table 8.5: Generalized linear mixed model analysis to compare the difference between single and multiple residual biofilms (%) covering the canal surface following passive or active irrigation with 2.5 % NaOCl irrigant (n = 10 per group).

Irrigation protocols	Comparable groups	*Coefficient (±SE)	95% CI	p value
Passive irrigation	Single vs multi-species	31.42 (±3.7)	24.13, 38.71	**0.001**
Manual agitation	Single vs multi-species	43.75(±1.8)	40.18, 47.32	**0.001**
Sonic agitation	Single vs multi-species	31.89(±2.9)	26.17, 37.61	**0.001**
Ultrasonic agitation	Single vs multi-species	36.31 (±3.2)	30.02, 42.60	**0.001**

*Coefficient for the residual biofilm, SE= standard error, CI = Confidence interval.

8.3.2. Microscopic images analysis

The CLSM images of the multi-species biofilm on the surface of the root canal models before and after irrigation using passive irrigation, manual and automated agitation (sonic & ultrasonic) protocols are presented in Figure 8.4.

In the untreated contaminated canal model (control group), the CLSM assessment of the multi-species biofilm (Fig. 8.4ai) depicted that the ratio of the live cell clusters (green) was greater than that of the dead cell clusters (red).

In the treated groups (b, c, d, e), the CLSM images exhibited no residual multi-species biofilm was detected at the 3 mm level from the canal terminus of the models treated with 2.5% NaOCl in all groups (Fig. 8.4aii). At the 2 mm level, the CLSM images showed no viable cells in all experimental groups. However, dispersed clusters of residual dead multi-species biofilm (red) were more abundant in the passive irrigation group (Fig. 8.4bi) followed by manual (Fig. 8.4ci), sonic (Figs. 8.4di), and ultrasonic (Figs. 8.4ei) agitation groups respectively.

The CLSM assessment of the multi-species biofilm at 1 mm from the canal terminus demonstrated both viable (green) and dead cells (red) in the passive irrigation group (Fig. 8.4bii) and the manual (Fig. 8.4cii) groups with greater live to dead cell amounts in the former group. In comparison, no viable cells were detected in the sonic (Fig. 8.4dii) and the ultrasonic groups (Fig. 8.4eii).

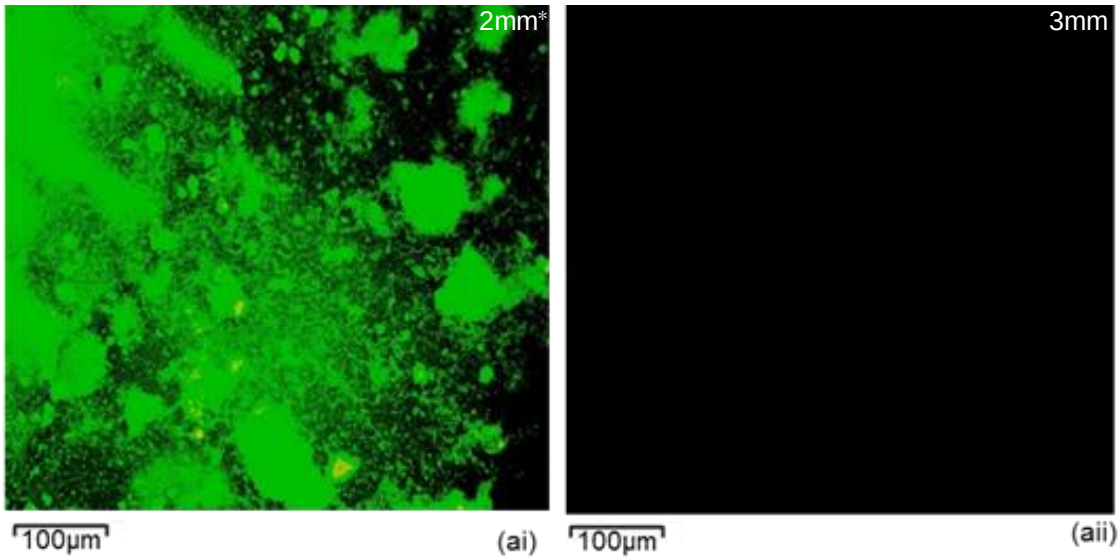

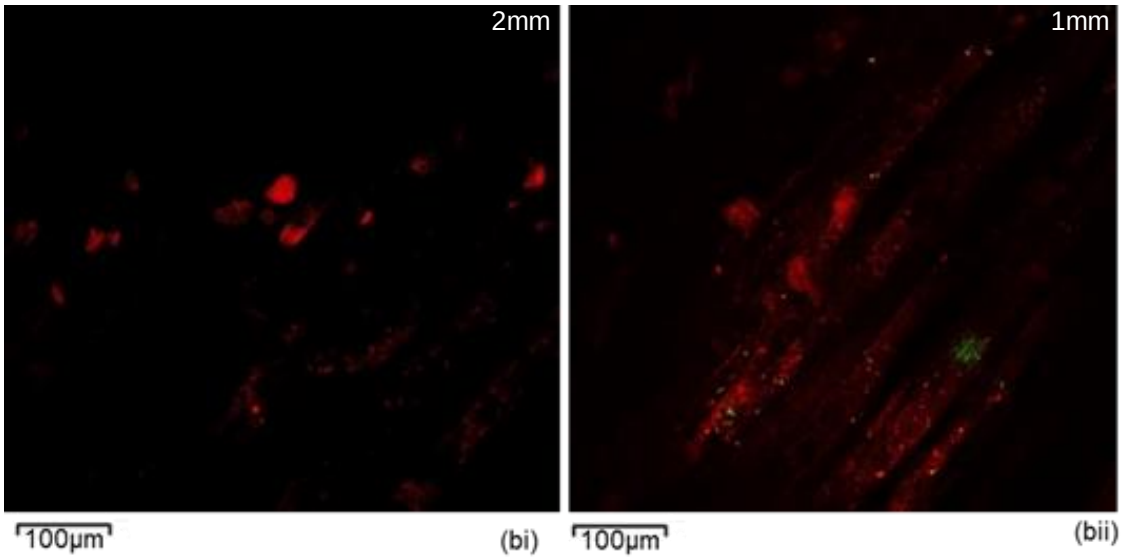
2mm
1mm
100µm
(bi)
100µm
(bii)

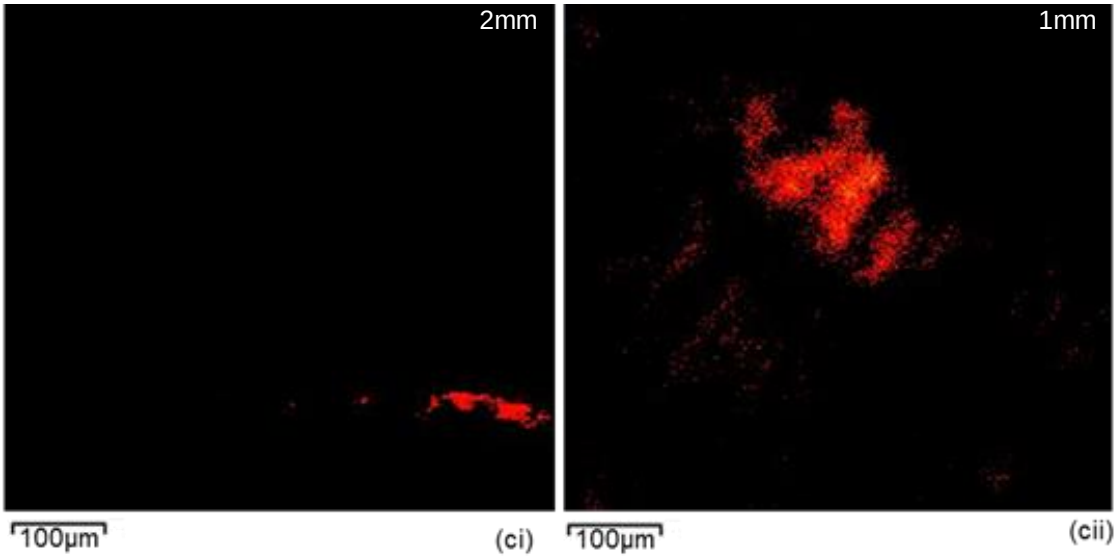
2mm
1mm
100µm
(ci)
100µm
(cii)

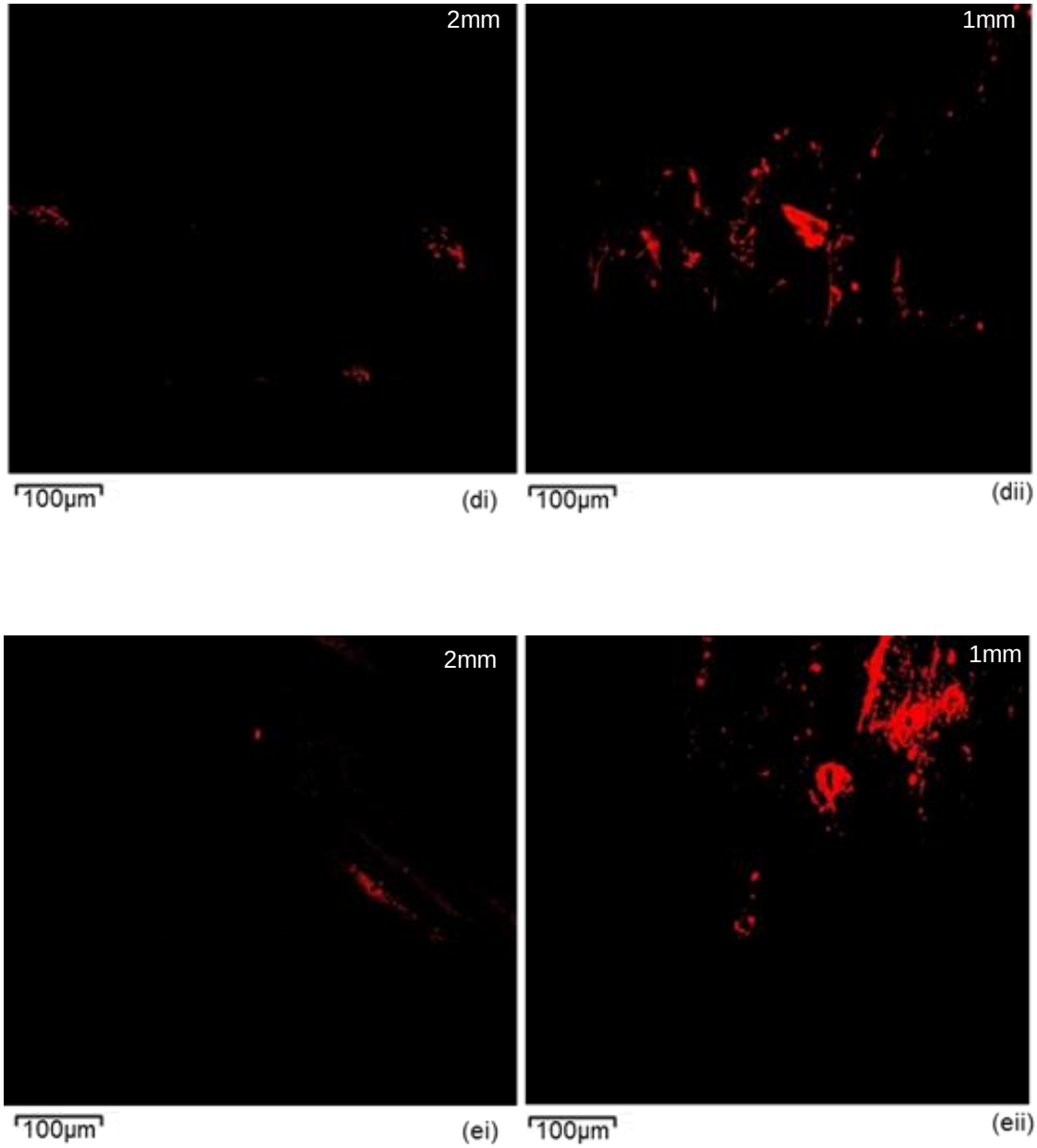

*The information at the upper right of each image indicates the level of the root canal (in mm) from the canal terminus where the residual biofilm was captured.

Figure 8.4: CLSM images (0.3 mm^2) from within the canal to illustrate (ai) *E. faecalis* biofilm grown for 10 days and stained using Live/Dead® viability stain with the green colour indicating live cells and the red colour showing the dead bacteria (control). (aii) residual biofilm at 3 mm from the canal terminus after passive irrigation. (b) Passive irrigation group; (i) residual biofilm at 2 mm from the canal terminus; (ii) residual biofilm at 1 mm from the canal terminus. (c) manual-agitation group; (i) residual biofilm at 2 mm from the canal terminus; (ii) residual biofilm at 1 mm from the canal terminus. (d) Sonic agitation group; (i) residual biofilm at 2 mm from the canal terminus; (ii) residual biofilm at 1 mm from the canal terminus. (e) Ultrasonic agitation group; (i) residual biofilm at 2 mm from the canal terminus; (ii) residual biofilm at 1 mm from the canal terminus.

SEM images of the multi-species biofilm on the surface of the root canal models before and after irrigation using passive irrigation, manual and automated agitation protocols are presented in Figure 8.5

SEM assessment of the untreated multi-species biofilm (Fig. 8.5ai) depicted different morphology of bacteria [cocci (blue arrow) & (white arrow) rod]. The EPS around the bacterial cell is shown with a yellow arrow. The two cocci-shape species (*E. faecalis* & *S. mutans*) of the biofilm are distinguishable from one another. *E. faecalis* is larger, has an ovoid morphology, while *S. mutans* is smaller, and has a spherical morphology. The two rod-shape species (*F. nucleatum* & *P. intermedia*) of the biofilm are also discernible from one another. *F. nucleatum* is longer, and has a fusiform rod morphology, whereas P*. intermedia* is shorter and has a distinct rod morphology. The framework of the biofilm is dominated by *S. mutans* (small cocci) followed by *E. faecalis* (large cocci), *P. intermedia* (short rods), and *F. nucleatum* (long rods).

After 2.5% NaOCl irrigation, SEM images exhibited no residual multi-species biofilm was detected at the 3 mm level from the canal terminus in all groups (Fig. 8.5aii). SEM images of the multi-species biofilm at 2 mm showed that the least EPS destruction and cell deformation was associated with the passive irrigation group (Fig. 8.5bi) followed by manual (Fig. 8.5ci), sonic (Fig. 8.5di), and ultrasonic (Fig. 8.5ei) groups respectively. At 1 mm from the canal terminus, SEM images illustrated that the multi-species biofilm appeared intact with the least bacterial cell deformation in the passive irrigation group (Fig. 8.5bii), followed by manual (Fig. 8.5cii), sonic (Fig. 8.5dii) groups respectively. The greatest multi-species biofilm removal and cell destruction were associated with the ultrasonic agitation group (Fig. 8.5eii).

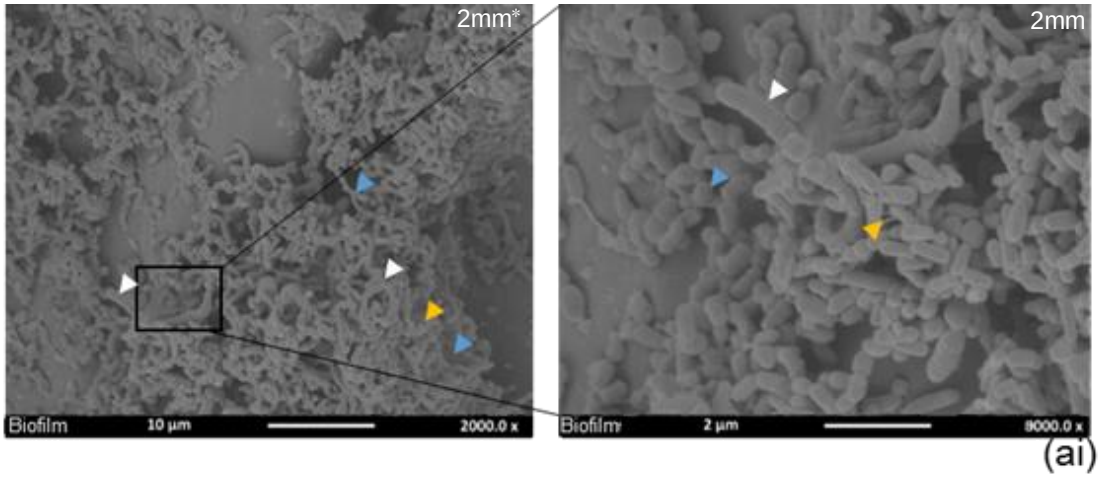
2mm*
2mm
Biofilm 10 µm 2000.0 x
Biofilm 2 µm 8000.0 x

(ai)

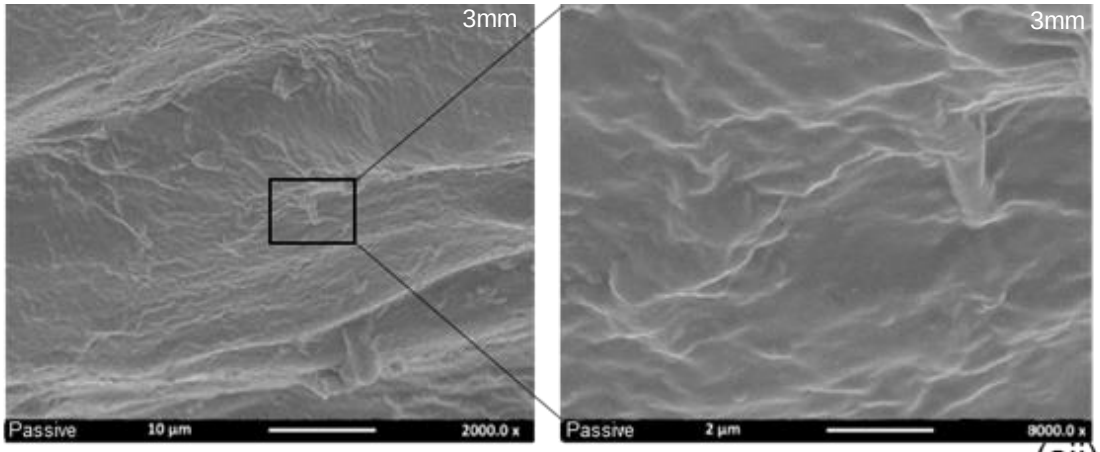
3mm
3mm
Passive 10 µm 2000.0 x
Passive 2 µm 8000.0 x

(aii)

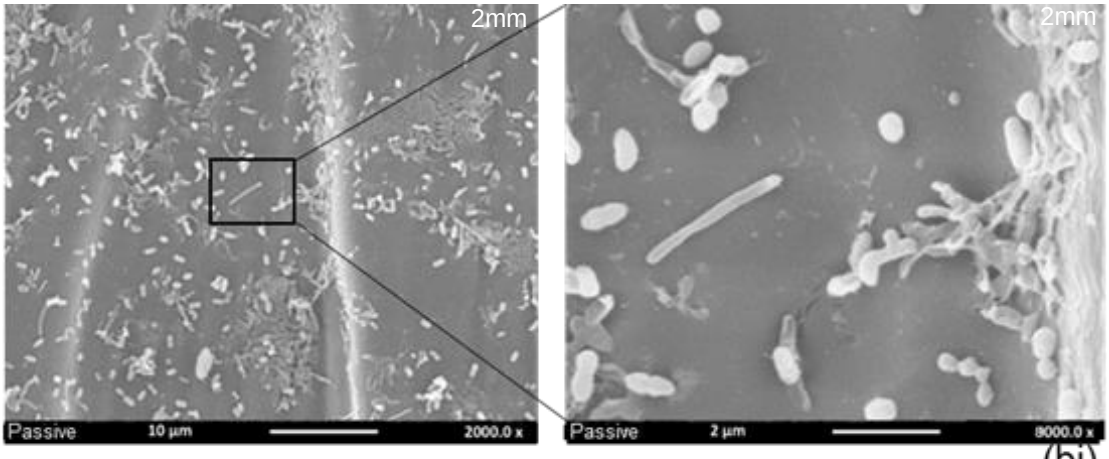
2mm
2mm
Passive 10 µm 2000.0 x
Passive 2 µm 8000.0 x

(bi)

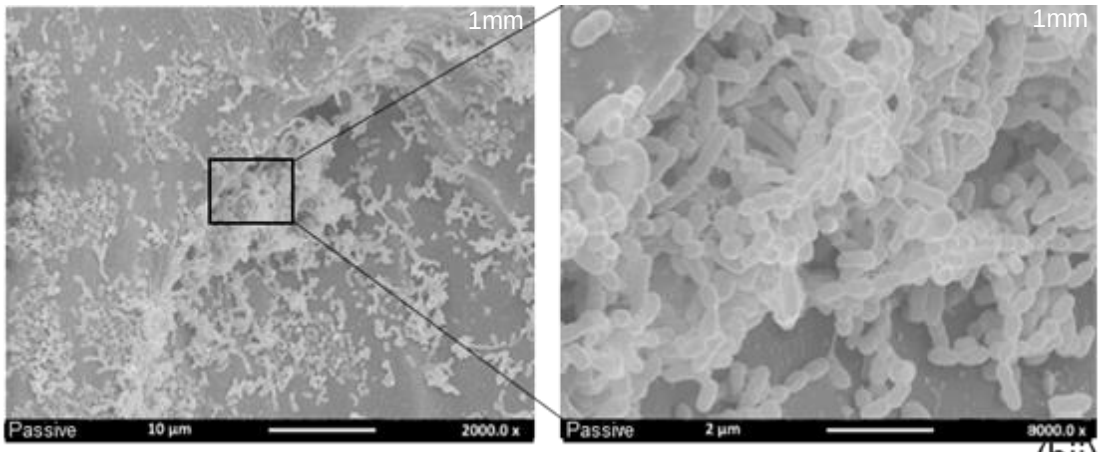
1mm
1mm
Passive
10 µm
2000.0 x
Passive
2 µm
8000.0 x

(bii)

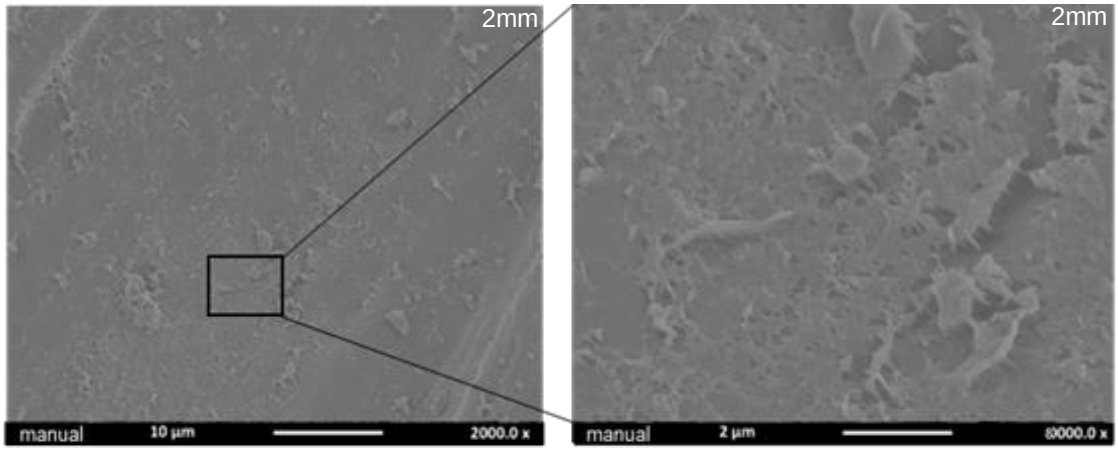
2mm
2mm
manual
10 µm
2000.0 x
manual
2 µm
8000.0 x

(ci)

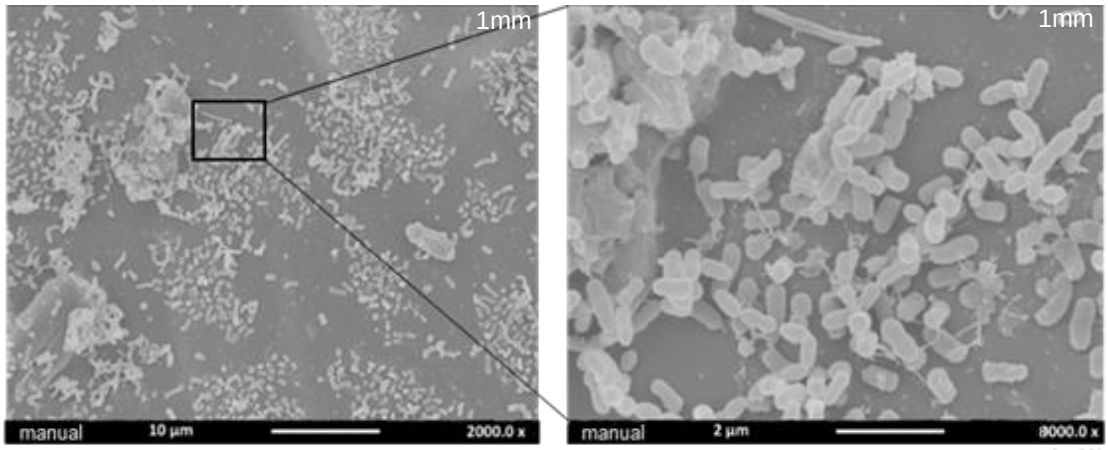
1mm
1mm
manual
10 µm
2000.0 x
manual
2 µm
8000.0 x

(cii)

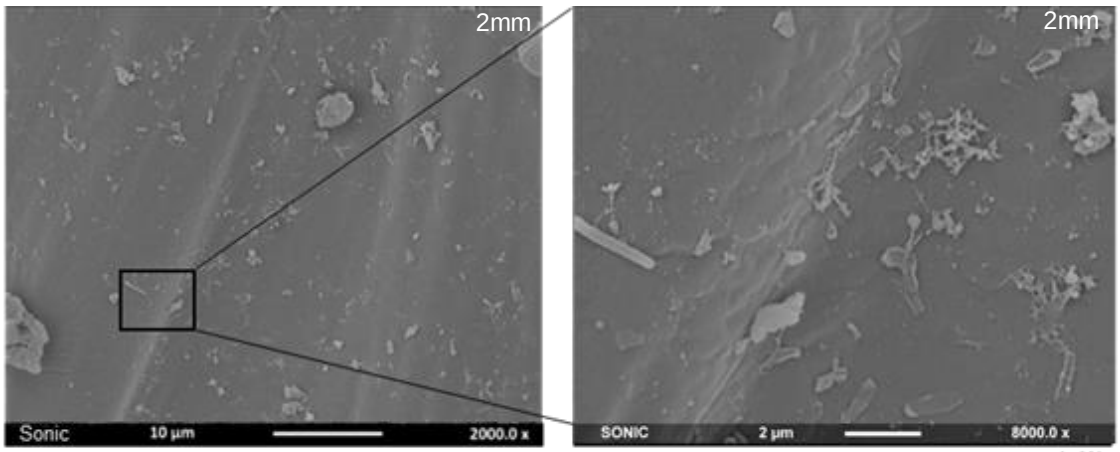
2mm
2mm
Sonic
10 µm
2000.0 x
SONIC
2 µm
8000.0 x

(di)

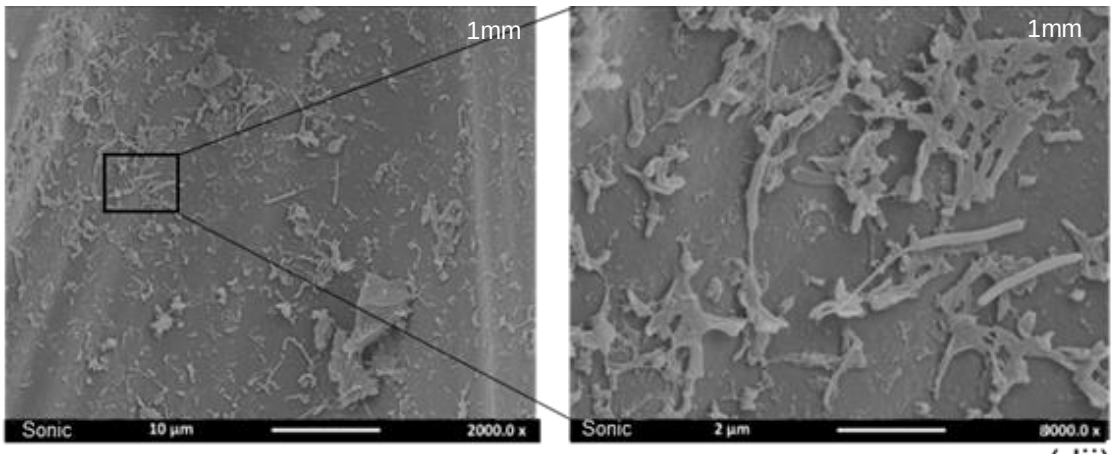
1mm
1mm
Sonic
10 µm
2000.0 x
Sonic
2 µm

(dii)

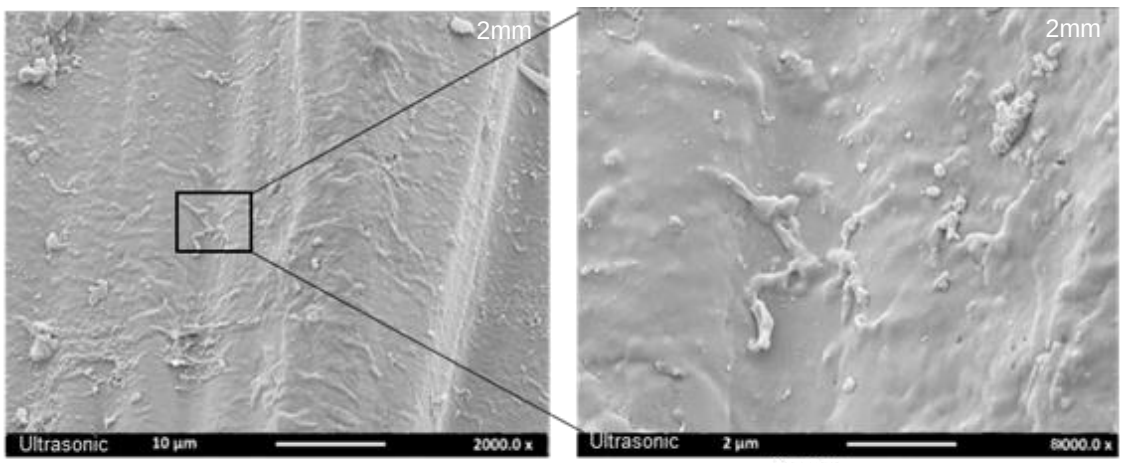
2mm
2mm
Ultrasonic
10 µm
2000.0 x
Ultrasonic
2 µm

(ei)

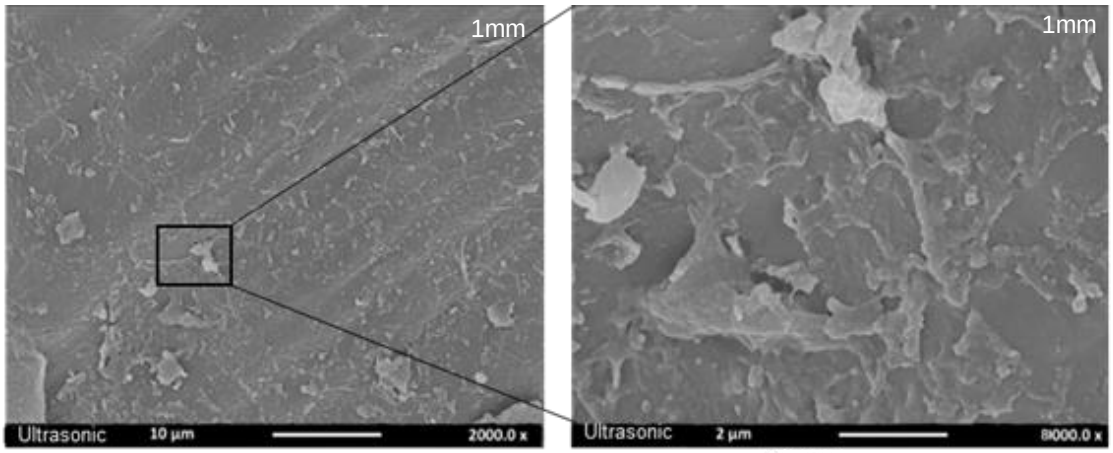

*The information at the upper right of each image indicates the level of the root canal (in mm) from the canal terminus where the residual biofilm was captured.

Figure 8.5: SEM images illustrate (ai) *E. faecalis* biofilm grown for 10 days. (aii) residual biofilm at 3 mm from the canal terminus after passive irrigation. (b) Passive irrigation group; (i) residual biofilm at 2 mm from the canal terminus; (ii) residual biofilm at 1 mm from the canal terminus. (c) manual-agitation group; (i) residual biofilm at 2 mm from the canal terminus; (ii) residual biofilm at 1 mm from the canal terminus. (d) Sonic agitation group; (i) residual biofilm at 2 mm from the canal terminus; (ii) residual biofilm at 1 mm from the canal terminus. (e) Ultrasonic agitation group; (i) residual biofilm at 2 mm from the canal terminus; (ii) residual biofilm at 1 mm from the canal terminus.

The TEM images of the multi-species biofilm on the surface of the root canal models before and after irrigation using passive irrigation, manual and automated agitation protocols are presented in Figure 8.6.

TEM images of the untreated multi-species biofilm on the root canal model (Fig. 8.6ai) displayed a complex arrangement of cells of different cocci and rod shapes, sizes and extracellular components. A clear discrimination between the rod and cocci bacteria could not be identified in the two-dimensional TEM images. At higher magnification, the bacterial cells exhibited a smooth and intact outer cell wall, a cell membrane surrounding the cytoplasm.

After 2.5% NaOCl irrigation, TEM images exhibited complete destruction and dissolution of the multi-species biofilm at the 3 mm level from the canal terminus in all groups (Fig. 8.6aii). The TEM images of the residual multi-species biofilm at 2 mm from the canal terminus showed a clear destructive effect of the NaOCl

irrigation on most of the cell that include ghost cell appearance because of cell content dissolution, cell wall deformations/perforations, and apparent removal of EPS in passive irrigation (Fig. 8.6bi) and manual (Fig. 8.6ci) groups. Ghost cells (black arrow) were greater in the latter group than the former. However, cells of different morphology retain their intact cell membrane and content (white arrow). In comparison, complete multi-species biofilm destruction, removal, and cell damage were associated with sonic (Fig. 8.6di) and ultrasonic (Fig. 8.6ei) groups. At 1 mm from the canal terminus, bacterial cells seem to maintain their cell wall and structural integrity in both passive irrigation (Fig. 8.6bii) and manual (Fig. 8.6cii) groups. On the other hand, ghost cells were more abundant than intact cells in the sonic (Fig. 8.6dii) group. The greatest multi-species biofilm disintegration was associated with the ultrasonic (Fig. 8.6eii) group.

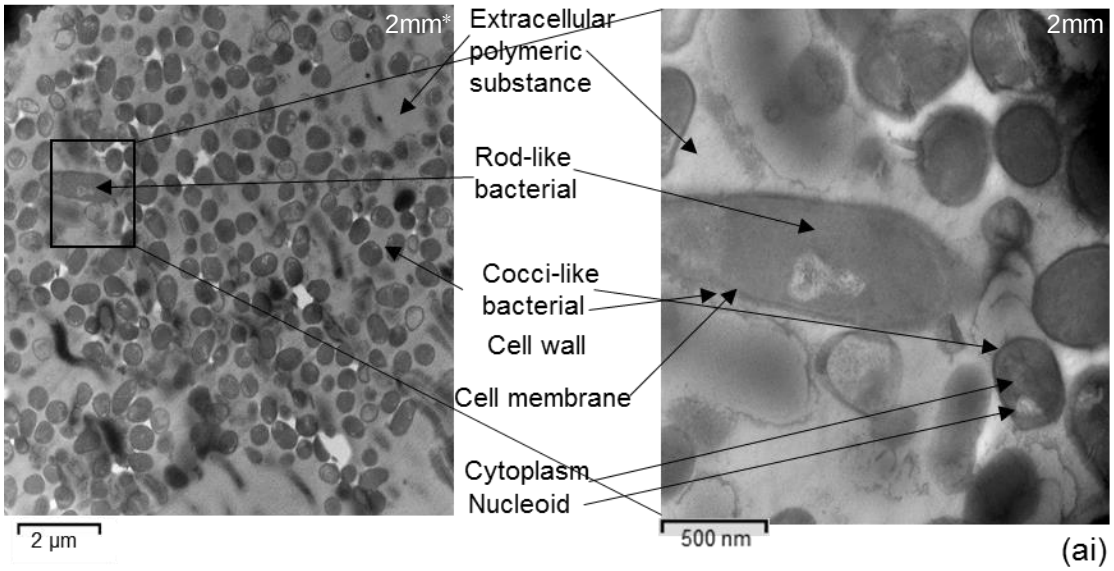

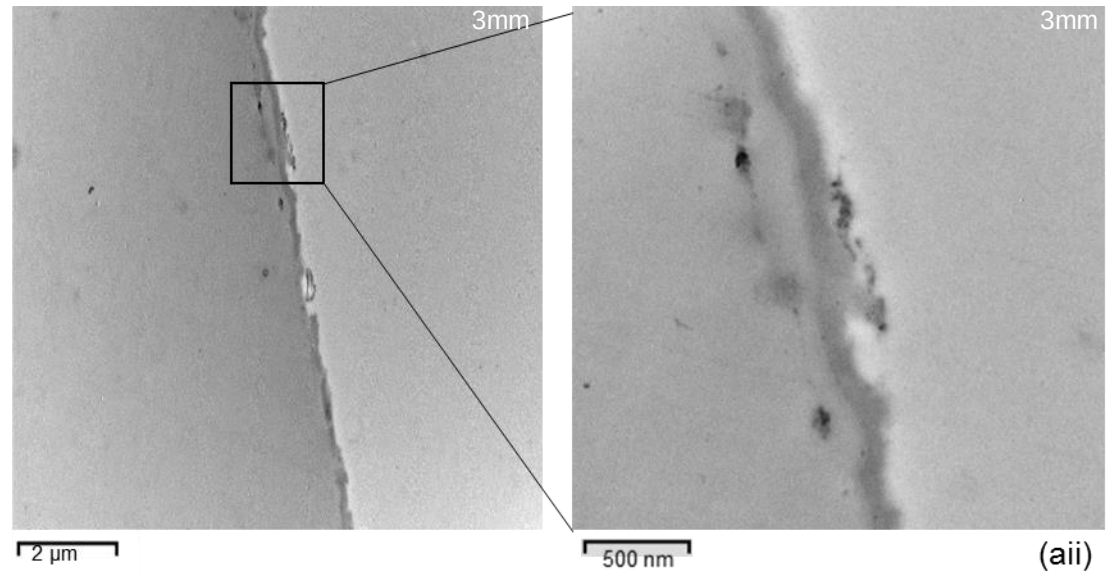
3mm
3mm
2 µm
500 nm
(aii)

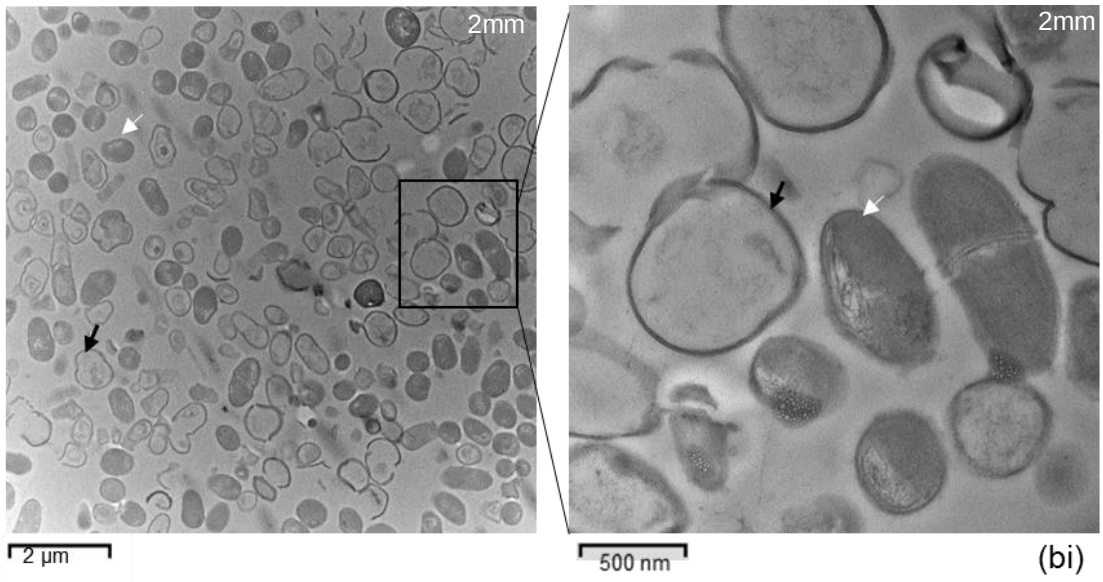
2mm
2mm
2 µm
500 nm
(bi)

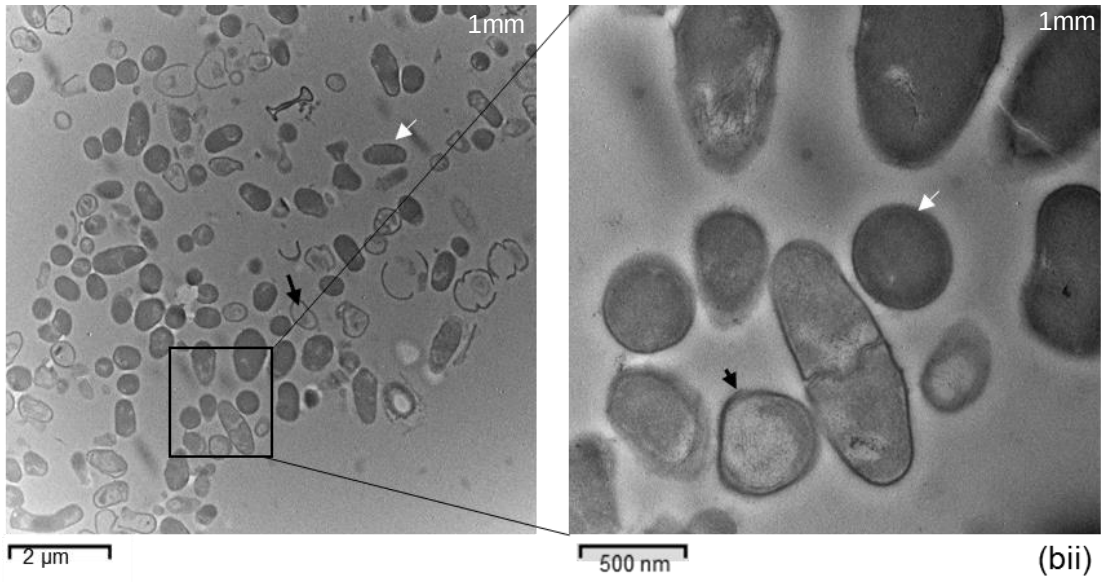
1mm
1mm
2 µm
500 nm
(bii)

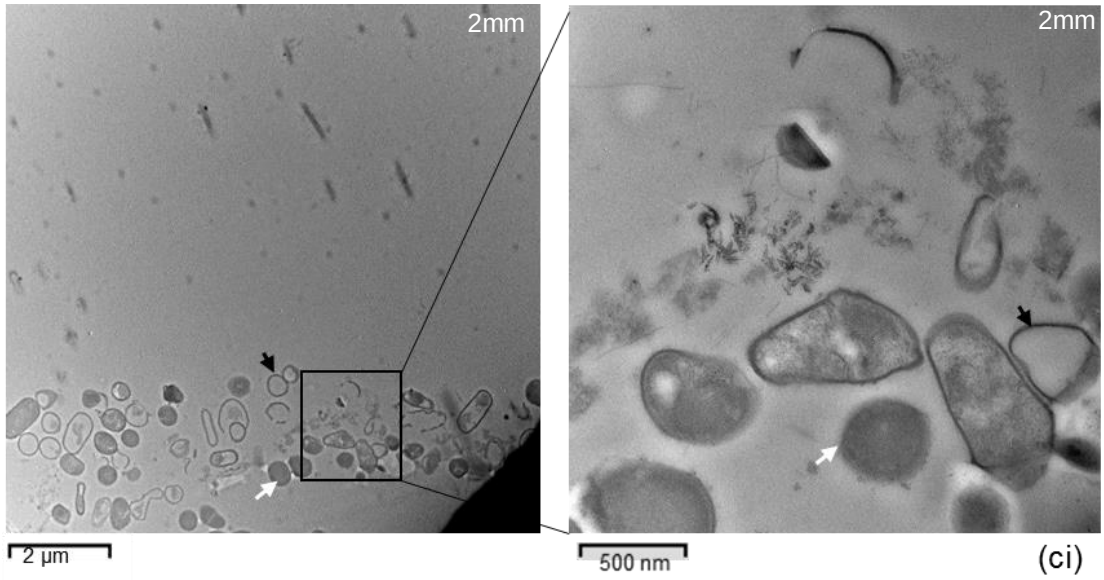
2mm
2mm
2 µm
500 nm
(ci)

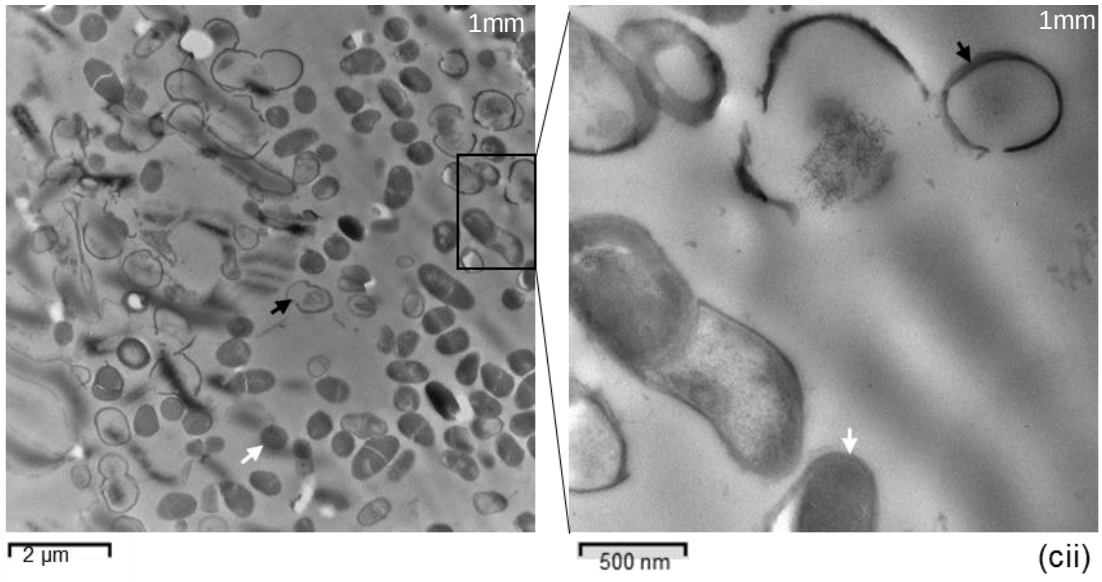
1mm
1mm
2 µm
500 nm
(cii)

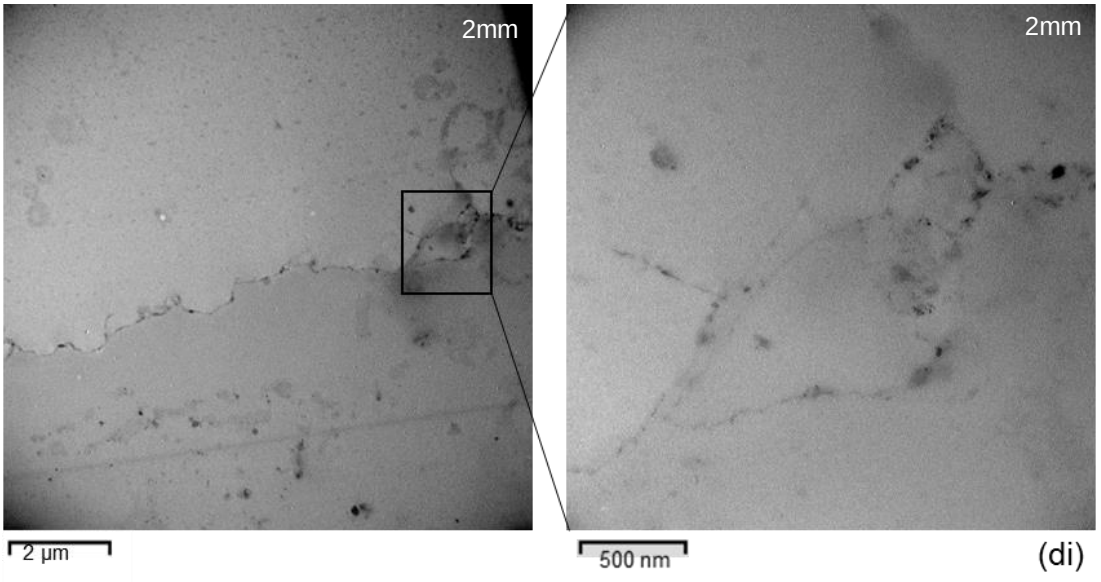
2mm
2mm
2 µm
500 nm
(di)

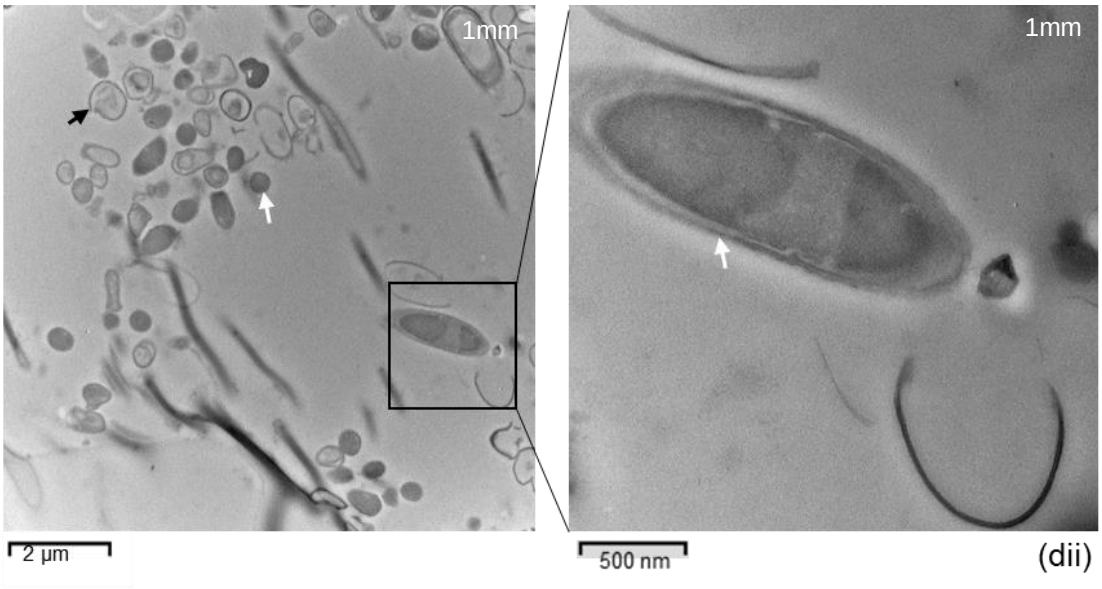

(dii)

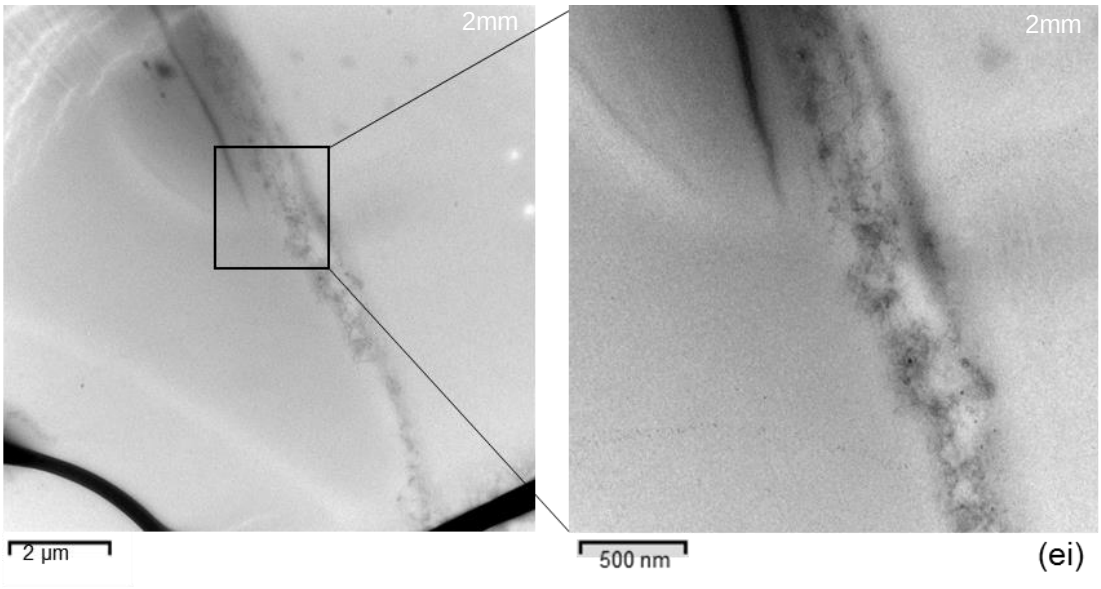

(ei)

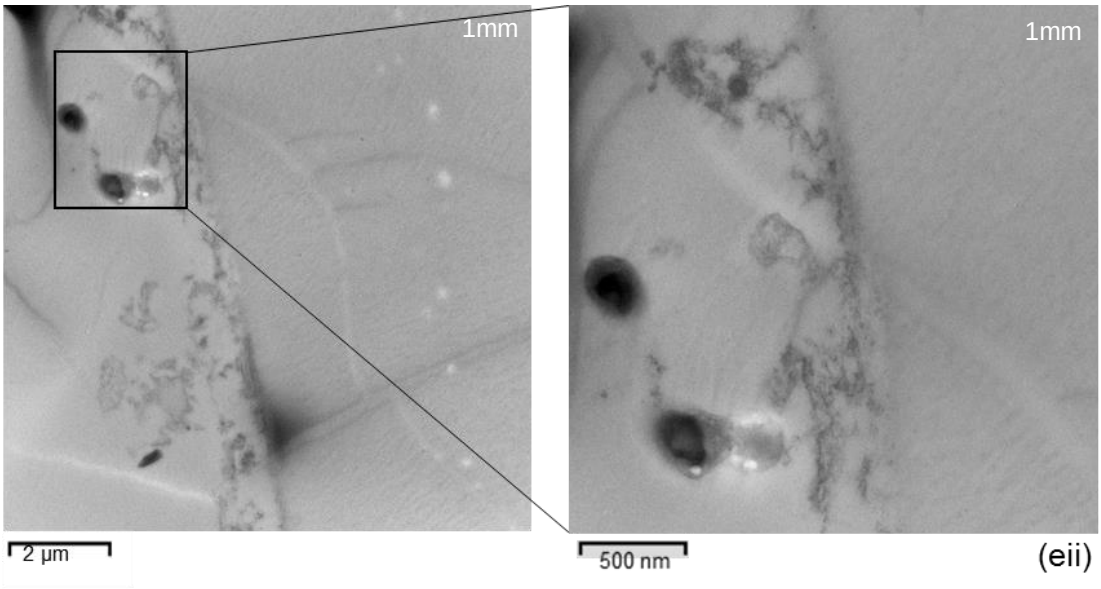

*The information at the upper right of each image indicates the level of the root canal (in mm) from the canal terminus where the residual biofilm was captured.

Figure 8.6: TEM images illustrate (ai) *E. faecalis* biofilm grown for 10 days. (aii) residual biofilm at 3 mm from the canal terminus after passive irrigation. (b) Passive irrigation group; (i) residual biofilm at 2 mm from the canal terminus; (ii) residual biofilm at 1 mm from the canal terminus. (c) manual-agitation group; (i) residual biofilm at 2 mm from the canal terminus; (ii) residual biofilm at 1 mm from the lateral canal terminus. (d) Sonic agitation group; (i) residual biofilm at 2 mm from the canal terminus; (ii) residual biofilm at 1 mm from the canal terminus. (e) Ultrasonic agitation group; (i) residual biofilm at 2 mm from the canal terminus; (ii) residual biofilm at 1 mm from the canal terminus.

8.4. Discussion

The present chapter was designed to provide comprehensive information about the effect of different irrigation protocols on the ability of 2.5% NaOCl irrigant to remove and destroy a multi-species biofilm within a simulated root canal model. The findings show a significant increase in the efficacy of NaOCl during manual, sonic, and ultrasonic agitation. Multi-species biofilm was more difficult to remove than single species biofilm to the effect of 2.5% NaOCl. The greatest destructive effect of multi-species structure was observed after ultrasonic agitation of 2.5% NaOCl.

In the present study, tryptic soya broth and agar were used to generate the multi-species biofilm. TSB media has been used to develop an *in vitro* multi-species biofilm model (Sedlacek and Walker, 2007). Furthermore, laboratory experiments

to optimize the culture conditions to obtain maximum growth of the relevant strains used herein to create multi-species biofilm were performed. For this, 50 µL of the multi-species baseline inoculum were added separately into 10 mL of three culture media (BHI. FAB, and TSB). Each mixture was vortexed and then incubated in an anaerobic chamber for up to 10 days with a change to fresh medium every 48 hours intervals (Sedlacek and Walker, 2007). Both optical density (OD) measurement and colony forming units per millilitre (CFUs/mL) were performed at 0h, 1h, 5h, 10h, 24h, 34h, 48h, 7days, and 10days incubation intervals. The results suggested that the TSB media allowed production of higher numbers of bacterial cells than BHI and FAB.

Analysis of the microscopic images (CLSM, SEM, and TEM) of the 1 mm^2 surface area of the root canals at 3 mm from the canal terminus showed no marked differences in the efficacy of passive and active irrigation, in terms of killing, cell wall destruction and complete removal of multi-species biofilm. The finding may be due to both high fluid dynamics the area around the needle tip (Verhaagen *et al.*, 2012), and chemical action of NaOCl, which related to the oxidizing effect of the OCl^- /$HOCl^-$ of the NaOCl (Christensen *et al.*, 2008).

Unlike the observations at 3 mm, a marked difference was found between the passive and active irrigation protocols at 2 and 1 mm from the canal terminus. The reduction in killing and destruction of the multi-species biofilm by NaOCl in the passive group could be related to the impact of canal confinement on the irrigant (Boutsioukis *et al.*, 2009; Verhaagen *et al.*, 2012). This may have reduced the irrigant refreshment and enhanced its stagnation (Ram, 1977). Another possible explanation for this is the viscous matrix of the multi-species biofilm may result in reduction of irrigant penetration (Burmølle *et al.*, 2006). This finding

suggests that it may be impossible to achieve complete removal of multi-species biofilm using passive irrigation in the apical part of the canal. In comparison, the greater destruction of multi-species biofilm and cell killing in active irrigation groups may be related to the impact of agitation on the dissolving capacity of NaOCl (Moorer and Wesselink, 1982). Furthermore, agitation enhances the mixing of fresh irrigant with the stagnant, used fluid in the apical part of the canal (Bronnec *et al.*, 2010). However, the difference in effectiveness of the techniques used to agitate NaOCl inside the root canal may be related to space restrictions of the root canal that interfere with the fluid dynamics and agitation method (Basrani, 2015). Another possible explanation is related to the exopolysaccharide matrix of mixed-species biofilms that could decrease the penetration of the antibacterial agent (NaOCl) (Burmølle *et al.*, 2006). Furthermore, the negative charged polymer of the matrix may prevent the penetration of active components of antimicrobial agent (e.g. NaOCl) (Stewart and Costerton, 2001). Moreover, bacterial surface protein, which is responsible for the hydrophobic property of bacterial cells, may play an important role in biofilm resistance by repelling the antimicrobial agent (Kobayashi and Iwano, 2012).

The findings of this study are in accordance with results reported by previous studies (Sena *et al.*, 2006; Shen *et al.*, 2010b), who showed that the mechanical agitation effectively enhanced the antimicrobial action of the irrigation procedure against multi-species biofilm.

The most obvious finding to emerge from this study is that multi-species biofilm was more resistant to the antibacterial action of 2.5% NaOCl than single species biofilm. The difference in resistance can be attributed to the cooperative behaviour exhibited by different bacterial cells of multi-species biofilm (Elias and

Banin, 2012). Also, this could be explained by the abundant exopolysaccharide matrix of multi-species biofilm, which provides an extra barrier against penetration of the antimicrobial agent (Pan *et al.*, 2006). The findings of the current study are consistent with those of Simoes *et al.* (2009), who reported an increase in resistance of multispecies biofilm when compared to single species biofilm.

8.5. Conclusion

Within the limitations of the current study, the passive irrigation using 2.5% NaOCl exhibited more residual multi-species biofilm on the model surface than 2.5% NaOCl irrigant activated by manual or automated (sonic, ultrasonic) method. Although non-viable cells were associated with the ultrasonic group, no complete biofilm dissolution was noted. The multi-species biofilm was more difficult to be killed or removed from the canal walls than the single species biofilm.

Chapter 9
General discussion and conclusions

9.1. General discussion

The issue of apical periodontitis has received considerable critical attention. Bacteria is integrated into communities, attached to surfaces and consequently form biofilm (Ricucci and Siqueira, 2010). The biofilm structure provides bacteria with a series of protection skills against antimicrobial agents (Marsh, 2005) and enhance pathogenicity (e.g. apical periodontitis). Sodium hypochlorite (NaOCl) has become the irrigant of choice for the elimination of bacteria from the root canal system based on its antimicrobial findings (Bystrom and Sundqvist, 1981). This thesis has described NaOCl irrigant refreshment during needle irrigation placed at a different level from the canal terminus using CFD models. In addition, the removal rate of bacterial biofilms from the apical part of the root canal system (3 mm) by sodium hypochlorite of different concentrations delivered by a syringe and needle, and how the irrigant agitation affects irrigant removal and destructive action were assessed. Furthermore, the effect of the canal complexity (lateral canal) and biofilm type on the efficacy of irrigation protocols was tested. The results of those investigations showed an increase in the irrigant penetration to the apical terminus increased as the irrigation needle was placed closer to the apical end, but the refreshment diminished. There was an increase in the removal efficacy of NaOCl when the concentration was increased and the needle was placed closer to the canal terminus. NaOCl agitation demonstrated an enhancement of its removal and destructive efficacy. Passive ultrasonic agitation showed a clear improvement in removal and destructive efficacy. Although canal complexity displayed no effect on the efficacy of NaOCl irrigation at the apical part, it reduced the effect of agitation on NaOCl irrigant in the lateral canal.

Multispecies biofilms were more resistant to the antimicrobial action of NaOCl than single species biofilm. According to the results, the null hypothesis tested in this study can be rejected that there exists no difference in the efficacy of passive and active sodium hypochlorite irrigation on the removal and destruction of single and multispecies bacterial biofilms from the walls of 3 mm of the apical third and lateral canal of the root canal system.

In the present study, all *in vitro* models were made of synthetic transparent materials. The surface and composition of such materials differ from that of the natural surface found in the root canal dentine. The porous nature of dentine (due to dentinal tubules) may act differently from a solid plastic material. An *in vitro* study that uses *ex vivo* (extracted teeth) to test the antimicrobial action of irrigants would be more relevant in terms of reflecting the clinical situation. Yet, tooth structures are concealed, which makes them unavailable for the direct visualisation needed to assess the antibacterial action of an irrigant during the process of irrigation. In this regard, the models advocated in this study have the advantage that the transparent canal model allows for a direct investigation in a time dependent way, into the removal action of the test targets (biofilm, simulant biofilms) by NaOCl irrigant. In addition, the results of investigation (chapter 2) to investigate the potential of the model material for development of suitable *in vitro* biofilm models showed that the relevant materials allowed for the adhesion and growth of biofilms on their surface.

In this study, the root canal model was created with an apical size 30, 0.06 taper because it has been suggested that the minimum apical size necessary to deliver the irrigant to the canal terminus is size 30 (Khademi *et al.*, 2006). A side cut 27-gauge endodontic needle was chosen for this study, as it is commonly used in

clinical practice, and to avoid the greater pressure required to deliver the irrigant at a rate of 9 mL per minute, as is the case when using a flat ended 30-gauge needle (Shen *et al.*, 2010a). A total of 9 mL of NaOCl were used during syringe irrigation protocol as it has been reported that 9 mL were sufficient to remove stained collagen simulating biofilm from the root canal system (Huang *et al.*, 2008). The volume of 9 mL per minute (0.15 mL s^{-1}) irrigant was selected as an attempt to improve the solution penetration (Bronnec *et al.*, 2010). Furthermore, this rate falls within the range of 0.01–1.01 mL s^{-1} reported in previous studies to be used in clinical practice (Boutsioukis *et al.*, 2007). One criticism may be generated about the high flow rate that may increase both apical pressure and irrigant extrusion (Park *et al.*, 2013); however, it has been argued that the healthy condition of the periapical tissue creates a barrier against the apical extrusion (Salzgeber and Brilliant, 1977).

The four strains used in this study (*E. faecalis* & *S. mutans, F. nucleatum* & *P. intermedia*) were selected to generate the multi-species biofilms because these species have been reported as a part of the microbial flora of the root canal system (Nair, 1987; Siqueira and Rôças, 2005). It has been reported that *E. faecalis* performs an essential role in secondary endodontic infections (Stuart *et al.*, 2006). *E. faecalis* persistence is related to their ability to invade dentinal tubules (Love, 2001), toleration to high pH and nutritional condition, and the ability to form a biofilm which is related to surface adhesins that facilitate the attachment to the surface as well as other cells (Distel *et al.*, 2002).

S. mutans plays a pioneer role in forming biofilms on the hard surface of the oral cavity (Kolenbrander *et al.*, 2006). *F. nucleatum* exhibits the capacity to coaggregate with other bacterial species and enhance adhesion of primary

colonized bacteria such as *S. mutans* and late colonized bacteria such as *P. intermedia.* (Kolenbrander *et al.*, 1989). Furthermore, Bolstad *et al.* (1996) reported bacterial synergism between *F. nucleatum* and *P. intermedia,* which could increase the pathogenic behaviour of the biofilm. In addition, studies have described the resistance and survival aptitude of the relevant bacteria to the root canal antimicrobial treatment (Molander *et al.*, 1998; Chavez De Paz *et al.*, 2003). However, the use of one community of four species biofilm may be considered a limitation of the present study and future investigations using different diversities of multi-species biofilms are recommended.

A total of ten days was selected for biofilm growth as it has been confirmed in investigation (chapter 2) that this period allowed microbial colonization and developed biofilm models. The relevant biofilm model allowed for the controlled investigation and comparison of the antimicrobial protocols (Halford *et al.*, 2012). Antimicrobial susceptibility of generated biofilms over time has been intensively explored. For instance, Wang *et al.* (2012) showed that young biofilm was more sensitive to intracanal medicaments, and bacteria were more easily killed than in old biofilm. It has been urged that the biofilms become increasingly difficult to be eliminated by antibacterial agents between 2 and 3 weeks (Stojicic *et al.*, 2013). However, another study suggested the biofilm resistance is inherent and it is possible to generate mature wild bacterial biofilm (*Pseudomonas aeruginosa*) after 5 days incubation (Klausen *et al.*, 2003).

In the present study, a fluorescent microscope has been selected to observe and record biofilm removal by NaOCl. The main advantage of this microscope was that it allowed direct vision of the biofilm removal without the need for sample fixation. However, the high resolution imaging proved difficult because of the

steeply curved sides of the canal walls, which interfere with light reflection from these areas. Furthermore, it was unachievable to assess single bacterial cell destruction in the biofilm because the lens of the microscope used herein was a 2.5-x objective lens. In this regard, residual biofilms were examined using CLSM, SEM, and TEM to assess cell viability, biofilm structure, and the extent of bacterial cells destruction respectively.

The use of crystal violet stain to render the biofilm visible under the microscope provoked an issue, because the stain may affect the oxidative capability of NaOCl. For this, experiments were performed to examine the effect of crystal violet stain on the oxidative capacity and capability of NaOCl . The results showed that crystal violet, which displayed a fluorescent capacity, showed neutral effect on NaOCl. This was interpreted by the evaluation of the available chlorine and pH of NaOCl before and after the addition of crystal violet. This result may be attributed to the alkaline property of the stain, or due to their concentration, which was not high enough to affect the oxidative capacity of NaOCl. The experiments were done in triplicate.

Image analysis software (Image-Pro Plus) has been used to analyse the images from the fluorescent microscope. This software has been adopted in other studies in order to analyse images (Huang *et al.*, 2008; McGill *et al.*, 2008). One criticism that can be made in relation to all image-analysis techniques is that the areas measured are to some extent subjectively chosen by the examiner. In order to reduce this limitation, inter- and intra-examiner assessments were carried out. A semi-automatic approach to measuring the biofilms was applied and imaging software was used to manually draw the template of the root canal outline and

quantify the biofilm. The same template was used to obtain and calculate the biofilm area after washing, without further interference of the operator.

Although the method of quantifying the biofilm from the root canal wall showed marked results, a single assessor performed the measurements and therefore there was a possibility of bias. In order to reduce this, a methodology was agreed using a standard protocol for outlining the root canal and for setting the threshold of the stain to be measured. The principal assessor and another observer who was experienced in using image analysis software measured 10% of the images and this was repeated until sufficient inter-observer agreement was achieved (Hartmann and Wood, 1990). Another attempt to reduce bias was attained by assessment of the intra-observer reliability. This was performed by recording ten replicate measurements of the residual biofilm in each group at specific intervals (every 10 s of the 90 s irrigation) and comparing the values taken. This comparison showed good agreement between the measurements (Koppe *et al.*, 2009). This semi-automatic method provided operator-independent quantitative results.

In the first chapter (the introduction), it was pointed out that the taper confinement and air bubble entrapment could affect the flow and penetration of an irrigant within the root canal system. The flow and velocity of 2.5% NaOCl within the root canal model used herein (size 30 taper 0.06) were demonstrated using CFD models, which revealed a clear decline in velocity toward the apical end. This finding is in agreement with Shen *et al.* (2010a)'s findings using CFD models, which showed that the highest irrigant velocity was at the tip of the needle, inserted at 3 mm from the canal terminus. The reduction in irrigant replacement was particularly likely when the irrigant needle was placed at 2 mm from the apical

end. For this, the irrigation needle was placed 3 mm from the canal terminus in all subsequent investigations.

In order to monitor the real-time effect of irrigation solution (NaOCl) on bacterial biofilm, the root canal model was used with closed or open-end (chapter 3). The results obtained from the closed end models, which were more clinically relevant, showed greater residual biofilms that explained to be related to the biofilm resistance, which affect the irrigant penetration (Ricucci *et al.*, 2009). Another possible explanation is related to reduction in velocity magnitude, which reduced the shear stress on the canal wall, as was confirmed with investigation using the CFD model. Another possible explanation is due to the effect of canal confinement (Verhaagen *et al.*, 2012) and air bubbles entrapment at the apical end (Tay *et al.*, 2010), which may reduce the mixing and replacement of irrigant. The open-end models were used to identify the maximum removal potential of NaOCl without interference of the canal confinement. However, residual biofilm was notified in the open-model, which may be related to the biofilm resistance or inadequate irrigation time (60 seconds). This total syringe irrigant time was selected as it was adopted in a previous study for irrigation protocol (Jiang *et al.*, 2012). After the irrigation procedure, the values of the available chlorine and pH of the outflow NaOCl were measured and compared with the values before irrigation in an attempt to identify the extent of interaction between NaOCl and biofilm. The results were interesting as the values were reduced, but the reduction was minimal, which was attributed to the irrigant stagnation and lowest replacement. The available chlorine determines the active component of NaOCl, whilst pH determines the equilibrium of the hypochlorous acid ($HOCl^-$), which has a strong bactericidal effect, and the hypochlorite ion (OCl^-), which has an

oxidative effect (de Macedo, 2013). Thus, minimal reduction of available chlorine and pH suggests that the outflow NaOCl still has a tissue dissolution effect (Baker *et al.*, 1975). Even when the interaction between NaOCl and the biofilm was performed on a flat surface in an attempt to reduce the effect of canal confinement, the reductions were also minimal (chapter 4). This was attributed to the biofilm thickness that requires more contact time to achieve complete removal (Spratt *et al.*, 2001). In an attempt to increase the chemical action of NaOCl, a higher concentration of NaOCl (5.25%) was delivered using a syringe placed closer to the apical end (2 mm) was performed (chapter 5). Although there was a clear improvement in biofilm removal, no complete biofilm removal was detected. This suggests that both the chemical action and mechanical action of NaOCl are required to remove the biofilm from the most apical part of the canal (Kishen *et al.*, 2008). In addition, the irrigating solution should be refreshed to allow the fresh NaOCl to be in contact with biofilm during the irrigation protocol (Macedo *et al.*, 2010). Previous research has already drawn attention to the agitation of an irrigant as a method to improve the outcomes of irrigation (Townsend and Maki, 2009; Parente *et al.*, 2010). The results of chapter 5 suggest the need for irrigant agitation as a tool that may enhance the chemical and physical action of the NaOCl within the root canal system.

With regard to the real-time effect of agitation on the efficacy of NaOCl, this thesis intended to determine the extent to which biofilms were removed and whether the destruction of the residual biofilm was intensified using different agitation techniques (manual, sonic, and ultrasonic). All agitation protocols used herein were found to cause a significant increase in the efficacy of NaOCl as less residual biofilm was notified ($p \leq 0.05$). In addition, an increase in the extent of

destruction of bacterial cells and structure of biofilm was identified. This might be related to that agitation of NaOCl which allows the inflow NaOCl to mix and replace the already exhausted NaOCl; it may also render the irrigant to be in contact with the biofilm surface for sufficient time required to achieve biofilm destruction biofilm (Spratt *et al.*, 2001). However, differences in removal and destruction level were found using different agitation protocols. The manual agitation of NaOCl was less effective in removing the biofilm and killing bacteria than the automated techniques (sonic & ultrasonic). This may be explained by the fact that the push-pull movement of gutta-percha points may have generated less shear stress than the automated techniques (Paragliola *et al.*, 2010). The results of the automated protocols may be attributed to the acoustic streaming and cavitation effects of the sonic and ultrasonic device within the main root canal (Van der Sluis *et al.*, 2005). This enhanced shear stress and intensified the chemical reactivity along the root canal wall at the apical part (Jiang *et al.*, 2010). The microscopic assessment of the residual biofilm supported the use of the ultrasonic agitation protocol to increase the efficacy of NaOCl as the complete destruction of biofilm was identified. It appears that the higher driving frequency of ultrasound results in a higher acoustic streaming (Ahmad *et al.*, 1988). This also may be responsible for the higher removal and destructive effect of NaOCl agitated using the ultrasonic protocol when compared with other irrigation protocols to remove biofilm from the lateral canal (chapter 7). However, this study confirmed that the efficacy of active and passive NaOCl was minimized at 1 mm from the lateral canal end in all irrigation groups. This could be related to the reduction in fluid convection (Verhaagen *et al.*, 2014a) and irrigant replacement (Wang *et al.*, 2014). Another possible factor, which can limit the outcome of

ultrasonic activation, is the resistance of bacterial biofilm. Biofilm type (single or multi-species) has also been confirmed in this study to affect the efficacy of active NaOCl irrigant (chapter 8). Although ultrasonic activation provided a clear improvement in the efficacy of NaOCl against multi-species biofilm, no complete destruction and removal from the apical part of the canal were detected. This may be attributed to the exopolysaccharide matrix of mixed-species biofilms, which could reduce the penetration of NaOCl irrigant (Burmølle *et al.*, 2006). Another possible explanation is related to the ability of different bacterial cells of multi-species biofilm to cooperate with each other and consequently enhance the resistance to irrigant penetration (Elias and Banin, 2012).

Based on the results of this study, it is evident that the concentration of NaOCl, the extent of the irrigation needle, the type of agitation, canal complexity, and type of bacterial biofilm have an influence on the outcome of root canal irrigation.

In order to effectively remove and eliminate the bacterial biofilm from the apical part of the root canal system, the following recommendations can be made:

- Apart from NaOCl concentration, the irrigation needle should be placed at a level which allows replacement of the irrigant as frequently as possible;
- NaOCl should be agitated to improve the mixing of the exhausted solution with the fresh solution;
- Agitation should be used to remove and eliminate bacterial biofilms from the root canal system as a final irrigation protocol, and within the tested protocols, ultrasonic agitation showed the best results.

9.2. Suggestions for future work

The 3D printing technology and materials used in the present study to create the root canal models could be adapted to manufacture root canal models of different apical size, taper, root curvature and complexity (e.g. oval canal), and further work on the current topic, which take these variables into account, should be undertaken.

Further research is required to explore the efficacy of active NaOCl on more mature multispecies biofilms of different bacterial strains within the root canal system.

Further work, which takes into account the use of high-speed cameras attached to a microscope to provide three-dimensional imaging of the effects of NaOCl on biofilm structure and bacterial cells should be undertaken.

The root canal model used herein is an *in vitro* approximation of what is present in a clinical scenario. In further research, a study in which people participate (randomized controlled trial) to test the outcome of the irrigation protocols within the root canal system is therefore recommended.

9.3. General conclusion

Within the limitations of the current study, the following conclusions are drawn:

- The stereolithography materials (Photopolymer and Accura) used herein demonstrated good potential to grow microorganisms in *in vitro* tests that require real-time investigation;
- The root canal model created using 3D printing technique served as a promising method by which to visualize and examine the efficacy of root

canal irrigation protocols to remove biofilms within simulated root canal systems.

- Both concentration and position of the irrigation needle affect the efficacy of NaOCl to remove bacterial biofilm from the apical part of the root canal system;
- The closed canal design adversely affect the removal efficacy of NaOCl.
- The passive irrigation using 2.5% NaOCl exhibited more residual biofilm (single & multi-species) on the model surface than 2.5% NaOCl activated by manual or automated (sonic, ultrasonic) methods.
- The results of the present study support the use of the ultrasonic agitation to optimise the effectiveness of irrigation using NaOCl to remove and destruct bacterial biofilm from the main and lateral canals;
- Canal complexity (lateral canal) had no effect on the efficacy of 2.5% NaOCl to remove bacterial biofilms from the apical part of the root canal system;
- The multi-species biofilm was more difficult to remove by passive or active NaOCl than the single species biofilm.

References

Abdullah, M., Ng, Y.-L., Gulabivala, K., Moles, D.R. & Spratt, D.A. 2005. Susceptibilties of Two Enterococcus faecalis Phenotypes to Root Canal Medications. *Journal of Endodontics,* 31 (1)**,** 30-36.

Abou-Rass, M. & Patonai, F.J. 1982. The effects of decreasing surface tension on the flow of irrigating solutions in narrow root canals. *Oral Surgery, Oral Medicine, Oral Pathology,* 53 (5)**,** 524-526.

Absolom, D.R., Lamberti, F.V., Policova, Z., Zingg, W., Van Oss, C.J. & Neumann, A. 1983. Surface thermodynamics of bacterial adhesion. *Applied and Environmental Microbiology,* 46 (1)**,** 90-97.

Adcock, J.M., Sidow, S.J., Looney, S.W., Liu, Y., Mcnally, K., Lindsey, K. & Tay, F.R. 2011. Histologic evaluation of canal and isthmus debridement efficacies of two different irrigant delivery techniques in a closed system. *Journal of Endodontics,* 37 (4)**,** 544-548.

Adorno, C.G., Yoshioka, T. & Suda, H. 2009. The effect of root preparation technique and instrumentation length on the development of apical root cracks. *Journal of Endodontics,* 35 (3)**,** 389-392.

Ahmad, M., Pitt Ford, T., Crum, L. & Walton, A. 1988. Ultrasonic debridement of root canals: acoustic cavitation and its relevance. *Journal of Endodontics,* 14 (10)**,** 486-493.

Akay, C., Karakis, D., Doğan, A. & Rad, A.Y. 2016. Effect of Chemical Disinfectants on Candida albicans Biofilm Formation on Poly (Methyl Methacrylate) Resin Surfaces: A Scanning Electron Microscope Study. *Journal of Advanced Oral Research/May-Aug,* 7 (2).

Al-Ahmad, A., Ameen, H., Pelz, K., Karygianni, L., Wittmer, A., Anderson, A.C., Spitzmüller, B. & Hellwig, E. 2014. Antibiotic resistance and capacity for biofilm formation of different bacteria isolated from endodontic infections associated with root-filled teeth. *Journal of Endodontics,* 40 (2)**,** 223-230.

Al-Jadaa, A., Paqué, F., Attin, T. & Zehnder, M. 2009. Necrotic pulp tissue dissolution by passive ultrasonic irrigation in simulated accessory canals: impact of canal location and angulation. *International Endodontic Journal,* 42 (1)**,** 59-65.

Al Shahrani, M., Divito, E., Hughes, C.V., Nathanson, D. & Huang, G.T.-J. 2014. Enhanced Removal of Enterococcus faecalis Biofilms in the Root Canal Using Sodium Hypochlorite Plus Photon-Induced Photoacoustic Streaming: An In Vitro Study. *Photomedicine and Laser Surgery,* 32 (5)**,** 260-266.

Almaguer-Flores, A., Olivares-Navarrete, R., Wieland, M., Ximénez-Fyvie, L., Schwartz, Z. & Boyan, B. 2012. Influence of topography and hydrophilicity on initial oral biofilm formation on microstructured titanium surfaces in vitro. *Clinical Oral Implants Research,* 23 (3)**,** 301-307.

Anderl, J.N., Franklin, M.J. & Stewart, P.S. 2000. Role of antibiotic penetration limitation in Klebsiella pneumoniae biofilm resistance to ampicillin and ciprofloxacin. *Antimicrobial Agents and Chemotherapy,* 44 (7)**,** 1818-1824.

Anderson, J.D. & Wendt, J. 1995. *Computational fluid dynamics.* 8 ed, McGraw-Hill Education, Springer.

Arias-Moliz, M., Ordinola-Zapata, R., Baca, P., Ruiz-Linares, M., García García, E., Duarte, H., Monteiro Bramante, C. & Ferrer-Luque, C. 2015. Antimicrobial activity of Chlorhexidine, Peracetic acid and Sodium hypochlorite/etidronate irrigant solutions against Enterococcus faecalis biofilms. *International Endodontic Journal,* 48 (12)**,** 1188-1193.

Baker, N.A., Eleazer, P.D., Averbach, R.E. & Seltzer, S. 1975. Scanning electron microscopic study of the efficacy of various irrigating solutions. *Journal of Endodontics,* 1 (4)**,** 127-135.

Ballal, N.V., Kandian, S., Mala, K., Bhat, K.S. & Acharya, S. 2009. Comparison of the efficacy of maleic acid and ethylenediaminetetraacetic acid in smear layer removal from instrumented human root canal: a scanning electron microscopic study. *Journal of Endodontics,* 35 (11)**,** 1573-1576.

Barthel, C.R., Zimmer, S. & Trope, M. 2004. Relationship of radiologic and histologic signs of inflammation in human root-filled teeth. *Journal of Endodontics,* 30 (2)**,** 75-79.

Basrani, B. 2015. *Endodontic Irrigation: Chemical disinfection of the root canal system.* second ed, Switzerland, Springer International Publishing.

Basrani, B. & Haapasalo, M. 2012. Update on endodontic irrigating solutions. *Endodontic Topics,* 27 (1)**,** 74-102.

Basrani, B.R., Manek, S., Mathers, D., Fillery, E. & Sodhi, R.N. 2010. Determination of 4-chloroaniline and its derivatives formed in the interaction of sodium hypochlorite and chlorhexidine by using gas chromatography. *Journal of Endodontics,* 36 (2)**,** 312-314.

Baumgartner, C., Mader, J. & Carson, L. 1987. A scanning electron microscopic evaluation of four root canal irrigation regimens. *Journal of Endodontics,* 13 (4)**,** 147-157.

Baumgartner, J.C., Siqueira, J., Sedgley, C.M. & Kishen, A. 2008. *Microbiology of endodontic disease*. *Ingle's endodontics.* 6th ed. Hamilton, Canada: BC Decker.

Bergenholtz Tz, G., Ahlstedt, S. & Lindhe, J. 1977. Experimental pulpitis in immunized monkeys. *European Journal of Oral Sciences,* 85 (6)**,** 396-406.

Bhuva, B., Patel, S., Wilson, R., Niazi, S., Beighton, D. & Mannocci, F. 2010. The effectiveness of passive ultrasonic irrigation on intraradicular Enterococcus faecalis biofilms in extracted single-rooted human teeth. *International Endodontic Journal,* 43 (3)**,** 241-250.

Blehert, D.S., Palmer, R.J., Xavier, J.B., Almeida, J.S. & Kolenbrander, P.E. 2003. Autoinducer 2 production by Streptococcus gordonii DL1 and the biofilm phenotype of a luxS mutant are influenced by nutritional conditions. *Journal of Bacteriology,* 185 (16)**,** 4851-4860.

Bolstad, A., Jensen, H. & Bakken, V. 1996. Taxonomy, biology, and periodontal aspects of Fusobacterium nucleatum. *Clinical Microbiology Reviews,* 9 (1)**,** 55-71.

Boutsioukis, C., Gogos, C., Verhaagen, B., Versluis, M., Kastrinakis, E. & Van Der Sluis, L. 2010a. The effect of apical preparation size on irrigant flow in root canals evaluated using an unsteady Computational Fluid Dynamics model. *International Endodontic Journal,* 43 (10)**,** 874-881.

Boutsioukis, C., Gogos, C., Verhaagen, B., Versluis, M., Kastrinakis, E. & Van Der Sluis, L. 2010b. The effect of root canal taper on the irrigant flow: evaluation using an unsteady Computational Fluid Dynamics model. *International Endodontic Journal,* 43 (10)**,** 909-916.

Boutsioukis, C., Kastrinakis, E., Lambrianidis, T., Verhaagen, B., Versluis, M. & Sluis, L. 2014. Formation and removal of apical vapor lock during syringe irrigation: a

combined experimental and Computational Fluid Dynamics approach. *International Endodontic Journal,* 47 (2)**,** 191-201.

Boutsioukis, C. & Kishen, A. 2012. Fluid dynamics of syringe-based irrigation to optimise anti-biofilm efficacy in root-canal disinfection. *Roots: International Magazine of Endodontology,* 2012**,** 22-31.

Boutsioukis, C., Lambrianidis, T. & Kastrinakis, E. 2009. Irrigant flow within a prepared root canal using various flow rates: a Computational Fluid Dynamics study. *International Endodontic Journal,* 42 (2)**,** 144-155.

Boutsioukis, C., Lambrianidis, T., Kastrinakis, E. & Bekiaroglou, P. 2007. Measurement of pressure and flow rates during irrigation of a root canal ex vivo with three endodontic needles. *International Endodontic Journal,* 40 (7)**,** 504-513.

Boutsioukis, C., Lambrianidis, T., Verhaagen, B., Versluis, M., Kastrinakis, E., Wesselink, P.R. & Van Der Sluis, L.W. 2010c. The effect of needle-insertion depth on the irrigant flow in the root canal: evaluation using an unsteady computational fluid dynamics model. *Journal of Endodontics,* 36 (10)**,** 1664-1668.

Boutsioukis, C., Verhaagen, B., Versluis, M., Kastrinakis, E. & Van Der Sluis, L.W. 2010d. Irrigant flow in the root canal: experimental validation of an unsteady Computational Fluid Dynamics model using high-speed imaging. *International Endodontic Journal,* 43 (5)**,** 393-403.

Brito, P.R., Souza, L.C., Machado De Oliveira, J.C., Alves, F.R., De-Deus, G., Lopes, H.P. & Siqueira Jr, J.F. 2009. Comparison of the Effectiveness of Three Irrigation Techniques in Reducing Intracanal Enterococcus faecalis Populations: An In Vitro Study. *Journal of Endodontics,* 35 (10)**,** 1422-1427.

Bronnec, F., Bouillaguet, S. & Machtou, P. 2010. Ex vivo assessment of irrigant penetration and renewal during the final irrigation regimen. *International Endodontic Journal,* 43 (8)**,** 663-672.

Brown, M. & Gilbert, P. 1993. Sensitivity of biofilms to antimicrobial agents. *Journal of Applied Bacteriology,* 74 (S22)**,** 87S-97S.

Bryce, G., O'donnell, D., Ready, D., Ng, Y.-L., Pratten, J. & Gulabivala, K. 2009. Contemporary root canal irrigants are able to disrupt and eradicate single-and dual-species biofilms. *Journal of Endodontics,* 35 (9)**,** 1243-1248.

Bukiet, F., Couderc, G., Camps, J., Tassery, H., Cuisinier, F., About, I., Charrier, A. & Candoni, N. 2012. Wetting properties and critical micellar concentration of benzalkonium chloride mixed in sodium hypochlorite. *Journal of Endodontics,* 38 (11)**,** 1525-1529.

Bürgers, R., Schneider-Brachert, W., Rosentritt, M., Handel, G. & Hahnel, S. 2009. Candida albicans adhesion to composite resin materials. *Clinical Oral Investigations,* 13 (3)**,** 293-299.

Burmølle, M., Webb, J.S., Rao, D., Hansen, L.H., Sørensen, S.J. & Kjelleberg, S. 2006. Enhanced biofilm formation and increased resistance to antimicrobial agents and bacterial invasion are caused by synergistic interactions in multispecies biofilms. *Applied and Environmental Microbiology,* 72 (6)**,** 3916-3923.

Bystrom, A. & Sundqvist, G. 1981. Bacteriologic evaluation of the efficacy of mechanical root canal instrumentation in endodontic therapy. *European Journal of Oral Sciences,* 89 (4)**,** 321-328.

Byström, A. & Sundqvist, G. 1983. Bacteriologic evaluation of the effect of 0.5 percent sodium hypochlorite in endodontic therapy. *Oral Surgery, Oral Medicine, Oral Pathology,* 55 (3)**,** 307-312.

Byström, A. & Sunvqvist, G. 1985. The antibacterial action of sodium hypochlorite and EDTA in 60 cases of endodontic therapy. *International Endodontic Journal,* 18 (1)**,** 35-40.

Castelo-Baz, P., Martín-Biedma, B., Cantatore, G., Ruíz-Piñón, M., Bahillo, J., Rivas-Mundiña, B. & Varela-Patiño, P. 2012. In vitro comparison of passive and continuous ultrasonic irrigation in simulated lateral canals of extracted teeth. *Journal of Endodontics,* 38 (5)**,** 688-691.

Cecic, P.A., Peters, D.D. & Grower, M.F. 1984. The comparative efficiency of final endodontic cleansing procedures in removing a radioactive albumin from root canal systems. *Oral Surgery, Oral Medicine, Oral Pathology,* 58 (3)**,** 336-342.

Cerca, N., Pier, G.B., Vilanova, M., Oliveira, R. & Azeredo, J. 2005. Quantitative analysis of adhesion and biofilm formation on hydrophilic and hydrophobic surfaces of clinical isolates of Staphylococcus epidermidis. *Research in Microbiology,* 156 (4)**,** 506-514.

Chalmers, N.I., Palmer, R.J., Cisar, J.O. & Kolenbrander, P.E. 2008. Characterization of a Streptococcus sp.-Veillonella sp. community micromanipulated from dental plaque. *Journal of Bacteriology,* 190 (24)**,** 8145-8154.

Chatterjee, R., Venugopal, P., Jyothi, K., Jayashankar, C., Kumar, S.A. & Kumar, P.S. 2015. Effect of sonic agitation, manual dynamic agitation on removal of Enterococcus faecalis biofilm. *Saudi Endodontic Journal,* 5 (2)**,** 125.

Chavez De Paz, L., Dahlén, G., Molander, A., Möller, Å. & Bergenholtz, G. 2003. Bacteria recovered from teeth with apical periodontitis after antimicrobial endodontic treatment. *International Endodontic Journal,* 36 (7)**,** 500-508.

Chen, J.E., Nurbakhsh, B., Layton, G., Bussmann, M. & Kishen, A. 2014. Irrigation dynamics associated with positive pressure, apical negative pressure and passive ultrasonic irrigations: A computational fluid dynamics analysis. *Australian Endodontic Journal,* 40 (2)**,** 54-60.

Chin, M.Y., Busscher, H.J., Evans, R., Noar, J. & Pratten, J. 2006. Early biofilm formation and the effects of antimicrobial agents on orthodontic bonding materials in a parallel plate flow chamber. *The European Journal of Orthodontics,* 28 (1)**,** 1-7.

Christensen, C.E., Mcneal, S.F. & Eleazer, P. 2008. Effect of lowering the pH of sodium hypochlorite on dissolving tissue in vitro. *Journal of Endodontics,* 34 (4)**,** 449-452.

Chugal, N., Wang, J.-K., Wang, R., He, X., Kang, M., Li, J., Zhou, X., Shi, W. & Lux, R. 2011. Molecular characterization of the microbial flora residing at the apical portion of infected root canals of human teeth. *Journal of Endodontics,* 37 (10)**,** 1359-1364.

Clegg, M., Vertucci, F., Walker, C., Belanger, M. & Britto, L. 2006. The effect of exposure to irrigant solutions on apical dentin biofilms in vitro. *Journal of Endodontics,* 32 (5)**,** 434-437.

Cohen, S. & Burns, R.C. 1998. *Pathways of the pulp.* 7 ed, the University of Michigan, Mosby.

Costerton, J.W., Lewandowski, Z., Caldwell, D.E., Korber, D.R. & Lappin-Scott, H.M. 1995. Microbial biofilms. *Annual Reviews in Microbiology,* 49 (1)**,** 711-745.

Costerton, J.W., Stewart, P.S. & Greenberg, E. 1999. Bacterial biofilms: a common cause of persistent infections. *Science,* 284 (5418)**,** 1318-1322.

Craig Baumgartner, J. & Falkler, W.A. 1991. Bacteria in the apical 5 mm of infected root canals. *Journal of Endodontics,* 17 (8)**,** 380-383.

Cunningham, W.T., Martin, H. & Forrest, W.R. 1982. Evaluation of root canal debridement by the endosonic ultrasonic synergistic system. *Oral Surgery, Oral Medicine, Oral Pathology,* 53 (4)**,** 401-404.

D'arcangelo, C., Varvara, G. & De Fazio, P. 1999. An evaluation of the action of different root canal irrigants on facultative aerobic-anaerobic, obligate anaerobic, and microaerophilic bacteria. *Journal of Endodontics,* 25 (5)**,** 351-353.

Dammaschke, T., Witt, M., Ott, K. & Schäfer, E. 2004. Scanning electron microscopic investigation of incidence, location, and size of accessory foramina in primary and permanent molars. *Quintessence International,* 35 (9).

De-Deus, G., Brandão, M., Fidel, R. & Fidel, S. 2007. The sealing ability of GuttaFlow™ in oval-shaped canals: an ex vivo study using a polymicrobial leakage model. *International Endodontic Journal,* 40 (10)**,** 794-799.

De Gregorio, C., Estevez, R., Cisneros, R., Heilborn, C. & Cohenca, N. 2009. Effect of EDTA, Sonic, and Ultrasonic Activation on the Penetration of Sodium Hypochlorite into Simulated Lateral Canals: An In Vitro Study. *Journal of Endodontics,* 35 (6)**,** 891-895.

De Gregorio, C., Estevez, R., Cisneros, R., Paranjpe, A. & Cohenca, N. 2010. Efficacy of Different Irrigation and Activation Systems on the Penetration of Sodium Hypochlorite into Simulated Lateral Canals and up to Working Length: An In Vitro Study. *Journal of Endodontics,* 36 (7)**,** 1216-1221.

De Macedo, R.G. 2013. *Optimizing the chemical aspect of root canal irrigation.* 1 ed, Amsterdam, The Netherlands, Academic Center for Dentistry Amsterdam.

De Moor, R.J., Meire, M.A. & Verdaasdonk, R.M. The power of the bubble: comparing ultrasonic and laser activated irrigation. Fifth International Conference on Lasers in Medicine, 2014. International Society for Optics and Photonics, 892504-892504-892509.

Defives, C., Guyard, S., Oularé, M., Mary, P. & Hornez, J. 1999. Total counts, culturable and viable, and non-culturable microflora of a French mineral water: a case study. *Journal of Applied Microbiology,* 86 (6)**,** 1033-1038.

Del Carpio-Perochena, A.E., Bramante, C.M., Duarte, M.A., Cavenago, B.C., Villas-Boas, M.H., Graeff, M.S., Bernardineli, N., De Andrade, F.B. & Ordinola-Zapata, R. 2011. Biofilm dissolution and cleaning ability of different irrigant solutions on intraorally infected dentin. *Journal of Endodontics,* 37 (8)**,** 1134-1138.

Derjaguin, B. & Landau, L. 1941. The theory of stability of highly charged lyophobic sols and coalescence of highly charged particles in electrolyte solutions. *Acta Physicochim. URSS,* 14**,** 633-652.

Diaz, P.I., Chalmers, N.I., Rickard, A.H., Kong, C., Milburn, C.L., Palmer, R.J. & Kolenbrander, P.E. 2006. Molecular characterization of subject-specific oral microflora during initial colonization of enamel. *Applied and Environmental Microbiology,* 72 (4)**,** 2837-2848.

Dick, E. 2009. *Introduction to finite element methods in computational fluid dynamics*. *Computational Fluid Dynamics.* 3rd ed. New York, USA: Springer.

Distel, J.W., Hatton, J.F. & Gillespie, M.J. 2002. Biofilm formation in medicated root canals. *Journal of Endodontics,* 28 (10)**,** 689-693.

Donlan, R.M. 2002. Biofilms: microbial life on surfaces. *Emerging Infectious Diseases,* 8 (9)**,** 881-890.

Dovgyallo, G., Migun, N. & Prokhorenko, P. 1989. The complete filling of dead-end conical capillaries with liquid. *Journal of Engineering Physics and Thermophysics,* 56 (4)**,** 395-397.

Doyle, R.J. 2000. Contribution of the hydrophobic effect to microbial infection. *Microbes and infection,* 2 (4)**,** 391-400.

Druttman, A. & Stock, C. 1989. An in vitro comparison of ultrasonic and conventional methods of irrigant replacement. *International Endodontic Journal,* 22 (4)**,** 174-178.

Dufour, D., Leung, V. & Lévesque, C.M. 2010. Bacterial biofilm: structure, function, and antimicrobial resistance. *Endodontic Topics,* 22 (1)**,** 2-16.

Dunne, W.M. 2002. Bacterial adhesion: seen any good biofilms lately? *Clinical Microbiology Reviews,* 15 (2)**,** 155-166.

Elias, S. & Banin, E. 2012. Multi-species biofilms: living with friendly neighbors. *FEMS Microbiology Reviews,* 36 (5)**,** 990-1004.

Ercan, E., Özekinci, T., Atakul, F. & Gül, K. 2004. Antibacterial activity of 2% chlorhexidine gluconate and 5.25% sodium hypochlorite in infected root canal: in vivo study. *Journal of Endodontics,* 30 (2)**,** 84-87.

Espersen, F., Wurr, M., Corneliussen, L., Høg, A.-L., Rosdahl, V.T., Frimodt-Møller, N. & Skinhøj, P. 1994. Attachment of staphylococci to different plastic tubes in vitro. *Journal of Medical Microbiology,* 40 (1)**,** 37-42.

Estrela, C., Estrela, C., Decurcio, D., Hollanda, A. & Silva, J. 2007. Antimicrobial efficacy of ozonated water, gaseous ozone, sodium hypochlorite and chlorhexidine in infected human root canals. *International Endodontic Journal,* 40 (2)**,** 85-93.

Estrela, C., Estrela, C.R., Barbin, E.L., Spanó, J.C.E., Marchesan, M.A. & Pécora, J.D. 2002. Mechanism of action of sodium hypochlorite. *Brazilian Dental Journal,* 13 (2)**,** 113-117.

Estrela, C., Holland, R., Bernabé, P.F.E., Souza, V.D. & Estrela, C.R. 2004. Antimicrobial potential of medicaments used in healing process in dogs' teeth with apical periodontitis. *Brazilian Dental Journal,* 15 (3)**,** 181-185.

European Society of Endodontology, E. 2006. Quality guidelines for endodontic treatment: consensus report of the European Society of Endodontology. *International Endodontic Journal,* 39 (12)**,** 921-930.

Evans, M., Davies, J., Sundqvist, G. & Figdor, D. 2002. Mechanisms involved in the resistance of Enterococcus faecalis to calcium hydroxide. *International Endodontic Journal,* 35 (3)**,** 221-228.

Fabricius, L., Dahlen, G., Holm, S.E. & Moller Jr, A. 1982. Influence of combinations of oral bacteria on periapical tissues of monkeys. *European Journal of Oral Sciences,* 90 (3)**,** 200-206.

Farrugia, C., Cassar, G., Valdramidis, V. & Camilleri, J. 2015. Effect of sterilization techniques prior to antimicrobial testing on physical properties of dental restorative materials. *Journal of Dentistry,* 43 (6)**,** 703-714.

Ferraz, C.C., Gomes, B.P., Zaia, A.A., Teixeira, F.B. & Souza-Filho, F.J. 2007. Comparative study of the antimicrobial efficacy of chlorhexidine gel, chlorhexidine solution and sodium hypochlorite as endodontic irrigants. *Brazilian Dental Journal,* 18 (4)**,** 294-298.

Figdor, D. 2004. Microbial aetiology of endodontic treatment failure and pathogenic properties of selected species. *Australian Endodontic Journal,* 30 (1)**,** 11-14.

Fimple, J.L., Fontana, C.R., Foschi, F., Ruggiero, K., Song, X., Pagonis, T.C., Tanner, A.C., Kent, R., Doukas, A.G. & Stashenko, P.P. 2008. Photodynamic treatment of endodontic polymicrobial infection in vitro. *Journal of Endodontics,* 34 (6)**,** 728-734.

Flemming, H.-C., Neu, T.R. & Wozniak, D.J. 2007. The EPS matrix: the "house of biofilm cells". *Journal of Bacteriology,* 189 (22)**,** 7945-7947.

Flemming, H.-C. & Wingender, J. 2010. The biofilm matrix. *Nature Reviews Microbiology,* 8 (9)**,** 623-633.

Fletcher, M. & Marshall, K. 1982. Bubble contact angle method for evaluating substratum interfacial characteristics and its relevance to bacterial attachment. *Applied and Environmental Microbiology,* 44 (1)**,** 184-192.

Fonseca, A., Granja, P., Nogueira, J., Oliveira, D. & Barbosa, M. 2001. Staphylococcus epidermidis RP62A adhesion to chemically modified cellulose derivatives. *Journal of Materials Science: Materials in Medicine,* 12 (6)**,** 543-548.

Fouad, A.F. 2009. *Endodontic microbiology.* 1 ed, Arnes-Spain, John Wiley & Sons.

Fowkes, F.M. 1964. Attractive forces at interfaces. *Industrial and Engineering Chemistry,* 56 (12)**,** 40-52.

Gao, Y., Haapasalo, M., Shen, Y., Wu, H., Li, B., Ruse, N.D. & Zhou, X. 2009. Development and validation of a three-dimensional computational fluid dynamics model of root canal irrigation. *Journal of Endodontics,* 35 (9)**,** 1282-1287.

George, S. & Kishen, A. 2007. Effect of Tissue Fluids on Hydrophobicity and Adherence of Enterococcus faecalis to Dentin. *Journal of Endodontics,* 33 (12)**,** 1421-1425.

Gibbons, R. & Van Houte, J. 1971. Selective bacterial adherence to oral epithelial surfaces and its role as an ecological determinant. *Infection and Immunity,* 3 (4)**,** 567-573.

Goldman, M. & Pearson, A.H. 1969. Postdebridement bacterial flora and antibiotic sensitivity. *Oral Surgery, Oral Medicine, Oral Pathology,* 28 (6)**,** 897-905.

Gomes, B.P.F.A., Martinho, F.C. & Vianna, M.E. 2009. Comparison of 2.5% Sodium Hypochlorite and 2% Chlorhexidine Gel on Oral Bacterial Lipopolysaccharide Reduction from Primarily Infected Root Canals. *Journal of Endodontics,* 35 (10)**,** 1350-1353.

Good, R.J. & Van Oss, C.J. 1992. *The modern theory of contact angles and the hydrogen bond components of surface energies*. *Modern Approaches to Wettability.* Springer.

Goode, N., Khan, S., Eid, A.A., Niu, L.-N., Gosier, J., Susin, L.F., Pashley, D.H. & Tay, F.R. 2013. Wall shear stress effects of different endodontic irrigation techniques and systems. *Journal of Dentistry,* 41 (7)**,** 636-641.

Gopikrishna, V., Kandaswamy, D. & Jeyavel, R.K. 2006. Comparative evaluation of the antimicrobial efficacy of five endodontic root canal sealers against Enterococcus faecalis and Candida albicans. *Journal of Conservative Dentistry,* 9 (1)**,** 2.

Grossman, L.I. 1955. *Root canal therapy.* 4 ed, the University of Michigan, Lea & Febiger.

Gu, L.-S., Kim, J.R., Ling, J., Choi, K.K., Pashley, D.H. & Tay, F.R. 2009. Review of contemporary irrigant agitation techniques and devices. *Journal of Endodontics,* 35 (6)**,** 791-804.

Guerisoli, D.M.Z., Silva, R. & Pécora, J.D. 1998. Evaluation of some physico-chemical properties of different concentrations of sodium hypochlorite solutions. *Braz Endod J,* 3 (2)**,** 21-23.

Guggenheim, B., Giertsen, E., Schüpbach, P. & Shapiro, S. 2001. Validation of an in vitro biofilm model of supragingival plaque. *Journal of Dental Research,* 80 (1)**,** 363-370.

Gulabivala, K. & Ng, Y.-L. 2014. *Endodontics.* 4th ed, Springer London/UK, Mosby/Elsevier Health Sciences.

Gulabivala, K., Ng, Y., Gilbertson, M. & Eames, I. 2010. The fluid mechanics of root canal irrigation. *Physiological Measurement,* 31 (12)**,** R49.

Gulabivala, K., Patel, B., Evans, G. & Ng, Y.L. 2005. Effects of mechanical and chemical procedures on root canal surfaces. *Endodontic Topics,* 10 (1)**,** 103-122.

Guyon, E. 2001. *Physical hydrodynamics.* 1 ed, U.S.A., Oxford University Press.

Halford, A., Ohl, C.-D., Azarpazhooh, A., Basrani, B., Friedman, S. & Kishen, A. 2012. Synergistic Effect of Microbubble Emulsion and Sonic or Ultrasonic Agitation on Endodontic Biofilm in Vitro. *Journal of Endodontics,* 38 (11)**,** 1530-1534.

Harrison, J.W. & Hand, R.E. 1981. The effect of dilution and organic matter on the antibacterial property of 5.25% sodium hypochlorite. *Journal of Endodontics,* 7 (3)**,** 128-132.

Hartmann, D.P. & Wood, D.D. 1990. *Observational methods*. *International handbook of behavior modification and therapy.* 2 ed. Plenum Press, New York: Springer/USA.

Hawkins, C., Pattison, D. & Davies, M.J. 2003. Hypochlorite-induced oxidation of amino acids, peptides and proteins. *Amino Acids,* 25 (3-4)**,** 259-274.

Hegde, J., Bashetty, K. & Krishnakumar, U.G. 2012. Quantity of sodium thiosulfate required to neutralize various concentrations of sodium hypochlorite. *Asian Journal of Pharmaceutical and Health Sciences,* 2 (3)**,** 390-393.

Holman, J. 2002. *Heat Transfer.* 9 ed, New York, McGraw-Hill.

Hsieh, Y., Gau, C., Kung Wu, S., Shen, E., Hsu, P. & Fu, E. 2007. Dynamic recording of irrigating fluid distribution in root canals using thermal image analysis. *International Endodontic Journal,* 40 (1)**,** 11-17.

Hsu, L.C., Fang, J., Borca-Tasciuc, D.A., Worobo, R.W. & Moraru, C.I. 2013. Effect of micro-and nanoscale topography on the adhesion of bacterial cells to solid surfaces. *Applied and Environmental Microbiology,* 79 (8)**,** 2703-2712.

Hu, X., Peng, Y., Sum, C.-P. & Ling, J. 2010. Effects of concentrations and exposure times of sodium hypochlorite on dentin deproteination: attenuated total reflection Fourier transform infrared spectroscopy study. *Journal of Endodontics,* 36 (12)**,** 2008-2011.

Huang, T.Y., Gulabivala, K. & Ng, Y.L. 2008. A bio-molecular film ex-vivo model to evaluate the influence of canal dimensions and irrigation variables on the efficacy of irrigation. *International Endodontic Journal,* 41 (1)**,** 60-71.

Hülsmann, M., Gressmann, G. & Schäfers, F. 2003. A comparative study of root canal preparation using FlexMaster and HERO 642 rotary Ni–Ti instruments. *International Endodontic Journal,* 36 (5)**,** 358-366.

Izano, E.A., Wang, H., Ragunath, C., Ramasubbu, N. & Kaplan, J.B. 2007. Detachment and killing of Aggregatibacter actinomycetemcomitans biofilms by dispersin B and SDS. *Journal of Dental Research,* 86 (7)**,** 618-622.

Jhajharia, K., Parolia, A., Shetty, K.V. & Mehta, L.K. 2015. Biofilm in endodontics: a review. *Journal of International Society of Preventive and Community Dentistry,* 5 (1)**,** 1.

Jiang, L.-M., Lak, B., Eijsvogels, L.M., Wesselink, P. & Van Der Sluis, L.W. 2012. Comparison of the cleaning efficacy of different final irrigation techniques. *Journal of Endodontics,* 38 (6)**,** 838-841.

Jiang, L.M., Verhaagen, B., Versluis, M. & Van Der Sluis, L.W. 2010. Evaluation of a sonic device designed to activate irrigant in the root canal. *Journal of Endodontics,* 36 (1)**,** 143-146.

Jucker, B.A., Harms, H. & Zehnder, A. 1996. Adhesion of the positively charged bacterium Stenotrophomonas (Xanthomonas) maltophilia 70401 to glass and Teflon. *Journal of Bacteriology,* 178 (18)**,** 5472-5479.

Jungbluth, H., Marending, M., De-Deus, G., Sener, B. & Zehnder, M. 2011. Stabilizing sodium hypochlorite at high pH: effects on soft tissue and dentin. *Journal of Endodontics,* 37 (5)**,** 693-696.

Kakehashi, S., Stanley, H. & Fitzgerald, R. 1965. The effects of surgical exposures of dental pulps in germ-free and conventional laboratory rats. *Oral Surgery, Oral Medicine, Oral Pathology,* 20 (3)**,** 340-349.

Kanagasingam, S., Lim, C., Yong, C., Mannocci, F. & Patel, S. 2016. Diagnostic accuracy of periapical radiography and cone beam computed tomography in detecting apical periodontitis using histopathological findings as a reference standard. *International Endodontic Journal*.

Kandaswamy, D. & Venkateshbabu, N. 2010. Root canal irrigants. *Journal of Conservative Dentistry,* 13 (4)**,** 256.

Kara, D., Luppens, S.B. & Cate, J.M. 2006. Differences between single-and dual-species biofilms of Streptococcus mutans and Veillonella parvula in growth, acidogenicity and susceptibility to chlorhexidine. *European Journal of Oral Sciences,* 114 (1)**,** 58-63.

Katsikogianni, M. & Missirlis, Y. 2004. Concise review of mechanisms of bacterial adhesion to biomaterials and of techniques used in estimating bacteria-material interactions. *Eur Cell Mater,* 8 (3).

Khademi, A., Yazdizadeh, M. & Feizianfard, M. 2006. Determination of the minimum instrumentation size for penetration of irrigants to the apical third of root canal systems. *Journal of Endodontics,* 32 (5)**,** 417-420.

Khaord, P., Amin, A., Shah, M.B., Uthappa, R., Raj, N., Kachalia, T. & Kharod, H. 2015. Effectiveness of different irrigation techniques on smear layer removal in apical thirds of mesial root canals of permanent mandibular first molar: A scanning electron microscopic study. *Journal of conservative dentistry: JCD,* 18 (4)**,** 321.

Kishen, A. 2010. Advanced therapeutic options for endodontic biofilms. *Endodontic Topics,* 22 (1)**,** 99-123.

Kishen, A. & Haapasalo, M. 2010. Biofilm models and methods of biofilm assessment. *Endodontic Topics,* 22 (1)**,** 58-78.

Kishen, A., Sum, C.-P., Mathew, S. & Lim, C.-T. 2008. Influence of Irrigation Regimens on the Adherence of Enterococcus faecalis to Root Canal Dentin. *Journal of Endodontics,* 34 (7)**,** 850-854.

Klausen, M., Heydorn, A., Ragas, P., Lambertsen, L., Aaes-Jørgensen, A., Molin, S. & Tolker-Nielsen, T. 2003. Biofilm formation by Pseudomonas aeruginosa wild type, flagella and type IV pili mutants. *Molecular Microbiology,* 48 (6)**,** 1511-1524.

Kobayashi, K. & Iwano, M. 2012. BslA (YuaB) forms a hydrophobic layer on the surface of Bacillus subtilis biofilms. *Molecular Microbiology,* 85 (1)**,** 51-66.

Kolenbrander, P., Andersen, R. & Moore, L. 1989. Coaggregation of Fusobacterium nucleatum, Selenomonas flueggei, Selenomonas infelix, Selenomonas noxia, and Selenomonas sputigena with strains from 11 genera of oral bacteria. *Infection and Immunity,* 57 (10)**,** 3194-3203.

Kolenbrander, P.E., Palmer, R.J., Rickard, A.H., Jakubovics, N.S., Chalmers, N.I. & Diaz, P.I. 2006. Bacterial interactions and successions during plaque development. *Periodontology 2000,* 42 (1)**,** 47-79.

Koppe, T., Meyer, G. & Alt, K. 2009. Comparative dental morphology. Preface. *Frontiers of Oral Biology,* 13**,** XI.

Korber, D.R., Lawrence, J.R., Lappin-Scott, H.M. & Costerton, J.W. 1995. Growth of microorganisms on surfaces. *Microbial biofilms***,** 15-45.

Krause, T.A., Liewebr, F.R. & Hahn, C.-L. 2007. The antimicrobial effect of MTAD, sodium hypochlorite, doxycycline, and citric acid on Enterococcus faecalis. *Journal of Endodontics,* 33 (1)**,** 28-30.

Lawrence, J., Korber, D., Hoyle, B., Costerton, J. & Caldwell, D. 1991. Optical sectioning of microbial biofilms. *Journal of Bacteriology,* 173 (20)**,** 6558-6567.

Layton, G., Wu, W.-I., Selvaganapathy, P.R., Friedman, S. & Kishen, A. 2015. Fluid Dynamics and Biofilm Removal Generated by Syringe-delivered and 2 Ultrasonic-assisted Irrigation Methods: A Novel Experimental Approach. *Journal of Endodontics,* 41 (6)**,** 884-889.

Lee, S.J., Wu, M.K. & Wesselink, P. 2004. The efficacy of ultrasonic irrigation to remove artificially placed dentine debris from different-sized simulated plastic root canals. *International Endodontic Journal,* 37 (9)**,** 607-612.

Lehner, A., Riedel, K., Eberl, L., Breeuwer, P., Diep, B. & Stephan, R. 2005. Biofilm formation, extracellular polysaccharide production, and cell-to-cell signaling in various

Enterobacter sakazakii strains: aspects promoting environmental persistence. *Journal of Food Protection®,* 68 (11)**,** 2287-2294.

Leriche, V., Briandet, R. & Carpentier, B. 2003. Ecology of mixed biofilms subjected daily to a chlorinated alkaline solution: spatial distribution of bacterial species suggests a protective effect of one species to another. *Environmental Microbiology,* 5 (1)**,** 64-71.

Leung, J.W., Liu, Y.L., Desta, T., Libby, E., Inciardi, J.F. & Lam, K. 1998. Is there a synergistic effect between mixed bacterial infection in biofilm formation on biliary stents? *Gastrointestinal Endoscopy,* 48 (3)**,** 250-257.

Levin, B.R. & Rozen, D.E. 2006. Non-inherited antibiotic resistance. *Nature Reviews Microbiology,* 4 (7)**,** 556-562.

Lewis, K. 2006. Persister cells, dormancy and infectious disease. *Nature Reviews Microbiology,* 5 (1)**,** 48-56.

Lewis, K. 2010. Persister cells. *Annual Review of Microbiology,* 64**,** 357-372.

Li, H., Chen, V., Chen, Y., Baumgartner, J.C. & Machida, C.A. 2009. Herpesviruses in endodontic pathoses: association of Epstein-Barr virus with irreversible pulpitis and apical periodontitis. *Journal of Endodontics,* 35 (1)**,** 23-29.

Liang, Y.-H., Jiang, L.-M., Jiang, L., Chen, X.-B., Liu, Y.-Y., Tian, F.-C., Bao, X.-D., Gao, X.-J., Versluis, M. & Wu, M.-K. 2013. Radiographic healing after a root canal treatment performed in single-rooted teeth with and without ultrasonic activation of the irrigant: a randomized controlled trial. *Journal of Endodontics,* 39 (10)**,** 1218-1225.

Liu, Y. & Zhao, Q. 2005. Influence of surface energy of modified surfaces on bacterial adhesion. *Biophysical Chemistry,* 117 (1)**,** 39-45.

Lloyd, G., Friedman, G., Jafri, S., Schultz, G., Fridman, A. & Harding, K. 2010. Gas plasma: medical uses and developments in wound care. *Plasma Processes and Polymers,* 7 (3-4)**,** 194-211.

Loebl, J. 1985. *Image analysis: principles and practice.* 6th ed, New York, Oxford University Press, USA.

Love, R. 2001. Enterococcus faecalis–a mechanism for its role in endodontic failure. *International Endodontic Journal,* 34 (5)**,** 399-405.

Love, R.M. 2010. Biofilm–substrate interaction: from initial adhesion to complex interactions and biofilm maturity. *Endodontic Topics,* 22 (1)**,** 50-57.

Macedo, R., Robinson, J., Verhaagen, B., Walmsley, A., Versluis, M., Cooper, P. & Sluis, L. 2014a. A novel methodology providing insights into removal of biofilm-mimicking hydrogel from lateral morphological features of the root canal during irrigation procedures. *International Endodontic Journal,* 47 (11)**,** 1040–1051.

Macedo, R., Wesselink, P., Zaccheo, F., Fanali, D. & Van Der Sluis, L. 2010. Reaction rate of NaOCl in contact with bovine dentine: effect of activation, exposure time, concentration and pH. *International Endodontic Journal,* 43 (12)**,** 1108-1115.

Macedo, R.G., Herrero, N.P., Wesselink, P., Versluis, M. & Van Der Sluis, L. 2014b. Influence of the Dentinal Wall on the pH of Sodium Hypochlorite during Root Canal Irrigation. *Journal of Endodontics,* 40 (7)**,** 1005–1008.

Macfarlane, S. & Macfarlane, G.T. 2006. Composition and metabolic activities of bacterial biofilms colonizing food residues in the human gut. *Applied and Environmental Microbiology,* 72 (9)**,** 6204-6211.

Malentacca, A., Uccioli, U., Mannocci, F., Bhuva, B., Zangari, D., Pulella, C. & Lajolo, C. 2017. The comparative effectiveness and safety of three activated irrigation techniques in the isthmus area using a transparent tooth model. *International Endodontic Journal*.

Marsh, P. 2005. Dental plaque: biological significance of a biofilm and community life-style. *Journal of Clinical Periodontology,* 32 (s6)**,** 7-15.

Marshall, K., Stout, R. & Mitchell, R. 1971. Mechanism of the initial events in the sorption of marine bacteria to surfaces. *Journal of General Microbiology,* 68 (3)**,** 337-348.

Matsumoto, H., Yoshimine, Y. & Akamine, A. 2011. Visualization of irrigant flow and cavitation induced by Er: YAG laser within a root canal model. *Journal of Endodontics,* 37 (6)**,** 839-843.

Mceldowney, S. & Fletcher, M. 1986. Variability of the influence of physicochemical factors affecting bacterial adhesion to polystyrene substrata. *Applied and Environmental Microbiology,* 52 (3)**,** 460-465.

Mcgill, S., Gulabivala, K., Mordan, N. & Ng, Y.L. 2008. The efficacy of dynamic irrigation using a commercially available system (RinsEndo®) determined by removal of a collagen 'bio-molecular film'from an ex vivo model. *International Endodontic Journal,* 41 (7)**,** 602-608.

Mckee, A.S., Mcdermid, A.S., Ellwood, D. & Marsh, P. 1985. The establishment of reproducible, complex communities of oral bacteria in the chemostat using defined inocula. *Journal of Applied Bacteriology,* 59 (3)**,** 263-275.

Mejare, B. 1974. Streptococcus faecalis and Streptococcus faecium in infected dental root canals at filling and their susceptibility to azidocillin and some comparable antibiotics. *Odontologisk Revy,* 26 (3)**,** 193-204.

Melchels, F.P., Feijen, J. & Grijpma, D.W. 2010. A review on stereolithography and its applications in biomedical engineering. *Biomaterials,* 31 (24)**,** 6121-6130.

Millward, T. & Wilson, M. 1989. The effect of chlorhexidine on Streptococcus sanguis biofilms. *Microbios,* 58 (236-237)**,** 155.

Molander, A., Reit, C., Dahlén, G. & Kvist, T. 1998. Microbiological status of root-filled teeth with apical periodontitis. *International Endodontic Journal,* 31 (1)**,** 1-7.

Möller, A. 1966. Microbiological examination of root canals and periapical tissues of human teeth. Methodological studies. *Odontologisk Tidskrift,* 74 (5)**,** Suppl: 1-380.

Moorer, W. & Wesselink, P. 1982. Factors promoting the tissue dissolving capability of sodium hypochlorite. *International Endodontic Journal,* 15 (4)**,** 187-196.

Mullis, K.B., Ferré, F. & Gibbs, R.A. 1994. *The polymerase chain reaction.* 1st ed, Boston, MA, USA, Birkhauser.

Munson, B.R., Young, D.F. & Okiishi, T.H. 1990. *Fundamentals of fluid mechanics.* 7th ed, UK, John Wiley and Sons

Nair, P. 1987. Light and electron microscopic studies of root canal flora and periapical lesions. *Journal of Endodontics,* 13 (1)**,** 29-39.

Nair, P., Henry, S., Cano, V. & Vera, J. 2005. Microbial status of apical root canal system of human mandibular first molars with primary apical periodontitis after "one-visit" endodontic treatment. *Oral Surgery, Oral Medicine, Oral Pathology, Oral Radiology, and Endodontology,* 99 (2)**,** 231-252.

Neelakantan, P., Devaraj, S. & Jagannathan, N. 2016. Histologic Assessment of Debridement of the Root Canal Isthmus of Mandibular Molars by Irrigant Activation Techniques Ex Vivo. *Journal of Endodontics,* 42 (8)**,** 1268-1272.

Ng, Y.L., Mann, V. & Gulabivala, K. 2011. A prospective study of the factors affecting outcomes of nonsurgical root canal treatment: part 1: periapical health. *International Endodontic Journal,* 44 (7)**,** 583-609.

Niazi, S., Al-Ali, W., Patel, S., Foschi, F. & Mannocci, F. 2015. Synergistic effect of 2% chlorhexidine combined with proteolytic enzymes on biofilm disruption and killing. *International Endodontic Journal,* 48 (12)**,** 1157-1167.

Niazi, S., Clark, D., Do, T., Gilbert, S., Foschi, F., Mannocci, F. & Beighton, D. 2014. The effectiveness of enzymic irrigation in removing a nutrient-stressed endodontic multispecies biofilm. *International Endodontic Journal,* 47 (8)**,** 756–768.

Nichols, W.W., Dorrington, S., Slack, M. & Walmsley, H. 1988. Inhibition of tobramycin diffusion by binding to alginate. *Antimicrobial Agents and Chemotherapy,* 32 (4)**,** 518-523.

Nouioua, F., Slimani, A., Levallois, B., Camps, J., Tassery, H., Cuisinier, F. & Bukiet, F. 2015. A preliminary study of a new endodontic irrigation system: Clean Jet Endo. *Odonto-Stomatologie Tropicale,* 38 (149)**,** 13-22.

Ordinola-Zapata, R., Bramante, C.M., Brandão Garcia, R., Bombarda De Andrade, F., Bernardineli, N., Gomes De Moraes, I. & Duarte, M.A. 2013. The antimicrobial effect of new and conventional endodontic irrigants on intra-orally infected dentin. *Acta Odontologica Scandinavica,* 71 (3-4)**,** 424-431.

Ordinola-Zapata, R., Bramante, C., Cavenago, B., Graeff, M., Gomes De Moraes, I., Marciano, M. & Duarte, M. 2012. Antimicrobial effect of endodontic solutions used as final irrigants on a dentine biofilm model. *International Endodontic Journal,* 45 (2)**,** 162-168.

Otake, K., Inomata, H., Konno, M. & Saito, S. 1989. A new model for the thermally induced volume phase transition of gels. *The Journal of Chemical Physics,* 91 (2)**,** 1345-1350.

Paiva, S.S., Siqueira Jr, J.F., Rôças, I.N., Carmo, F.L., Leite, D.C., Ferreira, D.C., Rachid, C.T. & Rosado, A.S. 2013. Molecular microbiological evaluation of passive

ultrasonic activation as a supplementary disinfecting step: a clinical study. *Journal of Endodontics,* 39 (2)**,** 190-194.

Pan, Y., Breidt, F. & Kathariou, S. 2006. Resistance of Listeria monocytogenes biofilms to sanitizing agents in a simulated food processing environment. *Applied and Environmental Microbiology,* 72 (12)**,** 7711-7717.

Paragliola, R., Franco, V., Fabiani, C., Mazzoni, A., Nato, F., Tay, F.R., Breschi, L. & Grandini, S. 2010. Final rinse optimization: influence of different agitation protocols. *Journal of Endodontics,* 36 (2)**,** 282-285.

Parente, J., Loushine, R., Susin, L., Gu, L., Looney, S., Weller, R., Pashley, D. & Tay, F. 2010. Root canal debridement using manual dynamic agitation or the EndoVac for final irrigation in a closed system and an open system. *International Endodontic Journal,* 43 (11)**,** 1001-1012.

Park, E., Shen, Y., Khakpour, M. & Haapasalo, M. 2013. Apical pressure and extent of irrigant flow beyond the needle tip during positive-pressure irrigation in an in vitro root canal model. *Journal of Endodontics,* 39 (4)**,** 511-515.

Pasqualini, D., Cuffini, A.M., Scotti, N., Mandras, N., Scalas, D., Pera, F. & Berutti, E. 2010. Comparative evaluation of the antimicrobial efficacy of a 5% sodium hypochlorite subsonic-activated solution. *Journal of Endodontics,* 36 (8)**,** 1358-1360.

Paz, L.E.C.D., Sluis, L., Boutsioukis, C., Jiang, L., Macedo, R., Verhaagen, B. & Versluis, M. 2015. *The root canal biofilm.* Verlag Berlin Heidelberg, Springer.

Pecora, J.D., Sousa-Neto, M.D., Guerisolo, D.M.Z. & Marchesan, M.A. 1998. Effect of reduction of the surface tension of different concentrations of sodium hypochlorite solutions on radicular dentine permeability. *Analysis,* 7 (11.15)**,** 1.47.

Peters, L.B., Wesselink, P.R., Buijs, J.F. & Van Winkelhoff, A.J. 2001a. Viable Bacteria in Root Dentinal Tubules of Teeth with Apical Periodontitis. *Journal of Endodontics,* 27 (2)**,** 76-81.

Peters, O.A., Bardsley, S., Fong, J., Pandher, G. & Divito, E. 2011. Disinfection of root canals with photon-initiated photoacoustic streaming. *Journal of Endodontics,* 37 (7)**,** 1008-1012.

Peters, O.A., Laib, A., Göhring, T.N. & Barbakow, F. 2001b. Changes in root canal geometry after preparation assessed by high-resolution computed tomography. *Journal of Endodontics,* 27 (1)**,** 1-6.

Popa, E.G., Gomes, M.E. & Reis, R.L. 2011. Cell delivery systems using alginate–carrageenan hydrogel beads and fibers for regenerative medicine applications. *Biomacromolecules,* 12 (11)**,** 3952-3961.

Precautions, M.S.B. & Flush, A.C. 2008. *Guideline for Disinfection and Sterilization in Healthcare Facilities, 2008* [Online]. Available: http://www.cdc.gov/hicpac/pdf/guidelines/Disinfection-Nov 2008.pdf [Accessed 08.07.2015].

Ragnarsson, K., Rechenberg, D., Attin, T. & Zehnder, M. 2014. Available chlorine consumption from NaOCl solutions passively placed in instrumented human root canals. *International Endodontic Journal,* 48 (5)**,** 435–440.

Ram, Z. 1977. Effectiveness of root canal irrigation. *Oral Surgery, Oral Medicine, Oral Pathology,* 44 (2)**,** 306-312.

Renslow, R.S., Majors, P.D., Mclean, J.S., Fredrickson, J.K., Ahmed, B. & Beyenal, H. 2010. In situ effective diffusion coefficient profiles in live biofilms using pulsed-field gradient nuclear magnetic resonance. *Biotechnology and Bioengineering,* 106 (6)**,** 928-937.

Retamozo, B., Shabahang, S., Johnson, N., Aprecio, R.M. & Torabinejad, M. 2010. Minimum contact time and concentration of sodium hypochlorite required to eliminate Enterococcus faecalis. *Journal of Endodontics,* 36 (3)**,** 520-523.

Rich, H., Odlyha, M., Cheema, U., Mudera, V. & Bozec, L. 2014. Effects of photochemical riboflavin-mediated crosslinks on the physical properties of collagen constructs and fibrils. *Journal of Materials Science: Materials in Medicine,* 25 (1)**,** 11-21.

Richardson, N., Mordan, N.J., Figueiredo, J.A., Ng, Y.L. & Gulabivala, K. 2009. Microflora in teeth associated with apical periodontitis: a methodological observational study comparing two protocols and three microscopy techniques. *International Endodontic Journal,* 42 (10)**,** 908-921.

Ricucci, D. & Siqueira, J.F. 2010. Biofilms and apical periodontitis: study of prevalence and association with clinical and histopathologic findings. *Journal of Endodontics,* 36 (8)**,** 1277-1288.

Ricucci, D., Siqueira, J.F., Bate, A.L. & Ford, T.R.P. 2009. Histologic investigation of root canal–treated teeth with apical periodontitis: a retrospective study from twenty-four patients. *Journal of Endodontics,* 35 (4)**,** 493-502.

Roberts, A.P. & Mullany, P. 2010. Oral biofilms: a reservoir of transferable, bacterial, antimicrobial resistance. *Expert Review of Anti-Infective Therapy,* 8 (12)**,** 1441-1450.

Rôças, I.N., Jung, I.-Y., Lee, C.-Y. & Siqueira Jr, J.F. 2004. Polymerase chain reaction identification of microorganisms in previously root-filled teeth in a South Korean population. *Journal of Endodontics,* 30 (7)**,** 504-508.

Rojekar, S., Mordan, N., Ng, Y., Figueiredo, J. & Gulabivala, K. In situ immunocytochemical colloidal gold probing of three bacterial species in the root canal system of teeth associated with apical periodontitis. BES Spring Scientific Meeting, 2006 London. International Endodontic Journal, 738–741.

Ronaghi, M., Karamohamed, S., Pettersson, B., Uhlén, M. & Nyrén, P. 1996. Real-time DNA sequencing using detection of pyrophosphate release. *Analytical Biochemistry,* 242 (1)**,** 84-89.

Rossi-Fedele, G., De Figueiredo, J.a.P., Steier, L., Canullo, L., Steier, G. & Roberts, A.P. 2010. Evaluation of the antimicrobial effect of super-oxidized water (Sterilox (R)) and sodium hypochlorite against Enterococcus faecalis in a bovine root canal model. *Journal of Applied Oral Science,* 18 (5)**,** 498-502.

Ruddle, C.J. 2007. Hydrodynamic disinfection. *Dentistry Today,* 11 (4)**,** 1-9.

Sabins, R.A., Johnson, J.D. & Hellstein, J.W. 2003. A comparison of the cleaning efficacy of short-term sonic and ultrasonic passive irrigation after hand instrumentation in molar root canals. *Journal of Endodontics,* 29 (10)**,** 674-678.

Sagvolden, G., Giaever, I. & Feder, J. 1998. Characteristic protein adhesion forces on glass and polystyrene substrates by atomic force microscopy. *Langmuir,* 14 (21)**,** 5984-5987.

Sáinz-Pardo, M., Estevez, R., Pablo, Ó.V.D., Rossi-Fedele, G. & Cisneros, R. 2014. Root canal penetration of a sodium hypochlorite mixture using sonic or ultrasonic activation. *Brazilian Dental Journal,* 25 (6)**,** 489-493.

Salzgeber, R.M. & Brilliant, J.D. 1977. An in vivo evaluation of the penetration of an irrigating solution in root canals. *Journal of Endodontics,* 3 (10)**,** 394-398.

Santos, J.M., Palma, P.J., Ramos, J.C., Cabrita, A.S. & Friedman, S. 2014. Periapical Inflammation Subsequent to Coronal Inoculation of Dog Teeth Root Filled with Resilon/Epiphany in 1 or 2 Treatment Sessions with Chlorhexidine Medication. *Journal of Endodontics,* 40 (6)**,** 837-841.

Savvides, M., Pratten, J., Mordan, N., Ng, Y. & Gulabivala, K. 2010. Development of an ex-vivo multi-species biofilm model in teeth for sequential low-magnification evaluation of the effect of root canal treatment procedures. *International Endodontic Journal,* 43 (9)**,** 830-830.

Schuurs, A., Wu, M.K., Wesselink, P. & Duivenvoorden, H. 1993. Endodontic leakage studies reconsidered. Part II. Statistical aspects. *International Endodontic Journal,* 26 (1)**,** 44-52.

Sedgley, C., Lennan, S. & Clewell, D. 2004. Prevalence, phenotype and genotype of oral enterococci. *Oral Microbiology and Immunology,* 19 (2)**,** 95-101.

Sedgley, C., Nagel, A., Hall, D. & Applegate, B. 2005. Influence of irrigant needle depth in removing bioluminescent bacteria inoculated into instrumented root canals using real-time imaging in vitro. *International Endodontic Journal,* 38 (2)**,** 97-104.

Sedlacek, M. & Walker, C. 2007. Antibiotic resistance in an in vitro subgingival biofilm model. *Oral Microbiology and Immunology,* 22 (5)**,** 333-339.

Seltzer, S., Bender, I. & Ziontz, M. 1963. The interrelationship of pulp and periodontal disease. *Oral Surgery, Oral Medicine, Oral Pathology,* 16 (12)**,** 1474-1490.

Şen, B.H., Safavi, K.E. & Spångberg, L.S. 1999. Antifungal effects of sodium hypochlorite and chlorhexidine in root canals. *Journal of Endodontics,* 25 (4)**,** 235-238.

Sena, N., Gomes, B., Vianna, M., Berber, V., Zaia, A., Ferraz, C. & Souza-Filho, F. 2006. In vitro antimicrobial activity of sodium hypochlorite and chlorhexidine against selected single-species biofilms. *International Endodontic Journal,* 39 (11)**,** 878-885.

Shaw, B.R., Creasy, K.E., Lanczycki, C.J., Sargeant, J.A. & Tirhado, M. 1988. Voltammetric Response of Zeolite-Modified Electrodes. *Journal of The Electrochemical Society,* 135 (4)**,** 869-876.

Shen, Y., Gao, Y., Lin, J., Ma, J., Wang, Z. & Haapasalo, M. 2012. Methods and models to study irrigation. *Endodontic Topics,* 27 (1)**,** 3-34.

Shen, Y., Gao, Y., Qian, W., Ruse, N.D., Zhou, X., Wu, H. & Haapasalo, M. 2010a. Three-dimensional numeric simulation of root canal irrigant flow with different irrigation needles. *Journal of Endodontics,* 36 (5)**,** 884-889.

Shen, Y., Stojicic, S., Qian, W., Olsen, I. & Haapasalo, M. 2010b. The synergistic antimicrobial effect by mechanical agitation and two chlorhexidine preparations on biofilm bacteria. *Journal of Endodontics,* 36 (1)**,** 100-104.

Silva, L.a.B.D., Leonardo, M.R., Assed, S. & Tanomaru Filho, M. 2004. Histological study of the effect of some irrigating solutions on bacterial endotoxin in dogs. *Brazilian Dental Journal,* 15 (2)**,** 109-114.

Simoes, M., Simões, L.C. & Vieira, M.J. 2009. Species association increases biofilm resistance to chemical and mechanical treatments. *Water Res,* 43 (1)**,** 229-237.

Siqueira, J., Machado, A., Silveira, R., Lopes, H. & Uzeda, M.D. 1997. Evaluation of the effectiveness of sodium hypochlorite used with three irrigation methods in the elimination of Enterococcus faecalis from the root canal, in vitro. *International Endodontic Journal,* 30 (4)**,** 279-282.

Siqueira, J. & Rôças, I. 2005. Exploiting molecular methods to explore endodontic infections: part 1—current molecular technologies for microbiological diagnosis. *Journal of Endodontics,* 31 (6)**,** 411-423.

Siqueira, J.F. & Rôças, I.N. 2008. Clinical implications and microbiology of bacterial persistence after treatment procedures. *Journal of Endodontics,* 34 (11)**,** 1291-1301. e1293.

Siqueira, J.F., Rôças, I.N., Favieri, A. & Lima, K.C. 2000. Chemomechanical reduction of the bacterial population in the root canal after instrumentation and irrigation with 1%, 2.5%, and 5.25% sodium hypochlorite. *Journal of Endodontics,* 26 (6)**,** 331-334.

Siqueira, J.F., Rôças, I.N. & Lopes, H.P. 2002. Patterns of microbial colonization in primary root canal infections. *Oral Surgery, Oral Medicine, Oral Pathology, Oral Radiology, and Endodontology,* 93 (2)**,** 174-178.

Siqueira Jr, J.F., Alves, F.R. & Rôças, I.N. 2011. Pyrosequencing analysis of the apical root canal microbiota. *Journal of Endodontics,* 37 (11)**,** 1499-1503.

Siqueira Jr, J.F., Antunes, H.S., Rôças, I.N., Rachid, C.T. & Alves, F.R. 2016. Microbiome in the Apical Root Canal System of Teeth with Post-Treatment Apical Periodontitis. *PLoS One,* 11 (9)**,** e0162887.

Sirtes, G., Waltimo, T., Schaetzle, M. & Zehnder, M. 2005. The effects of temperature on sodium hypochlorite short-term stability, pulp dissolution capacity, and antimicrobial efficacy. *Journal of Endodontics,* 31 (9)**,** 669-671.

Sjögren, U., Figdor, D., Persson, S. & Sundqvist, G. 1997. Influence of infection at the time of root filling on the outcome of endodontic treatment of teeth with apical periodontitis. *International Endodontic Journal,* 30 (5)**,** 297-306.

Sousa, C., Teixeira, P. & Oliveira, R. 2009. Influence of surface properties on the adhesion of Staphylococcus epidermidis to acrylic and silicone. *International journal of biomaterials,* 2009.

Spanó, J.C.E., Barbin, E.L., Santos, T.C., Guimarães, L.F. & Pécora, J.D. 2001. Solvent action of sodium hypochlorite on bovine pulp and physico-chemical properties of resulting liquid. *Brazilian Dental Journal,* 12 (3)**,** 154-157.

Spratt, D., Pratten, J., Wilson, M. & Gulabivala, K. 2001. An in vitro evaluation of the antimicrobial efficacy of irrigants on biofilms of root canal isolates. *International Endodontic Journal,* 34 (4)**,** 300-307.

Stashenko, P., Teles, R. & D'souza, R. 1998. Periapical inflammatory responses and their modulation. *Critical Reviews in Oral Biology and Medicine,* 9 (4)**,** 498-521.

Stewart, G.G. 1955. The importance of chemomechanical preparation of the root canal. *Oral Surgery, Oral Medicine, Oral Pathology,* 8 (9)**,** 993-997.

Stewart, P.S. & Costerton, J.W. 2001. Antibiotic resistance of bacteria in biofilms. *The lancet,* 358 (9276)**,** 135-138.

Stewart, P.S. & Franklin, M.J. 2008. Physiological heterogeneity in biofilms. *Nature Reviews Microbiology,* 6 (3)**,** 199-210.

Stojanović, N., Krunić, J., Popović, B., Stojičić, S. & Živković, S. 2014. Prevalence of Enterococcus faecalis and Porphyromonas gingivalis in infected root canals and their susceptibility to endodontic treatment procedures: A molecular study. *Srpski Arhiv za Celokupno Lekarstvo,* 142 (9-10)**,** 535-541.

Stojicic, S., Shen, Y. & Haapasalo, M. 2013. Effect of the source of biofilm bacteria, level of biofilm maturation, and type of disinfecting agent on the susceptibility of biofilm bacteria to antibacterial agents. *Journal of Endodontics,* 39 (4)**,** 473-477.

Stojicic, S., Shen, Y., Qian, W., Johnson, B. & Haapasalo, M. 2012. Antibacterial and smear layer removal ability of a novel irrigant, QMiX. *International Endodontic Journal,* 45 (4)**,** 363-371.

Stoodley, P., Cargo, R., Rupp, C., Wilson, S. & Klapper, I. 2002. Biofilm material properties as related to shear-induced deformation and detachment phenomena. *Journal of Industrial Microbiology and Biotechnology,* 29 (6)**,** 361-367.

Stuart, C.H., Schwartz, S.A., Beeson, T.J. & Owatz, C.B. 2006. Enterococcus faecalis: its role in root canal treatment failure and current concepts in retreatment. *Journal of Endodontics,* 32 (2)**,** 93-98.

Sundqvist, G. 1976. *Bacteriological studies of necrotic dental pulps.* 7 ed, Department of Oral Microbiology, University of Umeå.

Sundqvist, G. 1992. Associations between microbial species in dental root canal infections. *Oral Microbiology and Immunology,* 7 (5)**,** 257-262.

Sundqvist, G. 1994. Taxonomy, ecology, and pathogenicity of the root canal flora. *Oral Surgery, Oral Medicine, Oral Pathology,* 78 (4)**,** 522-530.

Suwarno, S., Hanada, S., Chong, T., Goto, S., Henmi, M. & Fane, A. 2016. The effect of different surface conditioning layers on bacterial adhesion on reverse osmosis membranes. *Desalination,* 387**,** 1-13.

Tanomaru, J., Leonardo, M., Tanomaru Filho, M., Bonetti Filho, I. & Silva, L. 2003. Effect of different irrigation solutions and calcium hydroxide on bacterial LPS. *International Endodontic Journal,* 36 (11)**,** 733-739.

Tawakoli, P., Ragnarsson, K., Rechenberg, D., Mohn, D. & Zehnder, M. 2017. Effect of endodontic irrigants on biofilm matrix polysaccharides. *International Endodontic Journal,* 50 (2)**,** 153-160.

Tay, F.R., Gu, L.-S., Schoeffel, G.J., Wimmer, C., Susin, L., Zhang, K., Arun, S.N., Kim, J., Looney, S.W. & Pashley, D.H. 2010. Effect of vapor lock on root canal debridement by using a side-vented needle for positive-pressure irrigant delivery. *Journal of Endodontics,* 36 (4)**,** 745-750.

Teixeira, P. & Oliveira, R. 1999. Influence of surface characteristics on the adhesion of Alcaligenes denitrificans to polymeric substrates. *Journal of Adhesion Science and Technology,* 13 (11)**,** 1287-1294.

Ter Steeg, P. & Van Der Hoeven, J. 1990. Growth stimulation of Treponema denticola by periodontal microorganisms. *Antonie van Leeuwenhoek,* 57 (2)**,** 63-70.

Thilo, B.E., Baehni, P. & Holz, J. 1986. Dark-field observation of the bacterial distribution in root canals following pulp necrosis. *Journal of Endodontics,* 12 (5)**,** 202-205.

Tilton, J.N. 2008. *Fluid and particle dynamics.* 8th edn ed, New York, McGraw-Hill.

Tomaras, A.P., Dorsey, C.W., Edelmann, R.E. & Actis, L.A. 2003. Attachment to and biofilm formation on abiotic surfaces by Acinetobacter baumannii: involvement of a novel chaperone-usher pili assembly system. *Microbiology,* 149 (12)**,** 3473-3484.

Torabinejad, M. & Walton, R.E. 2009. *Endodontics: principles and practice.* 4 ed, St. Louis, Missouri, USA, Saunders, Elsevier.

Townsend, C. & Maki, J. 2009. An In Vitro Comparison of New Irrigation and Agitation Techniques to Ultrasonic Agitation in Removing Bacteria From a Simulated Root Canal. *Journal of Endodontics,* 35 (7)**,** 1040-1043.

Tran, N., Kelley, M.N., Tran, P.A., Garcia, D.R., Jarrell, J.D., Hayda, R.A. & Born, C.T. 2015. Silver doped titanium oxide–PDMS hybrid coating inhibits Staphylococcus aureus and Staphylococcus epidermidis growth on PEEK. *Materials Science and Engineering: C,* 49**,** 201-209.

Tronstad, L., Barnett, F., Schwartzben, L. & Frasca, P. 1985. Effectiveness and safety of a sonic vibratory endodontic instrument. *Dental Traumatology,* 1 (2)**,** 69-76.

Trope, M., Delano, E.O. & Ørstavik, D. 1999. Endodontic treatment of teeth with apical periodontitis: single vs. multivisit treatment. *Journal of Endodontics,* 25 (5)**,** 345-350.

Van Der Sluis, L., Wu, M.K. & Wesselink, P. 2005. The efficacy of ultrasonic irrigation to remove artificially placed dentine debris from human root canals prepared using instruments of varying taper. *International Endodontic Journal,* 38 (10)**,** 764-768.

Van Der Sluis, L.W., Vogels, M.P., Verhaagen, B., Macedo, R. & Wesselink, P.R. 2010. Study on the influence of refreshment/activation cycles and irrigants on mechanical cleaning efficiency during ultrasonic activation of the irrigant. *Journal of Endodontics,* 36 (4)**,** 737-740.

Van Oss, C. 1995. Hydrophobicity of biosurfaces—origin, quantitative determination and interaction energies. *Colloids and Surfaces B: Biointerfaces,* 5 (3)**,** 91-110.

Vera, J., Siqueira Jr, J.F., Ricucci, D., Loghin, S., Fernández, N., Flores, B. & Cruz, A.G. 2012. One- versus Two-visit Endodontic Treatment of Teeth with Apical Periodontitis: A Histobacteriologic Study. *Journal of Endodontics,* 38 (8)**,** 1040-1052.

Verhaagen, B., Boutsioukis, C., Heijnen, G., Van Der Sluis, L. & Versluis, M. 2012. Role of the confinement of a root canal on jet impingement during endodontic irrigation. *Experiments in fluids,* 53 (6)**,** 1841-1853.

Verhaagen, B., Boutsioukis, C., Sleutel, C., Kastrinakis, E., Van Der Sluis, L. & Versluis, M. 2014a. Irrigant transport into dental microchannels. *Microfluidics and nanofluidics,* 16 (6)**,** 1165-1177.

Verhaagen, B., Boutsioukis, C., Van Der Sluis, L. & Versluis, M. 2014b. Acoustic streaming induced by an ultrasonically oscillating endodontic file. *J Acoust Soc Am,* 135 (4)**,** 1717-1730.

Versiani, M.A., De-Deus, G., Vera, J., Souza, E., Steier, L., Pécora, J.D. & Sousa-Neto, M.D. 2015. 3D mapping of the irrigated areas of the root canal space using micro-computed tomography. *Clinical Oral Investigations,* 19 (4)**,** 859-866.

Versteeg, H.K. & Malalasekera, W. 2007. *An introduction to computational fluid dynamics: the finite volume method.* 2nd ed, Harlow, UK, Pearson Education.

Verwey, E.J.W., Overbeek, J.T.G. & Overbeek, J.T.G. 1999. *Theory of the stability of lyophobic colloids.* Courier Corporation.

Vianna, M.E., Gomes, B.P., Berber, V.B., Zaia, A.A., Ferraz, C.C.R. & De Souza-Filho, F.J. 2004. In vitro evaluation of the antimicrobial activity of chlorhexidine and sodium hypochlorite. *Oral Surgery, Oral Medicine, Oral Pathology, Oral Radiology, and Endodontology,* 97 (1)**,** 79-84.

Vianna, M.E., Horz, H.P., Gomes, B.P.F.A. & Conrads, G. 2006. In vivo evaluation of microbial reduction after chemo-mechanical preparation of human root canals containing necrotic pulp tissue. *International Endodontic Journal,* 39 (6)**,** 484-492.

Walters, M.J., Baumgartner, J.C. & Marshall, J.G. 2002. Efficacy of irrigation with rotary instrumentation. *Journal of Endodontics,* 28 (12)**,** 837-839.

Waltimo, T., Siren, E., Torkko, H., Olsen, I. & Haapasalo, M. 1997. Fungi in therapy-resistant apical periodontitis. *International Endodontic Journal,* 30 (2)**,** 96-101.

Wang, X., Huang, J. & Huang, K. 2010. Surface chemical modification on hyper-cross-linked resin by hydrophilic carbonyl and hydroxyl groups to be employed as a polymeric adsorbent for adsorption of p-aminobenzoic acid from aqueous solution. *Chemical Engineering Journal,* 162 (1)**,** 158-163.

Wang, Y., Da Silva Domingues, J.F., Subbiahdoss, G., Van Der Mei, H.C., Busscher, H.J. & Libera, M. 2014. Conditions of lateral surface confinement that promote tissue-cell integration and inhibit biofilm growth. *Biomaterials,* 35 (21)**,** 5446-5452.

Wang, Z., Shen, Y. & Haapasalo, M. 2012. Effectiveness of endodontic disinfecting solutions against young and old Enterococcus faecalis biofilms in dentin canals. *Journal of Endodontics,* 38 (10)**,** 1376-1379.

Weller, R.N., Brady, J.M. & Bernier, W.E. 1980. Efficacy of ultrasonic cleaning. *Journal of Endodontics,* 6 (9)**,** 740-743.

Whiteley, M., Ott, J.R., Weaver, E.A. & Mclean, R.J. 2001. Effects of community composition and growth rate on aquifer biofilm bacteria and their susceptibility to betadine disinfection. *Environmental Microbiology,* 3 (1)**,** 43-52.

Williams, B.L., Mccann, G.F. & Schoenknecht, F. 1983. Bacteriology of dental abscesses of endodontic origin. *Journal of Clinical Microbiology,* 18 (4)**,** 770-774.

Williamson, A.E., Cardon, J.W. & Drake, D.R. 2009. Antimicrobial Susceptibility of Monoculture Biofilms of a Clinical Isolate of Enterococcus faecalis. *Journal of Endodontics,* 35 (1)**,** 95-97.

Wilson, M. 1996. Susceptibility of oral bacterial biofilms to antimicrobial agents. *Journal of Medical Microbiology,* 44 (2)**,** 79-87.

Wilson, S.M. & Bacic, A. 2012. Preparation of plant cells for transmission electron microscopy to optimize immunogold labeling of carbohydrate and protein epitopes. *Nat. Protocols,* 7 (9)**,** 1716-1727.

Wu, D., Fan, W., Kishen, A., Gutmann, J.L. & Fan, B. 2014. Evaluation of the Antibacterial Efficacy of Silver Nanoparticles against Enterococcus faecalis Biofilm. *Journal of Endodontics,* 40 (2)**,** 285-290.

Yang, Y., Shen, Y., Wang, Z., Huang, X., Maezono, H., Ma, J., Cao, Y. & Haapasalo, M. 2016. Evaluation of the Susceptibility of Multispecies Biofilms in Dentinal Tubules to Disinfecting Solutions. *Journal of Endodontics,* 42 (8)**,** 1246-1250.

Zandi, H., Rodrigues, R.C., Kristoffersen, A.K., Enersen, M., Mdala, I., Ørstavik, D., Rôças, I.N. & Siqueira, J.F. 2016. Antibacterial Effectiveness of 2 Root Canal Irrigants in Root-filled Teeth with Infection: A Randomized Clinical Trial. *Journal of Endodontics,* 42 (9)**,** 1307-1313.

Zavistoski, J., Dzink, J., Onderdonk, A. & Bartlett, J. 1980. Quantitative bacteriology of endodontic infections. *Oral Surgery, Oral Medicine, Oral Pathology,* 49 (2)**,** 171-174.

Zhang, F., Zhang, Z., Zhu, X., Kang, E.-T. & Neoh, K.-G. 2008. Silk-functionalized titanium surfaces for enhancing osteoblast functions and reducing bacterial adhesion. *Biomaterials,* 29 (36)**,** 4751-4759.

11.1. Appendix 1

University College London Hospitals NHS
NHS Foundation Trust

UCL Eastman Biobank for Studying Health and Disease

1/12/15

Dr. *Saifalarab Mohmmed*
UCL Eastman

Project Title: *Verification of substrates used to create in vitro root canal biofilm model to investigate biofilm removal by irrigation solutions*

Reference number: 1310

Dear Investigator
I am writing to inform you that your application to the UCL Eastman Biobank as detailed above was approved by the Committee on 1/12/15.

All researchers must complete and comply with the regulatory and governance requirements and information requested on the Biobank application form. Further information is available on the UCL Eastman biobank website, or on the UCL-CI WICI (http://www.ucl.ac.uk/biobank/regulatory)

Please keep this copy of the ethics approval letter for the Biobank for your records. The current duration of the ethical approval is until 3rd April 2017 in line with the duration of the Research Tissue Bank approval. This approval may be renewed for a further period in the future. We will be asking you to complete an annual return giving information on the number of patients consented and samples taken. We may at any time request to audit your project to ensure compliance with the necessary regulatory and governance requirements.

Thank you for your application to the Biobank and if you have any questions, please do not hesitate to contact Paul Ashley (p.ashley@ucl.ac.uk).

Yours Sincerely

Paul Ashley

Chair, UCL Eastman Biobank

11.2. Appendix 2

11.2.1. Identity of the strains used in the study

The identification of the strains was confirmed by performing polymerase chain reaction (PCR) to amplify copies of a segment of each species DNA, followed by nucleic acid electrophoresis, which shows bands corresponding to the nucleotides, and analysis of the 16S rRNA gene sequencing.

11.2.2. DNA extraction

The four strains used in the study were stored separately Eppendorf tubes containing broth and 30% glycerol at -70 °C. The frozen strains were left on ice to thaw, for 30 minutes, then vortexed for 1 minute. The procedure of DNA extraction was performed using the QIAamp DNA Mini Kit (QIAGEN Inc., Alameda, CA, USA) according to manufacturer's instructions. The procedure is as follows:

1. A total of 200 µL of each strain were transferred into sterile microfuge tubes (1.5 mL).

2. The tubes were then centrifuged at 6.000 x g (8.000 rpm) for 5 minutes to pellet the cells.

3. The supernatant was removed, and the pellet was suspended in 180 µL of ATL (tissue lysis buffer).

4. 20 µL of Proteinase K were added to improve the cell lysis, and the tubes were vortexed at maximum speed for 1 minute, followed by incubation at 56°C for approximately 30 minutes.

5. 200 µL of Buffer AL were added and the tubes were vortexed for 1 minute, followed by incubation at 70°C for approximately 10 minutes.

6. The tubes were then vortexed at maximum speed for 1 minute and 200 µL of ethanol were added to the solution followed by vortexing for 1 minute.

7. The mixture was then was centrifuged at 8.000 rpm for 1 minute. Following this, the filtrate was discarded.

8. 500 µL of Buffer AW1 were added to the mixture, and another cycle of centrifugation was performed at 8.000 rpm for 1 minute. At the end of this step, the filtrate was again discarded.

9. The spin column was carefully opened and 500 µL of Buffer AW2 were added. The mixture was centrifuged at 13.000 rpm for 3 minutes. At the end of this step, the filtrate was again discarded.

10. Finally, the QIAamp Spin Column was transferred to a sterile (1.5 mL) Eppendorf tube. The cap was opened and 100 µL of Buffer AE were added and left to incubate at room temperature for 3 minutes to increase DNA yield. The purified DNA was eluted with a final centrifugation step for 1 minute at 8.000 rpm.

11. The purity of DNA extracts was assessed using a UV spectrophotometer (NanoDrop™ Spectrophotometer ND-100, Wilmington, USA) at 260/280 nm (Appendix VIII) and the DNA samples were frozen at -20°C until qPCR quantification.

11.2.3. Protocol of polymerase chain reaction (PCR) technique

The PCR amplification includes thermal cycling of the PCR component (50 µL), consisting of 2 µL of genomic DNA of each species, 25 µL PCR Bio Mix red containing an ultra-stable *Taq* DNA (Bioline, Luckenwalde, Germany), 2 µL of 27 forward universal primer (5‟-AGAGTTTGATCMTGGCTCAG–3‟), 2 µL of 1392 reverse universal primers (5‟–ACGGGCGGTGTGTRC–3‟), and 19 µL of PCR grade water.

The PCR reaction was performed using Biometra thermocycler T 3000 (Biometra, Göttingen, Germany) as the following: I cycle of 4 minutes at 95°C for denaturation, followed by 30 cycles of denaturation at 94°C for 30s, annealing for 90s and extension at 72°C for 60s. Finally, 5 minutes at 72°C for extension step.

11.2.4. Protocol of gel electrophoresis of nucleic acids

The DNA fragments of the PCR product of each species were distinguished by size as they were placed in a gel slab, and an electric field was applied inducing the nucleic acids to migrate toward the anode depending on the fragment size, because the nucleic acid contains a negative charge phosphate backbone.

The gel slab consisted of agarose gel and prepared by mixing 0.3 g of agarose powder (Amresco, Solon, Ohio, USA) with 30 mL of TAE buffer (Promega Corporation, Madison, South Dakota, USA) in a flask. The mixture was heated up in a microwave at 750 Watts for approximately 80 seconds until the gel turned clear, which indicates dissolving of the agarose powder. Then, the gel was cooled down using running water. Following that, 2 µL of GelRed™ Nucleic Acid Gel Stain (Biotium Inc, Hayward, California, USA) were added into the gel and directly poured into the electrophoresis apparatus (Biometra, Göttingen, Germany) with the comb in its position. The gel was left approximately 30 minutes for solidification. Once solidified, the comb was removed, and the agarose gel was placed in the electrophoresis tank with wells nearer to the black cathode. The tank was then filled with TAE buffer. The samples of the electrophoresis were prepared by mixing separately 8 µL PCR product of each species with 2 µL DNA loading buffer (Bioline, Luckenwalde, Germany) using a pipette. Then 10 µL of the DNA Ladder (Promega Corporation, Madison, USA) (1000 bp) were placed in the first well of the gel, positive control (10 µL), electrophoresis samples (10

µL), and negative controls (10 µL) were then loaded separately into the other wells. Electrophoresis was performed for approximately 20 minutes at 90 V. The bands were visualised using a UV transilluminator (Alphalmager, Alpha Innotech Corporation, San Leandro, CA, USA) connected to a computer, and the images for the DNA bands of the four species were captured (Figure 11.1).

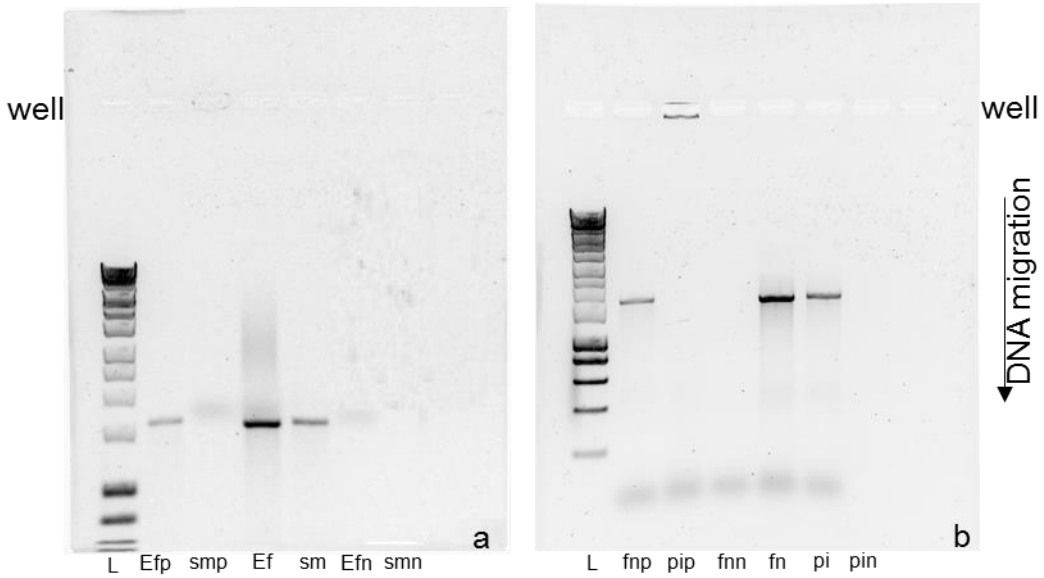

Figure 11.1: Images of DNA band of the 4 species used in the study on agarose gel stained with red gel stain. a) Bands of DNA ladder (L), *E. faecalis* positive control (efp), S*. mutans* positive control (smp), *E. faecalis* sample (ef), *S. mutans* sample (sm), *E. faecalis* negative control (efn), and S*. mutans* negative control (smn). b) Bands of DNA ladder (L), *fu. nucleatum* positive control (fnp), *P. intermedia* positive control (pip), *F.. nucleatum* sample (fn), P. *intermedia* sample (pi), *F.. nucleatum* negative control (fnn), and *P. intermedia* negative control (pin).

11.2.5. Protocol of DNA Sequencing

The purification process of the PCR product (10 µL) was performed using QlAquick PCR purification kit (QIAGEN, Hilden, Germany) to extract the DNA isolate. The extracted DNA (20 µL) were analysed by the DNA Sequencing facility of Beckman Coulter Genomics (www.BeckmanGenomics.com). After that, the sequences were compared with the online sequence database of the National Centre for Biotechnology Information (NCBI BLAST) of the PubMed website

(www.ncbi.nlm.nih.gov/pubmed). The results of each species sequencing are presented below:

11.2.5.1. Sequencing of *E. faecalis:*

AGCGGCNGCTCAANGGTTACCTCACCGACTTCGGGTGTTACAAACTCTCGTGGTGTGACG
GGCGGTGTGACAAGGCCCGGGAACGTATTCACCGCGGCGTGCTGATCCGCGATTACTAG
CGATTCCGGCTTCATGCAGGCGAGTTGCAGCCTGCAATCCGAACTGAGAGAAGCTTTAAG
AGATTTGCATGACCTCGCGGTCTAGCGACTCGTTGTACTTCCCATTGTAGCACGTGTGTAG
CCCAGGTCATAAGGGGCATGATGATTTGACGTCATCCCCACCTTCCTCCGGTTTGTCACCG
GCAGTCTCGCTAGAGTGCCCAACTAAATGATGGCAACTAACAATAAGGGTTGCGCTCGTTG
CGGGACTTAACCCAACATCTCACGACACGAGCTGACGACAACCATGCACCACCTGTCACTT
TGTCCCCGAAGGGAAAGCTCTATCTCTAGAGTGGTCAAAGGATGTCAAGACCTGGTAAGG
TTCTTCGCGTTGCTTCGAATTAAACCACATGCTCCACCGCTTGTGCGGGCCCCCGTCAATT
CCTTTGAGTTTCAACCTTGCGGTCGTACTCCCCAGGCGGAGTGCTTAATGCGTTTGCTGCA
GCACTGAAGGGCGGAAACCCTCCAACACTTAGCACTCATCGTTTACGGCGTGGACTACCA
GGGTATCTAATCCTGTTTGCTCCCCACGCTTTCGAGCCTCAGCGTCAGTTACAGACCAGAG
AGCCGCCTTCGCCACTGGTGTTCCTCCATATATCTACGCATTTCACCGCTACACATGGAAT
TCCACTCTCCTCTTCTGCACTCAAGTCTCCCAGTTTCCAATGACCCTCCCCGGTTGAGCCG
GGGGCTTTCACATCAGACTTAAGAAACCGCCTGCGCTCGCTTTACGCCCAATAAATCCGGA
CAACGCTTGCCACCTACGTATTACCGCGGCTGCTGGCACGTANTTAGCCGTGGCTTTCTG
GTTAGATACCGTCAGGGGACGTTCAGTTACTAACGTCCTTGTTCTTCTCTAACAACAGAGTT
TTACGATCCGAAAACCTTCTTCACTCACGCGGCGTTGCTCGGTCAGACTTTCGTCCATTGC
CGAANAATCCCTACTGCTGCCTCCCGTAGGAGTCTGGGCCGTGTCTCAGTCCCAGTNNGG
CCGATCACCCTCTCAGGTCGGCTATGCATCGGGNCCTTGGTGAACCGTTACCTNACAACT
AGCTAATGGCNNNNGGGGTCCTCCTTCANNGAANCCNGAANGGCCTTT

Sequences producing significant alignments:

Description	Max score	Total score	Query cover	E value	Ident	Accession
Enterococcus faecalis ATCC 19433. whole genome shotgun sequence	2180	8720	89%	0.0	99%	NC_004668.1

11.2.5.2. Sequencing of *S. mutans*:

AAGGTACCTCACCGACTTCGGGTGTTACAAACTCTCGTGGTGTGACGGGCGGTGTGTACA
AGGCCCGGGAACGTATTCACCGCGGCGTGCTGATCCGCGATTACTAGCGATTCCGACTTC
ATGGAGGCGAGTTGCAGCCTCCAATCCGAACTGAGATCGGCTTTCAGAGATTAGCTTGCC
GTCACCGGCTCGCAACTCGTTGTACCGACCATTGTAGCACGTGTGTAGCCCAGGTCATAA
GGGGCATGATGATTTGACGTCATCCCCACCTTCCTCCGGTTTATTACCGGCAGTCTCGCTA
GAGTGCCCAACTTAATGATGGCAACTAACAATAAGGGTTGCGCTCGTTGCGGGACTTAACC
CAACATCTCACGACACGAGCTGACGACAACCATGCACCACCTGTCTCCGATGTACCGAAG
TAACTTCCTATCTCTAAGAATAGCATCGGGATGTCAAGACCTGGTAAGGTTCTTCGCGTTG
CTTCGAATTAAACCACATGCTCCACCGCTTGTGCGGGCCCCCGTCAATTCCTTTGAGTTTC
AACCTTGCGGTCGTACTCCCCAGGCGGAGTGCTTATTGCGTTAGCTCCGGCACTAAGCCC
CGGAAAGGGCCTAACACCTAGCACTCATCGTTTACGGCGTGGACTACCAGGGTATCTAAT
CCTGTTCGCTACCCACGCTTTCGAGCCTCAGCGTCAGTGACAGACCAGAGAGCCGCTTTC
GCCACTGGTGTTCCTCCATATATCTACGCATTTCACCGCTACACATGGAATTCCACTCTCCC
CTTCTGCACTCAAGTCAGACAGTTTCCAGAGCACACTATGGTTGAGCCATAGCCTTTTACT
CCAGACTTTCCTGACCGCCTGCGCTCCCTTTACGCCCAATAAATCCGGACAACGCTCGGG
ACCTACGTATTACCGCGGCTGCTGGCACGTAGTTAGCCGTCCCTTTCTGGTAAGCTACCGT
CACTGTGTGAACTTTCCACTCTCACACACGTTCTTGACTTACAACAGAGCTTTACGATCCGA
AAACCTTCTTCACTCACGCGGCGTTGCTCGGTCAGACTTTCGTCCATTGCCGAAGATNCCC
TACTGCTGCCTCCCGTAGGAATCTGGGCCGGNTCTCAGTCCCAGTGGGNCCGATCACCTT
CTCAGGTCGGCTATGTATCGTCCCNTTGGTAAGCTCTTACCTTACAACT

Sequences producing significant alignments:

Description	Max score	Total score	Query cover	E value	Ident	Accession
Streptococcus mutans ATCC 700610, whole genome shotgun sequence	40.1	226	100%	0.033	100%	NC_004350.2

11.2.5.3. Sequencing of *F. nucleatum*

TTATGAAAGCTATATGCGCTGTGAGAGAGCTTTGCGTCCCATTAGCTAGTTGGAG
AGGTAACGGCTCACCAAGGCGATGATGGGTAGCCGGCCTGAGAGGGTGATCGG
CCACAAGGGGACTGAGACACGGCCCTTACTCCTACGGGAGGCAGCAGTGGGGAA
TATTGGACAATGGACCAAGAGTCTGATCCAGCAATTCTGTGTGCACGATGAAGTTT
TTCGGAATGTAAAGTGCTTTCAGTTGGGAAGAAAAAAATGACGGTACCAACAGAA
GAAGTGACGGCTAAATACGTGCCAGCAGCCGCGGTAATACGTATGTCACAAGCGT
TATCCGGATTTATTGGGCGTAAAGCGCGTCTAGGTGGTTATATAAGTCTGATGTGA
AAATGCAGGGCTCAACTCTGTATTGCGTTGGAAACTGTGTAACTAGAGTACTGGA
GAGGTAAGCGGAACTACAAGTGTAGAGGTGAAATTCGTAGATATTTGTAGGAATG
CCGATGGGGAAGCCAGCTTACTGGACAGATACTGACGCTGAAGCGCGAAAGCGT
GGGTAGCAAACAGGATTAGATACCCTGGTAGTCCACGCCGTAAACGATGATTACT
AGGTGTTGGGGGTCGAACCTCAGCGCCCAAGCAAACGCGATAAGTAATCCGCCT
GGGGAGTACGTACGCAAGTATGAAACTCATAGGAATTGACGGGGACCCGCACAA
GCGGTGGAGCATGTGGTTTAATTCGACGCAACGCGAGGAACCTTACCAGCGTTTG
ACATCTTAGGAATGAGACAGAGATGTTTCAGCGTCCCTTCGGGGAAACCTAAAGA
CAGGTGGTGCATGGCTGTCGTCAGCTCGTGTCGTGAGATGTTGGGTTAAGTCCC
GCAACGA

Sequences producing significant alignments:

Description	Max score	Total score	Query cover	E value	Ident	Accession
Fusobacterium nucleatum subsp. nucleatum ATCC 25586 chromosome, complete genome	1591	7944	100%	0.0	99%	NC_003454.1

11.2.5.4. Sequencing of *P. intermedia*

TGCAGTCGAGGGGAACGGCATTATGTGCTTGCACATTCTGGACGTCGACCGGCG
CACGGGTGAGTATCGCGTATCCAACCTTCCCTCCACTCGGGGATACCCCGTTGAA
AGACGGCCTAATACCCGATGTTGTCCACATATGGCATCTGACGTGGACCAAAGAT
TCATCGGTGGAGGATGGGGATGCGTCTGATTAGCTTGTTGGTGCGGGTAACGGC
CCACCAAGGCTACGATCAGTAGGGGTTCTGAGAGGAAGGTCCCCCACATTGGAA
CTGAGACACGGTCCAAACTCCTACGGGAGGCAGCAGTGAGGAATATTGGTCAAT
GGACGTAAGTCTGAACCAGCCAAGTAGCGTGCAGGATTGACGGCCCTATGGGTT
GTAAACTGCTTTTGTTGGGGAGTAAAGCGGGGCACGTGTGCCCCTTTGCATTTAC
CCTTCGAATAAGGACCGGCTAATTCCGTGCCAGCAGCCGCGGTAATACGGAAGG
TCCAGGCGTTATCCGGATTTATTGGGTTTAAAGGGAGTGTAGGCGGTCTGTTAAG
CGTGTTGTGAAATTTAGGTGCTCAACATCTACCTTGCAGCGCGAACTGGCGGACT
TGAGTGCACGCAACGTATGCGGAATTCATGGTGTAGCGGTGAAATGCTTAGATAT
CATGACGAACTCCGATTGCGAAGGCAGCGTACGGGAGTGTTACTGACGCTTAGCT
CCAAGTGCGGGTATCGAAAGGATTAGATACTTGGTAGTCCGCAGGTAAACGATGG
ATGCCCGCTGTTAGCGCAGGCGTAGCGGCTACCGANGCATTAGCATC

Sequences producing significant alignments:

Description	Max score	Total score	Query cover	E value	Ident	Accession
Prevotella intermedia DSM 20706, whole genome shotgun sequence	36.2	36.2	100%	0.52	100%	NC_017860.1

11.3. Appendix 3

11.3.1. The distributions of zeta potential of the test materials

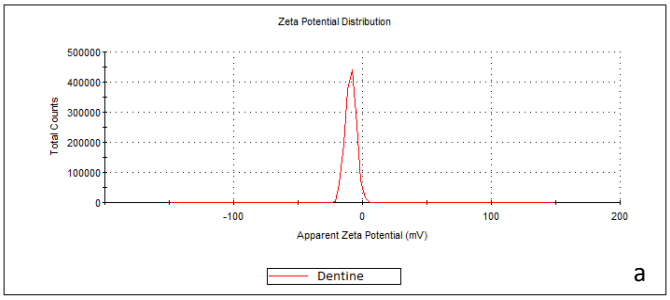

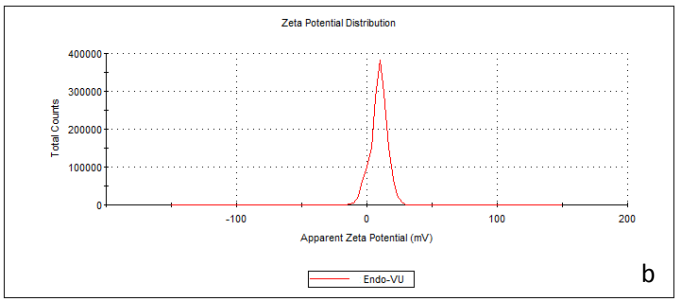

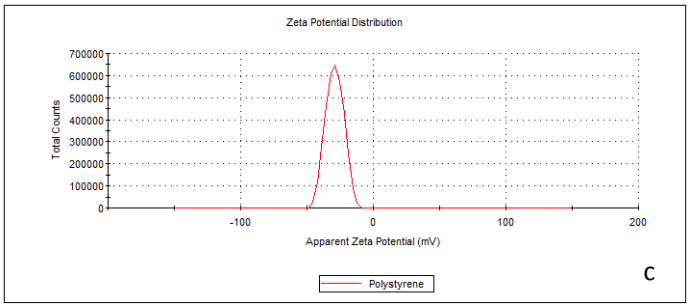

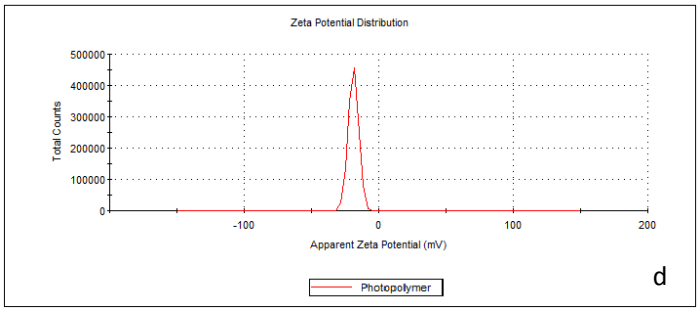

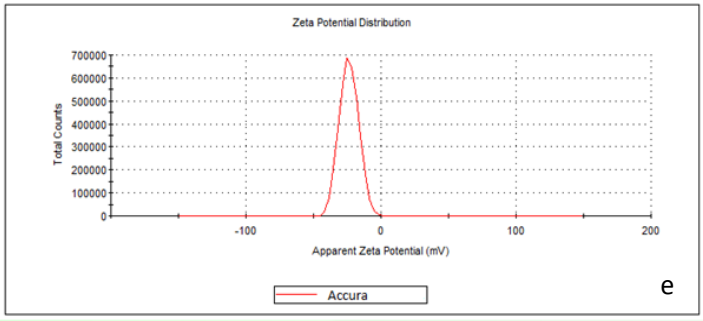

11.4. Appendix 4

11.4.1. Evaluation of the effect of sterilisation method on the surface structure of the biofilm model substrata

11.4.1.1 Aim of the experiments

The aim of these experiments was to assess the effect of sterilisation methods (autoclaving, gas plasma) on the surface characterization of substratum materials (Endo-Vu block, Polystyrene, Photopolymer, Accura) by comparing the images of the surfaces before and after sterilisation using scanning electron microscope (SEM).

11.4.1.2 Materials and Methods

A total of twelve samples of each substrata materials were prepared (as described in section 2.2.2.1.2), and then divided into two groups (A & B). Each group (n = 6) consists of 6 samples, and were then divided into two subgroups (1 & 2) (n = 3). For subgroup (1), the samples were directly prepared for evaluation using a scanning electron microscope (SEM) (as mentioned in section 2.2.2.5.1). For subgroup (2), the samples were sterilised using one sterilisation method (autoclaving or gas plasma). Following the sterilisation procedure, the samples were prepared for the SEM evaluation.

The autoclaving method was performed by placing each sample in an empty 7 mL plastic bijou bottle (Sarstedt Ltd, Nümbrecht, Germany) and then sterilised using a steam autoclave (Ascot Autoclaves Ltd, Berkshire, UK) (121°C, 103.421 kpa, 30 minutes) (Farrugia 2015).

The gas plasma method was performed by placing samples of each test material individually into packaging bags (Sterrad 100S, ASP®, Irvine, CA, USA) and then

sterilised using gas plasma with hydrogen peroxide vapour (Sterrad 100S, ASP®, Irvine, CA, USA) for fifty minutes (Precautions and Flush, 2008).

11.4.1.3 Results

11.4.1.3.1. Evaluation of substratum materials to withstand autoclaving procedures

SEM images of material surfaces before and after autoclaving procedure for each substratum material (Endo-Vu, Polystyrene. Photopolymer, Accura) are presented in Figures 11.2, 3, 4, and 5 respectively.

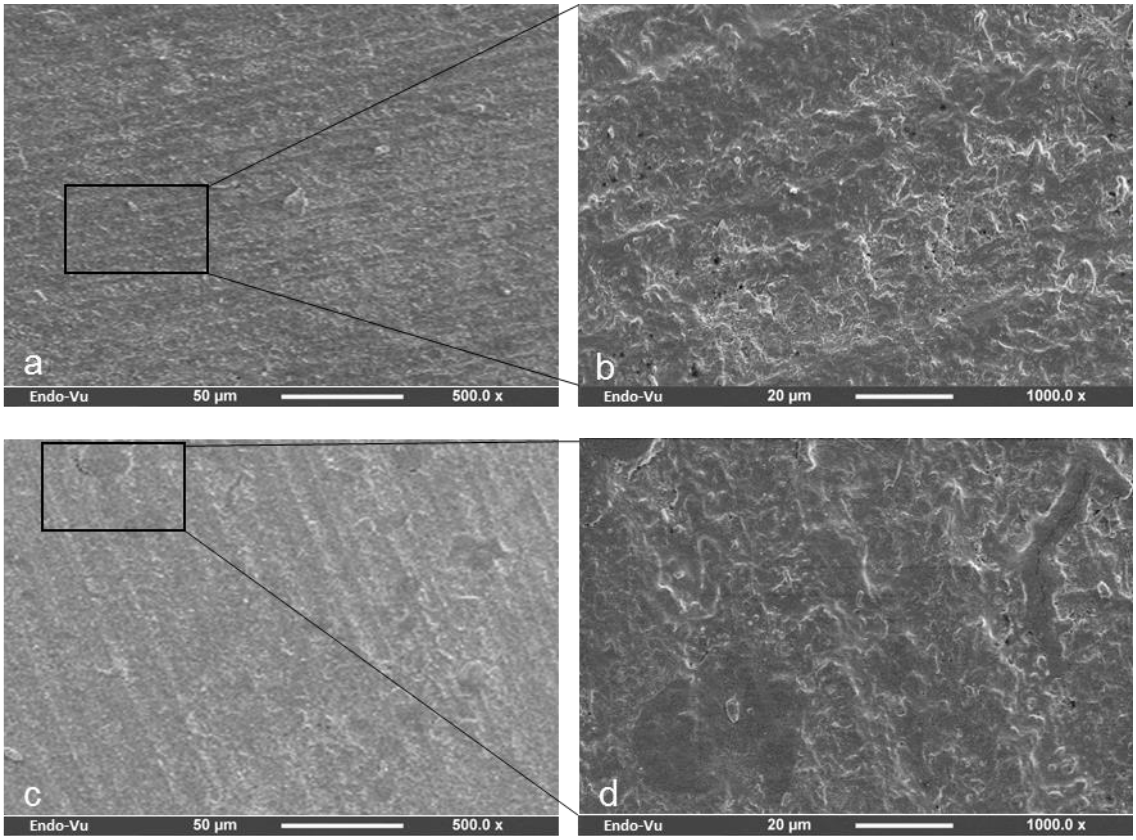

Figure 11.2: SEM images of the Endo-Vu material surface. a. and b. before, c. and d. after autoclaving.

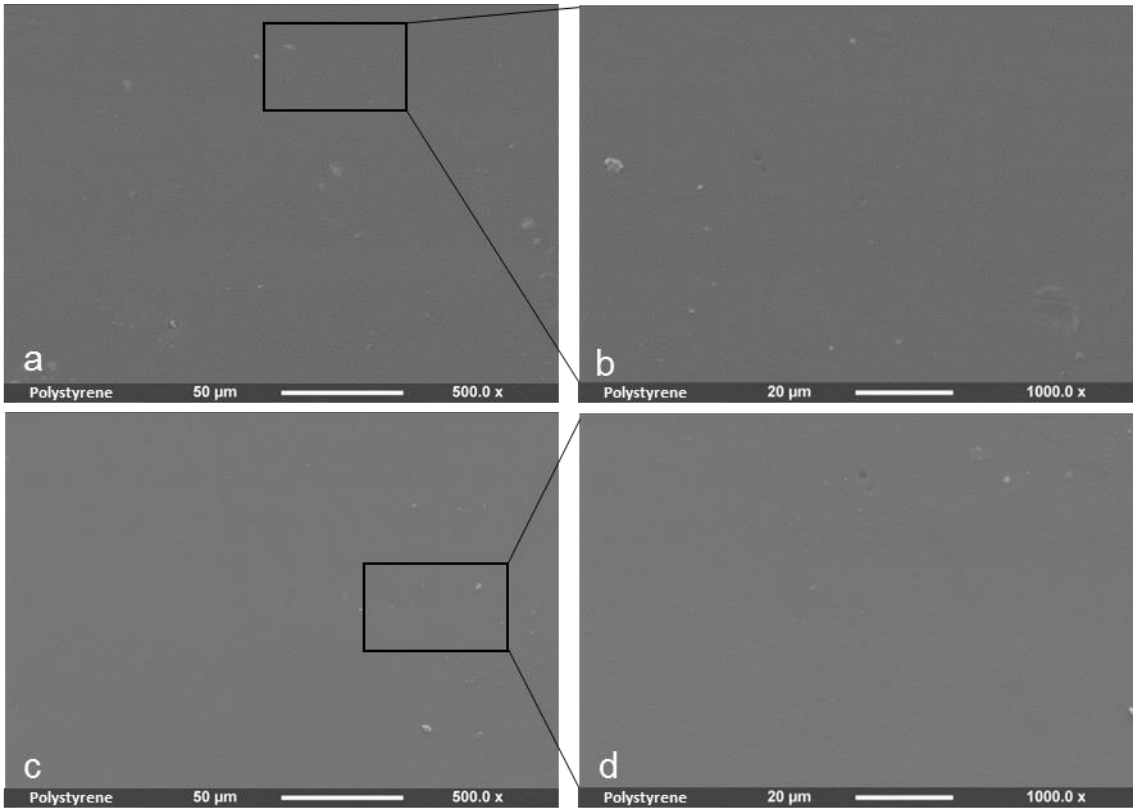

Figure 11.3: SEM images of the Polystyrene material surface. a. and b. before, c. and d. after autoclaving.

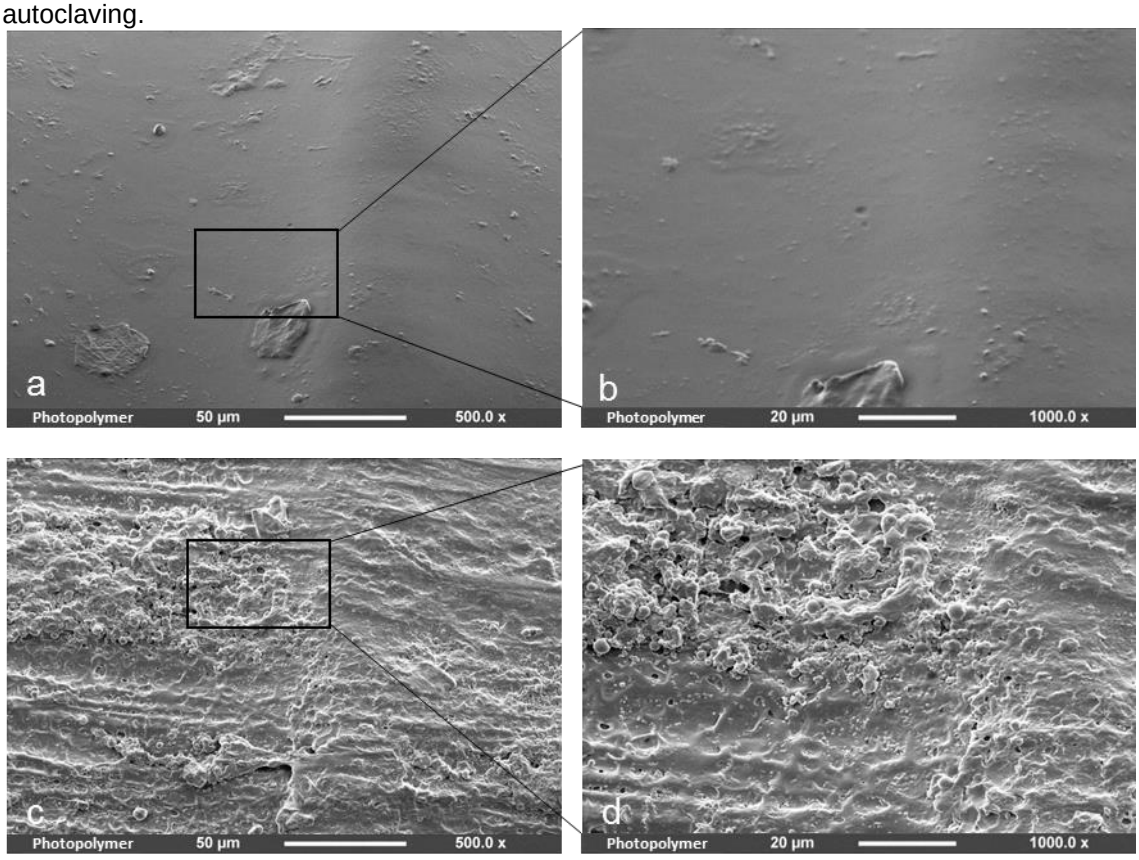

Figure 11.4: SEM images of the Photopolymer 3D material surface. a. and b. before, c. and d. after autoclaving.

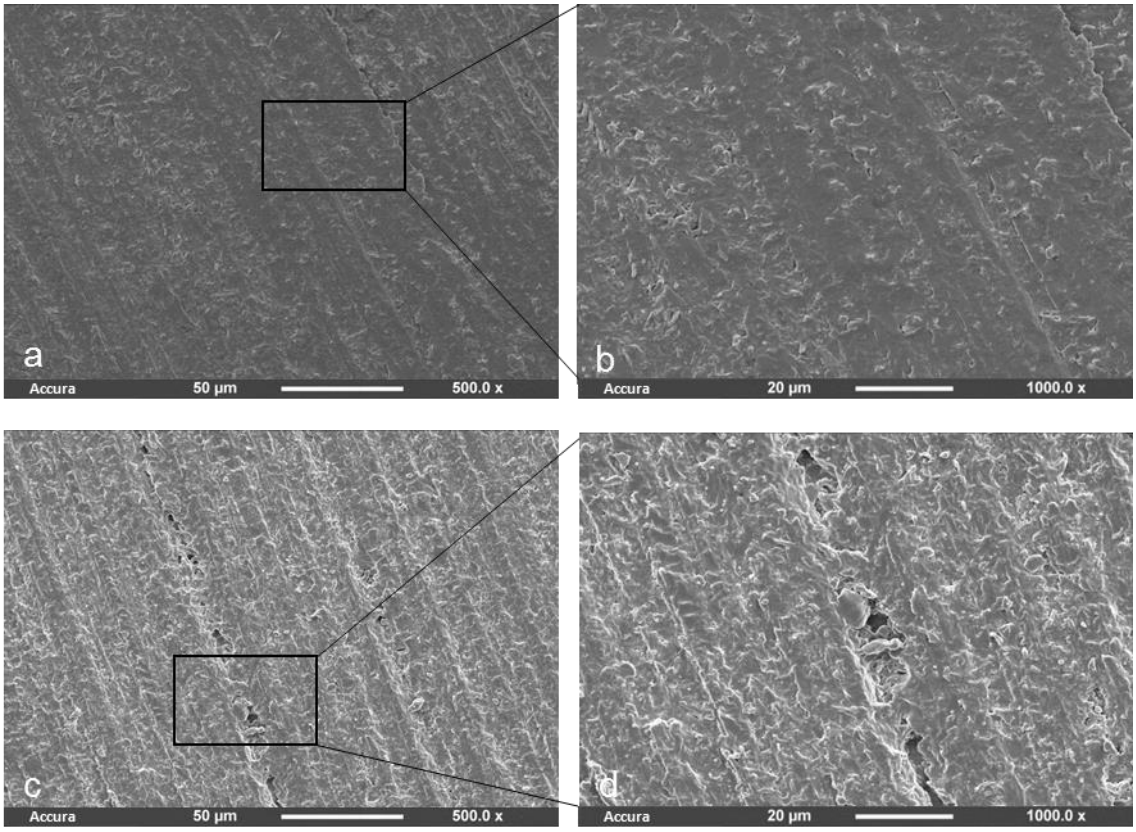

Figure 11.5: SEM images of the Accura 3D material surface. a. and b. before, c. and d. after autoclaving.

The images of the Endo-Vu block (Figure 11.2), and Polystyrene (Figure 11.3) revealed an even surface with no evidence of voids being detected along the surface of the autoclaved samples. Both substrata appeared unaffected following the autoclaving procedure. In comparison, the steam sterilisation caused degradation to the surface of the STL materials [Photopolymer (Figure 11.4), Accura (Figure 11.5)] with a number of pores present on the substratum surface.

11.4.1.3.2. Evaluation of substratum materials to withstand gas plasma procedures

SEM images of material surfaces before and after gas plasma procedure for each substratum material (Endo-Vu, Polystyrene. Photopolymer, Accura) are presented in Figures 11.6, 7, 8, and 9 respectively.

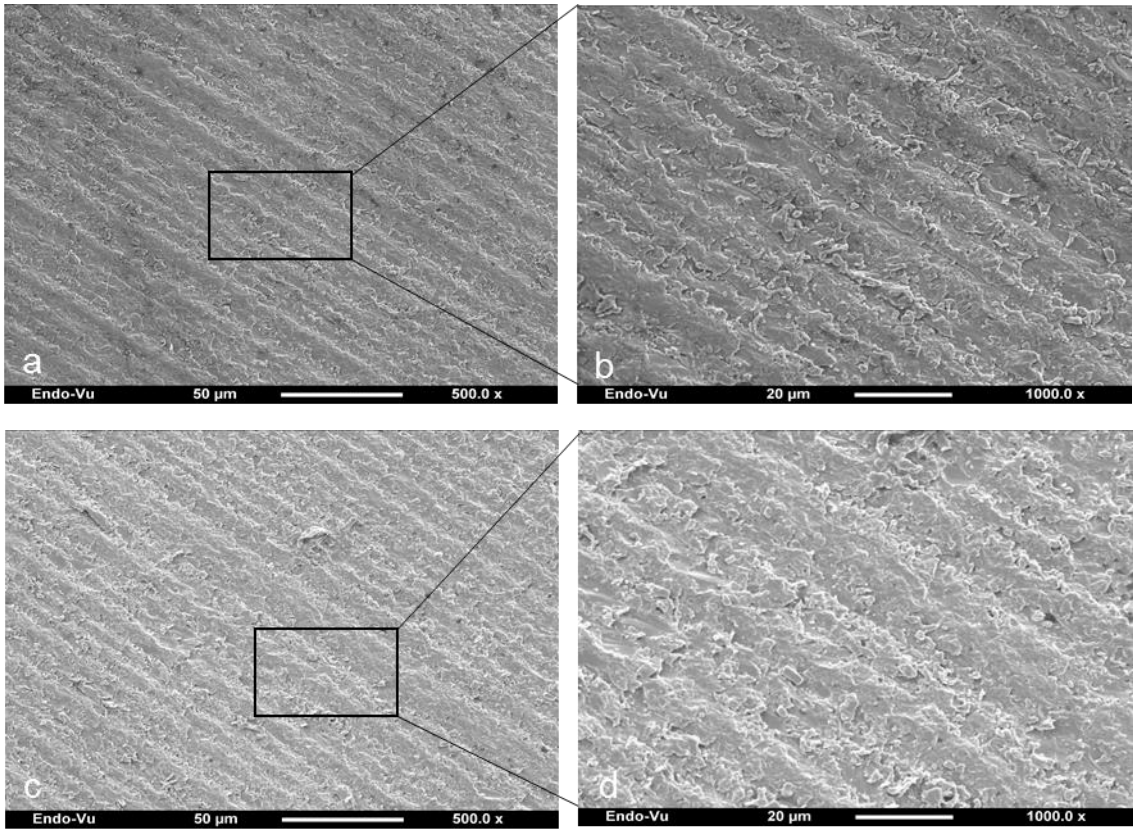

Figure 11.6 SEM images of the Endo-VU material surface. a. and b. before, c. and d. after gas plasma sterilisation.

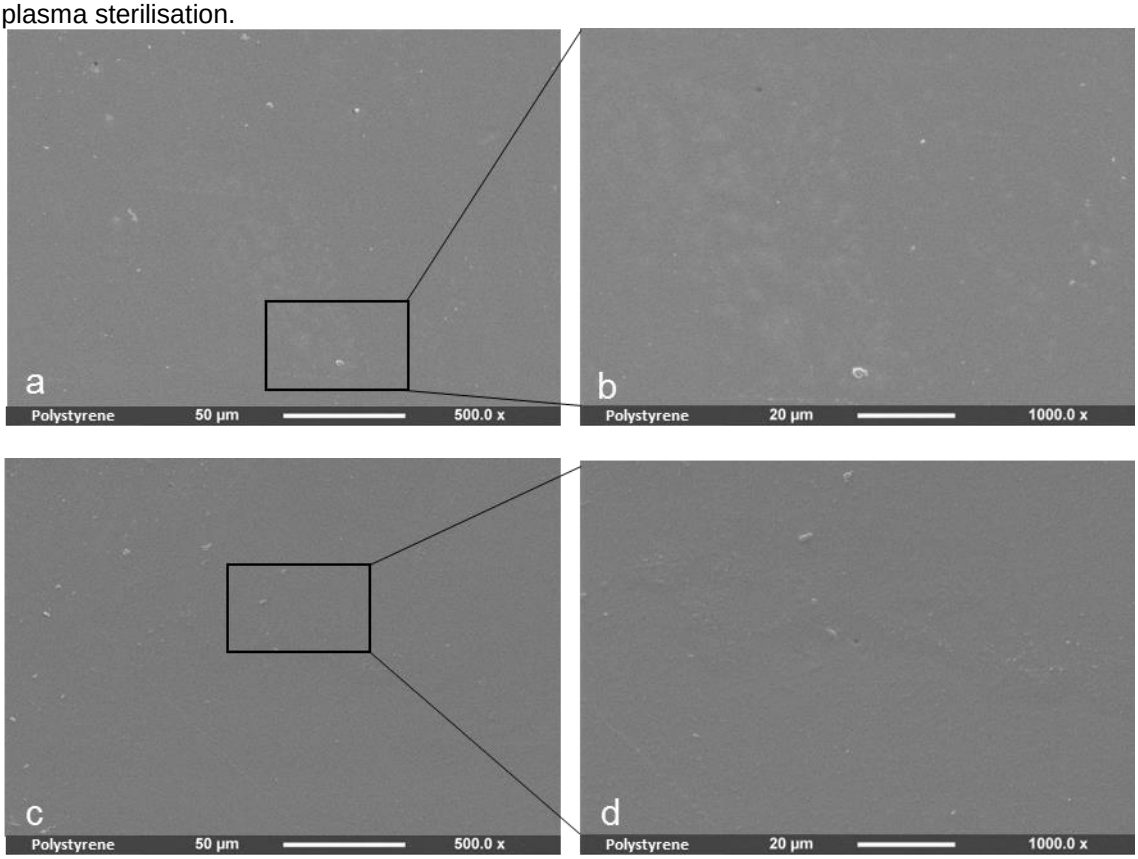

Figure 11.7: SEM images of the Polystyrene material surface. a. and b. before, c. and d. after gas plasma sterilisation.

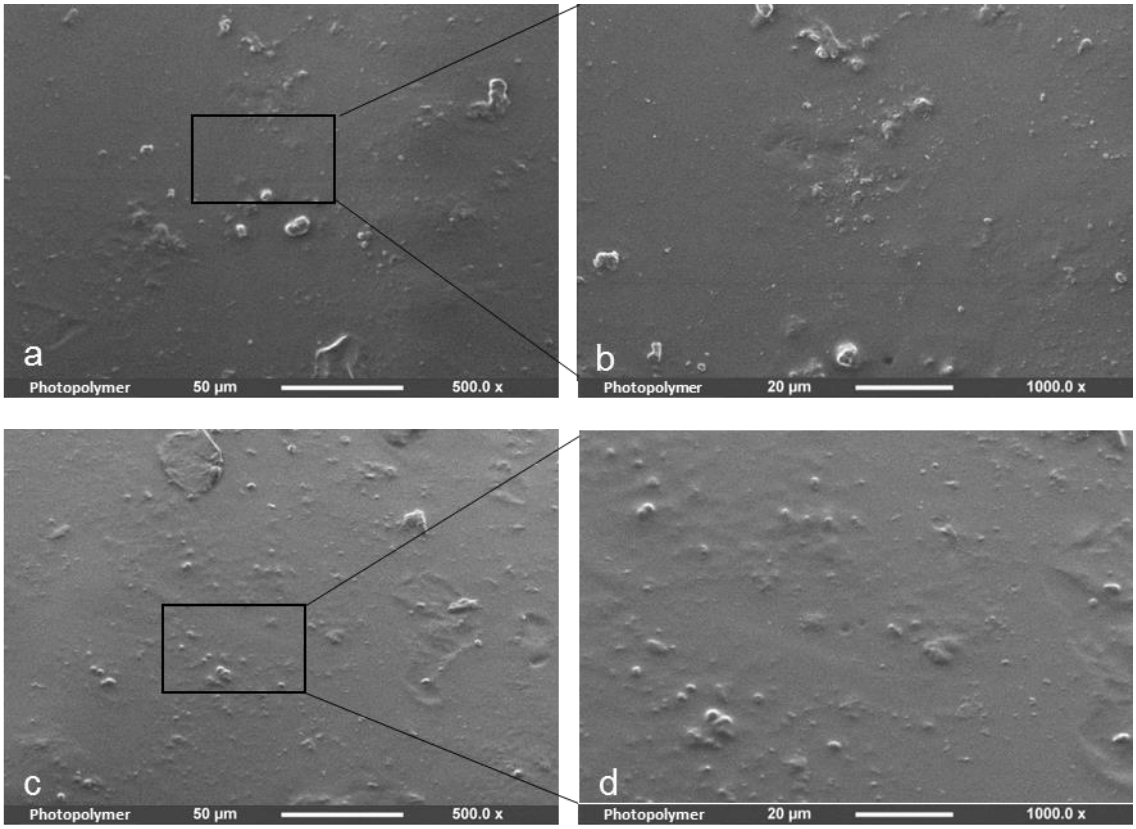

Figure 11.8: SEM images of the Photopolymer 3D material surface. a. and b. before, c. and d. after gas plasma sterilisation.

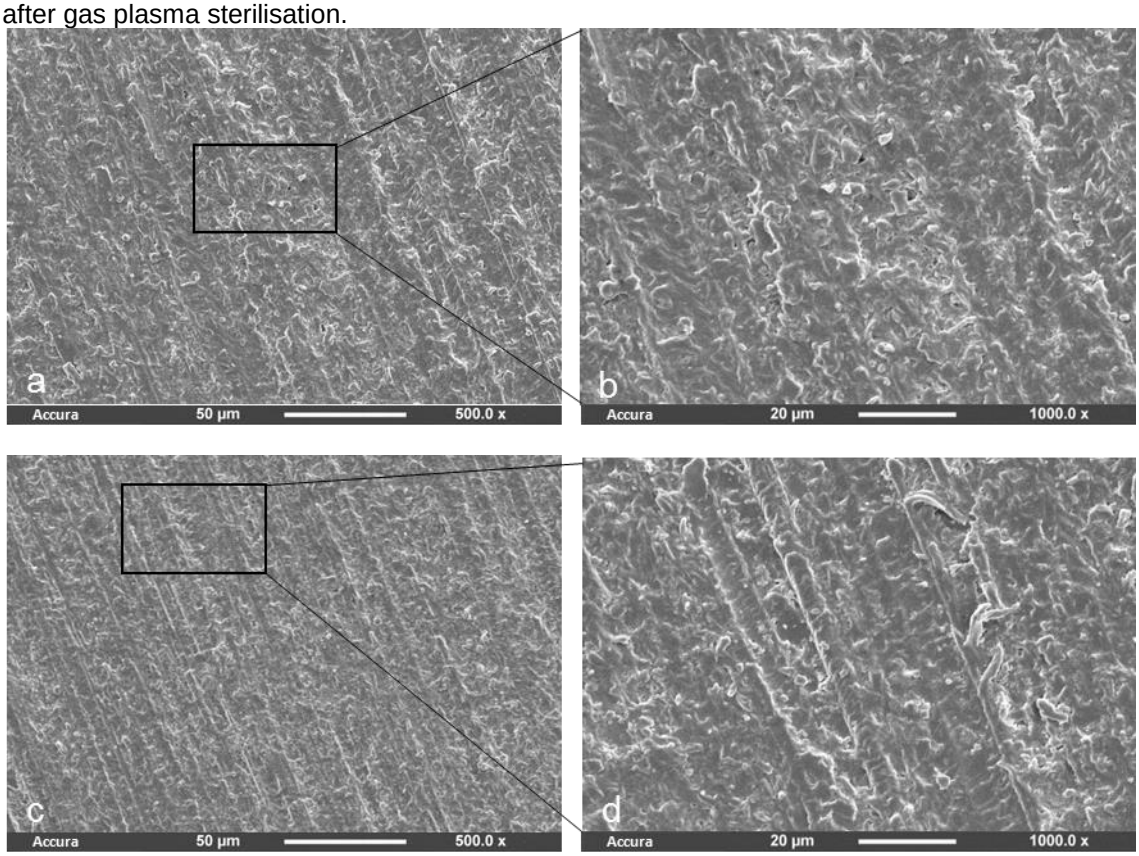

Figure 11.9: SEM images of the Accura 3D material surface. a. and b. before, c. and d. after gas plasma sterilisation.

The images of all substrata after sterilisation revealed an even surface with no evidence of voids being detected along the surface of the sterilised models. The substrata appeared unaffected following the sterilisation procedure.

Overall, these results indicated that the autoclaving method of sterilisation has no effect on the surface characteristic of two substrata materials (Endo-Vu and Polystyrene). In comparison, the gas plasma method allowed sterilisation of all substrata materials used in the present study without any destructive effect on the surface structure.

11.5. Appendix 5

11.5.1. Iodometric Titration of NaOCl

The NaOCl solution (Teepol® bleach, Teepol products, Egham, UK) was titrated and diluted with deionized water to a concentration of 2.5%, following the protocol detailed below. This procedure was performed immediately prior to use and the solution stored in a dark glass bottle in a cool place.

Titration of NaOCl for the determination of available chlorine:

1. A burette was filled with 0.1M of sodium thiosulphate solution
2. Potassium iodide (3 g) and 100 cm^3 of distilled water were mixed in a 250 cm^3 conical flask
3. 3 cm^3 of NaOCl was placed in the conical flask using a pipette, followed by 20 cm^3 of 10% acetic acid. The solution turned deep brown in colour
4. Titration was performed by adding sodium thiosulphate from the burette until the solution turned a pale straw colour
5. A few drops of starch were added to the solution, which then turned deep purple
6. Sodium thiosulphate was added slowly until the solution became colourless
7. A note was made of the titre and the procedure repeated until two consecutive readings were achieved within 0.1 cm^3
8. The average of the two readings was calculated
9. To calculate the amount of available chlorine the following equation was used:

$$Available\ chlorine\ (\%) = \frac{\text{Volume of sodium thiosulphate (X)} \times\ 0.003546}{\text{Volume of test NaOCl solution (1 mL)}} \times 100\%$$